Particle Interactions in Complex Dry Powder Inhaled Formulations and Single Particle Aerosol Mass Spectrometry

Inauguraldissertation

Zur

Erlangung der Würde eines Doktors der Philosophie
vorgelegt der
Philosophisch-Naturwissenschaftlichen Fakultät
der Universität Basel

von

Martin Jetzer

aus Baden (AG), Schweiz

Basel, 2019

Genehmigt von der Philosophisch-Naturwissenschaftlichen Fakultät auf Antrag von

Prof. Dr. Georgios Imanidis, Fakultätsverantwortlicher Universität Basel

Prof. Dr. Jörg Huwyler, Korreferent Universität Basel

Basel, 24.04.2018

Prof. Dr. Martin Spiess

«Anyone who stops learning is old, whether at twenty or eighty. Anyone who keeps learning stays young. The greatest thing in life is to keep your mind young»

Henry Ford

(Founder Ford Motor Company)

ACKNOWLEDGEMENTS

This thesis was conducted at the Pharmaceutical Development Unit (TRD PHAD PDU) Inhalation at Novartis Pharma AG Basel in collaboration with the University of Basel and Prof. Dr. Georgios Imanidis.

Foremost, I would like to express my sincere gratitude to my academic supervisor, Prof. Dr. Georgios Imanidis for the possibility to join his research group and particularly for his valuable scientific support, his advices for writing peer-reviewed publications and his enthusiastic guidance over the last three years. I would also like to thank him for giving me the freedom to explore my own ideas throughout my work. Furthermore, I am thankful for the great opportunities to present my work at numerous national and international conferences. I also very much appreciated his personal advice and the creation of a pleasant and creative working atmosphere in his group and seminars.

I would like to thank Prof. Dr. Jörg Huwyler (Department of Pharmaceutical Technology, University of Basel) for kindly accepting to co-examine my dissertation as well as Prof. Dr. Daniel Ricklin (Department of Molecular Pharmacy, University of Basel) to chair my defense.

Novartis Pharma AG is gratefully acknowledged for scientific, experimental, and financial support. My thanks go to Dr. Barbara Haeberlin, Dr. Thomas Storm, Dr. Kristina Kirch and Dr. Valerie Diart for the initiation of the project and for giving me this great opportunity to conduct my PhD studies at Novartis in cooperation with the University of Basel. I would also like to thank all of them for their guidance and valuable scientific support during my thesis.

My Special thanks go to Dr. Bradley Morrical and Dr. Marcel Schneider for taking over the supervision of this project at Novartis, for their support, enthusiastic guidance, and for all the scientific input and interesting scientific discussions we had. Thank you also for always being available for my questions and problems that raised during my daily work. I would also like to thank both of you for giving me the freedom to explore and bring in my own ideas during my thesis. I always appreciated your personal advice. Thank you for the fun times we had at several conferences.

Furthermore I would like to express my gratitude to Dr. Stephen Edge, Nuno Silva, Dr. Renato Guchardi, Dr. Malak Bitar, Laila El Yahyaoui, Aurelie Bubel and Dr. Grahame Woollam for their support with experiments in the lab and fruitful scientific discussions. I would also like to thank Dr. Anna Susz for training me on the SPAMS instrument. I would also like to express special thanks to all colleagues of the Novartis PDU Inhalation Unit for their support with experiments in the lab, the pleasant working environment and coffee breaks.

Special thanks go to Dr. David Fergenson and Wenchi Wang from Livermore Instruments Inc. for their technical support with the SPAMS instrument and their valuable scientific input to my work.

I would like to thank the group members of the Institute of Pharmaceutical Technology Laboratory Dr. Jonas Wedler, Kira Nultsch, Felix Ditzinger and Andreas Niederquell for the pleasant working atmosphere and coffee breaks at University. Thank you for your support and for the good time we spent together in- and outside the lab.

On a more personal level, I would like to thank my friends for their never ending patience, support and understanding during busy times at my work as well as all the afterwork beers.

Finally, I would like to thank my parents Eva Jetzer and Dr. Walter Jetzer and my sister Dr. Laura Jetzer for their encouragement and great support during all the years of my studies and beyond. Thank you for helping and allowing me to pursue my career goals as well as for your financial support. Without you I would not be where I am right now.

Last but not least I would like to thank Valentine Verhaeghe for her constant motivation and support whenever I needed it and also for the fantastic moments we spent together - thank you so much! Also thank you for your strong interest in my research and experiments.

Pursuing a doctorate can be very hard and demanding, but on the other hand it is also a very joyful and creative time where one can explore new areas of research. In the past three years I had the pleasure to work on various projects within different teams and I had the chance to meet and connect with many interesting people who not only helped me to further develop my scientific skills, but also contributed to my personal development. Finally and most important, I had the opportunity to build new friendships.

ABSTRACT

Pharmaceutical aerosols are an effective method to deliver therapeutic agents to the respiratory tract. Among aerosol generation systems, dry powder inhalers (DPIs) have been an attractive technology for both local and systemic delivery of drugs. DPIs combine several advantages compared to metered dose inhalers (MDIs) and other inhalation devices: DPIs are breath-actuated (patients do not require hand-lung coordination), no need for environmentally damaging chlorofluorocarbon (CFC) propellants or solvents, improved product stability, DPIs deliver a wide range of drugs (e.g. traditional anti-asthmatics, proteins) in high doses via one short inhalation and increased respirable fractions compared to MDIs. Furthermore, DPIs often have only low inspiratory flow resistances, which is beneficial for patients suffering from respiratory diseases [1, 2]. Inhalation devices are designed to deliver a reproducible predefined dose of drug to the small airways and alveolar regions of the human lung. It has been reported that particles with a mass median aerodynamic diameter (MMAD) of <5 μm are effectively deposited at these sites [3, 4]. The MMAD of an aerosol particle depends on its geometrical diameter, density, and morphology with these properties generally being optimized during the manufacturing process [5]. Most commercial DPI formulations (adhesive mixtures) consist of micronized drug blended with coarser carrier particles (usually alpha lactose monohydrate; ca. 20-300 μm), which is used to aid the handling, metering and dosing of the formulation. These components are usually combined in a manufacturing process with high- or low-shear blending, which is used primarily to distribute the cohesive drug particles throughout the bulk excipient of the formulation to create a homogeneous mixture. The interactions between drug and carrier are a major determinant of DPI performance. Due to interparticulate forces, such as mechanical interlocking, capillary, electrostatic, and van der Waals, micronized powders exhibit very adhesive and cohesive behavior and form spontaneously agglomerates [6, 7]. The extent of the combined forces is dependent on powder properties such as particle size, morphology, shape, and material characteristics (e.g. amorphous content, hydrophilicity, electrical resistivity) [8], as well as on environmental factors, such as relative humidity and temperature [9]. Since the extent of agglomeration negatively affects the fraction of the inhaled powder within the respirable range [10], these agglomerates must be deagglomerated effectively prior to or during the processes of aerosolization and inhalation [11].

In recent years, there has been great interest in the development of ternary mixing systems because the addition of a ternary component into carrier-based DPI formulations can lead to improved aerosol performance due to drug-carrier interaction modifications [12-19]. In lactose-based DPI formulations, ternary components can be either lactose fines [20], sugars (e. g. micronized glucose) [21], or a variety of force control agents (FCAs) such as magnesium stearate (MgSt) or leucine [13, 15, 16, 18, 22]. Blending lactose together with MgSt prior to adding the active pharmaceutical ingredient (API) has been shown to modify the performance of pharmaceutical inhaled products [14, 15]. Also pre-treatment of APIs with different FCAs has been shown to alter the performance and improve the drug deposition in the lowest impactor stages [23]. Various application processes such as mechanofusion, high- or low-shear mixing and particle smoothing have been used to apply different FCAs on carrier particles as very thin coating layers (<10 nm) [16, 22, 24, 25].

The current pharmacopoeial standard method for determining the aerodynamic particle size distribution (APSD) of APIs delivered from inhaled pharmaceutical products is to generate a size-segregated sample of the particles in a cascade impactor, typically the Next Generation Impactor (NGI) [26-28], followed by the dissolution of each size-fractionated particle sample into a solvent which is then analyzed by high-performance liquid chromatography (HPLC). While highly quantitative for the total concentration of API delivered, this technique does not yield any information regarding the relationships and interactions between the various product components (API(s), excipients) within the formulation. Cascade impaction testing also requires mastery of a complex technique before consistent results can be achieved and results in a large demand on resources in terms of laboratory personnel and solvents, and the measurements are very time-consuming [29, 30]. The development of more rapid techniques as application for routine product quality testing or in product development is therefore highly desired [31]. Mass spectrometry based aerosol analytical techniques have been undergoing continuous development since the 1970s [32, 33]. Aerosol-specific mass spectrometers are capable of providing both aerodynamic particle size distribution (APSD) profiles and

the chemical composition of particles by using a statistical sample of a high number of single particles in a very short timeframe (minutes). The single particle aerosol mass spectrometry (SPAMS) technique can be used to evaluate particle interactions/co-associations between drug product components in a way that is inaccessible via cascade impactor techniques. Importantly, since in recent years more complex inhaled products have become available on the market that deliver two (or even three) APIs within a single dose (e. g. Ultibro® Breezhaler®, Foster® NEXThaler®, Trelegy® Ellipta®) using highly sophisticated engineered formulation approaches with fine lactose and/or magnesium stearate [34-36]. Clinical research has shown that such combination inhalers provide an enhanced clinical effect beyond that achieved when the two drugs are administered concurrently from two separate inhalers. Preliminary tests using aerosol time-of-flight mass spectrometry and SPAMS determined that the respirable fraction can be composed of co-associated API particles, which could be the reason behind the increased effects of the combination drug inhalers [30, 37, 38].

This thesis focuses on the investigation of the complex mechanisms that affect the dispersion of drug particles during aerosolization and ultimately the *in vitro* aerosol performance of inhalation. Particular attention was paid to combinations of two APIs and formulations containing magnesium stearate as force control agent. Specifically prepared model dry powder inhaled formulations and commercial products were used. High- and low-shear blending techniques of lactose and magnesium stearate were explored and the effect of different storage regimes on physicochemical properties and performance of such dry powder inhaled formulations was assessed. Advanced powder characterization techniques such as single particle aerosol mass spectrometry (SPAMS) and time-of-flight secondary ion mass spectrometry (ToF-SIMS) were employed to improve the mechanistic understanding of particle interactions, drug detachment and dispersion during impaction analysis.

In a first study, aerodynamic particle size distribution profiles (APSD) of commercial metered dose inhaler (MDI) and dry powder inhaler (DPI) were obtained using single particle aerosol mass spectrometry (SPAMS; Livermore Instruments Inc., USA) and then compared to those obtained by the Aerodynamic Particle Sizer (APS; TSI Incorporated, USA) and Next Generation Impactor (NGI, Copley Scientific, USA). In addition, the transmission efficiency of SPAMS as well as potential size bias of APSD measurements that might result from a size dependent transmission profile were evaluated. It was demonstrated that the SPAMS can generate useful APSD measurements with both pMDI and DPI products. However, a consistent difference of particle transmission in the SPAMS in the region of 2-3 µm was found compared to NGI measurements.

In a second study, measurements of Advair® Diskus® and Seretide® using the SPAMS technique showed that a significant fraction of the emitted drug particles can form co-associated particles with other drugs (and likely excipients) in the same DPI or pMDI formulation. For this, unique mass spectral fragmentation patterns could be recognized and assigned for each API using the SPAMS data analysis software. SPAMS also revealed which particle size fractions are most likely forming these co-associations. In a third study it could be demonstrated that for example in Foster® NEXThaler® the degree of particle co-association was manipulated by the choice of formulation and manufacturing approach for DPIs. It is possible that in the manufacturing process APIs or carrier can be processed together with the force control agent magnesium stearate to improve dispersion mechanics. An explanation may be that the drug or the carrier receive an MgSt-coating that would prevent the co-association or agglomeration of the particles and moreover facilitate detachment from carrier. This results in high *in vitro* performance (and furthermore high extra fine particle fraction of particles <2 µm), as well as a relatively fine APSD profile compared to products not engineered in this way. Particle co-associations of API-MgSt were detected in the commercially available DPI product Foster® NEXThaler®.

The intensity of the blending technique is demonstrated in a fourth study in this work to affect the distribution of MgSt covering the lactose carrier. This coverage of lactose by MgSt as evidenced using the ToF-SIMS technique was shown to significantly influence the *in vitro* aerosol performance. The underlying mechanism of particle interaction between API and the carrier seems to be substantially different for high- and low-shear formulations. This provides the basis

for a modification in particle interactions from drug-lactose to drug-MgSt (in high-shear), which then is responsible for the improved performance by enhanced particle detachment from carrier due to lower interaction forces.

In a fifth study, the conditioning of DPI capsules at controlled temperature and humidity settings also showed to have a significant effect on the separation of drug and carrier particles. Significant differences were observed between adhesive and cohesive model compounds (with respect to lactose). This study highlights that electrostatic forces and interactions play a significant role in dry powder inhaled formulations. Large differences in the electrostatic charging behavior were observed. Fluticasone propionate seems to have a high propensity to electrostatic charging, while salmeterol xinafoate only showed negligible performance consequences as a result of its electrostatic charging behavior. Most of the common excipients used in DPI formulations, such as lactose monohydrate, do not seem to experience significant charge accumulation in stark contrast to MgSt, which tends to acquire high amounts of electrostatic charge. Other DPI drug product components such as HPMC capsules did not tend to charge significantly. Conditioning of certain APIs was found to be helpful to dissipate electrostatic charge which in turn increased aerosol performance.

In summary, this thesis combines improvements to the analytical methodologies such as SPAMS with the systematic investigation of dry powder inhalation formulations to advance the understanding of *in vitro* aerosol characteristics of drug product formulations at a fundamental mechanistic level.

CONTENTS

CHAPTER 1: GENERAL INTRODUCTION INTO PULMONARY DRUG DELIVERY & FORMULATION DEVELOPMENT

1. General Introduction

The respiratory tract is one of the oldest routes for the administration of drugs. Anesthetics, aerosolized drugs, smoke or steam have been inhaled for medical purposes for hundreds of centuries. Over the past decades inhalation therapy has established itself as a valuable tool in the local therapy of pulmonary diseases, such as asthma or chronic obstructive pulmonary disease (COPD) [39]. The benefits of local lung delivery include rapid clinical response and minimized systemic toxicity due to reduction of overall required doses. Regarding systemic therapy, the lungs are an efficient way for drugs to reach the bloodstream due to the large surface area available for absorption (ca. 100 m^2), the very thin absorption membrane (0.1–0.2 μm) and the elevated blood flow (5 L/min), which rapidly distributes molecules throughout the body. Moreover, the lungs exhibit relatively low local metabolic activity, and unlike the oral route, pulmonary inhalation is not subject to first pass metabolism [40]. However, pulmonary administration presents the difficulty of achieving efficient and regular deposition of the drug in the bronchial or alveolar regions of the respiratory tree, an aerodynamically efficient filter that hinders the deposition of the drug.

Historically, the evolution of inhalation therapy can be traced to India around 4000 years ago, where the leaves of the plant *Atropa Belladonna*, containing atropine as a bronchodilator, were smoked as a cough suppressant [41]. Asthma cigarettes containing stramonium leaves (*Datura Stramonium*) with atropine-like effects were widely used in the 19th century as "fuming asthma remedies" along with powders and cigars [42]. However, the development of modern inhalation therapy started in the 19th century with the invention of the glass bulb nebulizer. The development of the first pressurized metered dose inhaler (pMDI) for asthma therapy (Medihaler®) by Riker Laboratories Inc. (now 3M Drug Delivery Systems) in 1956 was a major advance in the use of (pharmaceutical) aerosols for drug delivery to the lungs [43]. However, the required hand-lung coordination of the patient and the use of environmentally damaging chlorofluorocarbon (CFC) propellants, are major drawbacks of the traditional pMDI. Dry powder inhalers (DPIs) were introduced to overcome these drawbacks. Since the first introduction of a DPI in 1971 (Spinhaler®) by Fisons, many DPIs have been marketed. DPIs represent a significant advance in pulmonary delivery technology. They are breath-controlled and therefore coordination problems have been overcome. DPIs are also potentially suitable for the delivery of a wide range of drugs apart from the field of asthma and COPD, such as anti-asthmatics, peptides and proteins. DPIs can also deliver a wide range of doses from 6 mg to more than 20 mg via one short inhalation [40, 43].

This chapter gives an overall introduction to inhalation therapy with modern dry powder inhaler technology, from the pulmonary diseases and human anatomy of the airways to dry powder formulation development.

2. Pulmonary Drug Delivery

2.1 From Inhalation to Clinical Effect

Pulmonary delivery has gained importance in the therapeutic field because of the numerous advantages this route of administration offers, in comparison to the oral or parenteral routes. The active pharmaceutical ingredient (API) can be delivered directly to the site of action in the respiratory tract in a high concentration to treat respiratory diseases such as asthma, chronic obstructive pulmonary disease (COPD), and bacterial or fungal pulmonary infections. Furthermore, this route could also be considered for treating lung tumors. The advantages of such targeted therapy include a reduction in local (deposition in oropharynx) and systemic side effects and a decreased incidence of potential drug-drug interactions [44]. These reductions are due to the decrease in systemic drug concentrations, whilst ensuring a therapeutic efficiency that is similar or superior to oral or parenteral delivery.

The major advantages of inhalation therapy are as follows [40]:

(a) Rapid onset of the therapeutic effect (huge surface area in the lungs allows a fast uptake of drug)
(b) Lowering of the required dose (compared to systemic administration)
(c) Reduction in unwanted side effects

It is well known that inhalation therapy, especially for asthma and COPD, is very successful even though only a small fraction of the inhaled dose (typically less than 20-30%) actually reaches the peripheral parts of the respiratory tract. The rest of the dose deposits in the mouth and in the upper airways [44]. The dry powder inhaler device is one of the types of delivery systems that enable the generation and delivery of aerosolized drug particles into the respiratory tract. The principle of this therapy is to transfer powdered medication into a clinical effect. However, the respiratory tract is a strongly branched system, which works excellently as filtering system to avoid penetration of particles into the lungs. To enable penetration into the lungs, the aerodynamic particle size of the inhaled medication has to be tailored, preferably below 5 μm [3, 4]. The particle size distribution of the drug is one of the major determinants in drug delivery to the respiratory tract. Special techniques, such as micronization of drugs in dry powder systems, are required to produce particles in this size range. Because of difficulties in powder handling of micronized particles and very low amounts of drug (5-500 mcg) that have to be metered in inhalation therapy, special formulations and devices have to be developed and applied to obtain the required clinical effect from the administered dose [7, 45].

2.2 Anatomy and Physiology of the Human Respiratory Tract

The main function of the respiratory tract is the exchange of oxygen from the alveolar gas into the pulmonary capillary blood and carbon dioxide exchange vice versa. The respiratory tract can be separated into two main parts (upper and lower lung). The upper part is divided into the head airway region with the nose, mouth, pharynx and larynx, and the tracheobronchial region from the trachea to the terminal bronchioles. Its main functions are warming and humidifying of air, and to retain foreign material to protect the lower lung. The lower lung is the pulmonary or alveolar region where the gas exchange takes place [46, 47]. The respiratory tract is characterized by a thin epithelium, very large surface area (ca. 100 m^2), low enzymatic activity, and a rich blood supply [48].

The human respiratory tract is a branching system of air channels with more than 23 bifurcations from the mouth to the alveoli with the appearance of an inverted tree. The human respiratory system can largely be divided into four regions. These regions clearly differ in structure, airflow patterns, function, and sensitivity to deposited particles. The most frequent used morphological model for describing the structures of the human lungs was initially given by Weibel (Figure 1) [49].

1. The first region is the upper respiratory tract, which includes the nose, mouth and pharynx. The main function of this region is the heating and moistening of air. Atmospheric air contains around 40-60% of moisture and has a temperature of ca. 20 °C. In the mouth, nose and throat the air is heated up to 37 °C and reaches 99% relative humidity.

2. The second region of the human lung is the conduction zone. This region consists of the first 16 generations of branching. The airways of the conducting zone are described as rigid tubes that consist primarily of cartilage in the walls and that symmetrically divide or bifurcate beginning with the trachea and ending with the terminal bronchioles.
3. The third region is the transitional zone. This region consists of the generations 17 through 19 of the branching. The respiratory bronchioles each consist of a few alveoli in which limited gas exchange can occur.
4. The fourth region is the respiratory zone. This region consists of the generations 20 through 23 of the branching, ending in the alveoli. Gas exchange occurs in the highly vascularized respiratory zone by adding oxygen, and removing carbon dioxide from the blood while passing the pulmonary capillary bed. With increasing generation number, the number of branches highly increases, while the distance between the branches and the airway diameter decrease. The summed cross sectional area from mouth to alveolar sacs exponentially increases and results in a tree shaped lung model, with a total surface area of up to 100 m^2 [49, 50].

	Generation		Diameter, cm	Length, cm	Number	Total cross-sectional area, cm^2
Conducting zone	Trachea	0	1.80	12.0	1	2.54
	Bronchi	1	1.22	4.8	2	2.33
		2	0.83	1.9	4	2.13
		3	0.56	0.8	8	2.00
	Bronchioles	4	0.45	1.3	16	2.48
	Terminal bronchioles	5 ↓ 16	0.35 ↓ 0.06	1.07 ↓ 0.17	32 ↓ 6×10^4	3.11 ↓ 180.0
Transitional and respiratory zones	Respiratory bronchioles	17	↓	↓	↓	↓
		18				
		19	0.05	0.10	5×10^5	10^3
	Alveolar ducts	T_3 20	↓	↓	↓	↓
		T_2 21				
		T_1 22				
	Alveolar sacs	T 23	0.04	0.05	8×10^6	10^4

Figure 1: Schematic representation of airway branching in the human lung. Adapted from [51].

2.3 Particle Deposition in the Lungs

In order to achieve the desired pharmacological effect, a drug particle designed for inhalation must deposit at the site of action [52]. The fate of inhaled particles either as a medicine or as environmental aerosol depends mainly on the particle properties (size/aerodynamic diameter, shape, and density) and lung physiology (geometry, respiratory flow rate, tidal volume). Over 90% of particles with an aerodynamic diameter larger than 10 µm are deposited in the oropharynx. The critical aerodynamic diameter for reaching the lungs is known to be <5 µm (Figure 2) [3, 4]. The relationship between aerodynamic particle size and deposition has been studied extensively [53]. Most studies confirm

the computations in their predictions that the most effective particles for inhalation are indeed within the aerodynamic size range of 1-5 µm [54-57]. It should be noted that particles with larger geometric diameters may be useful for inhalation if they have low densities, e.g. as the result of porous structures [58, 59]. Such particles may have an aerodynamic diameter between 1 and 5 µm, although their geometric diameter is much larger (e.g. in the size range of 10 to 30 µm) [5, 60].

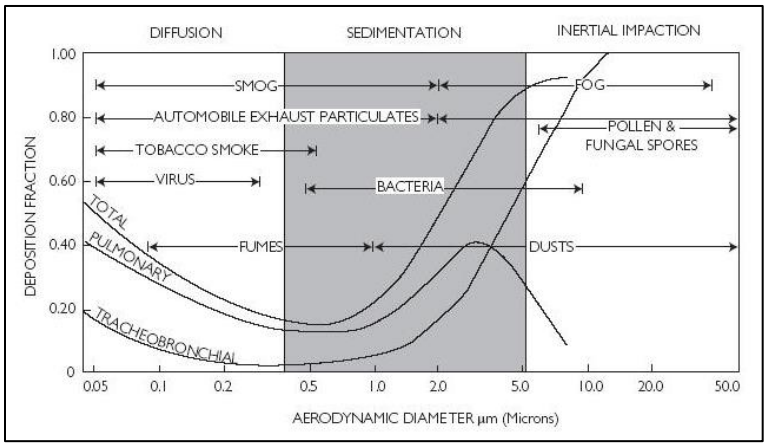

Figure 2: Relationship between particle size and lung deposition (from Labiris and Dolovich [3]).

The three most important particle deposition mechanisms are (1) impaction due to inertia of particles, (2) sedimentation due to gravitational forces, and (3) Brownian diffusion (Brownian motion of surrounding gas molecules) (Figure 3) [61]. Interception and electrostatic deposition only play a minor role in the lungs [62, 63].

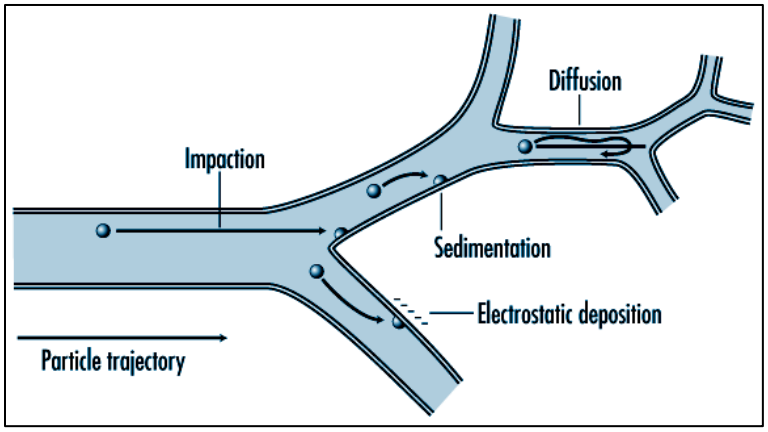

Figure 3: Schematic of particle deposition mechanisms at an airway branching site in the human lung adapted from [64]. Impaction takes place for particles >3 µm, sedimentation for particles with a diameter of 0.5-4 µm, and diffusion for particles <1 µm.

The deposition mechanisms can be explained with fluid and particle dynamics in the respiratory tract. As a result of the many branchings, the cross section for air flow increases exponentially from the trachea to the alveolar sacs. Accordingly, the air velocity decreases from nearly 4 m/s in the trachea to less than 1 mm/s in the alveoli (at a moderate inspiratory flow rate of 60 L/min). This has the consequence that the air flow is turbulent in the upper tract and laminar further downstream. Because filtering of airborne particles in the upper tract by inertial deposition (impaction) depends on the particle's aerodynamic diameter and the particle velocity, the cut-off value of the upper tract highly depends on the inhalation maneuver. At higher flow rates (>60 L/min), most particles larger than 3-5 µm cannot pass the oropharynx and the first bifurcations. In the upper tract, where the air velocity is still relatively high, particles may

collide with the inner walls of the large airways by inertial impaction. Particles with high inertia (large diameter; high density) are unable to follow the airflow in bifurcations and bends and deposit on the mucosa covering the inner airway walls. Filtering of the larger particles in the upper tract in combination with the reduced velocity decreases the deposition probability by inertial impaction further downstream, and increases the contribution of sedimentation to total deposition.

When the flow rate is decreased (less than 30 L/min), particles in the size range up to 3-5 μm may enter the central or even the deep lung. If such particles are able to enter the lung periphery, their deposition efficiency will be relatively high due to their high sedimentation velocity (compared to particles of 1 μm or smaller). The decreasing sedimentation velocity with decreasing particle size is the reason why particles <1 μm are often considered unsuitable for inhalation, which explains why the recommended aerodynamic size range is between 1-5 μm [53, 57]. The gravitational settling velocity of particles in the micron range is low, whereas their residence time in the lungs is relatively short. As a result, the deposition efficiency decreases as particle settling becomes more dependent of sedimentation than of inertial impaction. Deposition efficiency under normal breathing conditions reaches a minimum of only approximately 20% for particles of 0.5 μm, meaning that 80% of particles of this size are exhaled again. To increase the deposition efficiency, the residence time can be prolonged, which explains the benefit of a breath hold period in this respect. For particles smaller than 0.1 μm, the efficiency may increase also due to an increasing contribution of Brownian motion to particle deposition.

2.4 Pulmonary Drug Absorption

The optimal absorption characteristics of a pulmonary drug depend on the site of drug action. For locally acting drugs, the drug absorption process may determine the removal and consequently the termination of action of the drug in the lungs, as well as the onset of any systemically mediated adverse effects. For systemically acting drugs, absorption from the lungs determines the therapeutic effect profile (onset, intensity, and duration of action) of the drug. Therefore, when designing drugs for pulmonary delivery, it is important to consider both lung–tissue retention and permeability, irrespective of site of action. The air-to-blood transfer always begins with an interaction between the drug and the surfactant: following deposition onto the mucosa of the tracheobronchial airways or alveolar region, the drug solute or particle encounters at least a monolayer of surface-active agents in which the fatty acid tails of lipids project into the air. For a drug compound of macromolecular size (e.g. peptide or protein), this lung surfactant may induce aggregation and, thus, potentially compromise dissolution or enhance macrophage uptake and digestion [65]. By contrast, lung surfactant can enhance solubility of small, lipophilic drug molecules, as demonstrated for example with glucocorticosteroids [66], which may potentially increase the rate and extent of absorption. Immediately below the molecular layer(s) of lung surfactant lies the 0.01–10 μm thick lining fluid through which drug must diffuse to get to the epithelium. The routes of drug absorption across the epithelium include passive and active transport mechanisms involving paracellular and transcellular transport, pore formation, vesicular transport, and drainage into the lymphatics (depending on the drug and site of absorption). The drug solute will pass through a cellular barrier that varies from a monolayer of thick (about 60 μm) columnar cells in the bronchi to a monolayer of thin (0.2 μm) broad cells in the alveoli. Drug absorbed from the air spaces into the blood must traverse a final barrier after the surfactant layer, the lining fluid, the epithelium, its basement membrane, and the interstitium: the cell monolayer that makes up the walls of the microvessels, the endothelium. The alveolar–capillary endothelium is extremely thin (0.03–0.2 μm) and has a relatively large number of endocytic vesicles [67].

2.4.1 Dissolution

Once the drug aerosol has been deposited onto the lung surface, the immediate fate of the drug depends on its physical state. A free, solubilized drug will rapidly diffuse into the epithelial lining fluid and become available for absorption, while a drug deposited as particulate material has to be dissolved prior to absorption and may be subject to clearance by other mechanisms such as mucociliary clearance. The physicochemical properties of inhaled drugs vary considerably, from very hydrophilic to very hydrophobic (log P from −2 for the β2-agonist salbutamol sulfate and 5 for the corticosteroid fluticasone propionate; where P is the octanol-water-partition coefficient) with low aqueous

solubility from sub-microgram per milliliter (0.1 mg/mL fluticasone propionate) to that of hundreds of milligram per milliliter (250 mg/mL for salbutamol sulfate) [67]. For compounds with high aqueous solubility, dissolution is not considered to impact the lung clearance rate, and no or only small differences in pharmacokinetics are expected for different types of formulations unless the regional deposition is substantially different and/or absorption is altered by excipients. The very poorly soluble compounds show fairly rapid onset of absorption followed by sustained absorption over time, which is thought to be dissolution limited. For micronized lipophilic drugs, time of peak concentration has been suggested to correlate with intrinsic solubility [68]. The solubility of a drug depends on the compound, the formulation and physical form of the drug, as well as on the composition of the dissolving media in the lung. The composition of this fluid is mainly water (96%), salts, phospholipids, proteins, and mucins with a pH about 6.6 in healthy individuals [69, 70], while the surface-lining layer in the alveoli is composed of a thin layer of alveolar surfactant (phospholipids and proteins). The lipids and proteins in the lining fluid will increase the wetting, the solubility, and hence the dissolution rate of poorly soluble drugs [66, 71]. Generally, the solubility, and hence dissolution rate, is higher for a less thermodynamically stable material (crystalline polymorph or amorphous form) than that of a molecular high-order crystalline state.

The total liquid volume available for dissolution in the human lung is approximately 10–30 mL. Considering that a clinically relevant dose of fluticasone propionate, as an example of a poorly soluble drug, would require a volume in excess of 1 L for complete dissolution in a stationary system, the liquid volume in the lung is small. The thickness of the lining fluid varies from about 5–10 µm in the conducting airways and gradually decreases distally to about 0.01–0.08 µm in the alveoli [65, 72]. A drug particle deposited in the conducting airways can thus be immersed in the lining fluid while the lining fluid film may be much thinner than the diameter of a deposited drug particle in the alveoli. Consequently, the area of the solid liquid interface between the particles and the fluid is proportional to particle surface area in the conducting airways but limited by the thickness of the fluid in the alveoli. This suggests that particles deposited in the upper airways could dissolve more rapidly than particles deposited in the alveoli. However, other factors such as greater solubility, larger total interfacial surface area, and/or more rapid absorption in the periphery could arguably lead to the opposite. Assessing dissolution in the lungs is very complex as each of the governing parameters will be different in the different regions of the lungs, leading to several different dissolution processes occurring in parallel. By contrast, dissolution in the gastrointestinal tract can be described as a continuous process over a sequence of tanks with different properties [73]. Dissolution in the lungs has not been as systematically explored as dissolution in the gastrointestinal tract; rather the knowledge is derived from a number of diverse studies investigating *in vitro* dissolution models in the environmental and drug research area. Hence, there are presently no established *in vivo* predictive *in vitro* dissolution models for pulmonary formulations, in contrast to the standardized dissolution test methods available for oral solid dosage forms [74-76].

In conclusion, the dissolution rate of formulations or compounds may affect the rate and mode of clearance from the lungs, and therefore influence the pharmacodynamic properties of a drug. As a result of the difficulty in accounting for all the confounding factors, direct evidence is scarce, which limits the ability to predict how variations in formulations that affect solubility and/or dissolution will affect the pharmacokinetic and pharmacodynamic properties of a product.

2.5 Clearance and Defense Mechanisms in the Respiratory Tract

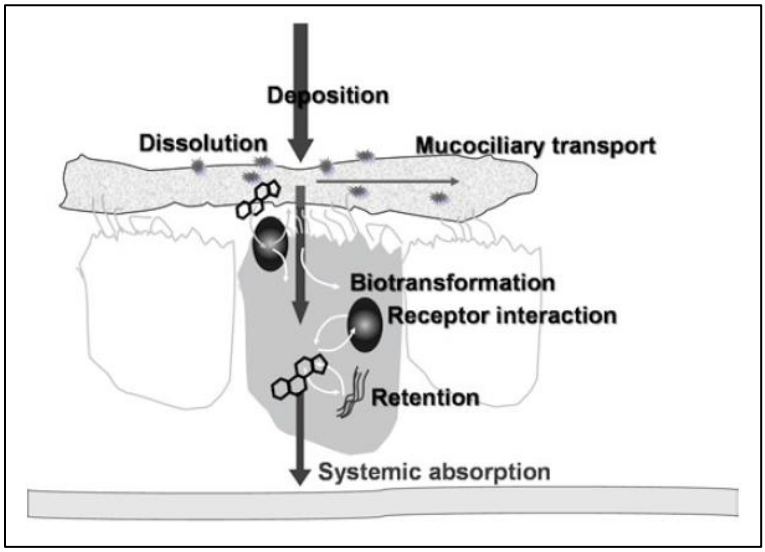

Figure 4: Possible routes of elimination of drug from the lungs. Pulmonary drug metabolism, clearance, and absorption depend on an interplay between factors occurring prior to target interaction (deposition, dissolution, and mucociliary transport), and events competing with target interaction (biotransformation, receptor interaction, and nonspecific retention), and following target interaction (systemic absorption). Adapted from [77].

Once deposited in the lungs, inhaled drugs are either cleared from the lungs, absorbed into the systemic circulation or degraded via drug metabolism. Drug particles deposited in the conducting airways are primarily removed through mucociliary clearance and, to a lesser extent, are absorbed through the airway epithelium into the blood or lymphatic system (Figure 5) [3, 78]. Mucociliary clearance is impaired in lung diseases such as immotile cilia syndrome, bronchiectasis, cystic fibrosis and asthma [79].

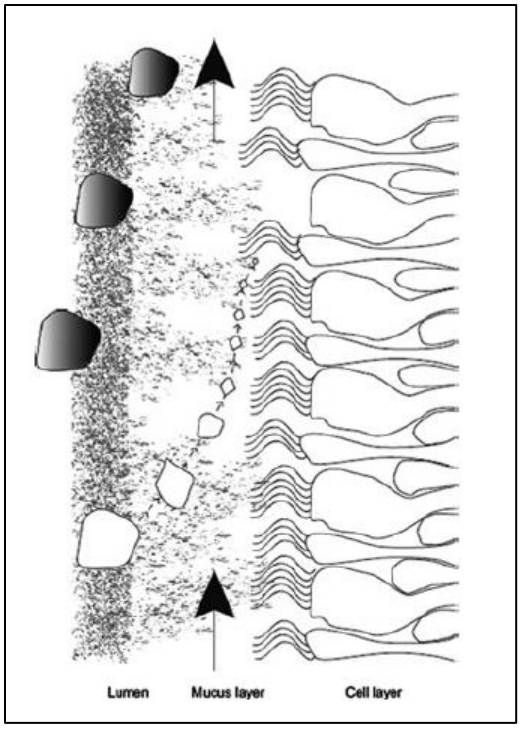

Figure 5: Mucociliary clearance competing with particle dissolution and absorption. Particles deposited on the mucus layer will gradually dissolve and diffuse toward the cell layer where the drug substance eventually may get absorbed. Particles of slowly dissolving compounds will be partly cleared by ciliary action thus reducing the amount absorbed. Adapted from [77].

In addition to mucociliary clearance, soluble particles also can be removed by absorptive mechanisms in the conducting airways [3]. Lipophilic molecules pass easily through the airway epithelium via passive transport. Hydrophilic molecules cross via extracellular pathways, such as tight junctions, or by active transport via endocytosis and exocytosis [80]. From the submucosal region, particles are absorbed into either the systemic circulation, bronchial circulation or lymphatic system.

Drugs deposited in the alveolar region may be phagocytosed and cleared by alveolar macrophages or absorbed into the pulmonary circulation. Alveolar macrophages are the predominant phagocytic cell for the lung defense against inhaled microorganisms, particles and other toxic agents. Macrophages phagocytose insoluble particles that are deposited in the alveolar region and are either cleared by the lymphatic system or moved into the ciliated airways along currents in alveolar fluid and then cleared via the mucociliary escalator [81]. This process can take weeks to months to complete [82]. Soluble drug particles deposited in the alveolar region can be absorbed into the systemic circulation. The rate of protein absorption from the alveoli is size dependent [83].

Very little is known about how the drug-metabolizing activities of the lung affect the concentration and therapeutic efficacy of inhaled drugs. All metabolizing enzymes found in the liver are present to a lesser extent in the lung (CYP450 enzymes are up to 20 times lower than in liver) distributed throughout the conducting airways and alveoli [81, 84-86].

3. Targets of Inhalation Therapy

Inhalation of drugs has been established successfully for a local treatment of lung diseases. A number of marketed products contain a wide range of different drugs for the treatment of asthma or chronic obstructive pulmonary disease (COPD) as the lung diseases with the highest prevalence [87]. Ongoing research is further focusing on the therapy of cystic fibrosis, lung cancer or the vaccination via the lungs since the lung provides the bronchus associated lymphoid tissue that enables mucosal vaccinations [88-90]. Systemically, inhalation therapy is of great interest as active pharmaceutical ingredients (APIs) or proteins delivered to the lungs avoid the hepatic first-pass effect and degradation in the gastro intestinal tract. Some marketed products such as for example inhaled insulin (Exubera® from Pfizer; withdrawn from market in 2007) proved this concept and raised hope for the development of pharmaceutics objected to all kinds of diseases [91, 92].

3.1 Asthma and Chronic Obstructive Pulmonary Disease (COPD)

Asthma is a chronic inflammatory disease of the airways characterized by reversible airway obstruction associated with exacerbations of coughing, wheezing, chest tightness, difficult of breathing, and airway hyper responsiveness [93]. Asthma has a high incidence and is a common disease among children. It is estimated, that over 235 million people worldwide suffer from asthma (2016 estimate by the World Health Organization). Risk factors for developing asthma include inhaling asthma "triggers", such as allergens, tobacco smoke and chemical irritants. Asthma cannot be cured, but appropriate management can control the disorder and enable people to enjoy a good quality of life [94].

Chronic Obstructive Pulmonary Disease (COPD) is characterized by chronic airway obstruction causing progressive loss of lung function. COPD is associated with symptoms of chronic cough and purulent sputum. COPD is strongly related to a history of smoking and is predominantly a disease of older patients [95]. Globally, it is estimated that about 3 million deaths were caused by COPD in 2015 (5% of all deaths worldwide) [94].

Airflow limitations and chronic inflammation are the main characteristics of both asthma and COPD. The most effective treatment is the administration of a medication which acts to reduce and prevent airway constriction and inflammation. The first-line treatments in both asthma and COPD are bronchodilators (short and long acting β2-agonists; SABA, LABA) and anti-inflammatory therapy (inhaled corticosteroids; ICS), which are administered to aid bronchodilation and reduce inflammation [96-98]. Asthma differs from COPD whereas there is a greater reversibility, spontaneously and after treatment with bronchodilators or inhaled corticosteroids. Some patients with asthma have progressive irreversible airway obstruction and therefore have a form of COPD, and some patients may have coexistent asthma and COPD.

Chronic respiratory diseases are not curable, however, various forms of treatment that help dilate major air passages and improve shortness of breath can help control symptoms and increase the quality of life for people with the disease. Therefore, the main goal of respiratory therapy is to improve the patient's quality of live by achieving and maintaining control of symptoms, preventing exacerbations, attaining normal lung function, maintaining normal activity levels, including exercise, and avoiding adverse effects from respiratory medications [99]. The Global Initiative for Asthma (GINA) and the Global Initiative for Chronic Obstructive Lung Disease (GOLD) release guidelines based on the latest state of the art and suggest the drug therapy with respect to disease severity [94, 100].

3.1.1 Bronchodilators

Bronchodilators are used to relieve symptoms of bronchoconstriction [101]. They typically stimulate β-adrenoceptors in the smooth-muscle of the airway, producing smooth-muscle relaxation and bronchodilation (β2-agonists) [102]. Short-acting β2-agonists (SABA) include for example salbutamol and terbutaline, which have a duration of action of approximately 3-4 hours with an onset of action of 15 minutes. Long-acting β2-agonists (LABA), including salmeterol xinafoate (SX) and formoterol fumarate dihydrate (FF), have a duration of action of more than 12 hours and are helpful in controlling chronic asthma [103]. Anticholinergic quaternary ammonium compounds such as tiotropiumbromide or glycopyrroniumbromide are a relatively novel class of bronchodilators [104]. Anticholinergic drugs act as a

competitive blockage of muscarinic cholinergic receptors, inhibiting bronchoconstriction and bronchial hypersecretion leading to airway dilation [105].

3.1.2 Anti-Inflammatory Drugs

Inhaled corticosteroids (ICS) are widely used for the treatment of asthma and COPD. ICS such as budesonide (BUD) and fluticasone propionate (FP) reduce airway inflammation which is the underlying pathophysiological process in both diseases [101].

3.1.3 Combination Therapy

Both the «Global Initiative for Asthma (GINA)» guidelines for the treatment of patients with asthma and the «Global Initiative for Chronic Obstructive Pulmonary Disease (GOLD)» guidelines for COPD patients mention the use of long-acting β2-receptor agonists (LABA) in addition to inhaled corticosteroids (ICS) for patients whose treatment with ICS alone is insufficient. This way, two fundamental processes of the diseases can be addressed: bronchoconstriction and inflammation.

It was found that the co-administration of the two types of drugs in one formulation resulted not only in increased patient convenience, but also showed improved β2-adrenoceptor and glucocorticoid receptor function, as well as a reduction in inflammation and, potentially, remodeling in the airways and lung due to synergistic effects [106]. For example, the co-administration of fluticasone propionate (ICS) and salmeterol xinafoate (LABA) was found to be superior in terms of clinical efficacy to the separate treatment with the two drugs [107]. In a Cochrane meta-analysis of 48 studies (including more than 15’000 patients) [108] the authors concluded that the combination therapy is modestly more effective in reducing the risk of exacerbations requiring oral corticosteroids than a higher dose of inhaled ICS alone. Combination therapy also led to a greater improvement in lung function, symptoms and use of rescue β2-agonists than with a higher dose of inhaled corticosteroids. For children under the age of 12, combination therapy did not contribute to a beneficial treatment, but rather showed a trend towards an increase in adverse effects.

A growing body of evidence suggests that triple therapy with an antimuscarinic agent, a LABA, and an ICS is efficacious in patients with more severe asthma and COPD, such as those with frequent exacerbations. A variety of triple combinations are currently under development [109].

4. Inhaler Devices

Formulations for inhaled medicines require either dry or liquid particles (or agglomerates) with a particle size <5 µm to penetrate the deeper airways as described earlier. For the generation of aerosol particles in the required size range for deep lung deposition, three different types of inhalation devices are currently available on the market. These are nebulizers, pressurized metered dose inhaler (pMDI) and dry powder inhaler (DPI). MDIs are currently the most frequently used system worldwide [110]. Nebulizers and pMDIs will only be introduced briefly in this section as the main focus in this thesis is on DPI formulations.

4.1 Nebulizers

Nebulizer systems are applied for drug solutions or suspensions, which are aerosolized either by air jet (atomization), using vibrating meshes or ultrasonic nebulization to generate droplets of appropriate size. To generate the aerosol from an air-jet nebulizer, compressed air is forced through an orifice over the open end of a capillary tube. The drug solution or suspension is drawn through the capillary by means of momentum transfer. In the nozzle region, shear forces disrupt the liquid into small particles that are entrained by the air towards a baffle. Only the smallest droplets, in the desired size range, are able to follow the streamlines of the air and pass the baffle, whereas larger droplets impact on the baffle and are returned to the liquid reservoir. The emerging aerosol is then inhaled over a mouthpiece or a facemask (Figure 6) [111]. Nearly any soluble drug or mixture of different drugs and in almost any dose can be administered by nebulization, which favors them for infant therapy. Nebulizers can further be used for ventilated patients or those suffering from diseases such as dementia or Alzheimer's since no specific coordination or device actuation is needed. However, such device systems are cost-intensive, bulky and require a consistent power supply, which limits the use in everyday life. Other major disadvantages of nebulizers are their poor deposition efficiency and long inhalation time [112].

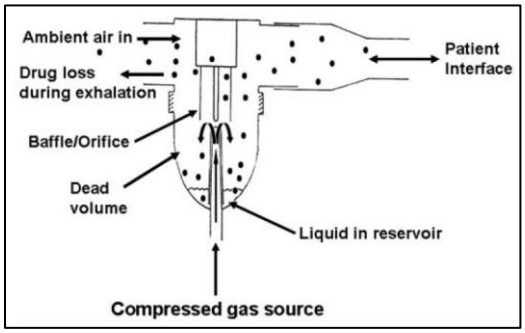

Figure 6: Schematic of a pneumatic jet nebulizer [111].

4.2 Metered Dose Inhalers

Pressurized metered dose inhalers (pMDIs) provide the aerosolization of drug solutions or suspensions upon actuation by the patient. The drugs are therefore either dispersed in a propellant to form a suspension or dissolved in a propellant to build a drug solution [113]. MDIs consist of four basic functional elements: container, metering valve, actuator and mouthpiece (Figure 7). The operation principle of pMDIs is based on a spray-can. A single dose is released from the inhaler device upon actuation forcing the drug solution or suspension through a spray orifice to generate an aerosol. The propellant evaporates rapidly to leave solid particles of adequate size (<5 µm) that are subsequently inhaled by the patient [114]. MDIs have been invented in the 1950s based on chlorofluorocarbon (CFC) propellants that have mostly been replaced by environmentally less harmful hydrofluoroalkanes (HFAs) at current stage [112, 115]. The inhalation maneuver for pMDIs is relevant for deposition efficacy as the hand-lung coordination is of major importance. For infants or elderly people, spacers are applied that help to reduce inhalation variability to improve hand-lung coordination during the inhalation maneuver to overcome oropharynx deposition issues.

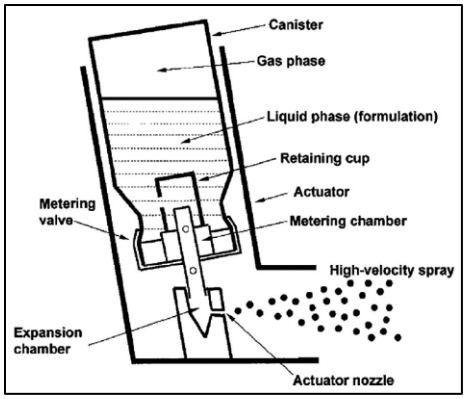

Figure 7: Schematic of a pressurized metered-dose inhaler [111].

Soft mist inhalers (non-pressurized metered dose inhalers) as invented with Boehringer Ingelheim´s Respimat® generate a low velocity spray from aqueous or ethanolic drug solutions that are forced through a nozzle system. Administration of the drug dose is actuated by the patient and independent from the inspiratory effort. Coordination between inhalation and actuation is simplified due to prolonged treatment times based on lower spray velocities, which in turn results in higher respirable fractions and lower dose variability due to less deposition in the oropharynx compared to traditional pMDIs [116, 117].

4.3 Dry Powder Inhaler Containing Adhesive Mixtures

Interest in DPIs for inhalation therapy grew strongly due to their potential to offer CFC-free alternatives to pMDIs [118]. The first single dose dry powder inhaler with a hard gelatin capsule technology (Spinhaler®, 1971) was initially developed for the inhalation of relatively large amounts of drug (50 mg of disodium cromoglycate) [43]. DPI devices combine several advantages such as prolonged long-term stability of drugs, higher drug contents per dose or increased respirable drug fractions compared to pMDIs [115, 119]. Most marketed DPI inhalers work breath-actuated and use the patients inspiratory forces for particle dispersion and deagglomeration, which results in reduced aerosol velocities and lower oropharyngeal drug depositions that in turn induce higher respirable fractions than exhibited for pMDIs [120]. However, despite better results in the overall dispersing mechanism, large differences from patient to patient can be observed with respect to the applied inspiratory airflow. Elderly people, younger children or patients suffering from severe asthma or COPD are known to not sufficiently inhale drugs with a DPI [121]. The aerodynamic performance of dry powder inhaler is a combination of powder properties, inhaler device and the patient's habits.

Most marketed DPIs contain micronized drug blended with larger carrier particles (mainly alpha lactose monohydrate, usually with a particle size distribution of ca. 50-300 µm), which prevents aggregation, assists in metering and helps flow. The dispersion of dry powder aerosols is conducted from a static powder bed. In order to generate the aerosol cloud, the particles have to be moved. Passive inhalers employ the inspiratory flow of the patient for fluidization and aerosol generation. When the patient activates the DPI by inhaling through it, the airflow within the device creates high shear forces and turbulence; and the generation of velocity gradients introduces air into the powder bed. Thus, the static powder blend is fluidized and enters the patient's airways. At the mouthpiece, the drug particles separate from the carrier particles and are carried deep into the lungs while the larger carrier particles impact in the oropharynx and are cleared. Thus, deposition in the lungs is determined by the patient's variable inspiratory airflow [6, 122-124]. One of the main reasons for the low deposition efficiency encountered with DPIs is inadequate drug/carrier separation [125]. Dose uniformity is a challenge in the performance of DPIs. This is a greater concern with powders than with liquids because of the discrete nature of particulates.

The main advantage of utilizing a patient's inspiratory airflow as the main source of energy is that such devices are breath actuated. This avoids the need to synchronize the actuation and inspiration maneuver by the patient. The downside of this approach is that devices currently available show a device-specific airflow resistance, and this often

demands a relatively high inspiratory effort [126] which might be a hurdle for patient populations suffering from obstructive airway diseases such as asthma or COPD, the elderly, or very young patients [127]. The extent of lung deposition is also highly dependent on the individual patient's inspiratory flow rate causing a potential difference in the dose effectively delivered due to this variability [128]. Since often times flow properties of micronized powders are poor, most formulations consist of physical blends of drug particles with larger (30-300 µm) carrier particles such as lactose, to facilitate deagglomeration and powder flow [129].

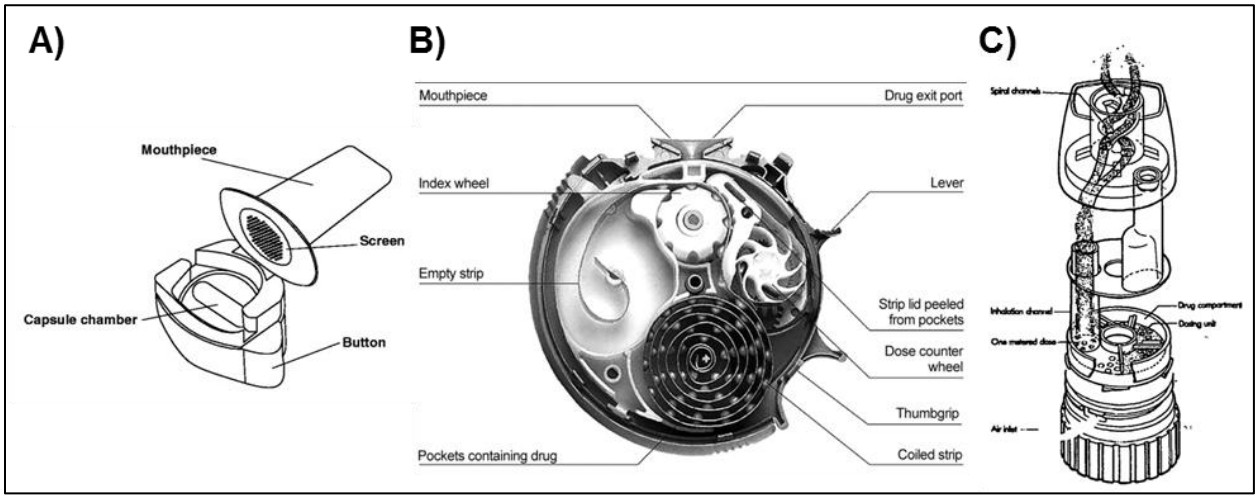

Figure 8: Schematic drawings of marketed example dry powder inhaler systems for adhesive mixtures. A) Capsule based single-dose inhaler (Breezhaler®), B) multi-dose blister inhaler (Diskus®) and C) multi-dose powder reservoir inhaler (Turbuhaler®). Modified from [130-132].

DPIs commonly consist of four functional elements: (1) a powder container, (2) a dosing or metering system, (3) a disintegration principle and a mouthpiece (4). Based on these functional elements, DPIs can be divided into two major groups: single dose and multi-dose inhalers. The multi-dose inhalers are divided in two different types of design: the reservoir systems (such as Turbuhaler®) and the multiple unit-dose inhalers (such as Diskus®). Each of these parts affects the inhaler efficiency with respect to dose dispensing and powder deagglomeration, and thus the amount of drug particles that can theoretically reach the deeper parts of the lung for deposition. A critical factor affecting the reproducibility of doses delivered by multi-dose inhalers is dose metering. While single-dose and multi-unit dose devices use pre-metered powders packed into blisters or capsules, powder bed bulk multi-dose inhalers use powder reservoirs so that the dose to be delivered has to be separated from the bulk material prior to actuation [133]. For both types of devices, suitable powder flow properties are essential, either for accurate dosing or emptying of the single-dose container entirely.

5. Challenges in the Development of Dry Powder Inhaled Formulations

Dry powder inhalers (DPIs) have been providing effective treatments for patients worldwide for more than 50 years. Throughout this period, the fundamental principles of DPI formulation have remained unchanged. A drug is formulated as a powder in which the drug particles are sufficiently small for deposition in the lungs. The powder must be homogeneous on a scale commensurate with the dose, and homogeneity must be preserved during manufacture, shipping, and use. And, for passive DPIs, a patient's inspiratory effort must provide sufficient energy to fluidize and disperse the powder. Although an inhalation product is commonly viewed as a drug and an inhaler, the formulation plays a critical role because it can influence both drug design and inhaler design. For example, most drugs for inhalation are small, highly crystalline molecules. Formulation technologies that relax or remove this constraint will enable development of a greater variety of drugs. Furthermore, formulation of a readily fluidizable and dispersible powder enables simpler device designs, benefitting both the manufacturer and, more importantly, patients. Although the drug substance, the formulated powder, the package, and the device are often times discussed in isolation, inhaled drug product development requires integration of these technologies into the drug product. A holistic approach to dry powder product development requires that engineering of the drug substance and particle be performed with consideration of how the formulated powder will be filled, packaged, and ultimately delivered to a patient's lungs (Figure 9).

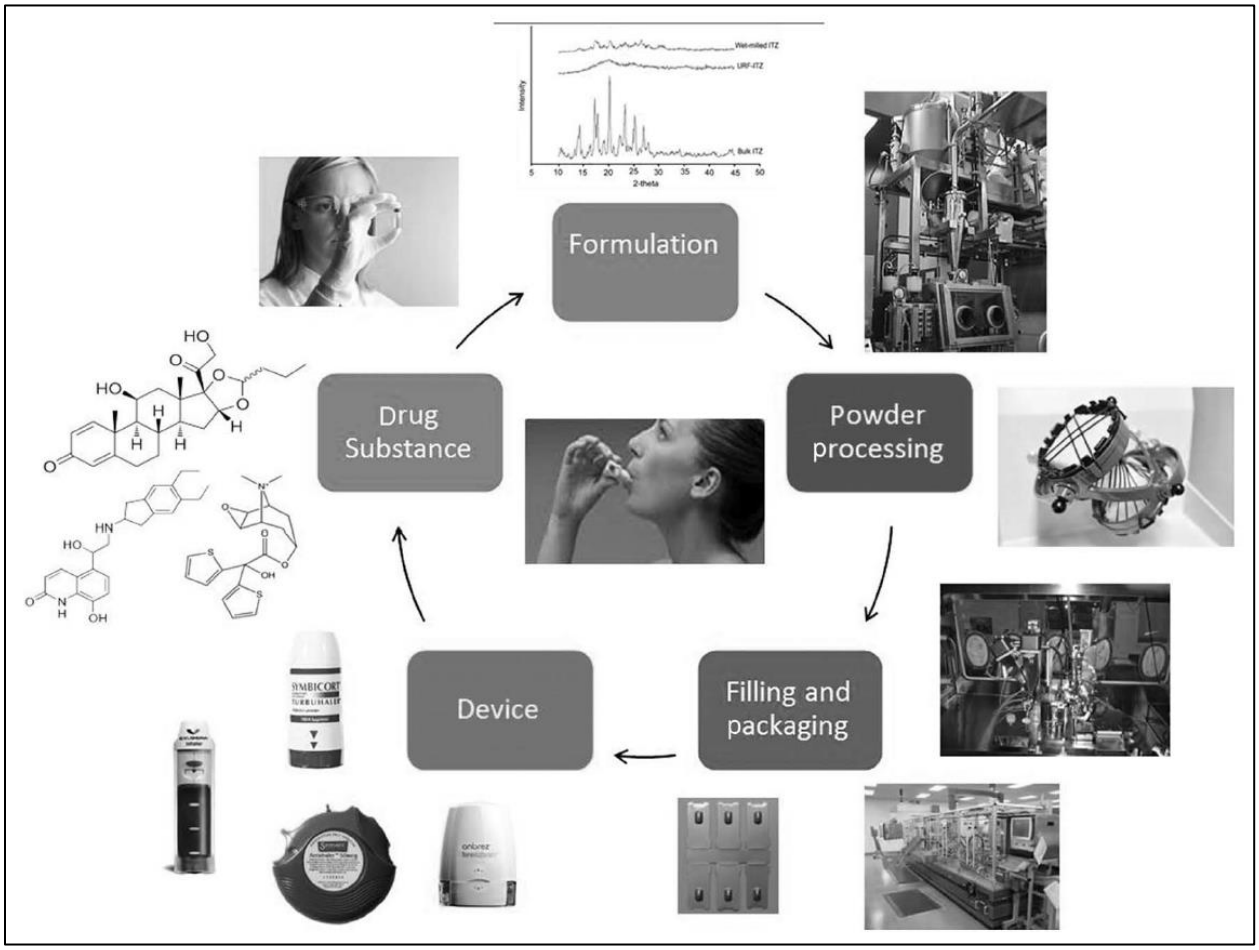

Figure 9: Formulation of a dry powder for inhalation requires integration of multiple technologies into the final drug product. Adapted from Weers et al. [134].

The development of new DPI formulations requires the consideration of a large number of factors that might influence the overall pharmaceutical performance of the new product. Apart from particle properties of all components (drug

and excipients), particle-particle interactions between all components (drug-drug, drug-carrier, carrier-carrier, drug-force control agent, carrier-force control agent) or particle-wall interactions between the formulation and inhaler device, and also the choice of inhaler device with its associated dispersing mechanism is of high importance.

Cohesiveness of drug particles is by far the main challenge in dry powder formulations. A pronounced tendency to build drug agglomerates can be attributed to the sum of cohesion forces (e.g. van der Waals forces, capillary forces or electrostatic forces). Drug bulk flowability is dramatically decreased for those small particles, which renders adequate dosing impossible for pre-metered capsules or blister stripes but also for container based devices.

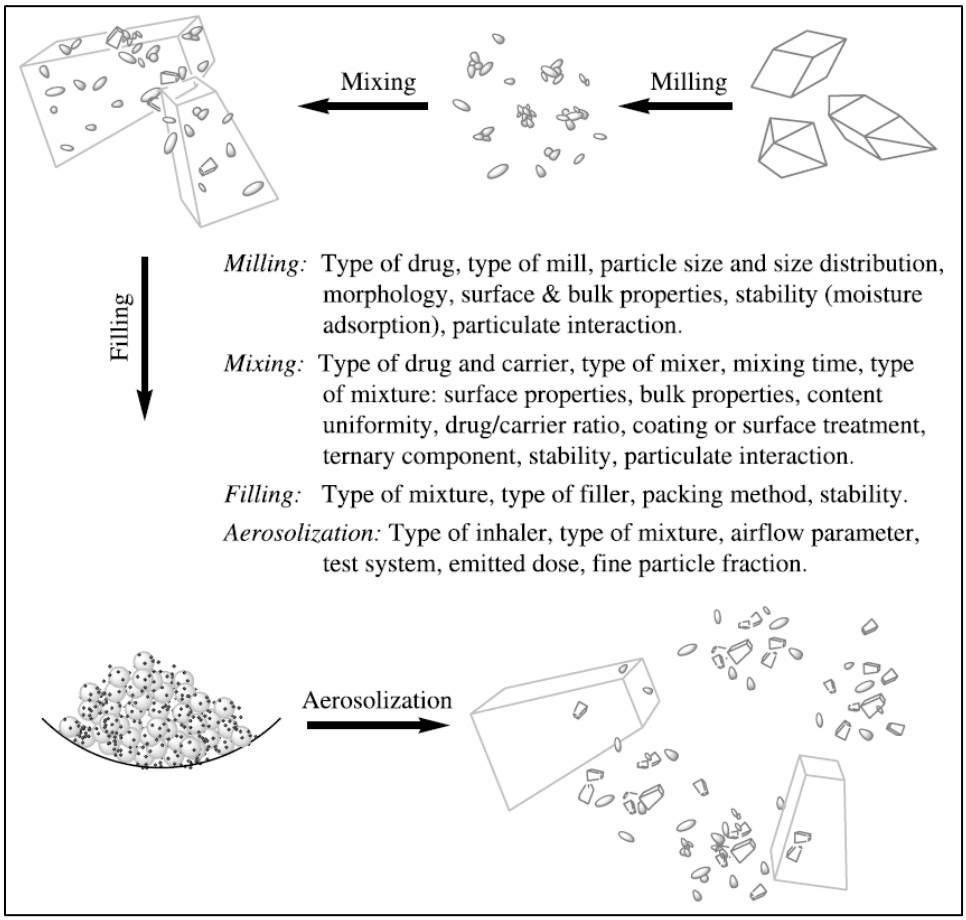

Figure 10: Dry powder inhaler formulation processing and variables associated with each process. Adapted from Xu et al. [135].

A large number of variables and processes can have a significant impact on the aerosol performance of the final DPI product. Figure 10 gives an overview of these variables in particular. Interparticulate interactions occur during milling, mixing, filling and storage and the end point of these coordinating steps of pharmaceutical processes are the beginning of the interparticulate interactions as they pertain to aerosolization performance [135].

6. Pulmonary Drug Delivery through Dry Powder Inhaled Formulations

As a consequence of the need to use drug particles below 5 µm in size, powders composed of such small particles are often strongly cohesive and show very poor flowability. In order to achieve an accurate metering of the desired small quantities, the drugs are either formulated with additional excipients or processed to soft spheres through spheronization. The goal of both is to improve powder flowability, which is essential to allow volumetric filling of the device reservoir or capsules and blister cavities, respectively. The addition of coarse lactose increases the total mass and therefore the metering volume, leading to fewer variations in dosing. Furthermore, the formation of an adhesive mixture improves the flowability significantly, as the used lactose is generally larger in size. A similar effect can be obtained through controlled agglomeration (spheronization) of the micronized drug particles. The increase in agglomerate size accompanies a decrease in interagglomerate forces and, hence, an increase in flowablity [7, 136-138].

In attempts to enhance the efficiency of delivery from DPIs, several techniques have been utilized to prepare particles of active pharmaceutical ingredients (APIs) and carriers (e.g. lactose or mannitol) under controlled conditions. These include simple crystallization techniques, spray-drying, freeze-drying, supercritical fluid technology and engineered carrier particles (adhesive mixtures). In this chapter, techniques like spray-drying, freeze-drying, supercritical fluid technology or crystallization techniques are only briefly introduced as the focus of this thesis is mainly on engineering of carrier based DPI systems (adhesive mixtures).

6.1 Drug Substance

Particle size is a driving factor with respect to deposition site in the lungs. The smaller the aerodynamic diameter of the particles, the deeper they may penetrate into the lungs [139, 140]. Target receptors are not always distributed uniformly throughout the lung. For example, Usmani *et al.* demonstrated in their study that variations to the particle size of inhaled salbutamol lead to a shift in deposition region and patient response [141]. Furthermore, for the treatment of infectious lungs diseases, or for a possible systemic uptake, it may be necessary to administer API particles uniformly throughout different lung regions [3]. Drug particles in the respirable size range can be generated via various processing methods.

6.1.1 Micronization of Drug Substance

The preparation of drug particles for inhalation purposes requires particles with an aerodynamic diameter <5 µm. Several approaches have been introduced to target this size range, but only a few are currently used for marketed products. Micronization techniques published in literature suggest freeze drying, micronization from supercritical fluids or air jet milling to be applicable for drug preparation since all techniques provide particles with a respective size range and appropriate aerodynamic behavior. Micronization by air jet milling is the most commonly used method to prepare drug particles for inhalation purposes. The process is cost-effective and is reliable with regards to batch-to-batch variations.

6.1.2 Air Jet Milling

The crystalline raw materials (drug substance) are introduced into a grinding chamber and grinded with high pressure nozzles using an inert gas. The resulting particle size is determined by the grinding pressure chosen since fine particles are separated based on the inert gas velocity in the chamber. It has been reported in literature that micronized materials can comprise amorphous areas on the surface due to the high-energy input during the micronization process. Drawbacks are not only related to the amorphous areas that might recrystallize during storage due to their high free Gibbs energy but also due to drug particle shape [142, 143]. Most drug substances appear with unevenly shaped particles upon air jet milling, so that particle adhesion to carrier particles cannot be derived from distinct controlled product properties (Figure 11) [144, 145]. It has been reported that approaches using spray drying techniques may overcome such challenges as this technique is known for creating a homogeneous overall particle shape.

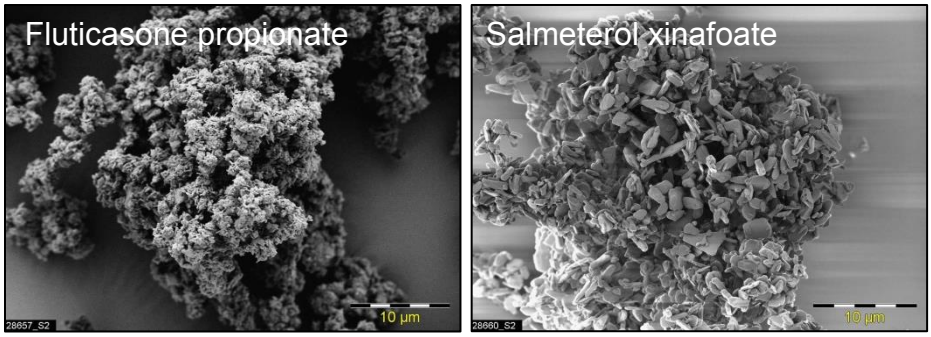

Figure 11: Scanning electron microscopy micrographs of micronized fluticasone propionate and salmeterol xinafoate by air jet milling. Adapted from [146].

6.1.3 Spray Freeze Drying

Spray freeze drying is a two-step process, during which the feed solution is sprayed into a freezing medium (usually liquid nitrogen). Eventually, the liquid nitrogen evaporates and the frozen particles can be lyophilized in a subsequent freeze drying step [147]. The typical process yield is >95% and the obtained particles are of light and porous nature with improved aerosolization characteristics compared with the micronized material [147, 148]. Particle properties can be modified through process adjustments (atomization) or formulation set-up [149, 150]. Generally, this technique can be used to create powders for various treatments, however, the time consuming and very expensive process narrows the use down to high-cost products, such as protein or antibody formulations. Furthermore, the ability to formulate liposomes [148] or encapsulated particles (e.g., in polylactid-co-glycolid; PLGA) [151] opens up a new strategy for formulation design of inhaled therapy. Sufficient stability of the material (protein) to shear, freezing and dehydration stresses is essential. Protein stability may be increased by adding sugars to the liquid feed, which can then build a glassy matrix and protect the protein during the process [152].

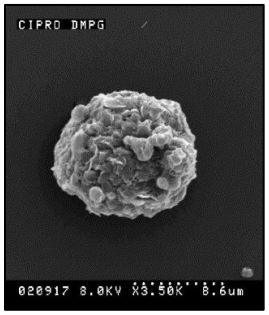

Figure 12: Scanning electron microscopy image (SEM) of a spray-freeze-dried liposomal ciprofloxacin powder particle [148].

6.1.4 Supercritical Fluid Technology

A liquid or gaseous phase can be transferred into its supercritical state by rising the pressure and temperature above their specific critical values. The obtained supercritical fluids (SCF) present an intermediate state that combines properties of both, gaseous (low viscosity) and aqueous (density) phase. Consequently, its often advantageous ability to serve as solvent or antisolvent for several drug substances offers a promising alternative approach for the generation of particles in the respirable size range [153, 154]. Supercritical carbon dioxide (above 31°C, 74 bar) is commonly used due to its low cost and non-toxicity. Particles can be generated mainly via three supercritical fluid techniques: (a) rapid expansion of supercritical solutions (RESS), (b) particles from gas-saturated solutions (PGSS) and (c) supercritical anti-solvent (SAS). Particles generated with such techniques are usually very uniform in size and exhibit a platelet-like morphology. They show improved flowability and smaller cohesive-adhesive interactions compared with jet-milled powders [155]. Such powders possess enhanced dispersion, which in turn generates increased

respirable particle fractions [156], especially at low airflow rates or low aerodynamic turbulent stresses [154, 155]. The generation via SCF precipitation has been shown to be a suitable approach for the production of low (water) soluble-drug and peptide particles. It is still subject of intense research and offers a promising alternative to spray drying and spray freeze drying methods. However, supercritical fluid technology is very complex and expensive set-up has so far limited its use on a routine basis.

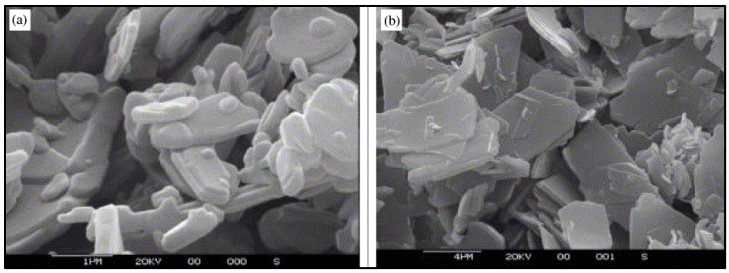

Figure 13: Scanning electron microscopy photographs of micronized salmeterol xinafoate (a) and salmeterol xinafoate produced by precipitation in supercritical CO_2 (b). Adapted from [156].

6.2 Spray Drying

The generation of fine particles using spray drying techniques can help to overcome some of the drawbacks of the micronization process. The technique can be used to generate particles with a narrow size distribution out of a solution, suspension or colloidal dispersion. The obtained particles reveal a more homogenous surface energy distribution and generally show a reduced area of contact between particles, thus leading to increased flowability and dispersion efficiencies (i.e., respirable fractions) [157]. Moreover, particle properties, such as density or morphology, can be customized by changing the process and/or formulation parameters [157-161]. However, spray drying often leads to the generation of amorphous particles. Modifications to the process set-up (introduction of a secondary drying step) [162] or change of material (type of carrier) [158] may be suitable approaches to overcome these challenges. The first inhaled dry powder treatment on the market using a spray dried formulation approach of tobramycin was the TOBI® Podhaler® (PulmoSphere® technology [163]). In this approach, the formulation containing volatile 'blowing agents' is spray-dried to produce large porous particles out of an oil-in-water emulsion. This way, powder flowability and deagglomeration is improved and no additional mixing step is needed. Also, a flow rate-independent, high-dose deposition in the lungs has been demonstrated [163]. Furthermore, spray drying was found to be a suitable technique to produce dry powder protein formulations for inhalation [164], and additional excipients, such as mannitol or trehalose, may be added to prevent possible degradation during processing and storage [165].

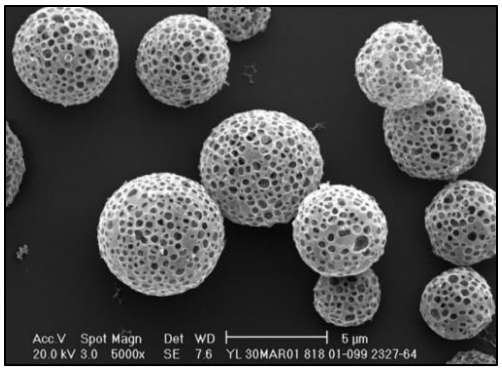

Figure 14: High resolution scanning electron microscopy image (SEM) of a spray dried PulmoSphere® particle of tobramycin. Copyright© Novartis Pharmaceuticals [166].

6.3 Adhesive Mixtures

Most marketed DPI products apply larger carrier particles to improve powder flow and dosing accuracy as well as to overcome the cohesive nature of the micronized APIs. Those single excipient platforms (interactive powder blends) usually consist of coarse carbohydrate particles (alpha lactose monohydrate) and small drug particles, but can be supplemented by fine sugar particles (lactose fines) or force control agents (e. g. magnesium stearate) to become dual excipient platforms (ternary interactive powder blends). Carrier particles, mostly consisting of lactose monohydrate with sizes ranging from ca. 50–300 µm are blended with micronized drug particles (<5 µm) to evenly distribute the drug on the carrier surface. The improved powder flow enables accurate dosing for all kinds of inhaler devices and inspiratory shear forces ensure the detachment of single drug particles or small drug agglomerates from the carrier surface to get entrained by the airflow to penetrate the lungs (Figure 15).

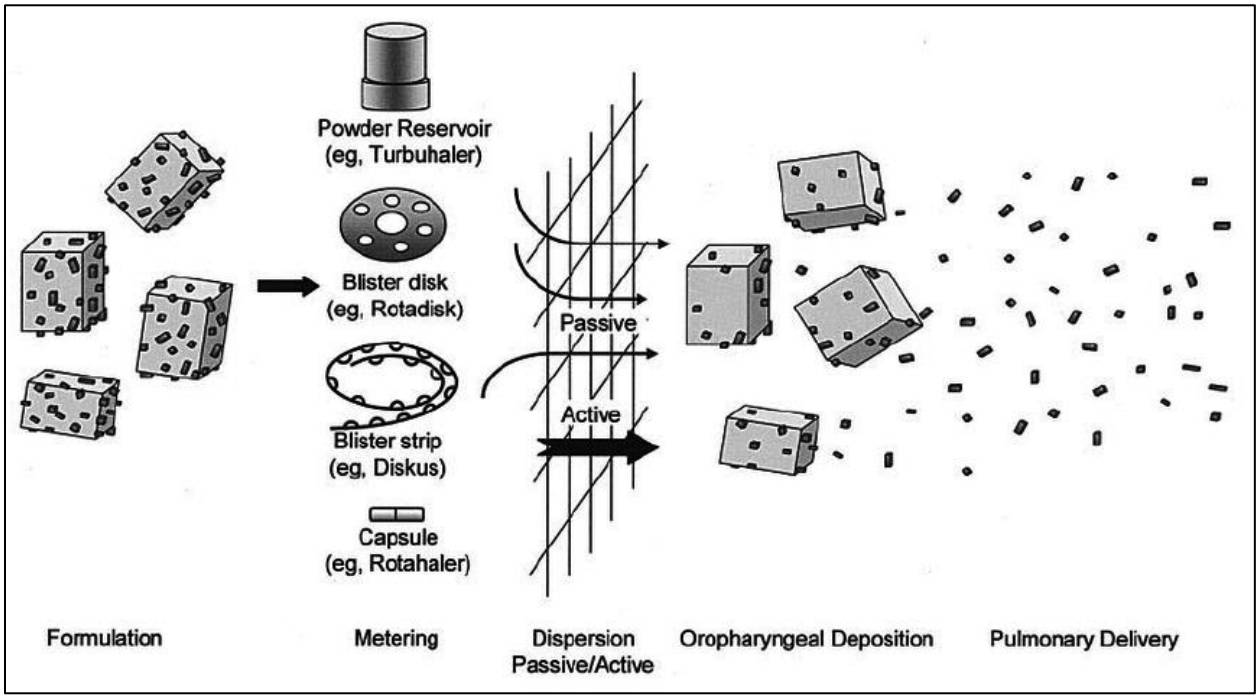

Figure 15: Principle of dry powder inhaler design of adhesive mixtures. The formulation, typically consisting of micronized drug blended with larger carrier particles is dispensed in a metering system. An active or passive dispersion system entrains the particles in the patient's airways where drug particles separate from the carrier and are carried into the lung [6].

6.3.1 Carrier Particles in Adhesive Mixtures

Since micronization of API crystals is still the most commonly used method to obtain particles in a respirable size range, further formulation steps to improve powder flowability are necessary. The aim is to use the adhesive forces of the micronized powder to build up agglomerates that are larger in size and, therefore, exhibit improved powder flowability. For such a process, the control over agglomerate strength (magnitude of interparticulate forces) is fundamental. Agglomerates need to be mechanically stable during storage, filling and dosing. But on the other hand, the thorough dispersion into single particles upon inhalation is essential to achieve reasonable respirable fractions of the drug. Most of the DPIs on the market contain a powder formulation with carrier material. In theory, the micronized drug binds to the host crystal surfaces to form an adhesive mixture [7] and gets separated again as single particles during the inhalation maneuver. Lactose monohydrate is currently the carrier of choice for almost all current DPIs on the market [167]. As carrier material, different sugars or sugar alcohols such as glucose monohydrate, mannitol, sorbitol, maltitol, xylitol, trehalose [168-170] and others have been tested. Nevertheless, Lactose has a well-established safety and stability profile, production is inexpensive, various qualities are easily available on the market, it is less hygroscopic compared with alternative sugars and there is extensive knowledge on its physico-chemical

properties [6]. Lactose is a suitable carrier for the majority of API molecules, however, lactose may not be applicable for formulations containing substances that are incompatible with its reducing sugar function (especially peptides). A typical carrier size ranges between 50 and 300 µm in diameter and the payload of drug is usually between 0.1 and 5% by weight [171, 172]. Deagglomeration efficiency of the mixture is dependent on a large number of factors and their interactions such as for example the flow rate during actuation, particle size of API and carrier or the blending technique. Extensive research has been performed to understand the influence of particle size, particle morphology, physico-chemical properties (e.g., pseudopolymorphs and amorphous contents), dose and environmental conditions on the drug deagglomeration behavior, but the very complex relationships are still not fully understood [7, 171, 173]. A very important factor is the addition of a third component to binary API-carrier mixtures. There are numerous publications on increased respirable API fraction with the addition of a ternary fine (mostly micronized lactose) component [15, 16, 20]. Supposed theories for the aerosol performance enhancement are the saturation of 'active sites' on the carrier surface with excipient fines (regions of increased adhesive forces on the carrier surface are covered with lactose fines before the carrier mixture is blended together with the API), and the formation of drug/fine excipient agglomerates with beneficial overall dispersion properties [7, 174]. It has been proposed that high-energy 'active sites' exist on coarse carrier particles. The addition of ternary fines (e. g. fine lactose or force control agents) preferentially bind and cover these active sites, forcing the drug to weaker binding sites, thus drug particles are more easily liberated from the surface of the carrier particles after actuation [175, 176]. The 'active site' theory has a vague definition that covers a multitude of phenomena including surface irregularities (pores, clefts, cavities, lattice discontinuities), surface rugosity, adhering fines, amorphous spots, water adsorption sites and impurities [7, 177]. The 'soft agglomerates' hypothesis describes that during interactive mixing, drug particles are distributed between the surface of carrier and fines, forming weak agglomerates of drug and fines that can be dispersed easily. The evidence for this mechanism can be found by direct observation of drug and fine agglomerates using scanning electron microscopy. This can be explained by the fact that agglomerates of drug and lactose fines weaken the cohesive interactions between drug particles [7, 178-180].

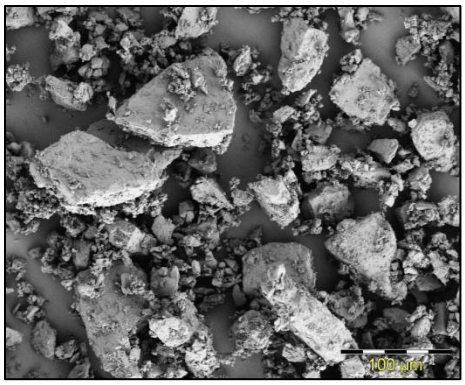

Figure 16: Scanning electron microscope image of alpha lactose monohydrate carrier particles (Respitose® ML001).

6.3.2 Blending of Adhesive Mixtures for Inhalation

The primary goal of a mixing process is the homogeneous distribution of drug particles within the excipient matrix in order to achieve acceptable content uniformity by volumetric dosing or filling. In detail, for an adhesive inhalation mixture, agglomerates of cohesive drug particles (and excipients fines) need to be broken up and distributed evenly across a carrier surface. Once adhered to their host crystals, the segregation tendency of an adhesive mixture is comparably low. Generally, two types of mixers can be utilized to produce such blends: tumbling blenders (low-shear) and high-shear mixers. The extent of energy input of the type of mixer during blending varies significantly and also does the magnitude of the driving diffusive, convective and shear mixing effects. Consequently, appropriate mixing speeds and process times for the production of homogeneous blends differ significantly. Mixing is a dynamic process, and particles may be redistributed across the carrier surfaces, become part of newly formed agglomerates, or may even act as carriers themselves over the time of the mixing process [7, 171]. The mixing efficiency is affected by multiple

factors, such as particle size, size distribution, morphology, density and other physico-chemical properties, and needs to be evaluated carefully for each new drug or component. Blending as a dynamic process leads to the further understanding that despite a homogenous distribution, redistribution effects of the particles may also be of importance for the correct choice of process parameters (mixing time, blending order, energy input, equipment) [181, 182]. Powder homogeneity (or blend uniformity) should not be looked at exclusively for an inhalation product. In particular, high shear mixing exerts a high mechanical stress on the larger carrier particles and may cause breakage or attrition or even changes to the solid state of the drug (small amorphous areas) [15, 17, 183, 184]. In addition, prolonged mixing time leads to a constant redistribution of particles and may hinder the detachment of drug particles from the host crystal surfaces ('press-on forces') [15, 185]. Short mixing times may be advantageous for high-shear formulations compared with low shear tumble mixers, however, research about the influence of differences in energy input on inhalation formulations has just moved into focus in recent years [181, 182, 186].

When mixing powders with different properties, particle sizes and drug-carrier ratios, inadequate mixing can cause poor dose uniformity, something that may not be improved with increasing mixing time. The choice of blender, mixing speed, mixing time, capacity, order of adding the ingredients, and fill level all require optimization, as they are likely to affect the blend homogeneity [181, 187]. In addition, blending conditions can also influence the interparticulate forces, which in turn determine the aerosol performance of a DPI formulation.

6.3.3 Magnesium Stearate as a Performance Enhancer and Force Control Agent in DPI Formulations

Using alpha lactose monohydrate as a single excipient has been the most prevalent excipient strategy in modern commercial DPI products. However, the use of only a single excipient may not always be capable of achieving the required performance efficiency, manufacturability and scale or commercial shelf-life using well understood product and company specific 'carrier' excipient based processing steps. Additionally, the single excipient platform may not be readily adaptable for intellectual property reasons or for the matching the performance of generic DPIs to their originator products [19]. While there has been a considerable number of academic publications and patents concerning the use of additional (ternary) excipients as functional additives for DPIs, their use in approved products has expanded since 2010 with no less than 6 product approvals by 3 companies in global regional markets between 2010 and 2015, all of which contain lactose monohydrate and magnesium stearate (Table 1). The traditional role of magnesium stearate in solid dosage forms has also been expanded to DPIs where its functionality in dual excipient platform formulations has been described in the literature as a 'lubricant', 'force control agent', 'water barrier', 'stabilizer' and 'chemical stabilizer', suggesting multi-functional properties of this excipient in this solid dosage form [19].

Table 1: Approved lactose monohydrate/magnesium stearate dual excipient platform inhalation drug products after 2010. Adapted from [19].

Brand name	Company	Drug	Therapy	Inhaler type/ Dose container	First approved
Foster® NEXThaler®	Chiesi	Beclometasone dipropionate/ formoterol fumarate	Combination, co-formulated	Reservoir	2012
Relvar® Ellipta®/ Breo™ Ellipta™	GSK	Vilanterol trifenatate/ fluticasone furoate	Combination, dual	Dual blister	2013
Anoro® Ellipta®/ Anoro™ Ellipta™	GSK	Umeclidinium bromide/ vilanterol trifenatate	Combination, dual	Dual blister	2013
Incruse® Ellipta®	GSK	Umeclidinium bromide	Mono	Single blister	2014
Seebri® Breezhaler®/ Seebri™ Neohaler®	Novartis	Glycopyrronium bromide	Mono	Capsule, HPMC	2012
Ultibro® Breezhaler®/ Utibron™ Neohaler®	Novartis	Glycopyrronium bromide/ indacaterol maleate	Combination, co-formulated	Capsule, HPMC	2013

The effect of ternary materials on the properties of powders and DPI product performance has been extensively investigated. In terms of the use of magnesium stearate, reports by Staniforth *et al.* had already described the influence of a ternary component, magnesium stearate, on the adhesion of salicylic acid to sucrose [188]. Such observations were further elaborated for the potential advantages of ternary materials for DPI product performance. Scientific

literature is claiming that the addition of magnesium stearate may improve the fine particle dose performance characteristics of DPI formulations [189-191]. The use of such ternary materials in DPI products may now be considered to be a somewhat standard formulation approach. With the increased understanding of the surface and particulate interactions in DPIs [23, 171, 192, 193], the use of such ternary materials in modern DPI development has led to the functionality of such a performance enhancer to also now being widely referred to as a 'force control agent' [14, 23]. Where such additives were added to DPIs their function was used to modify the characteristics of the powder formulation by impacting the inter-particulate interactions, or 'cohesive-adhesive balance' resulting in improved powder properties and aerosolization performance.

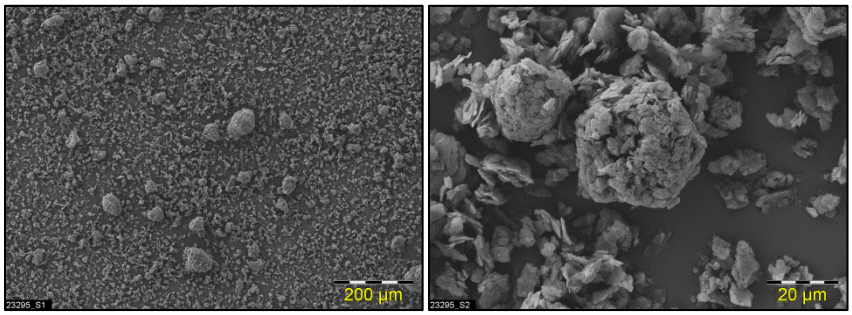

Figure 17: Scanning electron microscope images of magnesium stearate particles (Peter Greven).

Magnesium stearate (Figure 17), a hydrophobic, waxy fatty acid soap, has been used at low concentrations in lactose based formulations (MgSt content typically ca. 0.5%–3%, w/w) to improve drug delivery efficiency. Magnesium stearate can be mixed with the lactose carrier or the drug substance using conventional low-energy blending processes (for example Turbula mixer), or using energy-intensive process ("mechanofusion") designed to produce a thin coating layer on the carrier surface [14, 17, 24, 194]. Guchardi *et al.* proposed that the magnesium stearate increases the cohesive forces between fine and coarse lactose, thereby reducing adhesive forces between the drug and the carrier particles [195]. A variety of other force control agents such as Leucine, Lecithin, Pluronic F-68, Cremophor RH 40, Glyceryl monostearate, Polyethylene glycol 6000 using different application techniques have also been investigated previously [14, 22, 23].

7. Particle Interactions

Efficient drug dispersion of dry powder aerosol particles during aerosolization is governed by several factors that can be described as particle-particle interactions. The energy transferred from inspiratory forces to the powder blend needs to exceed the energy that arises from particle-particle interactions to effectively disperse drug and carrier particles (and eventually fines). The fundamental attractive forces/mechanisms of interaction between drug and carrier particles in DPI formulations can be summarized as van der Waals, electrostatic and capillary forces [7, 196]. Besides the mentioned adhesive and cohesive forces, friction and mechanical interlocking also play important roles in power flow and deaggregation [197]. Mechanical interlocking happens when fine particles are entrapped within the asperities or rough particles 'interlocked' with each other, resulting in increased area of contact and difficulty in separation [8, 198]. Particle aggregation is a result of interparticulate forces. The contribution of each force to the particle aggregation is dependent on numerous factors such as surface morphology, crystallinity, intrinsic material properties (e.g. amorphous content, polymorphism, hydrophilicity, electrical resistivity), and environmental conditions [8]. The drug-to-carrier interparticulate forces must be weak enough to allow substantial drug detachment during the inhalation/aerosolization process while strong enough to maintain powder blend homogeneity. The performance of DPI formulations is therefore a function of the relative magnitudes of cohesive (drug–drug) and adhesive (drug–excipient) interparticulate forces (Figure 18). In general, at normal environmental conditions, the strength of van der Waals forces is about two orders of magnitude higher than electrostatic and capillary forces. However, capillary forces would dominate at condition of high relative humidity [7, 199].

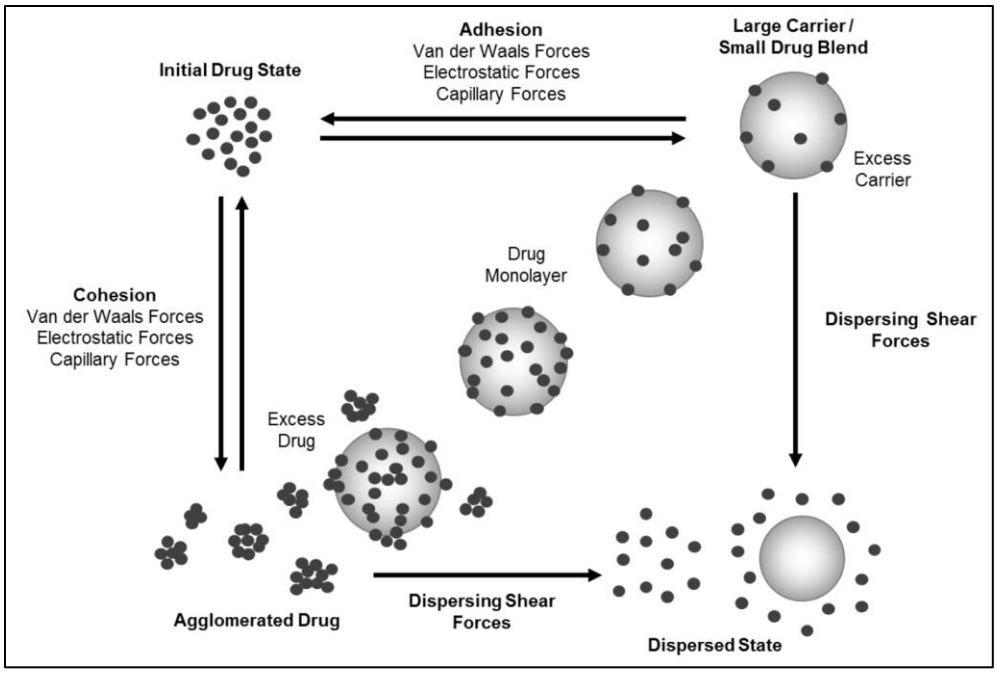

Figure 18: Particle interactions between carrier (large light grey particles) and drug particles (small black particles). Modified from [200].

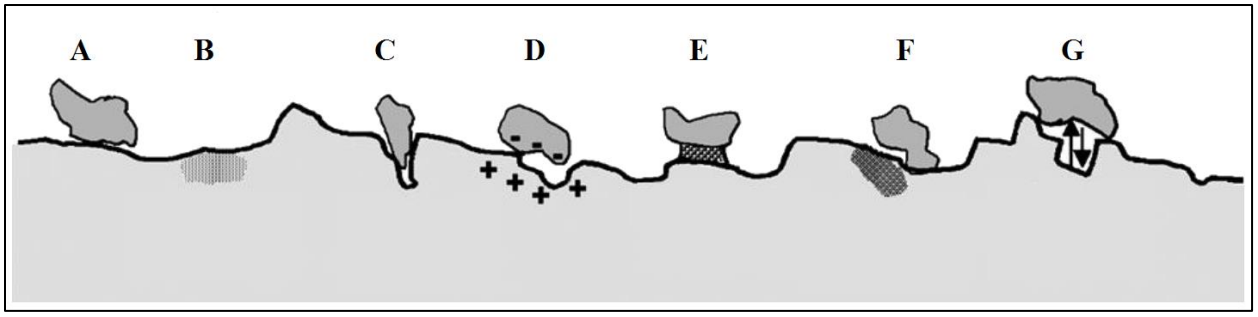

Figure 19: Particle-particle interactions between carrier surface and small particles adhered to the surface. Adapted from Hickey et al. [201].

Van der Waals forces (F_{vdW}) can be defined as below [7]:

$$\boldsymbol{F_{vdW} = \frac{A}{6h^2} * \frac{R_1 R_2}{R_1+R_2} = \frac{AR}{12h^2}\ (R_1 = R_2 = R, \text{for two identical spheres})} \qquad \textbf{Equation 1}$$

$$\boldsymbol{F_{vdW} = \frac{AR}{6h^2}\ (R_1 \ll R_2, \text{for sphere and surface})} \qquad \textbf{Equation 2}$$

Where A is the Hamaker constant (typically ~10^{-19} J) dependent on the molecular properties of the materials, R is the particle radius, and h is the separation distance. As compared to van der Waals forces, gravitational forces are lowered greater when size of drug particles becomes small. Therefore, the dry particles, with size less than 10 μm, become adhesive/cohesive as van der Waals forces become predominant. Van der Waals forces are effective within a separation distance of <100 μm and diminish rapidly with increasing separation distance [7]. Therefore, van der Waals forces are sensitive to the change of particle shape and surface morphology [202]. The magnitude of van der Waals forces is greatly affected by the number of mutual points of contact (coordination number) [8]. The van der Waals forces of particles could be also influenced by surface roughness (such as kinks and defects) by several orders of magnitude. The surface roughness of particles can be evaluated by mathematical models (e.g. Fourier, fractal analysis) in terms of irregular oscillations around a mean value [203]. At distances of typical pharmaceutical powders (e.g. separation distance ~5 nm), van der Waals forces are about 1-2 orders of magnitude stronger than electrostatic forces [8]. The force–distance curves indicate that capillary forces are significantly higher than both van der Waals and electrostatic forces [204], but are produced only at high RH (>65%) [8]. Electrostatic forces are 'long'-range forces compared to van der Waals forces, but decay quickly at high RH [205].

Electrostatic forces (including contact charging, coulombic interaction, and induced charging) can be either attractive or repulsive. Contact charging involves the contact of a charged object to a neutral object until electron transfer reaches equilibrium. The contact charging force (F_c) is defined as [7]:

$$\boldsymbol{F_c = \frac{2\pi q^2}{A}} \qquad \textbf{Equation 3}$$

Where q is charge detachment between two objects, A is the contact area between two objects.

Coulombic interaction occurs in two charged objects. Dependent upon the sign of electrical charge, it could be either attraction or repulsion. Coulombic force (F_q) is expressed as [7]:

$$\boldsymbol{F_q = \frac{q_1 q_2}{4\pi\varepsilon h^2}} \qquad \textbf{Equation 4}$$

Where q_1 and q_2 are the charge on two objects, respectively, ε is the permittivity, and h is the separation distance.

Induced charging appears when a charged object approaches an uncharged object. Induced charging (F_e) is calculated as [7]:

$$F_e = q^2 \left(1 - \frac{h}{(R^2+h^2)^{0.5}}\right) * \frac{1}{16\pi\varepsilon h^2} \qquad \textbf{Equation 5}$$

Where q is the charging on charged object, h is the separation distance, R is the radius of uncharged object, and ε is the permittivity.

The accumulation of electrostatic charge in DPI particles can occur during formulation preparation, where the API is micronized, sieved and blended with coarser carrier particles, and processing, where the formulation is placed in storage, filled into capsules or blister strips or transferred to a powder reservoir device. During these different manufacturing processes as particles are disturbed and agitated they undergo collisions with themselves and the surfaces with which they come in contact with. During such collisions particles will become charged via the mechanism of triboelectrification, which may result in a bipolar charge distribution [206, 207]. Since triboelectrification arises from interactions between surfaces, the composition of equipment surfaces will directly affect charging. This is due to the fact that different materials have different abilities to transfer electrons from or to a surface depending on their relative abilities to donate or accept electrons. Therefore, interactions between particles and different material surfaces may result in different charge levels and polarity in the powder [199]. This can potentially affect the physical structure of the blend and result in processing problems such as adhesion to container surfaces, agglomeration, poor flow behavior, reduced API recovery, loss of content uniformity and manual handling difficulties [208]. The presence of charge on a DPI formulation, which may not decay quickly with time, can result in variable formulation performance. In addition to a build-up of electrostatic charge during manufacturing and processing, DPI formulations also undergo triboelectrification upon aerosolization within an inhaler device. During drug dispersion in a DPI, interactions between the powder, air turbulence and inhaler device surface build up electrostatic charge in the aerosol cloud. Particles deagglomerate from each other, fluidize and enter the air stream. The particles circulate within the internal cavity of the inhaler where they also undergo numerous interparticulate collisions and collisions with the device material. Other factors influencing the extent of electrostatic charge during DPI aerosolization include the deaggregation mechanism of the device, device material, capsule material, physico-chemical and electrical properties of the particles, humidity and temperature [205, 209].

Water can interact with solid particles in three ways: adsorption, capillary condensation, and deliquescence process based on the relative humidity (RH) and the particle characteristics [210]. Capillary forces rise between particles following capillary condensation of water vapor at relatively high humidity (typically RH >65%). The Laplace pressure developed due to the water meniscus formed in the contact zone pulls particles together [8]. An increase in RH can induce profound change in particulate interactions in dry powder aerosol formulation, in most cases, resulting in reduced dispersion efficiency [173, 211-215]. The water vapor at or above critical RH may induce deliquescence followed by solid bridge formation by recrystallization.

The capillary forces (*Fcp*) between two spherical particles are described as [7]:

$$F_{cp} = 4\pi R * \gamma_L cos\theta + 4\pi R * y_{SL} \qquad \textbf{Equation 6}$$

Where R is the harmonic mean of radii of the particles, γ_L is the surface tension of water, γ_{SL} is the solid-liquid interfacial energy, and θ is the contact angle of liquid film to particle surface.

In reality, the forces of interaction between pharmaceutical particles are difficult to characterize or to be controlled due to the heterogeneity in particle composition and physicochemical characteristics. Therefore, it is not practical to consider each of these forces independently. However, key features of inhalation powders that critically influence interparticulate forces should be evaluated, including particle size and size distribution, particle shape, surface

asperities (roughness), crystallinity, particle density, and presence of impurities (Figure 20) [7]. Adhesion or cohesion of dry powder formulations can be indirectly estimated by using inverse gas chromatography (IGC) [136, 216-223] and contact angle [216], and directly measured by using atomic force microscopy (AFM) [193, 224, 225]. However, techniques like AFM only enable the measurement of interpaticulate or surface forces at the individual particle level, but due to the lack of understanding of the actual form of bodies in contact such as the contact area and coordination number, the exact description of the powder formulation and the correlation of measured forces with aerosol performance are still challenging. The efficiency of deaggregation in aerosolization is highly influenced by existing adhesive/cohesive forces in formulations. For instance of carrier-based dry powder formulation for inhalation, strong adhesive (drug-carrier) interaction may prevent the release of respirable drug particles from the surface of carriers, leading into a high deposition in upper airways. Therefore, the adhesive forces between respirable drug particles and large carrier particles strongly influences the delivered dose, since only drug particles separated from carrier surface are able to reach to the deep lungs. Similarly, excessive cohesive forces could lead to agglomerate formation, affecting powder fluidization and dispersion characteristics of formulations [193]. The balance of these forces is very critical in drug-carrier blending, drug particle deaggregation, and drug particle resuspension.

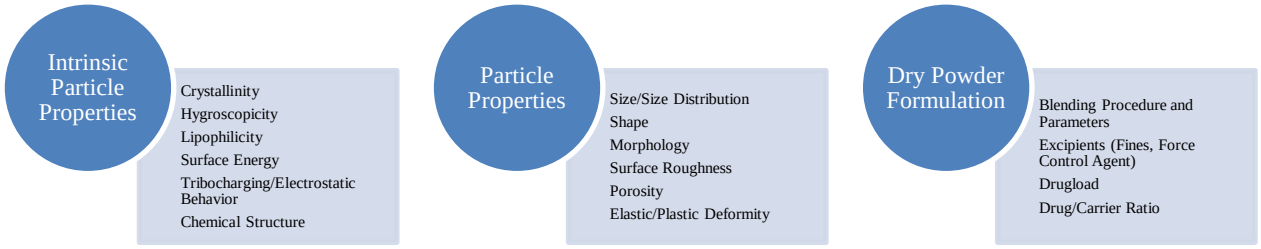

Figure 20: Overview of factors impacting particle interactions in adhesive powder mixtures.

A lot of work has been done earlier to discover dependencies between particle characteristics and performance during inhalation (Figure 20) [12, 21, 139, 219, 226-230]. Impaction analysis as a technique to study the detachment and dispersion of drug particles upon device actuation was introduced to investigate these dependencies and is required by the European Pharmacopoeia (Ph. Eur.) to assess the fine particle dose (FPD) of any formulation applied for inhalation [231].

8. Pharmaceutical Aerosol Testing

The fraction of the aerosol that is deposited in different locations of the respiratory tract is a function of the distribution of the aerodynamic particle size of the particles, the mode of inhalation and the morphology of the respiratory tract [139, 232]. The aerodynamic diameter (D_{ae}) is the most appropriate measure of aerosol particle size because it correlates directly with the efficiency of lung delivery and ultimately the therapeutic effect [6].

For the assessment of the aerodynamic particle size distribution (APSD) of orally inhaled pharmaceutical aerosols, typically the full resolution multi-stage cascade impactor (for example Next Generation Impactor, NGI, Copley Scientific, UK; Figure 21) is regarded in the compendial literature as the "gold standard"-method [233, 234]. Cascade impactors are the instruments of choice for the *in vitro* assessment of delivery efficiency of inhalation products for three reasons. First, by using a specific drug assay, the size distribution of drug particles that is obtained is drug specific, not confounded with any non-drug material that may be in the sample. Second, the size distribution is measured of the total amount of drug that is delivered, rather than of only a sub-sample that may or may not be representative. Third, impactors classify particles according to their aerodynamic diameter. However, it is important to recognize that the cascade impactor is not a lung simulator because of many features, including the geometry at the point of impact, collection surface hardness and coating, and operation at constant flow rate. In particular, collection stages in the impactor do not correspond to any specific deposition sites in the lung [28].

Particles entering a cascade impactor pass through different plates containing nozzles of a well-defined size (cutoff stages). A collection cup located immediately beyond a plate at a defined separation distance deflects the airflow; the inertia of the particles causes them to cross the flow stream, with the result that those with a size greater than a critical value impact on the surface, whereas smaller particles remain airborne [235, 236]. Usually, such instruments size-fractionate the incoming aerosol into eight discrete components by size, depending on the incoming air flowrate. About five stages in an NGI collect particles within a size range from 0-5 μm in aerodynamic diameter [26, 27, 237], where most information is acquired in connection with the respiratory deposition to receptors located in the human airways beyond the oropharynx [238, 239]. Cascade impactor measurements provide direct measures of both mass of active pharmaceutical ingredient (API) and aerodynamic particle size [235].

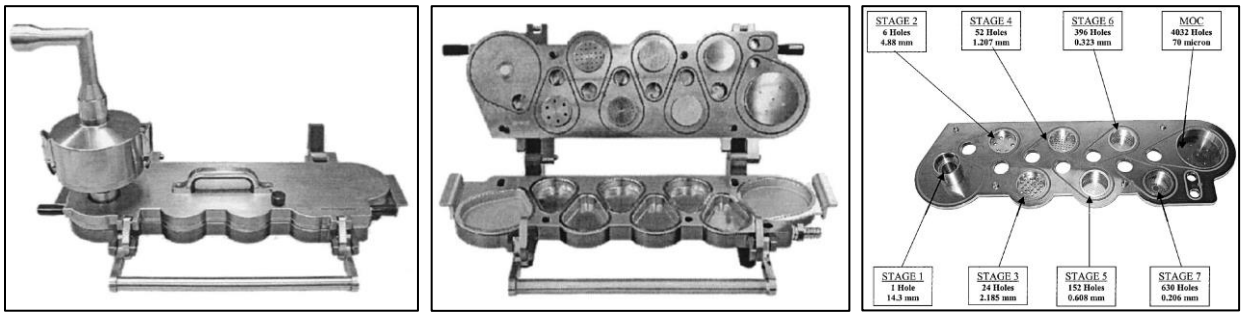

Figure 21: Next Generation Impactor equipped with a pre-separator and USP throat model (left), open NGI with collection cups (middle) and seal body with the eight cutoff stages (right). Adapted from [28].

After generating a size-segregated sample of the particles in a cascade impactor, each size fractionated particle sample is dissolved into a solvent which is then analyzed by high-performance liquid chromatography (HPLC). While highly quantitative for the total concentration of API delivered, this technique does not yield any information regarding the relationships between the various product components (drugs and excipients) within the formulation.

Cascade impaction testing requires mastery of a complex technique before consistent results can be achieved. NGI-testing results in a large demand on resources in terms of laboratory personnel and solvents, the measurements are very time-consuming and results are typically returned days or even weeks later [29, 30]. There is, therefore, an interest in the development of more rapid techniques that might have particular application for routine product quality testing

as well as in product development applications in which many similar impactor measurements are often necessary [31].

An alternative technique for aerosol characterization is single particle aerosol mass spectrometry (SPAMS), which determines both the aerodynamic diameter and the chemical composition of many individual particles in real-time. SPAMS is descended from other single particle characterization techniques.

Rapid single-particle mass spectrometry (RSMS) could determine the chemical composition of each particle at a rate of one per second but only determined the particle size very inaccurately by measuring the light scattering intensity collected by a relative large diameter fiber optic perpendicular to the scattering laser [240]. In 1994, the group of Prather *et al.* improved the RSMS design into aerosol time-of-flight mass spectrometry (ATOFMS), which was the first analytical technique capable of the in-situ simultaneous characterization of both the chemical composition and aerodynamic diameter of individual aerosol particles in real-time [241]. In 1997 the first portable ATOFMS was constructed and commercialized later by TSI Corporation [242]. The system was primarily developed for environmental air sampling and monitoring but its capabilities for characterizing aerosols generated with pMDIs have been demonstrated [37, 243, 244]. Unfortunately, while promising, the limitations the ATOFMS instrument limited the effectiveness of the technique as demonstrated by their specific analytical methods. First, the tendency of the ATOFMS light scattering detection system to saturate at particle concentrations common to pMDIs prevented quantitation of the particle concentrations. Second, the ATOFMS instruments were unable to efficiently analyze particles across the therapeutically relevant size range. While the overall approach of using on-line single particle mass spectrometry was innovative and remains robust, the experiments failed to demonstrate its utility. Therefore, there was the need for a real-time identifier of individual aerosol particles with a higher total particle analysis throughput and that would degrade progressively once the level of saturation is reached at very high particle concentrations. The SPAMS system developed by Lawrence Livermore National Laboratory prevented the light scattering system saturation and added high speed mass spectral acquisition and analysis in real-time [245]. The SPAMS was unique in its ability to acquire mass spectra rapidly and analyze data within seconds. The SPAMS technology was subsequently commercialized by Livermore Instruments Inc. (SPAMS 3.0 in Figure 22) [246].

Figure 22: Livermore Instruments Inc. single particle aerosol mass spectrometer (SPAMS 3.0).

Aerosol-specific mass spectrometers such as the Livermore Instruments Single Particle Aerosol Mass Spectrometer (SPAMS 3.0) are capable of providing both aerodynamic particle size distribution (APSD) profiles of particles and the chemical composition of particle statistical sampling of 10’000 single particles in two minutes. The SPAMS has a very high rate of data acquisition (up to 250 particles per second) compared to earlier aerosol MS designs measuring only 1-4 particles per second. By analyzing a large number of particles and using application-specific chemometric software, the instrument is able to determine mass loadings for particular components (both APIs and excipients), which can be compared to results obtained by NGI. Previous experiments using both aerosol time-of-flight mass spectrometry (ATOFMS) and SPAMS have demonstrated that particle co-associations between drug product components could be evaluated in a way that is inaccessible via impactor techniques [30, 37, 146, 247-249].

9. Outline and Aims of this Thesis

Current marketed dry powder inhalation products generate fine particle fractions (FPF; the proportion of dose containing particles <5 μm in aerodynamic diameter) that are roughly between only 10-50% of the label claim [137, 138]. Several powder inhalation products have recently been marketed of which the carrier-based formulations contain additional excipients such as the 'force control agent' magnesium stearate to obtain a satisfactory dispersion performance (e.g. Foster® NEXThaler®, Seebri® Breezhaler® or Anoro® Ellipta®), even though no evidence can be found in literature about the mechanism of action. Development and production of safer, more efficient and effective dry powder inhalation products is a goal worthwhile of striving towards. Understanding the dispersion performance of adhesive mixtures is pivotal in this respect. Therefore, the aim of this thesis is to improve the understanding of the relationships between particle interactions, the dispersion performance, formulation variables and inhalation variables of adhesive mixtures for inhalation.

This thesis focuses on the preparation of dry powder inhaled formulations and the investigation of the complex mechanisms that affect the dispersion of drug particles during aerosolization. Despite several years of research on particle interactions that occur in carrier-based systems, there are still essential issues that remain unclear (Figure 23). There is only a limited understanding of how blending processes affect material properties and the resulting distribution of drug and excipient in the final dosage form, as well as its final aerosol performance. A great number of variables are considered relevant to the interfacial forces in adhesive mixtures, but their effects have mostly been investigated individually, without taking account of the influence they may have on each other. Currently, there is a strong focus on exploring techniques for the characterization of drug and carrier surface properties that are believed to have an influence on the interparticulate forces in adhesive mixtures. For a number of surface properties it may be questioned whether they are really the key parameters to investigate [134, 136, 171, 177].

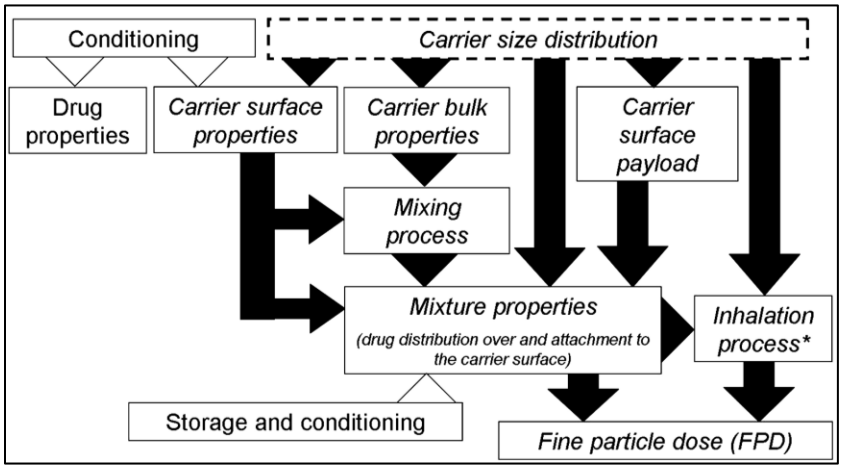

Figure 23: Scheme of variables in lactose carrier-based formulations showing the effects linked to a change of *in vitro* aerosol performance. Modified from [171].

Advanced powder characterization techniques such as single particle aerosol mass spectrometry (SPAMS) and time-of-flight secondary ion mass spectrometry (ToF-SIMS) were employed to improve the mechanistic understanding of particle interactions, drug detachment and dispersion during impaction analysis. ToF-SIMS is one of the most sensitive surface composition analysis techniques, with elemental detection limits ranging from parts per million to parts per billion. It can elucidate the microscopic structure of powders in form of an image. An introduction into ToF-SIMS measurements of dry powder carrier particles for inhalation is given in Jetzer *et al.* (Chapter 2) [146].

The overall objective of this PhD thesis was to improve the understanding of physical processes that determine the aerosol performance of dry powder inhalation drug product formulations and also to further develop the SPAMS analytical technique for testing pharmaceutical aerosols.

The objectives can be grouped in the following areas:

- Further development of the SPAMS analytical technique and application of the technique in the investigation of complex dry powder inhaled drug products. The focus was on the validation of the aerosol performance data such as aerodynamic particle size distribution (APSD) and fine particle fraction (FPF) generated with SPAMS and the evaluation of the suitability of the method to identify and quantify compound/compound interactions of different active ingredients in dry powder blends.
- Investigation of compound/compound (and/or excipient) interactions in dry powder blends (e.g. interactions between two APIs as a fixed dose combination in dry powder blends that affect aerosol performance of the DPI drug products when compared with the monotherapy dry powder blends). Previous experiments using the SPAMS technique have demonstrated that particle co-associations between drug product components can be evaluated in a way that is inaccessible via traditional impactor techniques
- The functionalizing of lactose carriers with a 'force control agent' (magnesium stearate) was studied by using different blending techniques. The parameters involved in this carrier modification were elucidated, e.g. the degree of carrier surface coverage/distribution with MgSt, the amount of particle co-association, changes in the excipient carrier's particle size distribution, physical characteristics changing on the microscopic level and their impact on *in vitro* aerosol performance. This may enable more rationale formulation process development and allow better control of DPI drug product critical quality attributes.
- Identification and study of model systems where the underlying physical processes determining the aerosol performance (APSD and FPF) of dry powder inhalation drug products are not fully understood at the mechanistic level.
- Conditioning processes of different dry powder inhaled formulations were studied. Exposure of the DPI capsules to specific environmental conditions such as elevated temperature or elevated humidity can alter the *in vitro* aerosol performance characteristics of a DPI drug product. The understanding of the root cause is limited and it is not clear if dissipation of electrostatic charge, a change in triboelectrification behavior or agglomeration of the APIs is the main root cause. Differences in conditioning behavior of different APIs was investigated. Several ways to measure electrostatic charge before, during and after conditioning as well as during DPI aerosolization were explored.

CHAPTER 2: PEER-REVIEWED PUBLICATIONS

1. Comparison of Different Aerodynamic Sizing Techniques for the Evaluation of Metered Dose and Dry Powder Inhalers

Jetzer et al. Respiratory Drug Delivery 2016. Volume 3, 2016 459-462

Summary

For the evaluation of the aerosol performance of inhaled pharmaceutical products, the current state of the art is the use of the next generation impactor (NGI, Copley Scientific, UK) [250], typically with chemical analysis using high performance liquid chromatography (HPLC), to characterize the aerodynamic particle size distribution (APSD). In this study, we compare the APSD profile of single particle aerosol mass spectrometry (SPAMS) to the aerodynamic particle sizer ((APS) TSI Incorporated, MN, USA) and NGI when tested with a pMDI and DPI. In addition, we evaluate the transmission efficiency of SPAMS as well as potential size bias of APSD measurements that might result from a size dependent transmission profile.

Introduction

SPAMS can be utilized for APSD measurements of pharmaceutical aerosols [30]. SPAMS data was found to correlate well with the fine particle mass (FPM) data obtained by NGI for Onbrez® and Arcapta™ dry powder inhalers (DPIs) as a function of dosage strength [251]. In this study, APSD data was obtained from APS and NGI to compare to SPAMS results. Since SPAMS samples a small fraction of the total emitted dose uniform transmission is required to prevent size bias. Therefore, this study also evaluates the transmission efficiency of particles of indacaterol maleate in a metered dose inhaler (pMDI) and DPI formulations in the SPAMS in order to better characterize the performance of the inlet interface and to determine if the results are closer to established standard aerodynamic sizing techniques.

Materials and Methods

A Livermore Instruments SPAMS 3.0 was used for this study. The experimental setup of the SPAMS instrument and sample testing has been described earlier by Morrical *et al.* [30]. For DPI formulations, a pre-separator was mounted between the USP throat and reservoir. In addition to the SPAMS, an APS was used with a single-stage impactor to take a size-segregated sample at a predefined air flow at 28.3 L/min. The NGI testing was conducted with a flow rate of 90 L/min for 2.7 seconds. The powder deposited on each stage was recovered via solvent extraction and analyzed with reverse-phased high performance liquid chromotography (HPLC). Indacaterol maleate DPI formulations (Arcapta™ Neohaler™ and Onbrez® Breezhaler®) and a proprietary indacaterol maleate pMDI suspension formulations were tested in the comparative studies.

Results

A comparison of APSD results from SPAMS for indacaterol maleate pMDI formulations with APS is shown in Figure 24A. While the profiles are similar, there are differences observed in the range from 2-3 μm where the SPAMS results are lower than those from the APS. But when comparing DPI profiles measured by APS and SPAMS technique (Figure 24B), it can be seen that there is a larger difference in the size distribution profile. DPI formulations are composed mostly of lactose carrier particles and the APS does not discriminate between lactose and API. The APS measurement indicates that there are more large particles > 6.7 μm, and also particles < 3.8 μm present, which are not counted by SPAMS because lactose is not ionized.

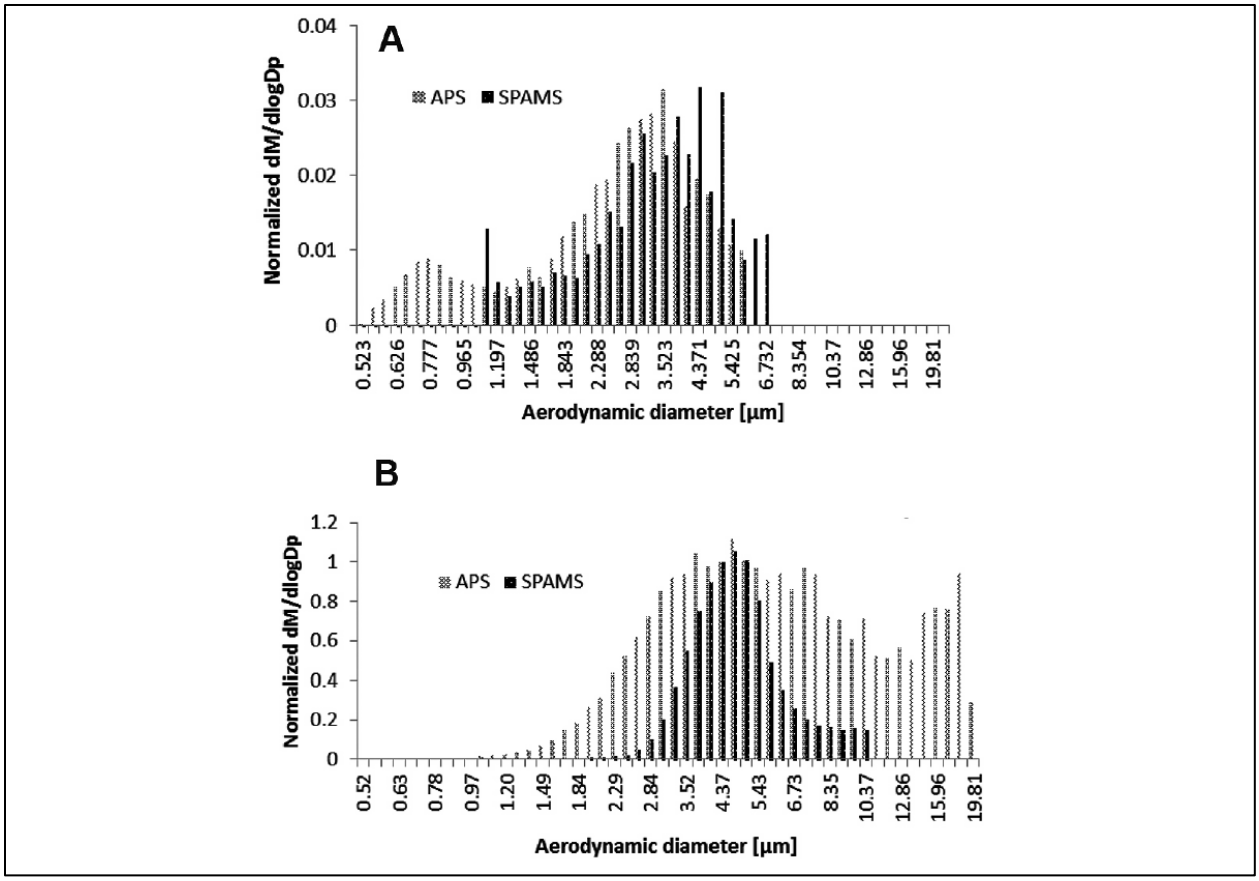

Figure 24: A) pMDI actuation with APS and calculated from SPAMS data. B) DPI actuation (Onbrez®) with APS and calculated from SPAMS data.

Table 2: Aerodynamic diameter estimated from indacaterol maleate pMDI and DPI formulations for both aerodynamic sizing methods APS and SPAMS at 28.3 L/min.

	pMDI Indacaterol maleate		DPI 150 mcg Indacaterol maleate (Onbrez®)	
	APS (µm)	SPAMS (µm)	APS (µm)	SPAMS (µm)
Median	2.8	2.6	2.3	3.9
Mean	2.9	2.9	2.7	4.1
Geom. Mean	3.1	2.3	2.3	4.0
SD	1.8	0.3	1.8	1.1

As can be seen in Table 2, there is good agreement overall between the APS and SPAMS for pMDI, while there is not a good agreement between APS and SPAMS for the DPI measurement. The results above indicate that the SPAMS does not have the same transmission efficiency for particles of all sizes. There are two potential factors that may cause this bias in the SPAMS APSD analysis: the sampling chamber and differences in the particle inlet interface. These two factors can result in differences in the settling velocity and deposition of larger particles and most likely have significantly different particle transmission efficiencies. SPAMS was also compared to the widely used NGI to see if it was possible to compare the results of a particle counting technique to one that obtains mass directly. In order to do this, the counted particles were summed into different size "bins" that match the impactor cup size cutoffs in the NGI at 90 L/min. Then the total mass of API particles was calculated for each size bin assuming unity density and a spherical shape. The mass was normalized to give the same relative mass scale of the NGI results. When comparing

NGI results with SPAMS data for DPI, it is observed that at the 6.48 and 3.61 µm stages results match well, but there is a consistent difference with the next stage (2.3 µm), where SPAMS results appear to be lower than these from NGI (Figure 25). This result mirrors what was observed for the pMDI results when comparing the SPAMS with the APS (Figure 24) and suggests that there is a significantly lower transmission of particles in this size range than would be expected from other sizing techniques. It is important to note that for the pMDI APS/SPAMS experiment only pure indacterol maleate particles were used and for the DPI NGI/SPAMS experiment the particles plotted are chemically specific to indacaterol maleate, so the interference with lactose observed in the DPI APS/SPAMS experiment is negated.

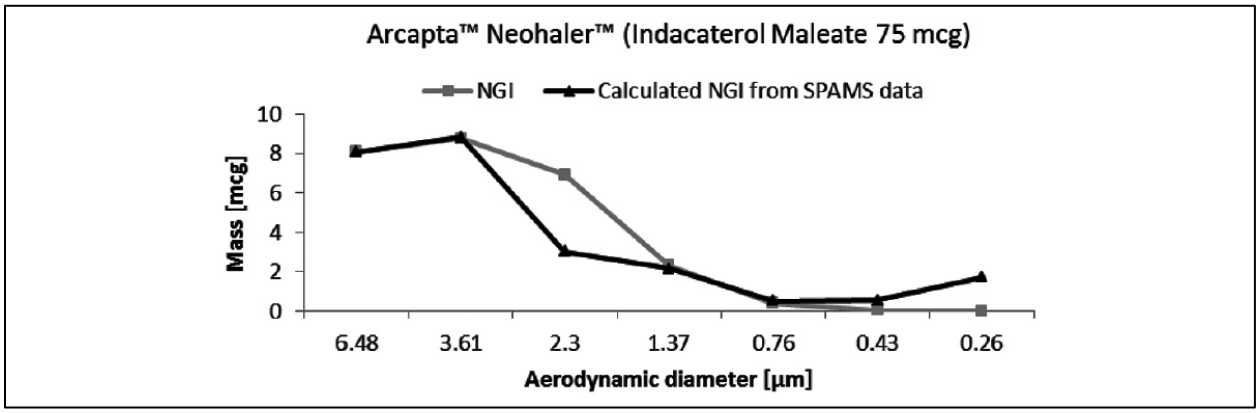

Figure 25: Indacaterol maleate DPI NGI data compared to calculated SPAMS data.

A potential reason for this is caused by the SPAMS interface that appears to have a discontinuity in the transmission of particles with the main gap centered around 2.3 µm, which will likely result in an underestimate of FPM (particles < 5 µm). Figure 26 shows the transmission efficiency of the SPAMS interface using calibration latex spheres. In Figure 26, the expected number of particles is the total number of particles introduced into the system and real counts is the actual number counted by the SPAMS. As can be seen, the transmission of particles in the range from 2-3 µm appears to be lower than for particles with a size of 1 or 6 µm. This again confirms what was observed in the previous experiments.

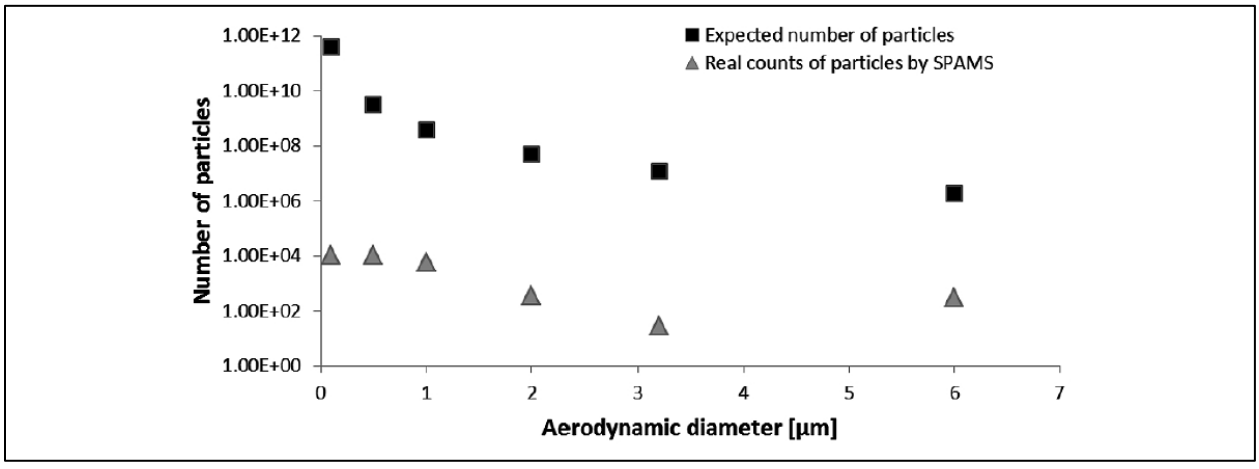

Figure 26: Real number of particle counts of a SPAMS compared with calculated expected number of counts.

Conclusions

It was demonstrated that the SPAMS can generate useful APSD measurements with both pMDI and DPI. However, there is still lack of a good correlation to date because of a consistent anomaly of particle transmission in the SPAMS. More work characterizing the particle interface is needed, particularly in the region of 2-3 μm, based on observations when comparing SPAMS with APS and NGI for the characterization of particles.

2. Particle Interactions of Fluticasone Propionate and Salmeterol Xinafoate detected with Single Particle Aerosol Mass Spectrometry (SPAMS)

Jetzer et al. International Journal of Pharmaceutics (2017) 532:218-228

Abstract

Particle co-associations between the active pharmaceutical ingredients fluticasone propionate and salmeterol xinafoate were examined in dry powder inhaled (DPI) and metered dose inhaled (MDI) combination products. Single Particle Aerosol Mass Spectrometry was used to investigate the particle interactions in Advair Diskus® (500/50 mcg) and Seretide® (125/25 mcg). A simple rules tree was used to identify each compound, either alone or co-associated at the level of the individual particle, using unique marker peaks in the mass spectra for the identification of each drug. High levels of drug particle co-association (fluticasone-salmeterol) were observed in the aerosols emitted from Advair Diskus® and Seretide®. The majority of the detected salmeterol particles were found to be in co-association with fluticasone in both tested devices. Another significant finding was that rather coarse fluticasone particles (in DPI) and fine salmeterol particles (both MDI and DPI) were forming the particle co-associations.

Introduction

The two most common chronic respiratory diseases are asthma and chronic obstructive pulmonary disease (COPD). According to the 2016 estimate by the World Health Organization, 235 million people currently suffer from asthma and over 3 million people die each year from COPD, accounting for an estimated 6% of all deaths worldwide [252]. Two major classes of drugs widely used in the treatment of these diseases are inhaled corticosteroids (ICS) and beta2-agonists (LABA), both preferably being delivered directly to the lungs by inhalation. The active pharmaceutical ingredients (APIs) are typically administered to patients via either a pressurized metered dose inhaler (pMDI) or a dry powder inhaler (DPI) device. The two classes of compounds have very different modes of action, targeting different aspects of the respiratory disease process (airway inflammation in the case of ICS and smooth muscle dysfunction in the case of LABA). Thus these two classes of drugs in combination address complementary aspects of the disease pathophysiology of asthma that neither drug class is able to achieve alone [101].

Clinically, prescribing both classes of drugs has become a method of taking advantage of their complementarity. There is, however, significant clinical and in-vitro evidence to suggest that the co-association of ICS and LABA at the level of the single administered aerosol particle leads to a synergetic effect with improved clinical outcomes. Studies have shown increasing evidence of complementary and synergistic effects of LABA and ICS, interacting at the molecular receptor [253-257] and cellular [258-261] level. Previous studies have ruled out systemic pharmacokinetic or pharmacodynamic interactions between inhaled fluticasone propionate (FP) and salmeterol xinafoate (SX) when administered in combination [262]. One postulated reason for this synergetic increase in pharmacological efficacy is the co-association of APIs at the point of deposition within the lung [38, 263]. Specifically, salmeterol was observed to retard the transport of fluticasone across cell cultures of lung epithelial tissues, prolonging its localized anti-inflammatory effects [38]. The co-administration of the two drugs is expected to improve the likelihood of the two APIs being delivered to the same location in adequate concentrations, maximizing the likelihood of these synergetic effects [107]. Partly for patient convenience and partly to take advantage of this synergetic phenomenon, "combination products" have been introduced which contain both APIs in a single formulation administered simultaneously by a single device.

Interestingly, the presence of one API in these products was demonstrated to affect the delivered dose of the other that reached the lung [107, 263-266] but that phenomenon was ruled out as the cause of the improved clinical outcomes for the combination products versus the administration of two single API products [267, 268], indicating that the postulated synergetic phenomenon is, indeed, taking place *in vivo*. Previously, it was demonstrated that there is some

affinity between fluticasone and salmeterol in solution, indicating that they may also be co-associated at the level of the individual administered aerosol particle [269]. Attempts have been made to observe particle co-associations with Raman microscopy by Theophilus *et al* [270]. Determining the chemical composition of individual particles with a technique such as single particle aerosol mass spectrometry (SPAMS) should yield more definitive data. Preliminary runs with the SPAMS technique have already shown promising results [30].

The current pharmacopoeial standard method for determining the aerodynamic particle size distribution (APSD) of drugs delivered from inhaled pharmaceutical products is to generate a size-segregated sample of the particles in a cascade impactor, typically the recently developed Next Generation Impactor (NGI) [26-28], followed by dissolving of each size-fractionated particle sample into a solvent which is then analyzed by high-performance liquid chromatography (HPLC). While highly quantitative for the total concentration of API delivered, this technique does not yield any information regarding the relationships between the various product components (API(s), excipients) within the formulation.

Mass spectrometry based aerosol analytical techniques have been undergoing continuous development since the 1970s [24, 32, 33, 271, 272]. Aerosol-specific mass spectrometers such as the Livermore Instruments SPAMS 3.0 are capable of providing both aerodynamic particle size distribution (APSD) profiles of particles and the chemical composition of particle statistical sampling of 10,000 single particles in two minutes.

The SPAMS is descended from an earlier instrument, the Aerosol Time-of-Flight Mass Spectrometer, that was also capable of determining the aerodynamic size and chemical composition for individual particles in real-time, first reported by Prather *et al* in 1994 [32]. This instrument was initially developed for environmental and air pollution studies but was applied to the analysis of inhaled pharmaceutical products soon after its invention [37, 237].

Recently, SPAMS was developed as a more advanced instrument capable of characterizing single aerosol particles, providing both the aerodynamic diameter and chemical composition of each measured particle. The SPAMS has a very high rate of data acquisition (up to 250 particles per second) compared to earlier aerosol MS designs measuring only 1-4 particles per second. By analyzing a large number of particles and using application-specific chemometric software, the instrument is able to determine mass loadings for particular components (both APIs and excipients), which can be compared to results obtained by NGI. Previous experiments using both ATOFMS and SPAMS have demonstrated that particle co-associations between drug product components could be evaluated in a way that is inaccessible via impactor techniques [30, 37, 247]. A deeper understanding about product performance and interactions can be gained, providing valuable information for combination products. If a higher degree of co-associated particles would indeed be beneficial for patients, product developers could design formulations with a greater degree of co-associated API. This makes the SPAMS technique an attractive alternative in the field of pharmaceutical aerosol analysis (complementary to NGI/HPLC-analysis).

The objective of these experiments was to determine the degree of particle co-associations between fluticasone and salmeterol and the mass distributions of the particles containing the two different APIs across multiple size ranges in real-time. Axotide® and Serevent®, each a single API product containing fluticasone and salmeterol, respectively, were used to identify unique marker peaks from mass spectral signals of each API.

Materials and Methods

In the current study, commercially available inhalation drug products containing fluticasone propionate (FP) and salmeterol xinafoate (SX) were investigated using a SPAMS 3.0. Table 3 lists the products used in this study. The experimental matrix consisted of both pMDI and DPI fluticasone mono, salmeterol mono and fluticasone-salmeterol combination formulations.

Table 3: Overview of DPI and pMDI product groups used in this study.

Brand Name	Inhaler	API/Dosage Strength
Advair Diskus®	DPI	Fluticasone Propionate / Salmeterol Xinafoate 500/50 mcg
Axotide Diskus®	DPI	Fluticasone Propionate 500 mcg
Serevent Diskus®	DPI	Salmeterol Xinafoate 50 mcg
Seretide®	pMDI	Fluticasone Propionate / Salmeterol Xinafoate 125/25 mcg
Axotide®	pMDI	Fluticasone Propionate 125 mcg
Serevent®	pMDI	Salmeterol Xinafoate 25 mcg

Chemical structures for fluticasone and salmeterol are given in Table 4.

Table 4: The structures of fluticasone propionate and salmeterol xinafoate.

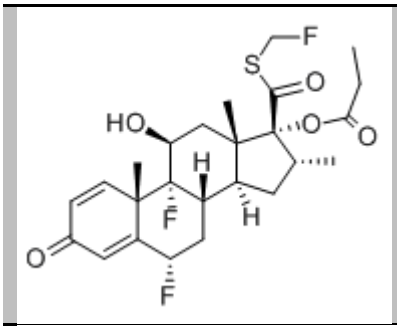

Fluticasone Propionate (FP)
$C_{25}H_{31}F_3O_5S$
MW 500 g/mol

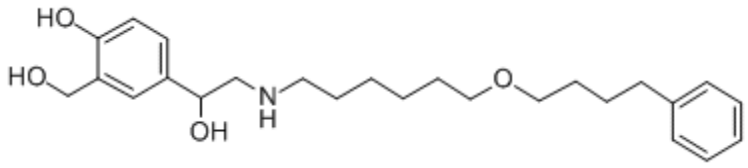

Salmeterol Xinafoate (SX)

Salmeterol
$C_{25}H_{37}NO_4$
MW 415 g/mol

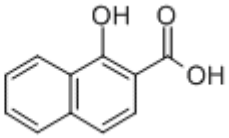

Xinofoate
$C_{11}H_8O_3$
MW 188 g/mol

Single Particle Aerosol Mass Spectrometry

The SPAMS instrument has been described elsewhere previously, but a brief description will be given here [30, 273]. Figure 27 is a schematic of the SPAMS instrument as configured for DPI measurements. An inhalation device is fitted to a USP throat (UIP, MSP Corp., Minnesota, USA) which is, in turn, mated to an aerosol residence chamber. The chamber is necessary to mediate between the higher flow rate of the devices under actuation and the SPAMS which draws 1.16 liters/minute through a KF-16 port at the bottom of the chamber. The relaxation chamber is also a source of sampling bias due to the loss of particles from wall adhesion and from gravitational settling of particles in the size range of interest [274]. In these experiments, no attempt was made to scale the data according to shape or transmission efficiency of the SPAMS inlet interface. The devices are actuated via a vacuum pump (HCP5, Copley Scientific Ltd., UK) / critical flow controller (TPK-2000, Copley Scientific Ltd., UK) which are connected through a third port in the side of the chamber.

The SPAMS system is maintained under vacuum. Aerosol particles are introduced from the chamber into its top through an inlet nozzle and proceed through a series of aerodynamic focusing lenses. The lenses collimate the particles into a beam and also serve to accelerate the particles in the beam to a terminal velocity that is a function of their

aerodynamic diameters. The SPAMS determines each particle's size in real-time by measuring its transit time as it traverses a square profiled laser beam and its scattered light is detected by a photomultiplier tube (2). This transit time is compared to a calibration made from particles of known size and density, returning their aerodynamic diameters at the level of the individual particle. The light scattering event is also used to trigger the firing of a pulsed ionization laser which desorbs and ionizes the particle. The desorption/ionization process occurs at the center of the source region of a dual polarity time-of-flight mass spectrometer. Both positive and negative ion spectra are simultaneously acquired and stored along with that particle's transit time. Up to 250 of these mass spectra/aerodynamic diameters can be acquired per second, each from an individual aerosol particle (3).

The mass spectra are analyzed in real-time using SPAMS-specific analysis software. First, the mass spectra are compared to a library of known mass spectra from previous training experiments to determine the general nature of the particle. Subsequently, the presence and absence of specific mass peaks are confirmed according to a decision tree to categorize the particles more precisely [246].

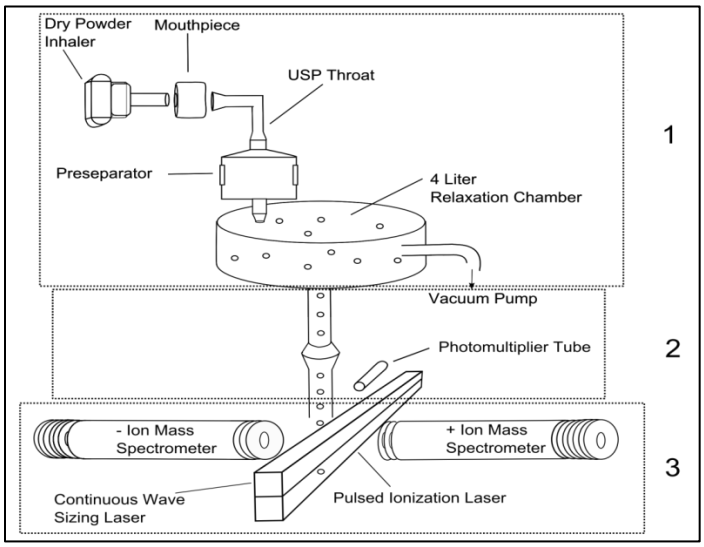

Figure 27: Schematic of a SPAMS instrument with a setup for dry powder inhaler measurements.

The first step in characterizing the acquired data is the removal of particles where a sizing event was recorded but no corresponding mass spectrum was observed. The remaining particles that generate both sizing and mass spectral data are referred to as "hit" particles, whereas particles with only sizing data acquired are referred to as "missed" particles. The hit rate in this work is defined as the ratio between the number of particles that generate ions detectable by mass spectrometry when the D/I laser has fired versus the total number of particles sized in the same time period.

Aerodynamic Diameter and Mass Calculation

As mentioned above, the aerodynamic diameter of the individual aerosol particles, d_{ae} was obtained from the correlation between transit time and an aerodynamic particle size calibration. The computation of d_{ae}, using Eq. (1) was based on the assumption that particles behave like spheres with a unit density in the air stream [275].

$$\boldsymbol{d_{ae} = d_{geo}\sqrt{\left(\frac{\rho_p}{\rho_0 \chi}\right)}} \qquad \textbf{Eq. 1}$$

where d_{ae} is the aerodynamic diameter in micrometers; d_{geo} is the geometric diameter of a volumetrically equivalent sphere in micrometers; ρ_p and ρ_0 are particle and unit densities; and χ is the dynamic shape factor (unity for a perfect sphere). The density of the polystyrene spheres was given by the manufacturer as 1.05 g/cm^3.

By making the approximation that particles have a perfectly spherical shape ($\chi \equiv 1$), their mass can be calculated by multiplying the volume of the particle by the API density, according to Eq. (2).

$$\boldsymbol{M = V \times \rho_0 = \frac{4}{3}\pi R^3 \times \rho_0} \qquad \textbf{Eq. 2}$$

where M is the mass (g); V is the volume of the sphere; ρ_0 is the particle density; and R is the radius.

With the SPAMS technique, the fine particle mass can be estimated on the basis of a conversion from particle counts per size bin into estimated mass per bin; by contrast, the NGI mass is based directly on gravimetric measurement or by chemical determination per impactor stage (defined size cut-offs) using HPLC. Additionally, whereas a SPAMS analyzes a statistical sampling of particles which can be scaled to the total mass, an NGI theoretically samples all particles which are dissolved and analyzed in their entirety.

Calibration of the SPAMS instrument

For the calibration of the SPAMS particle sizing section over the range of 0.1-10 µm, polystyrene microspheres (Thermo-Fisher Scientific, USA) were used. A size calibration curve was obtained by analyzing aqueous standard particle solutions in proper concentration with geometric diameters of 0.1, 0.5, 1.0, 2.0, 3.2 and 6.0 µm were introduced into the SPAMS by using a nebulizer (Salter Labs®, USA). The nebulized droplets were dried to individual particles by passing the aerosol stream through a two-stage diffusion dryer (Livermore Instruments, USA), containing silica gel desiccant. The aerodynamic diameters of the unknown particles from the inhalers were obtained from the generated calibration curve by plotting the median particle transit time as determined by the SPAMS against the calculated aerodynamic diameter. The smaller particles (aerodynamic diameter below 0.1 µm) are traveling at the approximate velocity of the gas molecules and thus their sizes cannot be distinguished from each other. Additionally, as the particles become smaller in size, they are more difficult to focus into a tight particle beam through the aerodynamic lens inlet [33] and behave more like gas molecules and can be pumped away [276]. The SPAMS interface is designed deliberately to take advantage of this phenomenon in order to bias towards the less numerous large particles and against the more numerous smaller particles roughly as a function of the mass of the particle.

Dry Powder Inhaler/pressurized Metered Dose Inhaler Testing by SPAMS

The experimental setup of the SPAMS instrument for inhalational device testing is similar to that described by Morrical *et al* [30]. Diskus® inhaler devices were fitted to an universal induction port (MSP Corp., Minnesota, USA) which was in turn fitted to a pre-separator (Copley Scientific, UK) which was filled with 15 mL of water and then connected to the 4L relaxation chamber. This assembly of pre-separator and relaxation chamber was then fitted to the SPAMS inlet. The primary purpose of the pre-separator was to filter out coarse lactose carrier particles (>10 µm) to prevent clogging of the SPAMS inlet interface. The actuation of the DPIs was made with a 2.7 seconds draw of air into the relaxation chamber, at a flow rate 90 L/min (i.e. 4 liters of air drawn). The pMDIs were actuated simultaneously with a 1.7 second draw of air at a flow rate 30 L/min (~1 liter of air drawn) through a universal induction port without a pre-separator into the relaxation chamber. Approximately the same number of particles was analyzed for each sample run (ca. 10,000 individual particles each). SPAMS experiments were alternated with clean air blank runs to flush the relaxation chamber for one minute each.

Preliminary experiments have been performed to investigate optimal parameters for pMDI and DPI measurements by SPAMS [30, 247, 277]. Both fluticasone and salmeterol have previously been demonstrated to generate ions well at a wavelength of 248 nm [278]. Therefore, the desorption/ionization laser was set to fire at a wavelength at 248 nm. In the configuration being operated, the SPAMS was able to analyze up to 64 particles per second (laser repetition rate 64 Hz). The laser energy was maintained at approximately 12 mJ per pulse to obtain a high and consistent hit rate.

Determination of the Chemical Identity of Particles

Determination of APIs present in a given particle of a combination product such as Advair Diskus® or Seretide® requires the acquired mass spectra to be analyzed. The comparison of multiple data sets of the combination product with the two mono products' data sets allows for the identification of unique marker peaks that distinguish one particle type from another. Most APIs are significantly structurally different or have a different counter ion (for compounds in a specific salt form), a mass spectrum should contain an ion or multiple ions that are unique for that compound. Once these ions have been identified in the single component products mass spectra, then combination particles are identified by the observation those unique markers in combination in an individual particle mass spectrum. Analyzing pure lactose in the SPAMS instrument did not result in any mass spectral data (lactose does not absorb significantly at a wavelength of 248 nm) (Figure 30).

A simple rules tree of mass-to-charge ratios and signal thresholds can then be applied to the single API and combination DPIs or pMDIs to determine which particles have either, both or neither API present (Figure 28) [30, 277]. Most likely, these particles are agglomerations of one or both API particles possibly in aggregation with excipients.

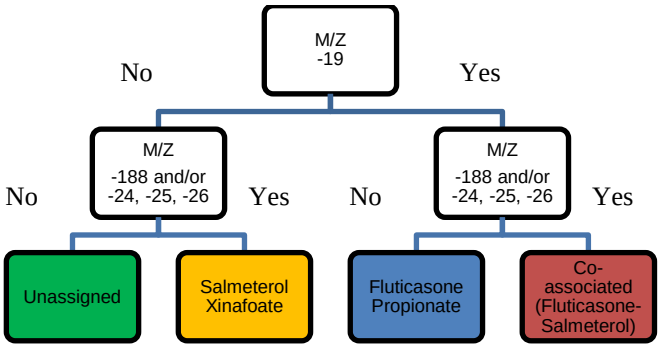

Figure 28: Rules tree to identify fluticasone propionate and salmeterol xinafoate in mass spectra.

Results and Discussion

The hit rate for the combination products was 92% for Advair Diskus® DPI and 78% for Seretide® pMDI. The hit rate for the mono products was at 71% for Axotide® pMDI, 87% for Serevent® pMDI, 79% for Axotide Diskus® DPI and 92% for Serevent Diskus® DPI. The hit rate for the different device types depends on several factors. For example, the ionization rate of each API itself plays an important role. Also imperfect alignment between the ionization laser and the aerosol beam or between the ionization laser and the tracking laser may result in reduced energy being received by the particle. Higher dosage strength in the product will also result in an increase in the hit rate. Excipients in a formulation, such as lactose, will significantly decrease the hit rate. However, in Advair Diskus®, Axotide Diskus® and Serevent Diskus® a lactose type with a very narrow particle size distribution around 60-100 µm was determined to be used by the manufacturer. In our experiments, a pre-separator was used to cut off particles with an aerodynamic diameter above 10 µm. Thus, the hit rate for the measured DPI products was very high since nearly all of the particles with an aerodynamic diameter below 10 µm were API particles. A possible explanation could be that during DPI actuation some smaller lactose particles may be formed through particle collision, abrasion and shear forces and reduce the hit rate [15]. MDI products are suspensions of API in a combination with excipient and vehicle so not every particle created during nebulization may contain an active substance.

Mass spectral data

Figure 29 shows the averaged mass spectra acquired from a single dose each of Axotide®, Serevent® and Seretide® pMDI formulations acquired over a 3 min period from each single actuation. Per the formulations, Figure 29 shows

spectra of pure fluticasone (top) and salmeterol (middle) respectively, while on the bottom a spectra of co-associated particles of fluticasone and salmeterol is shown. A spectrum from excipient particles (lactose) from a DPI is shown in Figure 30. The molecular weight of fluticasone propionate is 500 g/mol, of salmeterol is 415 g/mol and of xinafoate is 188 g/mol.

The molecular ion generally cannot be seen when analyzing particles by this method [30, 277] due to the extensive fragmentation of the molecule during the desorption and ionization process. The structures of both fluticasone and salmeterol contain strong chromophores, which absorb well at $\lambda = 248$ nm [278]; however, the required energy needed to break the crystal lattice of the particle and then to ionize the free molecules is substantially higher than the ionization threshold of the APIs. As a result, there is often sufficient excess energy to result in extensive fragmentation of the molecule into the fragment ions seen in Figure 29.

The mass spectra were individually evaluated for the presence of unique marker peaks with optimal predictive value for the identity of each API. The marker peaks inferred from the two products containing a single API were used to discern those APIs in the combination product. Negative ions were primarily used as markers since unique peaks were more readily identified there. It was determined that a peak at M/Z = -19 was found in fluticasone, indicating the liberation of fluorine from the fluticasone structure. For salmeterol xinafoate, peaks at M/Z = -188 and -24, -25, -26 were identified as originating for the xinafoate counter ion (M/Z=-188) and salmeterol (hydrocarbons: C_2, C_2H, C_2H_2), respectively.

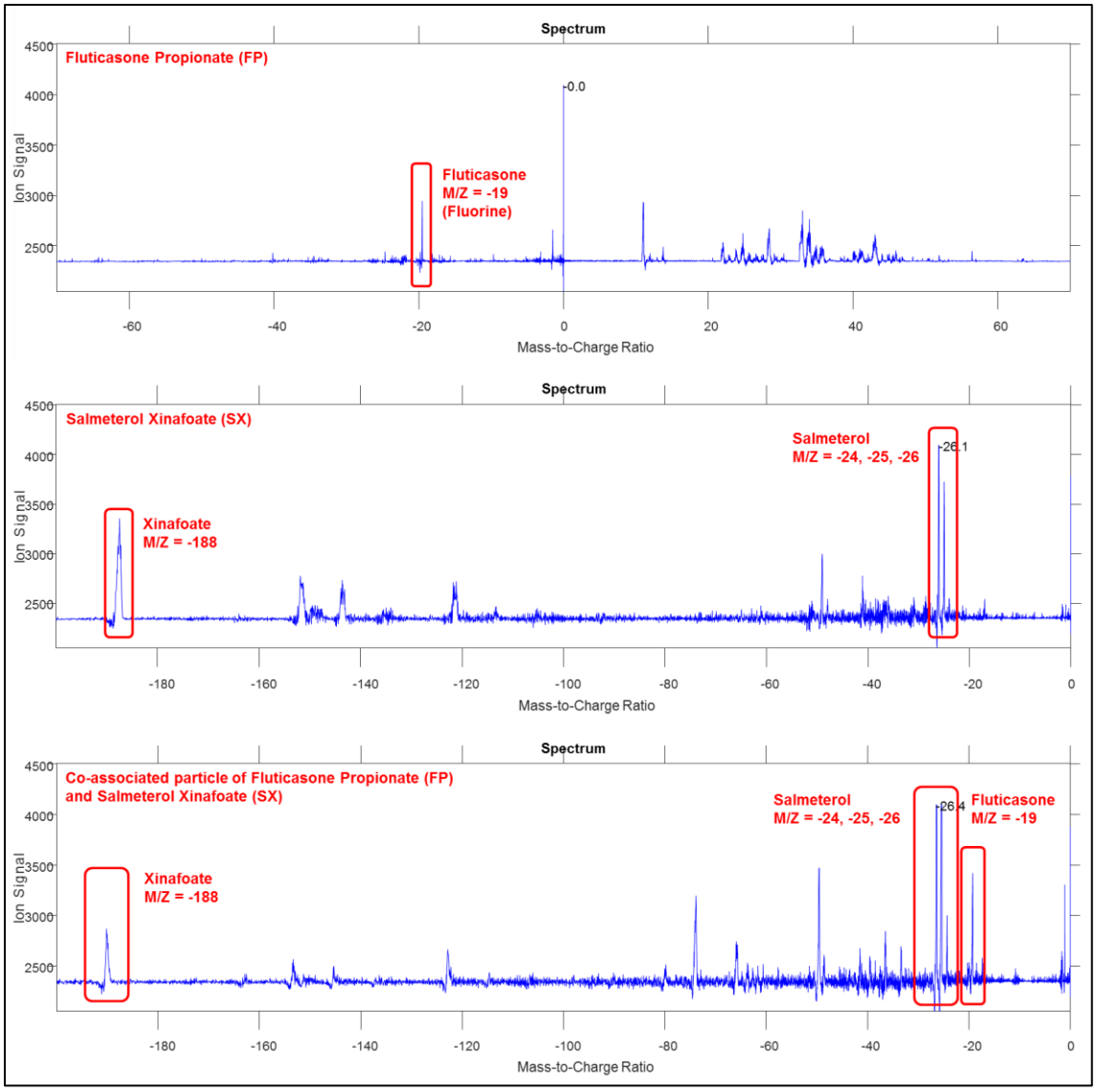

Figure 29: Top: Averaged mass spectra of pure fluticasone propionate (FP) particles (M/Z = -19) from Axotide® pMDI. Middle: Averaged mass spectra for pure salmeterol xinafoate (SX) particles (M/Z = -188; -24, -25, -26) from Serevent® pMDI. Bottom: Mass spectra for co-associated single particles of fluticasone propionate (FP) (M/Z = -19) and salmeterol xinafoate (SX) (M/Z = -188; -24, -25, -26) from the combination products.

It can be clearly seen that the spectra in Figure 29 at the bottom contain marker ions that correspond to those seen in the spectra taken from pure standards of both fluticasone and salmeterol and must therefore be agglomerates of co-associated particles.

Very few spectra were acquired for pure lactose and those that were acquired had an extremely weak sign for both positive and negative ions, presumably due to the lack of a strong chromophore in the lactose molecule capable of absorbing radiation at 248 nm (Figure 30). As a result, lactose does not interfere with the detection of particles containing an API. By eliminating all of the pure API particles and comparing them to the maximum known hit rates typically achieved, we estimate that less than 10% of all particles detected by mass spectrometry were pure lactose.

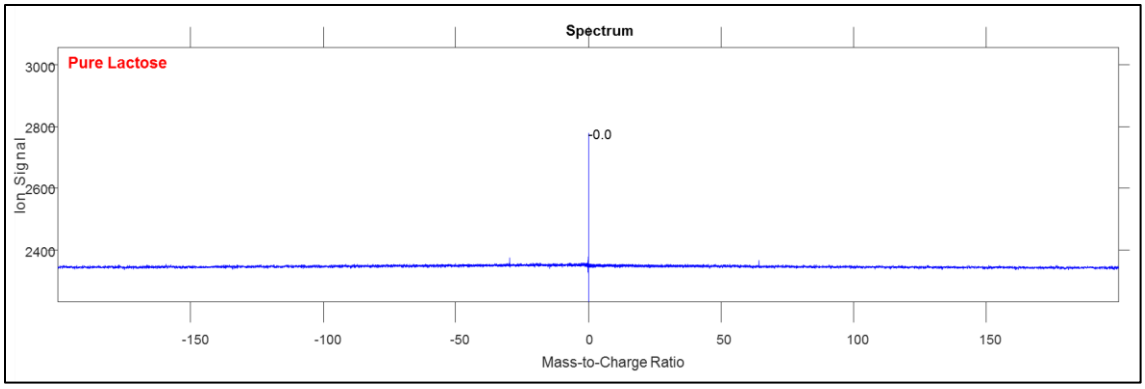

Figure 30: Averaged mass spectra for excipient (Lactose).

Aerodynamic Particle Size Distributions

As mentioned above, the SPAMS interface deliberately size biases in favor of larger particles and this bias was not accounted for in this work. Nevertheless, even the biased aerodynamic particle size distribution (APSD) histograms can be informative given that they all have the same bias. Those APSDs are plotted in Figure 31 and Figure 33 and Supplementary Figures 1-2. The histograms show the distribution of active and unassigned or excipient particles in 10,240 measured particles. MDIs show a normal (Gaussian) distribution curve shape with a median aerodynamic diameter (MAD) around 2.00 µm for fluticasone (Axotide®) and 1.39 µm for salmeterol (Serevent®) as can be seen in Table 5 and Supplementary Figures 1-2. In Figure 31, the MAD of total API (fluticasone-salmeterol, fluticasone and salmeterol) in Seretide® was 1.79 µm. Salmeterol seems to be much finer than fluticasone in the tested pMDI formulations and, as a result, many more small salmeterol particles were detected in the range from 0-0.7 µm.

The DPI mono products Axotide Diskus® and Serevent Diskus® had an MAD of 2.06 µm and 1.86 µm, respectively (as can be seen in Table 5 and Supplementary Figures 1-2). The DPI combination product Advair Diskus® had an MAD for both APIs combined around 2.02 µm (Figure 33, Table 5). Generally, the MAD for fluticasone, salmeterol and co-associated particles was found to be coarser in DPI formulations compared to corresponding pMDI products. However, the MAD of pure fluticasone was coarser in both the DPI mono and pMDI mono formulations than in the combination products.

The particle co-associations and interactions in combination products may influence the ratio and MAD of fluticasone, salmeterol and fluticasone-salmeterol (co-associated particles). It is possible that a certain particle size of each API preferentially forms heterogeneous agglomerates. Alternatively, it is possible that the drug substance was milled to a different fineness by the manufacturer. DPIs also have some larger agglomerate particles compared to pMDI profiles, with an aerodynamic diameter around 5.9-6.7 µm (Table 5). Because DPI formulations also contain excipients such as lactose, it seems likely that pure particles (fluticasone or salmeterol) and co-associated particles (fluticasone-salmeterol) are made of agglomerates of API and excipient, resulting in the larger particle size.

Table 5: Median aerodynamic diameter (MAD) calculated from pMDI and DPI products measured by SPAMS.

MAD [µm]	Axotide® pMDI	Serevent® pMDI	Seretide® pMDI	Axotide Diskus® DPI	Serevent Diskus® DPI	Advair Diskus® DPI
FPSX	---	---	1.64	---	---	2.02
FP mono	2.00	---	1.96	2.06	---	1.36
SX mono	---	1.39	2.25	---	1.86	2.12
Overall	2.00	1.39	1.79	2.06	1.86	2.02

Figure 31 shows the APSD of APIs in Seretide® pMDI, both as mono API particles and as co-associated API particles. The APSD histogram shows the fractionation of the "hit" particles and the collected data demonstrates that a majority of particles emitted from Seretide® contained both APIs in co-association. A fraction of particles (11%) could not be identified, most likely due to insufficient ionization. Due to the higher dosage strength of fluticasone compared to salmeterol in Seretide® (125/25 mcg), many more fluticasone particles were present to be detected than salmeterol particles. 45% of all hit particles contained fluticasone and salmeterol in co-association. A majority of salmeterol particles (70%) were co-associated with fluticasone.

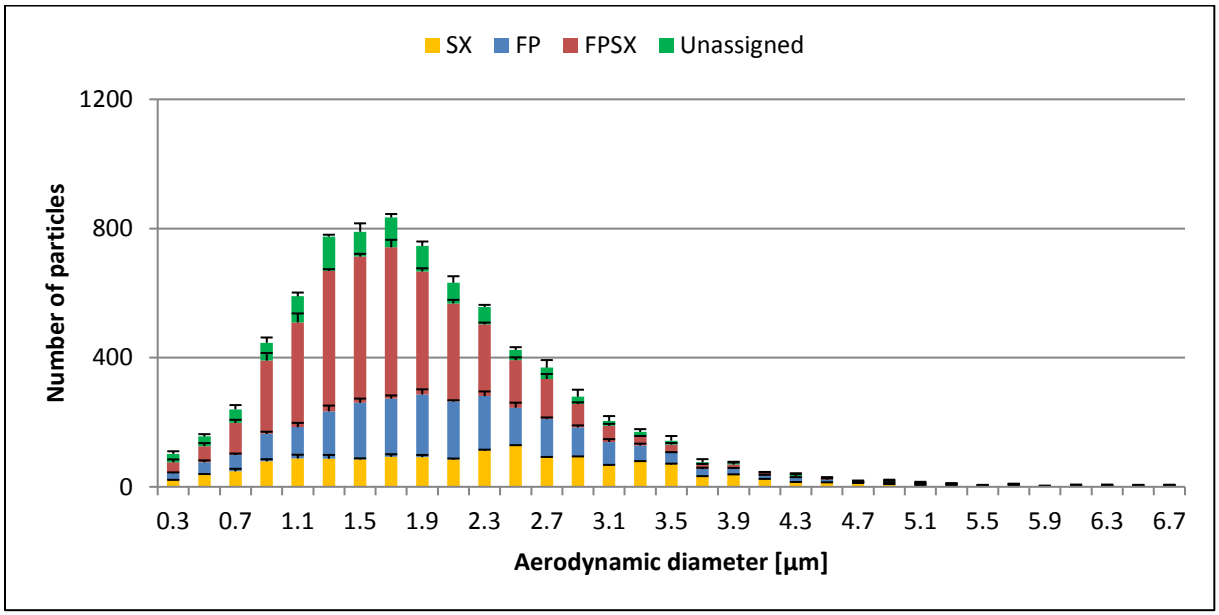

Figure 31: Aerodynamic particle size distribution of Seretide® pMDI obtained by SPAMS (n=3 pMDI actuations; error bars represent one standard deviation). The plot shows the distribution of number of particle co-associations of fluticasone-salmeterol (FPSX), pure fluticasone (FP), pure salmeterol (SX) and unassigned particles.

In Seretide® the MAD for pure fluticasone is around 1.96 µm while the MAD for salmeterol particles was found to be much coarser for pure SX particles (MAD 2.25 µm). The co-associated drug particles in Seretide® had an MAD around 1.64 µm. Interestingly, pure fluticasone and salmeterol particles had a coarser MAD compared to the co-associated particles in the pMDI combination product. In the tested pMDI combination formulation, it appears that fine salmeterol particles are preferentially co-associating with fluticasone particles (Figure 32). As can be seen in Figure 32, the majority of salmeterol particles in the finest size fraction are nearly 100% co-associated and the distribution is very different compared to the salmeterol mono pMDI.

The picture for pure fluticasone in the combination product is somewhat different. Although there is a slight shift in pure fluticasone in the combination product compared to the fluticasone mono pMDI, it appears that the fluticasone particle sizes that are involved in co-association are more evenly distributed across the entire size distribution rather than preferentially finer particles as observed with pure salmeterol particles in the combination product (Figure 32).

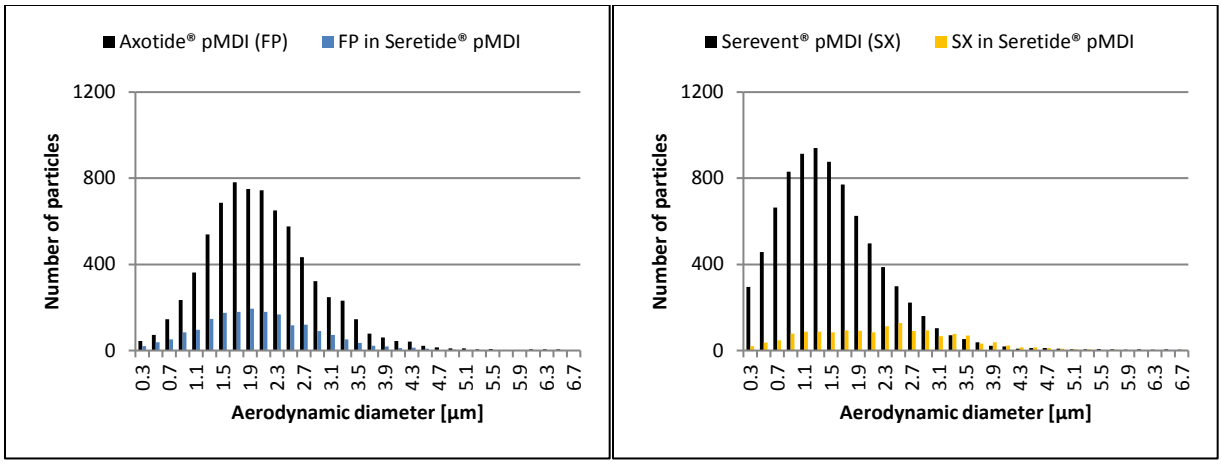

Figure 32: Overlay of aerodynamic particle size distribution of mono pMDI products (Axotide® and Serevent®) with pure fluticasone (FP) and salmeterol (SX) found in Seretide® pMDI.

Interestingly, the two mono DPIs give very similar distributions, unlike the fluticasone and salmeterol mono pMDIs, which look very different in their APSD (Supplementary Figures 1-2). The lactose carrier seems to have a big influence on the aerodynamic particle size distribution profiles of salmeterol.

The plot in Figure 33 illustrates the APSD of APIs in the Advair Diskus®, either as single API particles or as co-associated API particles. The APSD histogram shows the fractionation of the "hit" particles and the collected data demonstrates that there are also a high number of co-associated particles emitted from the Advair Diskus®. Only a small fraction of particles could not be assigned probably due to insufficient ionization (5%). 41% of all the hit particles contained fluticasone and salmeterol in co-association. Due to the far higher dosage strength of fluticasone compared to salmeterol in Advair Diskus® (500/50 mcg), there are many more fluticasone particles present and detected than salmeterol particles. A large fraction of salmeterol (74% of total salmeterol) is in co-association with fluticasone. While only about 52% of fluticasone is co-associated. This could be a simple result of the statistical mechanics given the 10x difference in dosage strength between the APIs in the product. But the cohesive nature of fluticasone [279] (with regards to salmeterol) could plausibly also play a role for this occurred effect.

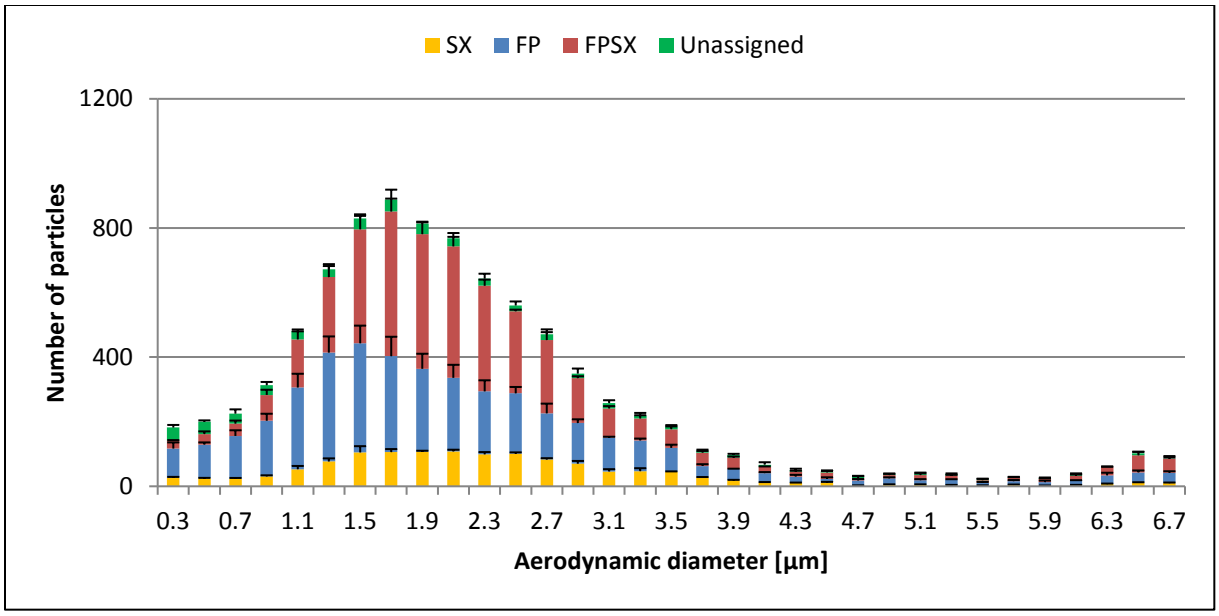

Figure 33: Aerodynamic particle size distribution of Advair Diskus® DPI obtained by SPAMS (n=3 DPI actuations; error bars represent one standard deviation). The plot shows the distribution of number of particle co-associations of fluticasone-salmeterol (FPSX), pure fluticasone (FP), pure salmeterol (SX) and unassigned particles.

In Axotide Diskus® the MAD for fluticasone is 2.06 µm whereas the MAD for fluticasone in Advair Diskus® is around 1.36 µm. This can be seen clearly in Figure 34 where it appears that primarily larger particles of fluticasone are involved in co-association with salmeterol particles.

Also shown in Figure 34 is the comparison of Serevent Diskus and the pure salmeterol particles from Advair Diskus. The MAD for Serevent Diskus salmeterol particles is 1.86 µm and for the pure salmeterol particles in Advair Diskus it is 2.12 µm, indicating the finer particles are the ones involved in co-association. This effect was also observed for the pMDI formulation.

For the co-associated drug particles (fluticasone-salmeterol), the MAD is somewhat coarser than the free fluticasone particles at approximately 2.02 µm, also strongly indicating that those particles result from the agglomeration of fine salmeterol and coarser fluticasone particles. Comparing the MAD in combination products of pure fluticasone and salmeterol particles, there appeared to be a difference between the DPI and pMDI formulations (Table 5). It may be possible that the lactose is changing the adhesive/cohesive behavior of the APIs in the tested products [225].

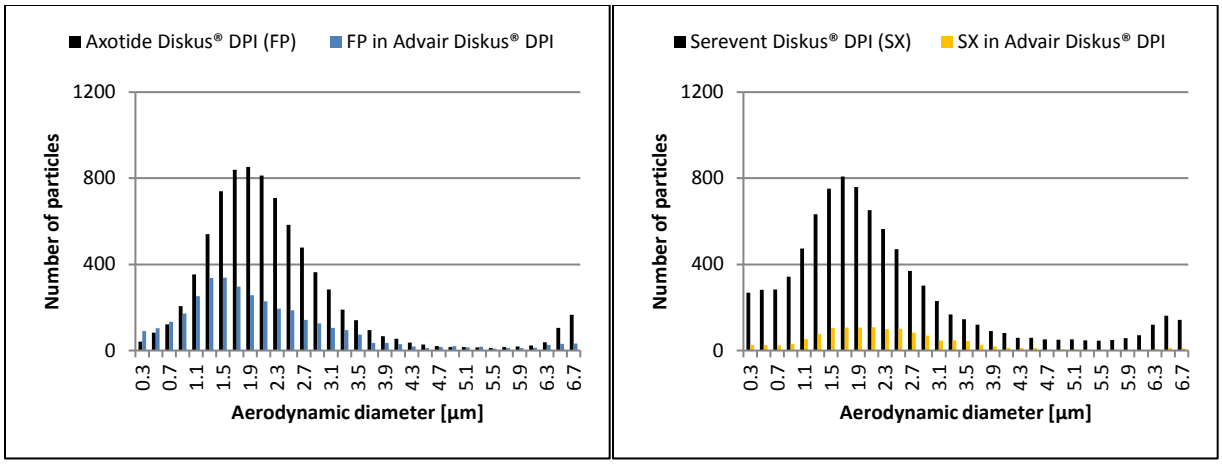

Figure 34: Overlay of aerodynamic particle size distribution of mono DPI products (Axotide Diskus® and Serevent Diskus®) with pure fluticasone (FP) and salmeterol (SX) found in Advair Diskus® DPI.

MADs for co-associated particles in the DPI were found to be larger than those in the pMDI product (Table 5 and Supplementary Figure 3). The pure salmeterol particles were coarser than the pure fluticasone particles in both DPI and pMDI. The manufacturer may have formulated APIs with a different particle size distribution but a more likely scenario is that there may be a greater tendency of salmeterol particles with small aerodynamic diameters to co-associate with coarser fluticasone in the DPI combination product. The mechanism and effect of the formation of co-associated particles or agglomerates appears substantially different between the two tested inhaler types and, in light of the synergetic effects of the two APIs, merits further investigation.

Theophilus *et al.* [270] made an attempt to investigate particle co-associations of fluticasone and salmeterol with Raman microscopy in 2006 and found interesting results. However, their sampling method likely biased their results. Collecting a sample on stage 4 of the Andersen Cascade Impactor at particle concentrations similar to those reported is expected to result in powder piles accumulating under the nozzles on the plate. Therefore it is impossible to disambiguate whether particle co-associations were formed before or after impaction on the plate. Nevertheless, if their detected particle co-associations of fluticasone and salmeterol are correct, one can assume, as in our own observations, that there is a greater tendency of smaller particles to form co-associations. The higher rate of diffusion for smaller particles could influence the phenomenon. But it is important to note that the particle size of salmeterol was found to be smaller than that of fluticasone and therefore many more small salmeterol particles are present in the formulation, suggesting statistical mechanics as a rival hypothesis.

Looking at the aerosol populations in their entireties, significant levels of API particle co-associations were detected in both of the tested combination products. 45% of all particles in the pMDI and 41% of all particles measured from the DPI were found to contain both APIs. The levels of particle co-association of fluticasone and salmeterol in DPIs and pMDIs were found to be different (Table 6 and Table 7). The adhesive API salmeterol [225] (with respect to fluticasone) was found to be highly co-associated with fluticasone for both inhaler types. A high fraction of salmeterol seemed to be in co-association with fluticasone, while only a smaller fraction of salmeterol seemed to be free (14% in DPI and 20% in pMDI, Table 6). Meanwhile, a significantly higher fraction of pure fluticasone could still be found in the tested formulations. Fluticasone is a cohesive compound (with respect to salmeterol) and agglomerates primarily with itself [279]. At a sufficiently high fluticasone to salmeterol ratio, all available salmeterol particles are used up in co-association and there is an excess of fluticasone particles given the far higher dosage strength of fluticasone in the analyzed formulations.

Table 6: Percentage of individual particles measured in the DPI and pMDI formulations (10'240 particles per run).

[%]	Axotide® pMDI	Serevent® pMDI	Seretide® pMDI	Axotide Diskus® DPI	Serevent Diskus® DPI	Advair Diskus® DPI
FPSX	---	---	44.9	---	---	41.3
FP	71.3	---	24.6	79.1	---	38.8
SX	---	87.0	19.5	---	91.5	14.4
Unassigned	28.7	13.0	11.1	20.9	8.5	5.4

Comparing the percentage of distribution of fluticasone and salmeterol particles in the formulation in either pure or co-associated state, it seems that overall more fluticasone and salmeterol is in co-association in the pMDI formulation (Table 7).

Table 7: Percentage distribution of total fluticasone propionate (FP) and salmeterol xinafoate (SX) in the formulation in co-associated or pure state in the tested DPI and pMDI combination products.

[%]	Advair Diskus® DPI	Seretide® pMDI
FP co-associated	51.6	64.6
SX co-associated	74.1	69.7
FP pure	48.4	35.4
SX pure	25.9	30.3

Overall, higher levels of API co-association were found in the pMDI combination product than in the DPI (Table 7). This may be explained by the different dosage strengths of the inhalers used in this study. Advair Diskus® contains a dosage strength of 500/50 mcg while Seretide® is only 125/25 mcg of fluticasone and salmeterol, respectively so the fluticasone to salmeterol ratio in the DPI was twice that of the pMDI. On the one hand, there are more total salmeterol particles available for co-association in the DPI and a higher percentage of observed particles were co-associated; on the other hand, there was less salmeterol initially and so a smaller percentage of particles were observed as pure salmeterol. This phenomenon was mitigated to some degree via the division of the API mass among a larger number of smaller salmeterol particles as the salmeterol particles were significantly smaller than the fluticasone particles (Table 5) [167]. Further studies with different dosage strengths and controlled particle sizes could clarify the statistical mechanical effects influencing the level of co-association.

Since, the pMDI and DPI formulations were considerably different, the mechanisms by which co-association of APIs may occur could also be different. In the pMDI, co-association can to occur between the two types of solid particles (fluticasone and salmeterol particles) while still in the suspension within the inhaler [269]. Depending on the dosage strength, multiple particles will be emitted within individual droplets to a greater or lesser degree upon the actuation [280]. When an emitted droplet collapses in the air stream through propellant evaporation, these particles can remain associated [281]. If both, fluticasone and salmeterol particles are within the droplet then they may remain co-associated. Alternatively, coalescence of droplets within the plume could also lead to particle co-association. API co-associations in DPIs can arise from interactions between different API-containing particles as a result of high shear forces during the blending process or via the formation of weak agglomerates of API with lactose fines [7]. In the case of the Advair Diskus®, the APIs were processed together and could furthermore also mix in the aerosol plume following the actuation of the device. Soft agglomerates of API and fine lactose formed during device actuation that could effectively co-associate the two APIs without direct binding of the one API to the other. Nevertheless, this co-association could well deliver both APIs to the same site in the patient. Adding lactose to the blend as an excipient would presumably reduce the level of co-association by acting as a diluent. These and other mechanisms contributing

to the levels of API co-association in inhaled products merit further study to optimize that co-association for increased pharmacological efficacy [38, 281].

SPAMS Mass Estimates

Mass estimates were made by multiplying the number of particles with active ingredient counted in each size bin by the mass of the average particle found in that bin (Figure 35 and Figure 36). This estimate was based on assuming all counted particles to be spheres with a density of 1 g/mL and to be pure API. In the mass spectra of the combination products, if both ions were present, the mass of the particle was assumed to be split evenly between each API, while if only one or the other were found then the mass of the particle was assumed to result entirely from that API. It is possible to use NGI data to develop a scaling factor for the SPAMS data for each size bin [247].

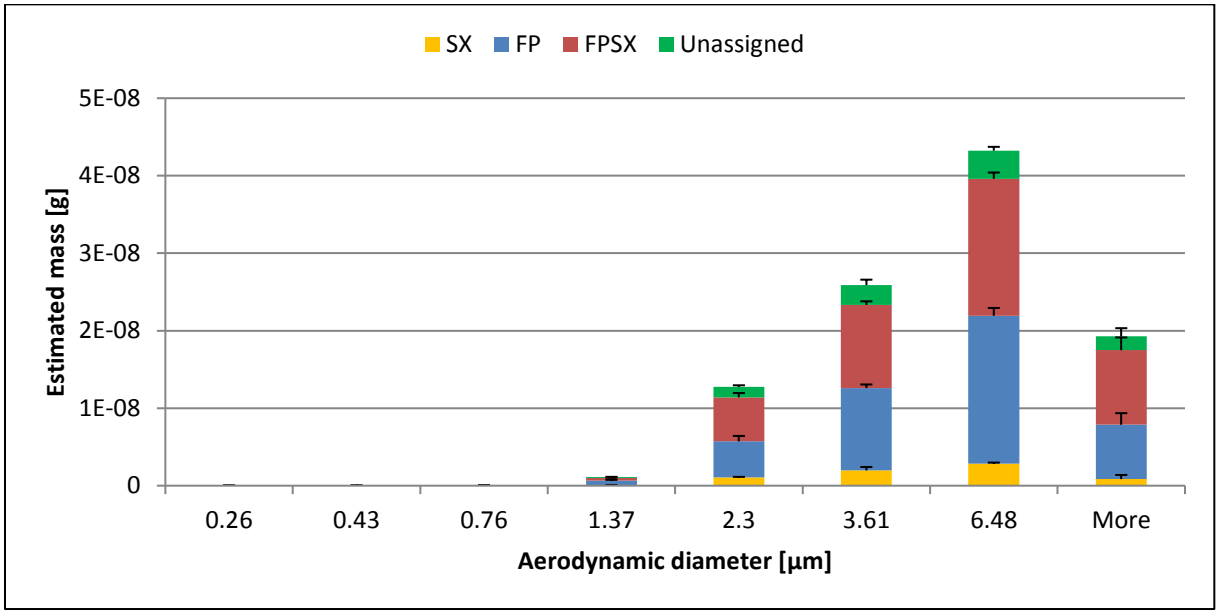

Figure 35: Computed masses of particles of the combination product Advair Diskus® DPI which contain either, both or neither active ingredients as determined by the SPAMS 3.0 (n=3; error bars represent one standard deviation).

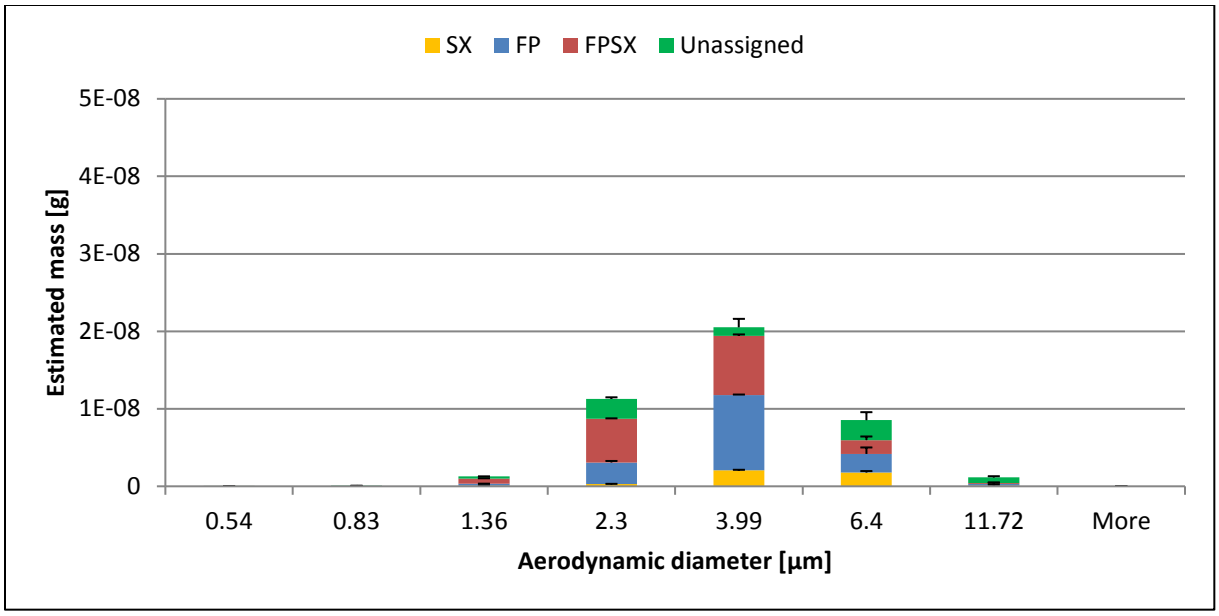

Figure 36: Computed masses of particles of the combination product Seretide® pMDI which contain either, both or neither active ingredients as determined by the SPAMS 3.0 (n=3; error bars represent one standard deviation).

The mass distribution profiles differ for dry powder formulations (Figure 35) from metered dose inhaled formulations (Figure 36). Particle mass is shifted to larger sizes in the DPI most likely due to the fact that insufficient de-agglomeration of the powders may occur [45]. This is often the case with formulations with strong adhesive forces [193, 282]. For the pMDI formulation the mass distribution plot is similar to a normal (Gaussian) distribution. Furthermore, co-association of APIs will also increase the particle size by simple virtue of the fact that multiple smaller particles are necessarily agglomerated.

Conclusions

The collected data confirms that high levels of co-associated particles are emitted from both fluticasone-salmeterol DPI and pMDI combination products examined after actuation of the device. Using the SPAMS technique reveals that approximately 41% of the respirable particles in the tested DPI product and 45% of the respirable particles in the pMDI product contained both fluticasone and salmeterol. Unique mass spectral fragmentation patterns were recognized and assigned for each API using software that has been specifically designed for the analysis of SPAMS data. A large fraction of the detected salmeterol was found in co-association with fluticasone in both DPI and pMDI devices while a large fraction of pure fluticasone particles was also detected. A significant finding was also that rather coarse fluticasone particles (in DPI) and fine salmeterol particles (both MDI and DPI) were forming the particle co-associations. The underlying mechanism for the formation of co-associated particles seems to be different between the DPI and pMDI. There is high potential for the association of fluticasone or salmeterol or both with lactose or other excipients present in a formulation and future work should involve the development of techniques to further differentiate, identify and quantify both APIs and excipients at the level of the individual particle. SPAMS was able to reveal particle co-associations successfully in combination pMDI and DPI products and provides an interesting tool for formulation design.

Future Outlook

In an effort to avoid extensive fragmentation and make the identification of the analyte compounds easier, a modification to the SPAMS to allow for a two-step laser desorption/ionization would potentially make identification of analytes less problematic than the current single laser system. This was successfully demonstrated for single particle

mass spectrometry by Morrical *et al* [283], who successfully coupled a "soft" two-step laser desorption/ionization technique (L2MS) with ATOFMS. L2MS decouples the desorption process from the ionization process by using a different laser for each step. By decoupling desorption from ionization, L2MS permits the independent optimization both laser energy and wavelength for each step. For the desorption process, it has been shown that an infrared laser, typically a CO_2 laser, efficiently thermally desorbs most molecules. The ionization step is performed subsequently with a UV laser at typical wavelengths of 193, 248, 266, or 308 nm [284, 285]. Such an upgrade to the SPAMS instrument would be highly valuable for the analysis of pharmaceutical aerosols. An upgraded SPAMS with separate desorption and ionization lasers firing at a different wavelength could potentially detect co-associations not only between APIs, but also between API and excipients (lactose or force control agents) in the future if an appropriate ionization wavelength were selected.

Acknowledgements

This work was funded by Novartis Pharma AG's internal research funds. The authors are grateful to B. Haeberlin, T. Storm and M. Schneider for scientific oversight and guidance.

Supplementary Data

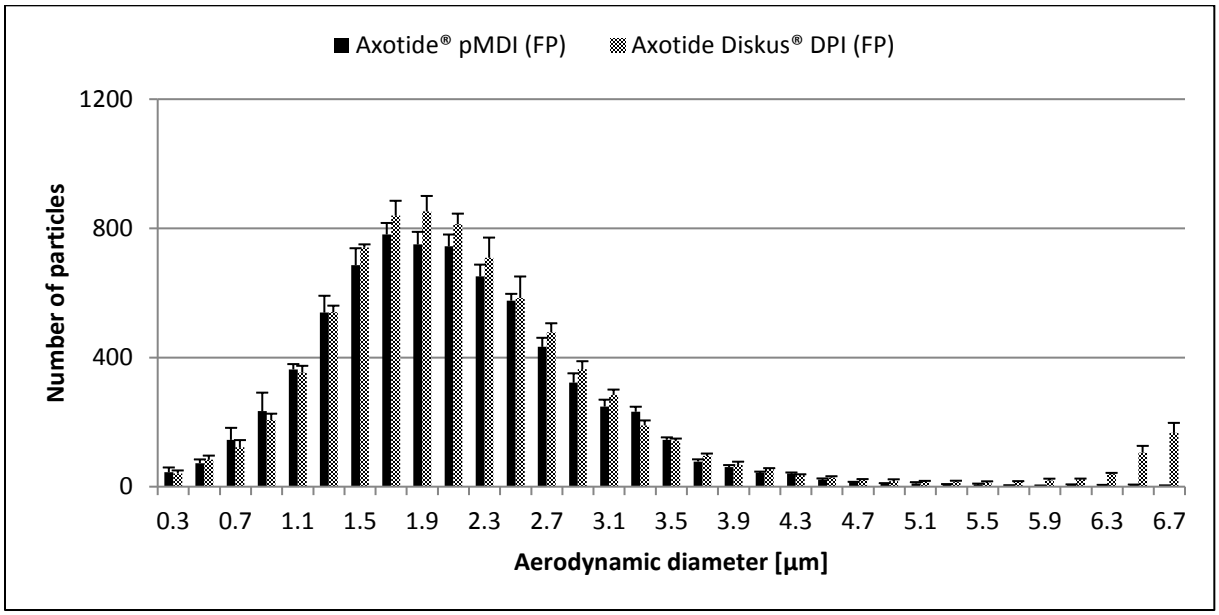

Supplementary Figure 1: Aerodynamic particle size distribution of fluticasone propionate (FP) particles in Axotide® pMDI and Axotide Diskus® obtained by SPAMS (n=3 pMDI actuations; error bars represent one standard deviation).

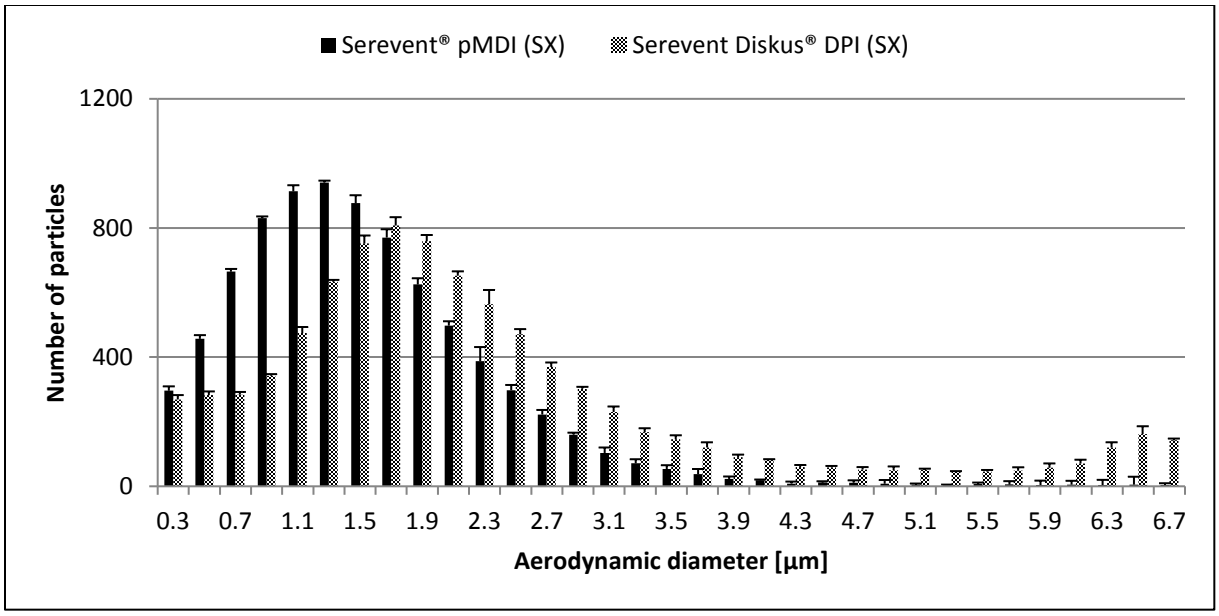

Supplementary Figure 2: Aerodynamic particle size distribution of salmeterol xinafoate (SX) particles in Serevent® pMDI and Serevent Diskus® DPI obtained by SPAMS (n=3 pMDI actuations; error bars represent one standard deviation).

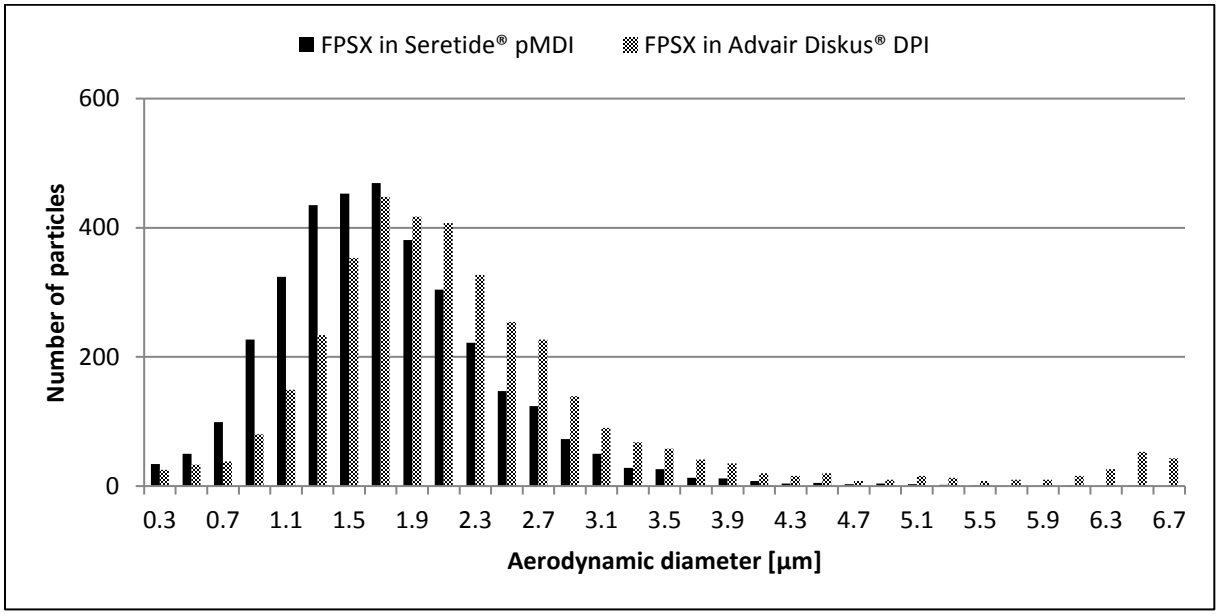

Supplementary Figure 3: Overlay of aerodynamic particle size distribution of co-associated particles of fluticasone-salmeterol (FPSX) in the combination products (Advair Diskus® and Seretide®).

3. Probing the Particulate Microstructure of the Aerodynamic Particle Size Distribution of Dry Powder Inhaler Combination Products

Jetzer et al. International Journal of Pharmaceutics (2018) 538:30-39

Abstract

The *in vitro* aerosol performance of two combination dry powder inhaler (DPI) products, Foster® NEXThaler® and Seretide® Diskus® were investigated with single particle aerosol mass spectrometry (SPAMS). The in-vitro pharmaceutical performance is markedly different for both inhalers. Foster® NEXThaler® generates a higher fine particle fraction (FPF <5 μm) and a much higher relative extra fine particle fraction (eFPF <2 μm). In terms of the composition of the aerodynamic particle size distribution (APSD), it could be verified with SPAMS that overall Foster® NEXThaler® emits a significantly higher number of fine and extra fine particles with a median aerodynamic diameter (MAD) of 2.1 μm while Seretide® Diskus® had a larger MAD of 3.1 μm. Additionally, the interactions between the two active pharmaceutical ingredients (APIs) in both products are different. While Seretide® emits a significant (37%) number of co-associated API particles, only a negligible number of co-associated API particles were found in Foster® NEXThaler® (<1%). A major difference with Foster® NEXThaler® is that it contains magnesium stearate (MgSt) as a second excipient besides lactose in a so-called 'dual excipient' platform. The data generated using SPAMS suggested that nearly all of the beclomethasone dipropionate particles in Foster® NEXThaler® also contain MgSt and must therefore be co-associated with this additional excipient. This may help explain why beclomethasone dipropionate in Foster® NEXThaler® forms less particle co-associations with the second API, formoterol fumarate, shows a lower cohesive strength in respect to beclomethasone itself and why both APIs exhibit superior detachment from the carrier as evidenced by the increased eFPF and smaller MAD.

Introduction

Dry powder inhalers (DPIs) are used to deliver an efficacious dose of active pharmaceutical ingredients (API) to a target region of the lung. DPIs are available as capsule, blister and reservoir based products, most of which employ excipients as carriers. The delivery of an efficacious dose to the target region of the lung is dependent on the fine particle dose (FPD), or more precisely, the aerodynamic particle size distribution (APSD) of the API emitted from the DPI during its use by the patient. Aerodynamic particle sizes of <5 microns are usually considered optimal for drug delivery to the lungs [286].

There is an increasing interest in the development and use of the so-called 'extrafine' aerosols to target the small airways in the treatment of peripheral airways in asthma and chronic obstructive pulmonary disease (COPD) [141, 287-289]. It has been reported that the inhalation of very small drug particles (<2μm) leads to an increased total lung deposition, improved distal airway penetration and a higher peripheral lung deposition [140]. Leach *et al.* used imaging single-photon emission computed tomography (scintigraphy) to compare the lung deposition of inhaled drugs from pressurized metered dose inhalers (pMDIs) with different particle size formulations. It was observed that up to 77% of the 'non-extrafine' fluticasone/salmeterol HFA-suspension pMDI was deposited in the oropharynx and about 16% in the lungs compared with 35% and 58% of the 'extrafine' HFA-solution of beclomethasone/formoterol [36, 290].

The development of DPIs now appears to follow somewhat 'standard' processes and analytical control methodologies with many DPI products being granted marketing authorization. In terms of the efficacious dose, the APSDs of DPIs are typically characterized using cascade impaction methods, which involve aerosolizing the powder in the DPI under standard conditions. For example, for the uniformity of delivered dose of DPIs, the European Pharmacopoeia requires testing 4 L of air at a flow rate, which generates a pressure drop across the device of 4 kPa [291]. The aerosolized particles are then fractionated in the impactor based on their aerodynamic particle size and collected on the

plates/stages of the impactor. The API deposited on the plates/stages of the impactor is then assayed to obtain the mass of fractionated API and ultimately the APSD.

There is one important aspect to consider for any assessment of the aerodynamic particle size of DPIs, namely that such techniques assume that the total mass of an API on any impactor stage/plate has been deposited as 'API only' particles/particulates. If the mass of the API is not deposited as 'API only' particles then this would mean that any generated APSD may not represent the true APSD of the idealized 'API only' particles, but instead the APSD would be API-excipient assemblies, such as agglomerates. This means that in reality, the pure API particles would be smaller than the agglomerates and therefore theoretically able to penetrate deeper in the respiratory system. The situation is even more complex for combination products, where two or more APIs and/or excipients are present. The physical association of API particles with any excipient particles and/or any of the secondary API particles (in the case of combination products) would constitute an apparent 'growth' of the API particle(s), but without any increase in API mass. Consequently, the aerodynamic particle size of an API-excipient or $API_{(1)}$-$API_{(2)}$ assembly would be expected to be greater, albeit sometimes only marginally, than that of the discrete API particle(s).

The presence of other components in the APSD of mono therapy DPIs evaluated by Srichana and co-workers suggested that lactose was detected in the lower stage of a twin stage impinger from Rotahaler® and Diskhaler® commercial Ventolin® formulations [292]. Thalberg *et al.* confirmed the presence of both lactose and MgSt in the Next Generation Impactor (NGI) stages by investigating the "total fines" in their formulations [15]. This suggests that the excipient in these formulations is indeed aerosolized and emitted from the device. However, the nature of this mass of excipient was not further elaborated in terms of particulate structure i.e., whether the excipient particles were present as discrete excipient only entities, or as some form of API-excipient 'assembly'.

One way to determine the morphology of the API particulates in the APSD of DPIs is the use of Raman chemical imaging to study particles aerosolized from DPIs. For example, it was reported that API-lactose agglomerates were identified as being deposited on NGI impaction plates from DPI formulations [270, 293, 294]. Whilst such studies begin to shed light on the qualitative chemical nature of the particles in the APSD they do not provide quantitative information concerning the nature and composition of any individual particles/particulates, for example, whether particles are single entities or co-associated agglomerates. Indeed, the main challenge to any such investigations is that there is no way to demonstrate that such identified particulate assemblies were not created during impaction, or that, due to the scale of analytical scrutiny particulate assembles are truly co-associated or simply geographically co-located.

Recent scientific advances in aerosol measurement technology are now allowing real possibilities to better understand the aerosol particles, which comprise the APSD and the fate of particles in the lung, for example by scintigraphy [295]. Additionally, it is now possible to visualize, in real time, the fluidization and aerosolization of DPI formulations [296] and to model their behavior using computational fluid dynamics [297]. However, even though such techniques offer further insight into the understanding of behavior of the fluidized and aerosolized powder, they do not provide any information concerning the chemical compositions of the particulates, which could be of particular relevance for any *in vivo* observations and correlations.

The chemical characterization of DPI particulates is achievable using mass spectrometry. The use of mass spectrometry to study aerosols has undergone continual development since the 1970s [33, 241]. These techniques have, like impaction methods, focused on attempting to characterize aerosols by generating the aerodynamic particle size distribution (APSD) profiles of particles. However, advances in technology are providing an increasing level of information about the chemical composition of single aerosolized particles. The first instrument capable of generating aerodynamic particle size and chemical composition for single particles for real-time analysis, the aerosol time-of-flight mass spectrometer (ATOFMS), was initially developed for environmental and air pollution studies [241]. The possibility of utilizing the technique to analyze pharmaceutical inhaled products was investigated by New *et al.* who studied the detection and assessment of co-association in inhalable drug particles using ATOFMS [37]. More recently,

the technique was further developed and improved for the specific characterization of single aerosol particles, namely single particle aerosol mass spectrometry (SPAMS). SPAMS has, in contrast to ATOFMS, a very high data acquisition rate and when coupled with chemometric analysis, allows the determination of the chemical composition for the particulates. Importantly for DPIs, the technique is also capable of studying APIs and excipients. The APSD results generated using SPAMS can be transformed and compared to APSD data generated using cascade impactors. But importantly, SPAMS allows the possibility to evaluate the chemical nature of the particulates in the APSD without the need for offline chemical analysis, such as HPLC [30].

Even though excipients have been detected in the lower stages of impactors, the physical morphology of the deposited excipient is not fully known. For example, it is not clear whether any excipient is present as discrete particles or aggregated with other excipients or to what degree, if any, co-association exists between particles of a mono API and excipient. This is a complex situation, especially when considering that the APSD impacts the efficacious dose of a DPI and any interpretation of the nature of APSD may have both *in vitro* and *in vivo* implications. In the case of combination products, or formulations where more than one excipient is present, the situation is even more complex since multiple particulate interactions are possible. For single excipient based DPI mono therapies, any API detected in the impactor stages/plates could be present as: API only (single API particles or API particle aggregates) or API-excipient assemblies (single or multiple API particle/single or multiple excipient particles; so called "soft-agglomerates").

In the case of combination products, it has been reported that the addition of another API to a mono formulation can affect the *in vitro* and, importantly, *in vivo* performance of one or both APIs [107, 263, 265, 266]. The mechanism for how any potential interactions may impact apparent in-vitro performance has not, so far been elucidated using cascade impaction studies. Preliminary investigations of DPI mono and combination products have suggested that SPAMS is a useful tool for the evaluation of any particle co-associations between APIs (and possibly excipients) and that such approaches may generate results that would otherwise not be available using impactor techniques in terms of the APSD and chemical composition of aerosolized particles [30, 37, 277]. Recently, the possibility of using SPAMS was further expanded to study mono DPI formulations containing a second excipient, a so-called force control agent, namely magnesium stearate [18]. The SPAMS technique allows characterization of the particulate interactions/compositions of the APIs in the APSD of such products, by clearly determining a chemical signature for each component in the agglomerate.

There has been great interest in the development of ternary mixing systems because the addition of a ternary component into carrier-based DPI formulations can lead to improved aerosol performance due to drug-carrier interaction modifications [12-19]. In lactose-based DPI formulations, ternary components can be either lactose fines [20], (other) sugars [21], or force control agents (FCAs) such as magnesium stearate or leucine [13, 15, 16, 18, 22]. Blending lactose together with MgSt prior to adding the API has been shown to modify the performance of pharmaceutical inhaled products [14, 15]. Also pre-treatment of APIs with different FCAs has been shown to alter the performance and improve the drug deposition in the lowest impactor stages [23]. Various application processes such as mechanofusion and particle smoothing have been used to apply different FCAs on carrier particles as very thin coating layers (<10 nm) [22, 24, 25]. Furthermore it has been published recently that a co-milled formulation of BDP and MgSt (5% w/w) led to a significant reduction in agglomerate size and strength after storage at elevated humidity compared to a formulation without MgSt. In addition to an enhanced pharmaceutical performance, another benefit of adding an FCA can be an enhanced stability and therefore a potentially longer shelf life of the product [19, 22].
To investigate particle interactions between API and carrier, Jones *et al.* [225] examined the drug-carrier cohesive-adhesive balance (CAB) ratio in DPI formulations containing different APIs. It was reported in this study that fluticasone propionate is strongly adhesive and salmeterol xinafoate is strongly cohesive with respect to lactose. On the other hand, formoterol fumarate is only slightly cohesive with respect to lactose (the cohesive-adhesive balance for beclomethasone dipropionate has not been published so far). The results of this study suggested that carrier-based

DPI formulation performance is optimized when the drug-carrier CAB ratio is slightly cohesive. A more cohesive drug-carrier CAB ratio would represent a stronger drug-drug cohesion, and relatively weaker drug-carrier adhesion.

In order to investigate product performance and interactions in DPIs and to test the applicability of SPAMS for the study of different DPIs, this study reports the particulate and chemical composition of the emitted particles from two DPI combination products: one containing a single excipient (lactose monohydrate), Seretide® Diskus®, and one containing two excipients (lactose and MgSt), Foster® NEXThaler®, with particular focus on the interactions of the two APIs. It should be noted that in each product two totally different sets of APIs are contained (Foster® NEXThaler®: beclomethasone dipropionate (BDP)/ formoterol fumarate (FF) and Seretide® Diskus®: fluticasone propionate (FP)/ salmeterol xinafoate (SX)). Particle interactions might have a significant influence on the performance of inhaled formulations as for example fine particles show a much faster dissolution *in vitro [76]*. Another aim of this work was to determine the fate of the aerosolized MgSt in Foster® NEXThaler® and whether it also interacts with the APIs in the formulation. The effect on the aerosol performance of the force control agent MgSt in commercial combination DPI formulations was further investigated.

Materials and Methods

Seretide® Diskus® (250/50 mcg) and Foster® NEXThaler® (100/6 mcg) were used for the study. Seretide® Diskus® contains the APIs fluticasone propionate (FP) and salmeterol xinafoate (SX) in a blister and Foster® NEXThaler® contains the APIs beclomethasone dipropionate (BDP) and formoterol fumarate (FF) in a reservoir. The products were stored at room temperature prior to opening the blister pouches and studied at ambient conditions. The analysis was performed within the instruction for use expiry date in the product information documentation. Chemical structures for the APIs FP, SX, BDP and FF; and for the excipients lactose monohydrate and MgSt are given in Table 8.

Table 8: The chemical structures of fluticasone propionate (FP), salmeterol xinafoate (SX), beclomethasone dipropionate (BDP), formoterol fumarate (FF), lactose monohydrate and magnesium stearate (MgSt).

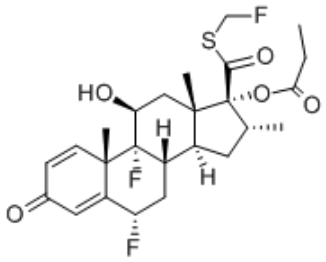	Fluticasone propionate (FP) $C_{25}H_{31}F_3O_5S$ MW 500 g/mol
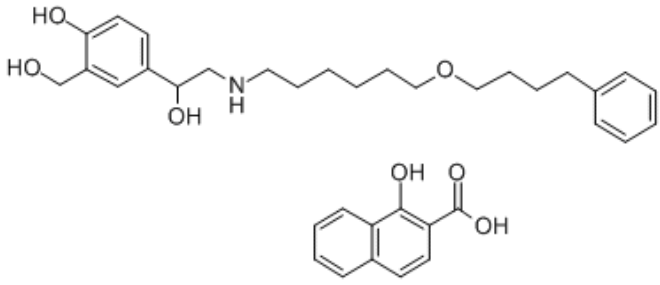	Salmeterol xinafoate (SX) Salmeterol $C_{25}H_{37}NO_4$ MW 415 g/mol Xinafoate $C_{11}H_8O_3$ MW 188 g/mol

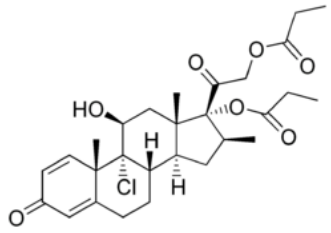	Beclomethasone dipropionate (BDP) $C_{22}H_{29}ClO_5$ MW 521 g/mol
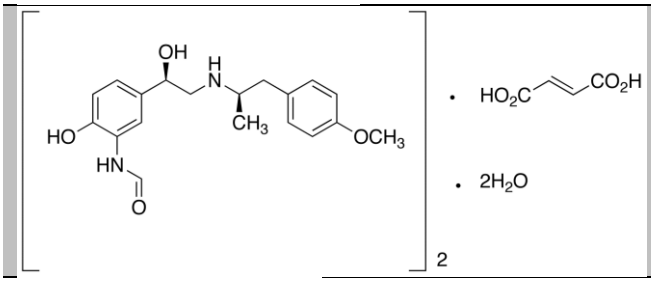	Formoterol fumarate (FF) Formoterol $C_{19}H_{24}N_2O_4$ MW 344 g/mol Fumaric acid $C_4H_4O_4$ MW 116 g/mol
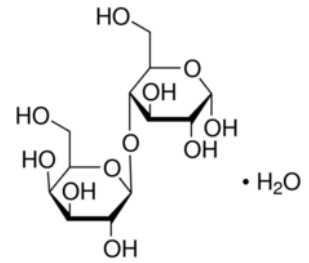	Lactose monohydrate $C_{12}H_{22}O_11$ MW 342 g/mol
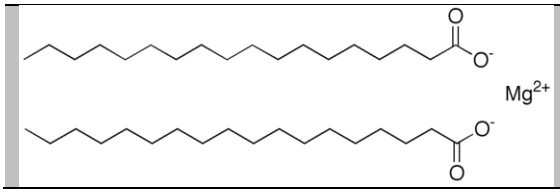	Magnesium stearate (MgSt) $Mg(C_{18}H_{35}O_2)_2$ MW 591 g/mol

Single Particle Aerosol Mass Spectrometry / DPI Testing by SPAMS

A SPAMS 3.0 (Livermore Instruments Inc., USA) was used for this study. The experimental setup of the SPAMS instrument and sample testing has been described earlier by Morrical *et al* [30] and Jetzer *et al* [248]. For the calibration of the SPAMS instrument in the region of 0.1-10 μm, polystyrene (PLS) microspheres (Thermo-Fisher Scientific, USA) were used. The DPI samples were acquired by actuating the inhaler device via an induction port through a pre-separator into the relaxation chamber. The induction port was connected to a pre-separator (Copley Scientific, UK), which was filled with 15 mL of water and then connected to the 4 L relaxation chamber. This assembly of pre-separator and relaxation chamber was then fitted to the SPAMS inlet. The primary purpose of the pre-separator was to filter out coarse lactose carrier particles (>10 μm) to prevent clogging of the SPAMS inlet interface. The sampling chamber allows for dilution of the particles and flow rate matching. The NEXThaler® and Diskus® have similar device resistances, and at a 4 kPa pressure drop and a 4 L test volume would require test flow rates of 55 L/min and 67 L/min respectively [35]. Since it is reported that Seretide® and NEXThaler® are relatively unaffected by flow rate, a test flow rate of 60 L/min was used for both devices [35]. The actuation of both DPI devices was made three times with a 4 sec. draw of air into the relaxation chamber, at a flow rate 60 L/min (i.e. 4 L of air drawn). The same number of particles was analyzed for each sample run (*ca.* 10'000 individual particles each). SPAMS experiments were alternated with background blank runs for one minute each.

Previous studies have been performed to investigate optimal parameters for pMDI and DPI measurements by SPAMS [30, 247, 277]. Based on these studies, the desorption/ionization laser was set to fire at a wavelength at 248 nm. In the configuration being operated, the SPAMS is able to analyze up to 64 particles per second (laser repetition rate 64 Hz). The laser energy was maintained at approximately 12 mJ per pulse to obtain a high and consistent acquisition rate of particles with mass spectral data. It is important to note that the SPAMS interface is known to size bias in favor of larger particles and that that bias was not accounted for in this work. Nevertheless, the relative differences in the aerodynamic particle size distribution (APSD) histograms can be evaluated for all tested formulations with SPAMS.

Results and Discussion

The Foster® NEXThaler® and Seretide® Diskus® are both co-formulated multi-dose combination product DPIs, containing two APIs, with the Foster® NEXThaler® being a reservoir product, and the Seretide® Diskus® consisting of a single blister strip containing single dose blisters of the formulation. Both products contain the excipient lactose monohydrate; however, the Foster® NEXThaler® contains the additional excipient MgSt as force control agent, the so-called 'dual excipient platform' [19]. Foster® NEXThaler® is equipped with a breath-actuated mechanism while Seretide® Diskus® is a regular device (contains no such feature). Additionally, the products have shelf-lives of 18 months and 36 months for Seretide® Diskus® and Foster® NEXThaler® respectively and can be stored at room temperature, suggesting they are stable pharmaceutical products.

Figures 1-8 show mass spectra of particles acquired from the tested combination DPI formulations Seretide® Diskus® and Foster® NEXThaler® acquired with SPAMS. Lactose and MgSt are not easily ionized at a wavelength of 248 nm using the SPAMS technique, therefore pure lactose and MgSt will not give a mass spectrum (Figures 7 and 8). However, it was found that if MgSt is co-associated with certain APIs, a large peak at M/Z=+24 (for Mg^+) will be detected in the mass spectral data (Figure 40 and Figure 44). For sizing, the majority of excipient particles is larger than 10 μm and thus is not analyzed. The relative number of excipient particles <10 μm depends on the lactose grade and dosage strength of the API(s).

The first step in characterizing the acquired data is the removal of particles where a sizing event was recorded but no corresponding mass spectrum was observed. The remaining particles that generate both sizing and mass spectral data are referred to as "hit" particles, whereas particles with only sizing data acquired are referred to as "missed" particles. The hit rate in this work is defined as the ratio between the number of particles that generate ions detectable by mass spectrometry when the D/I laser has fired versus the total number of particles sized in the same time period.

The hit rate with SPAMS was at 43% for Foster® NEXThaler® and 81% for Seretide® Diskus®. The different hit rates for the two different DPI products is dependent on several factors: A higher dosage strength in the product will generally result in an increase in the hit rate, if the API has relatively good absorption of the desorption/ionization laser. Excipients in a formulation, such as (fine) lactose or MgSt, will significantly decrease the hit rate because of dilution.

Interestingly, the hit rate for Foster® NEXThaler® (43%) is relatively high when comparing the dosage strength to Seretide® Diskus® and knowing there are fine excipient particles in the formulation. In Seretide® Diskus® a lactose type with a very narrow particle size distribution of approximately 50-100 μm was used by the manufacturer [298] thus minimizing the number of fine lactose particles present in the formulation to form agglomerates. In the experiments reported here, a pre-separator was used to cut off particles with an aerodynamic diameter above 10 μm. Thus, the hit rate for Seretide® Diskus® was very high since nearly all of the particles with an aerodynamic diameter below 10 μm were API particles. A possible explanation why the hit rate is reduced to 81% in Seretide® Diskus® could be that during DPI actuation some smaller lactose particles may be formed through particle collision, abrasion and shear forces. Last but not least, the ionization efficiency of each API itself plays an important role.

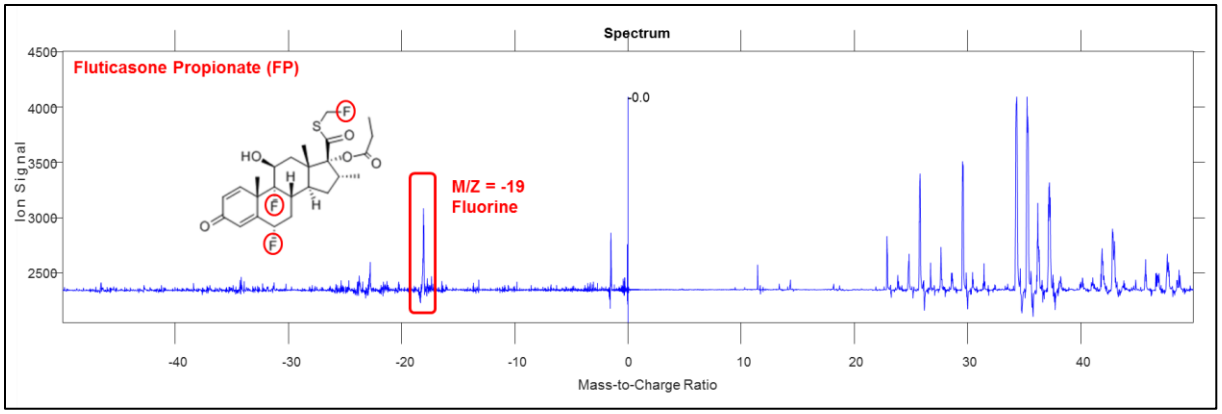

Figure 37: Mass spectrum of a single FP particle from Seretide® Diskus®.

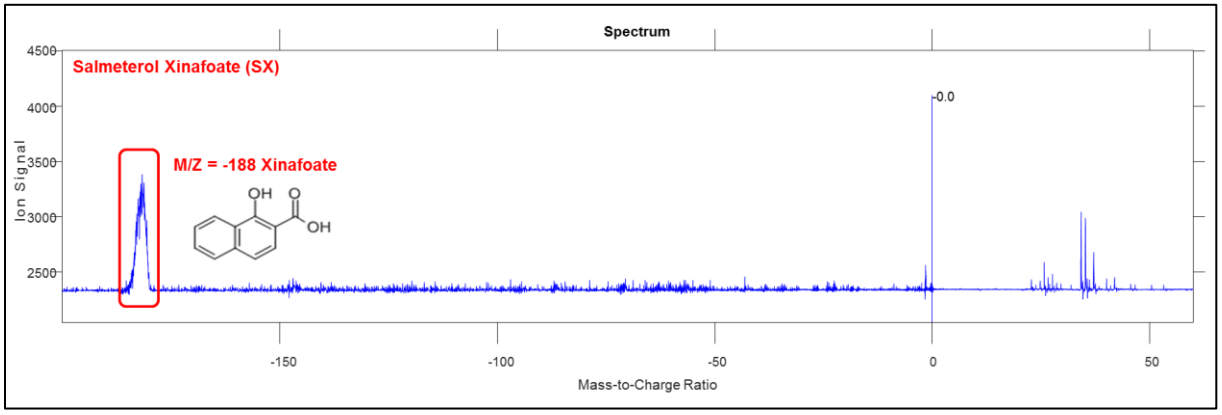

Figure 38: Mass spectrum of a single SX particle from Seretide® Diskus®.

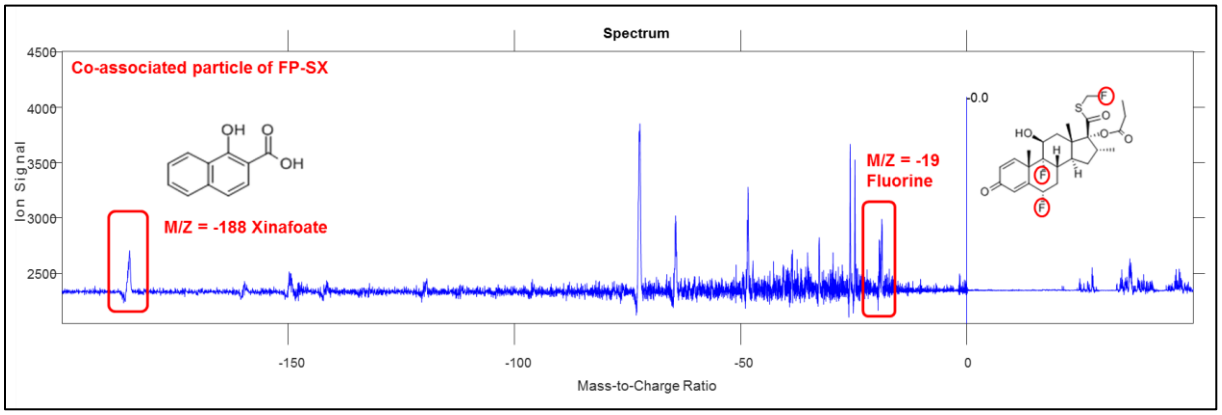

Figure 39: Mass spectrum of co-associated particles of FP and SX from Seretide® Diskus®.

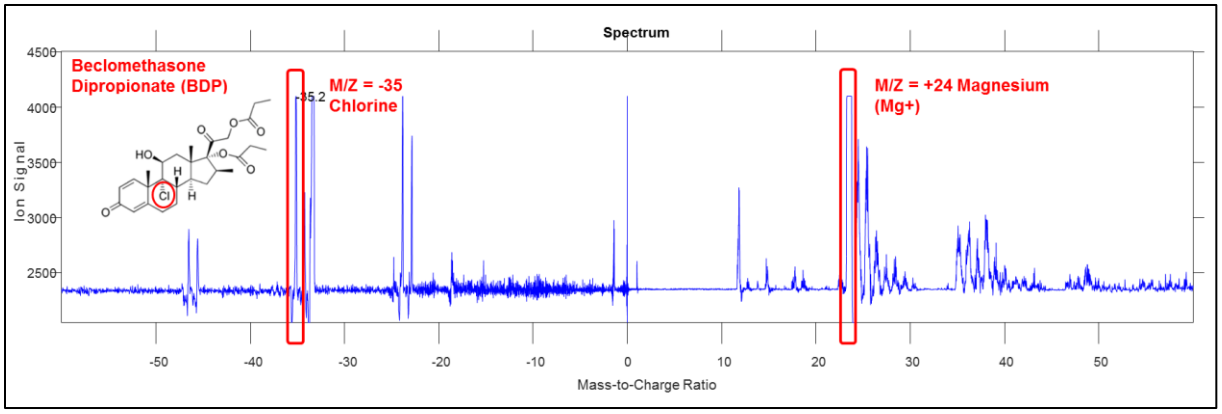

Figure 40: Mass spectrum of a single BDP particle from Foster® NEXThaler®.

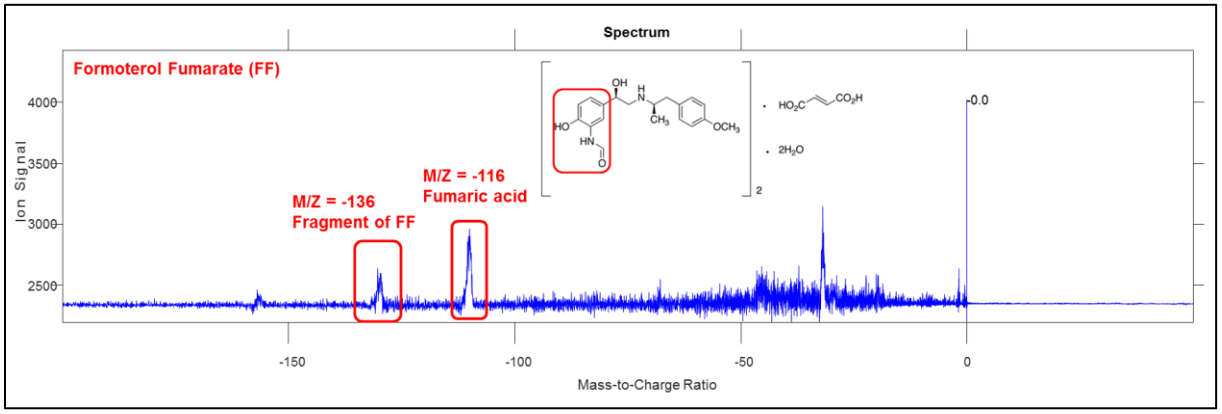

Figure 41: Mass spectrum of a single FF particle from Foster® NEXThaler®.

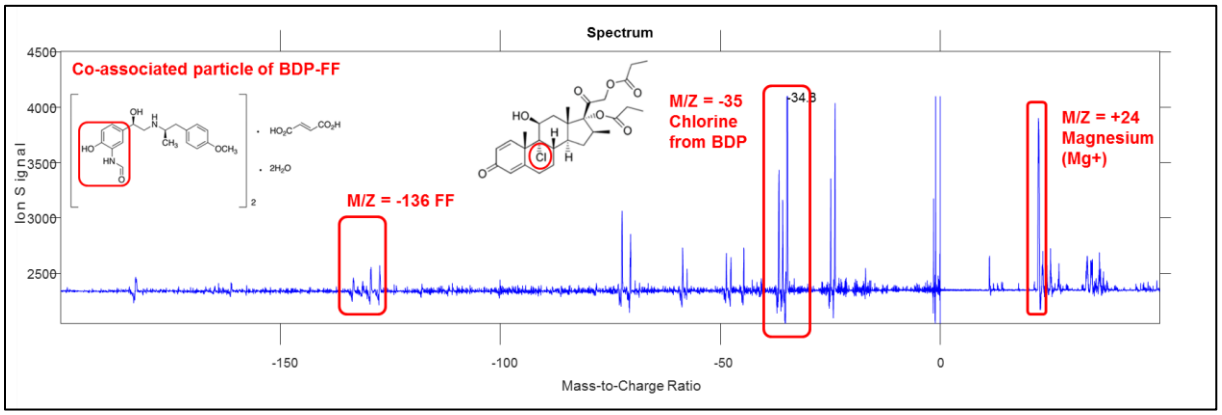

Figure 42: Mass spectrum of co-associated particles of BDP and FF from Foster® NEXThaler®.

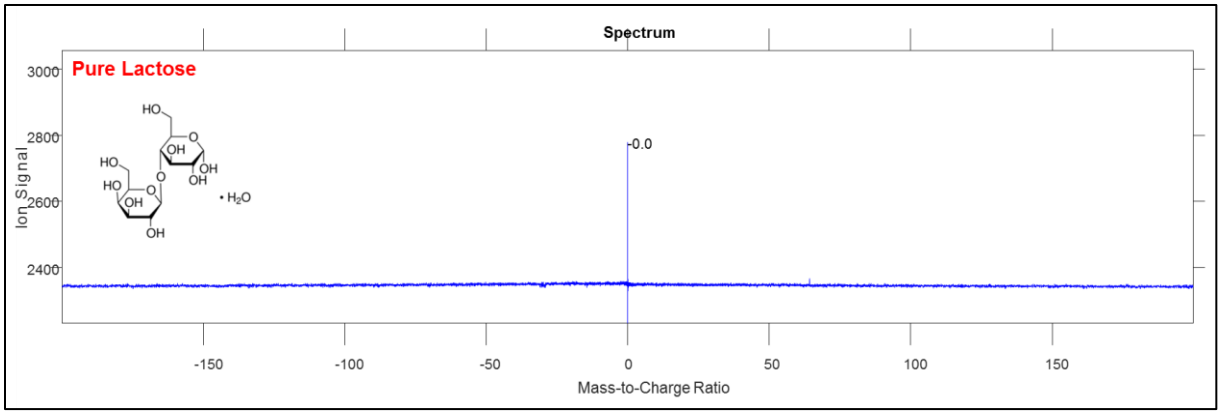

Figure 43: Averaged mass spectrum of pure lactose monohydrate.

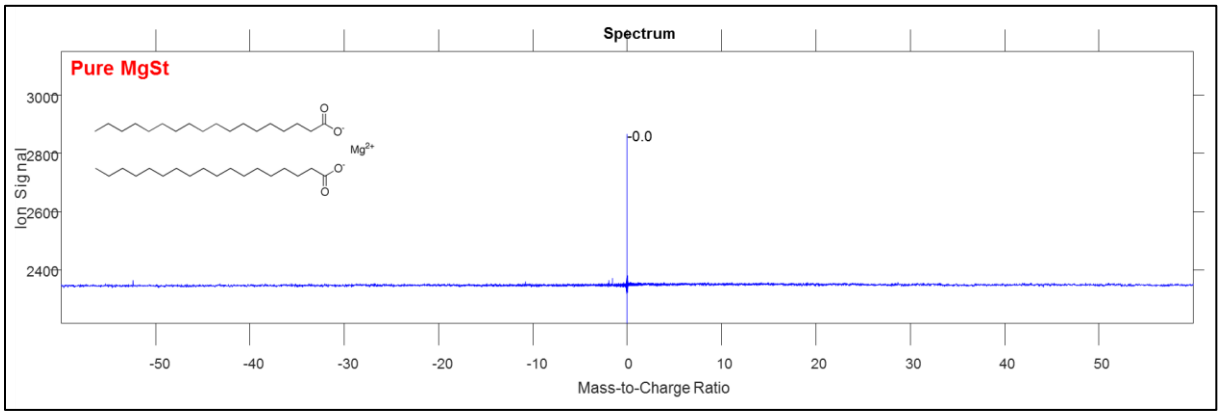

Figure 44: Averaged mass spectrum of pure MgSt.

The pharmaceutical performance of both products has been reported [35]. The delivered dose, fine particle mass (FPM), fine particle fraction (FPF, % loaded dose) determined by NGI/HPLC are presented in Table 9. Additionally, similar data is presented for the extra-fine FPM (particles <2 µm in size) for each API in both products.

Table 9: Pharmaceutical performance of Seretide® Diskus® and Foster® NEXThaler® at a flow rate of 60L/min, total inhalation volume, 4 L. Data adapted from [35].

Product	API	Loaded dose [µg]	Delivered Dose [%LD]	FPM <5µm [µg]	FPF <5µm [%LD]	eFPM <2µm [µg]	eFPF <2µm [%LD]
Seretide®	FP	250	92	52.9	21	29.9	12
Diskus®	SX	50	96	9.3	19.3	2.4	5
Foster®	BDP	100	88	58.4	58	46.6	46
NEXThaler®	FF	6	80	3.4	56	2.3	38

It can be seen from Table 9 that even though both products are established commercial products, the pharmaceutical performance is markedly different with Foster® NEXThaler® not only generating a higher FPF (<5 µm) but also, interestingly, a higher relative eFPF (<2 µm). Such a relatively high fine particle fraction has been assigned to the presence of the breath-actuated mechanism in Foster® NEXThaler® by Chiesi [299]. In a very recent published article by Farkas *et al.* [299] it is reported that the breath-actuated mechanism in Foster® NEXThaler® leads to a reduction of emission of larger particles (lower upper airway deposited doses) and an increase in the available therapeutic fine

particle fraction resulting in a significantly higher lung dose. The breath-actuated mechanism is delaying the emission of the drug until the inhalation flow rate of the patient is sufficiently high to detach the drug particles from their carriers. The generation of such a high FPF would also indicate that the interparticulate interactions are such that they allow a very high level of detachment. It has been demonstrated as well that the breath-actuated mechanism is capable to provide a reproducible and similar emitted dose and FPF of FF and BDP when activated using inhalation profiles of asthmatic patients. The results decreased when a capsule inhaler was employed [300].

Several DPI have been commercialized containing the two excipients lactose monohydrate and magnesium stearate [19], but there is to date no public information for any pharmaceutical performance or rationale, such as stability, processing or manufacturing for choosing this dual excipient approach in commercial products. It has been reported that MgSt can act as a force control agent and modify the performance of DPI formulations [194]. It is interesting to note that the FPM (<5 µm) of the capsule based mono therapy product Seebri® Breezhaler®, which also contains the excipients lactose monohydrate and MgSt, is reported to exhibit a FPF_{LD} of 40-66% based on a loaded dose of 50 µg of glycopyrronium [301]. These levels of FPF_{LD} are comparable with those reported for Foster® NEXThaler®, albeit with different APIs.

Although it has been reported that MgSt can behave as an effective force control agent to potentially improve product performance [15, 194, 195], any apparent differences in performance may also be due to the particle size of the APIs and lactose monohydrate, manufacturing process, dosing and API/excipient ratios etc.

The SPAMS APSD and chemical composition of particles in the aerosolized DPI doses results for Seretide® Diskus® and Foster® NEXThaler® are presented in Figure 45 and Figure 46, respectively. The APSD results summary of data generated from SPAMS is presented in Table 10. It can be seen from Table 10 that for Seretide® Diskus® and Foster® NEXThaler® the number of API particles determined with the SPAMS technique is in general agreement with the reported impaction data (Table 9). The number of particles measured with SPAMS displays for both tested products a similar proportionality to loaded dose as cascade impaction tests (co-associated particles influenced the ratio only minimal) (Table 11). Furthermore, the SPAMS results seem to confirm the results obtained with the cohesive-adhesive balance (CAB) technique as the FF performance is extremely high (FF is slightly cohesive with respect to lactose) [225].

Table 10: SPAMS APSD results for Seretide® Diskus® and Foster® NEXThaler® at a flow rate of 60L/min, total inhalation volume, 4 L. Number of particles measured in total. Average (n=3) of 10240 particles ± SD.

Product	API(s)	Loaded dose (µg)	Number of particles <5 µm	Number of particles <2 µm
Seretide® Diskus®	FP	250	3805 ± 105	488 ± 21
	SX	50	998 ± 29	76 ± 6
	Co-associated particles (FP+SX)	-	2743± 63	594 ± 34
Foster® NEXThaler®	BDP	100	2865 ± 79	1121 ± 28
	FF	6	181 ± 9	142 ± 5
	Co-associated particles (BDP+FF)	-	8 ± 1	3 ± 0

It can be seen in Figures 37-42 that the SPAMS technique has appropriate specificity and is capable of identifying the 2 APIs in the APSDs of each of the formulations. However, in terms of compositions of the particles/particulates in the APSDs it appears that the interactions between the 2 APIs in both products are very different. Both APSDs containing single API, however Seretide® Diskus® appears to contain a significant number of co-associated drug particles compared to NEXThaler®. This result, like the differences in the pharmaceutical performance, is somewhat

unexpected and could be a consequence of the presence and the way MgSt is used in the formulation in Foster® NEXThaler®. Besides the manufacturing and processing with the MgSt in the Foster® formulation, there are a number of other contributing factors such as the API properties, lactose monohydrate properties and the breath actuated mechanism (in Foster® NEXThaler®). It should be noted that in each product two totally different sets of APIs with different dosage strengths are contained (Foster® NEXThaler®: 100 mcg BDP and 6 mcg FF / Seretide® Diskus®: 250 mcg FP and 50 mcg SX).

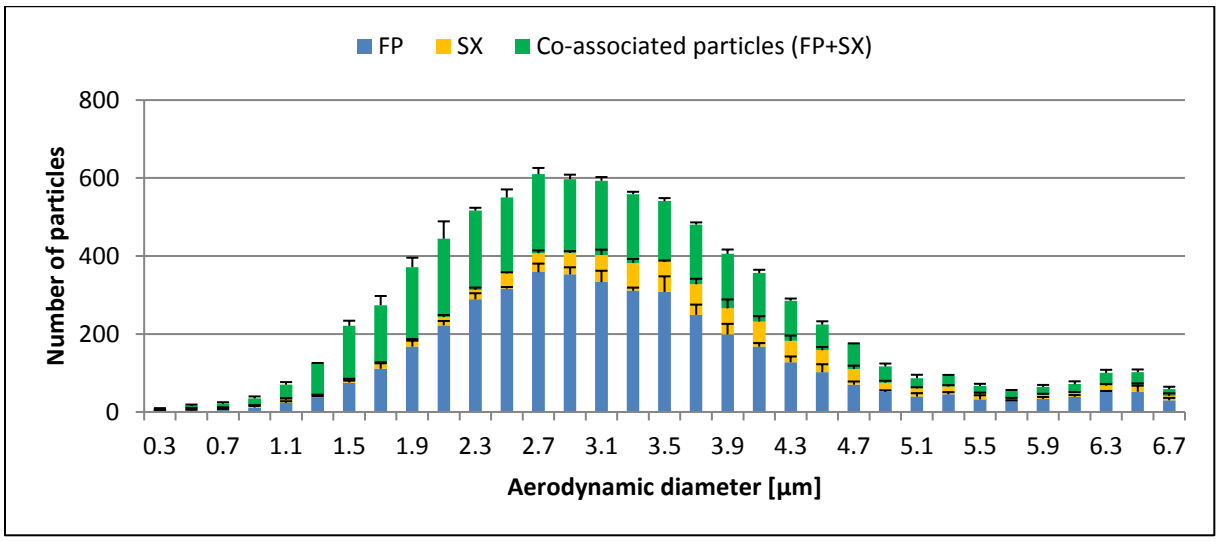

Figure 45: APSD Seretide® Diskus® DPI (250/50 mcg) obtained by SPAMS (n=3 DPI actuations; error bars represent one standard deviation). The plot shows the distribution of number of particle co-associations (FP+SX), pure FP and pure SX.

Figure 45 illustrates the APSD of the two APIs in Seretide® Diskus® and suggests that the APIs exist as single API particles or as co-associated API particles. The APSD histogram shows the fractionation of the "hit" particles and the collected data demonstrates that there are a high number of co-associated particles (37%) emitted (Table 11).

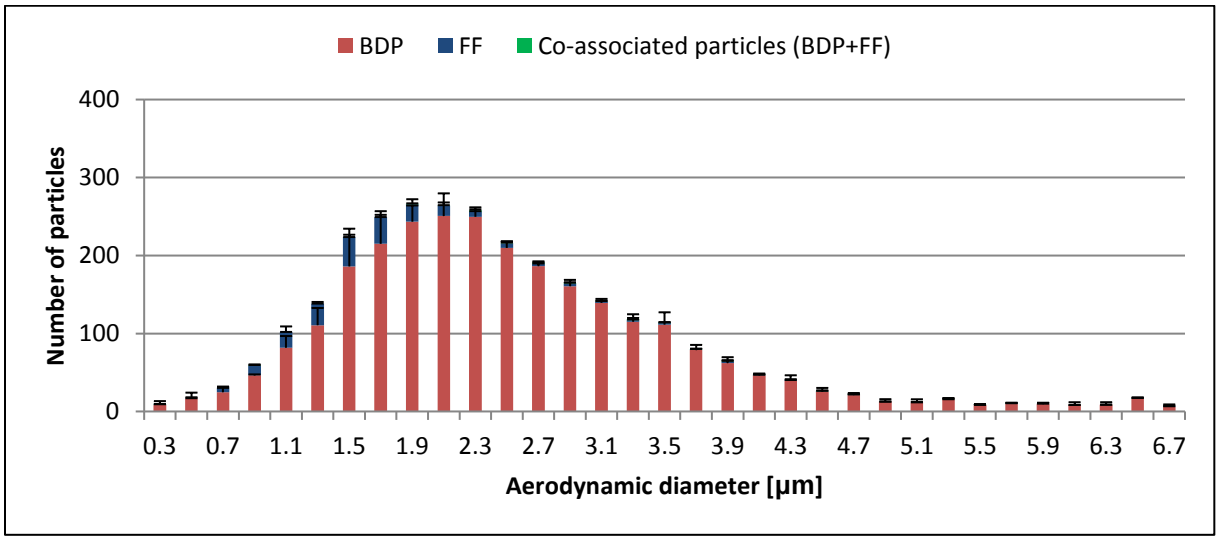

Figure 46: APSD of Foster® NEXThaler® (100/6 mcg) obtained by SPAMS (n=3 actuations; error bars represent one standard deviation). The plot shows the distribution of number of particle co-associations (BDP+FF), pure BDP and pure FF.

Figure 46 shows the APSD determined by SPAMS of the two APIs BDP and FF in Foster® NEXThaler® as single API particles or co-associated API particles. It is clearly evident that there are significant differences between the two tested products. In contrast to Seretide® Diskus® there appears to be only a negligible number of co-associated API particles (<1%) in Foster® NEXThaler® with the vast majority of the particles being present as single API particles (FF) or in co-association with MgSt in case of BDP (Table 11 and Figure 40).

Table 11: Percentage of individual particles measured in the DPI products (10'240 particles per run).

[%]	Seretide® Diskus®	[%]	Foster ® NEXThaler®
FP	51.3	**BDP**	92.6
SX	11.8	**FF**	7.0
FP-SX co-associated	36.9	**BDP-FF co-associated**	0.4

Table 12 shows the mean aerodynamic diameter (MAD, number average from SPAMS APSD measurements) measured with SPAMS. Generally, the MAD of the individual APIs and co-associated particles in Foster® NEXThaler® seem to be much smaller than these from Seretide® Diskus®. Similarly, the overall MAD of the Foster® NEXThaler® DPI was measured to be much smaller than Seretide® Diskus®.

Table 12: Median aerodynamic diameter (MAD [um], number average from SPAMS APSD measurements) calculated from the DPI products measured by SPAMS.

	Seretide® Diskus®		Foster ® NEXThaler®
FP	3.1	**BDP**	2.3
SX	3.7	**FF**	1.5
FP-SX co-associated	3.0	**BDP-FF co associated**	2.5
Overall	3.1	**Overall**	2.1

For Seretide® Diskus®, the API particulates in the aerosolized dose may consist of 6 simplistic particulate states: API_{FP} (single particles and assemblies), API_{SX} (single particles and assemblies), API_{FP}-API_{SX} assemblies, API_{FP}-lactose assemblies, API_{SX}-lactose assemblies and API_{FP}-API_{SX}-lactose assemblies. Normally lactose and MgSt do not give any mass spectral signals when using a D/I laser wavelength of 248 nm (Figure 43 and Figure 44). In this case, only the size of the particle is then recorded and it is classified as a "miss".

This study has shown that SPAMS can detect MgSt if it is (co-)associated with API. A large peak at m/z +24 for Mg^+ is present in the mass spectrum of an API particle that also contains or is associated with MgSt. In addition to using mass spectrometry to determine the API APSD contents, it was also used to investigate the chemical composition of any MgSt in the single API particles in APSD of Foster® NEXThaler®. The results are presented in Figure 6 and 7 for BDP and FF, respectively. It can be seen from Figure 6 that the large peak at m/z 24 is present in single BDP particles, but not in the FF particles. This was compared to a pure BDP pMDI measured with SPAMS where no peak at m/z 24 was measured (data not shown).

It has been reported that the formulation in Foster® NEXThaler® is constituted of a coarse lactose (212–355 µm) blended with a micronized lactose/MgSt mixture [35, 302]. Even though quantification of the relative Mg-content is not possible, it is clear from this study that MgSt is in some way 'associated' with BDP, but apparently not with FF in the Foster® NEXThaler®. However, it cannot be ascertained whether the MgSt has simply 'transferred' to the BDP particles during actuation, storage or processing. It has also been reported that if any additional MgSt is added in any other part of the manufacturing process to either the carrier or API itself, such as in co-milling [303] or mechanofusion

[23] of API and MgSt, also leads to improved fine particle performance. Last but not least, the device itself can play an important role in aerosolization and de-agglomeration mechanisms of the product as mentioned before.

It is clear from the composition selected APSD profiles (impactor and SPAMS results) that the aerosolized formulation in Foster® NEXThaler® not only exhibits a higher NGI generated FPF_{LD} but may also be engineered/manufactured with MgSt in such a way as to reduce the level of co-association between APIs, with MgSt also contributing to this effect. This is in stark contrast with the Seretide® formulation which has a lower FPF_{LD} and does not contain MgSt and has very high levels of co-association. Adding fine lactose to the blend as an excipient will presumably reduce the level of co-association by acting as a diluent. But adding lactose might increase the likelihood of particle co-association between fine lactose APIs which are adhesive with respect to lactose (such as for example FP) and thus increase particle size. Any reduction in co-association and/or API/excipient agglomeration will decrease the aerodynamic particle size distribution of the particulates, which is observed in the Foster® NEXThaler® both using an impactor and the SPAMS measurements.

Importantly, if the generation of a relatively high eFPF is possible in a DPI, as observed with the NEXThaler®, then these particles may reach the lower part of the airways. This has been reported for the pMDI version of Foster [304]. It also appears that an effort was made to limit the interactions of API in the Foster® NEXThaler® DPI formulation to achieve a high eFPF. A pre-treatment of the APIs and/or the carrier with a force control agent can furthermore facilitate drug detachment overall and thus increase *in vitro* aerosol performance [15, 23, 195].

This study demonstrates that combination DPIs, which are developed using "force control" agents such as MgSt in addition to carriers such as lactose monohydrate, may exhibit improved relative pharmaceutical performance, as measured by FPF. This effect is in addition to the function of the force control agent MgSt on single API formulations which has been demonstrated extensively in literature. Additionally, the increasing use of MgSt in other commercial products, such as in Anoro® Ellipta®, Relvar® Ellipta® or Seebri® Breezhaler®, suggest that the use of MgSt with lactose monohydrate is in part also responsible for enhanced pharmaceutical performance and becoming a standard approach in the development of DPI products [301, 305].

Conclusions

There are distinct differences in the relative *in vitro* pharmaceutical performance of Foster® NEXThaler® and Seretide® Diskus®. Foster® NEXThaler® generates a higher fine particle fraction for both APIs (FPF <5 μm) and furthermore also emits a significantly higher relative eFPF (extra fine particle fraction <2 μm). SPAMS was able to successfully distinguish and characterize the two different formulations in the range of 0-10 μm where a much higher number of particles with a small MAD were detected from Foster® NEXThaler® compared to Seretide® Diskus®. Furthermore, SPAMS showed that both products emit APIs in different relative particulate states and particulates with distinctly different characteristics, suggesting that the interactions between the APIs and excipients in both tested combination products are very different. The Seretide® APSD profile contained a relatively high number of co-associated API particles of FP and SX. As there is no fine lactose in the Seretide® Diskus® formulation, the co-associated particles are formed of APIs without any excipient particles involved. The Foster® NEXThaler® formulation only exhibited a negligible number of co-associated API particles of BDP and FF. Interestingly, large peaks for the presence of magnesium stearate (m/z=+24) were detected in the mass spectra of beclomethasone dipropionate in Foster® NEXThaler®. This would suggest that the BDP particles in Foster® NEXThaler® are somehow co-associated with MgSt (but not with FF). It is possible that in the manufacturing process BDP was processed (co-milled) together with MgSt to improve dispersion mechanics. Another explanation may be that the BDP or the lactose carrier are receiving a MgSt-coating that would prevent the co-association or agglomeration of the particles and moreover facilitate detachment from carrier. This would then result in high *in vitro* performance (eFPF) and a relatively fine APSD profile compared to a product not engineered in this way like the Seretide® formulation. It is not possible to explain this as being simply due to the presence of MgSt. However, since MgSt has been described as being a FCA in DPI

formulations, it is possible that this ternary excipient is indeed capable of affecting the interparticulate forces in DPI formulations resulting in high *in vitro* performance.

These studies suggest that the SPAMS technique may be used to investigate the nature of API particulates and provide feedback control for the level of particle co-association (API-API or API-excipient) in early-phase development of inhaled products. A SPAMS with separate desorption and ionization lasers firing at a different wavelengths could potentially detect co-associations not only between APIs, but also between API and excipients (lactose or force control agents) [283]. This makes the SPAMS technique an attractive additional technique in the field of pharmaceutical aerosol analysis and complementary to the current standard of impactor/HPLC-analysis.

Acknowledgements

This work was funded by Novartis Pharma AG's internal research funds.

4. Investigations on the Mechanism of Magnesium Stearate to Modify Aerosol Performance in Dry Powder Inhaled Formulations

Jetzer et al. Journal of Pharmaceutical Sciences (2018) 107:984-998

Abstract

The potential of the force control agent (FCA) magnesium stearate (MgSt) to enhance the aerosol performance of lactose-based dry powder inhaled (DPI) formulations was investigated in this study. Two different blending methods of lactose and MgSt have been examined. Excipient-blends were manufactured either by high-shear or low-shear blending lactose carrier with different amounts of MgSt in the range from 0-10% (w/w). Fluticasone propionate (FP) and salmeterol xinafoate (SX) were used as model APIs. The excipient blends were investigated with analytical techniques including time-of-flight secondary ion mass spectrometry (ToF-SIMS) and Single Particle Aerosol Mass Spectrometry (SPAMS). Particle size, morphology and surface properties were evaluated. The *in vitro* aerosol performance in terms of aerodynamic particle size distribution (APSD) and fine particle fraction (FPF) of the FP and SX DPI formulations were evaluated with the Next Generation Impactor (NGI) and also with SPAMS using a Breezhaler® inhalation device. The distribution of MgSt on the lactose carrier in the blends was visualized and found to depend strongly on the blending method. This affected drug particle detachment from the carrier and thus impacted aerosol performance for FP and SX. Compared to blends without FCA, low-shear blending of MgSt increases the FPF of the model drug SX, while high shear blending significantly increased FPF of both SX and FP. The interactions between drug and carrier particles were substantially affected by the choice of blending technique of MgSt with lactose. This allows detailed control of aerosol performance of a DPI by an adequate choice of the blending technique. SPAMS successfully demonstrated that it is capable to distinguish changes in DPI formulations blended with different amounts of MgSt and additional information in terms of dispersibility of fine particles could be generated.

Introduction

Dry powder inhalers (DPIs) are a widely used method of aerosol drug delivery for the local treatment of respiratory diseases. DPI products commonly consist of large carrier particles (usually alpha-lactose monohydrate) and a relatively small amount (0.05–10%) of micronized active pharmaceutical ingredient (API) having a particle size typically below 6 μm. The addition of a carrier particle has the effect of preventing agglomeration of cohesive APIs, improving the respirable fraction by facilitating drug aerosol formation, and acting as a bulking agent increasing powder flowability for uniform filling [7]. Extensive research in the field of DPI formulations has been conducted in the past 40 years; however, the development of DPI formulations still presents multiple challenges [138]. Deposition of an aerosol particle in the respiratory tract depends on many factors but the most important parameter in a DPI formulation is the particle size of the drug substance, which has to be tailored to give deposition at the desired locations within the lung [167]. Particle size analysis is required to assure the performance and reproducibility of the final dosage forms and drug delivery systems [306]. A variety of factors such as particle size and size distribution, shape, surface morphology (roughness) and surface energy can be critical, of which many are directly or indirectly connected with each other [171, 172, 178, 181, 307, 308]. In addition to the formulation composition and material properties, the choice of blender, order of mixing of ingredients, the process parameters and storage also play an important role [7, 143, 181, 182, 309].

The addition of lactose fines and/or functional additives such as magnesium stearate (MgSt) as a ternary force control agent (FCA) make DPI systems even more complex [14-16, 20, 310]. Even a small amount of formulation components can potentially have a big influence on the performance of the DPI product due to their impact on surface characteristics. They play an important role in particle interactions between excipient and API. Particle co-associations can occur between API and excipient, but also between two or more APIs in a formulation and may affect the *in vitro*

and possibly clinical performance of combination products [30, 38, 277]. The presence of fine lactose particles in a DPI formulation improves the formulation performance in terms of delivered dose and fine particle fraction up to some extent. Numerous articles on the topic of adding lactose fines to coarse carrier with different blending methods have been published over the last years [15, 16, 20]. Surface modifications of carrier particles have been reported to improve inhalation performance of DPI formulations [308, 311]. Blending lactose together with a FCA such as MgSt prior to adding the API has been shown to modify the performance of pharmaceutical inhaled products [15, 16]. A number of researchers are investigating the role of FCA's in pharmaceutical inhaled products with different analytical techniques. Various application processes such as mechanofusion and particle smoothing have been used to apply different FCAs on carrier particles [13, 15, 16, 184, 194].

Mechanofusion is a term used for various intensive mechanical dry coating processes. During the mechanofusion mixing process, a very thin coating layer of a material is applied onto a solid surface through high compression and shear forces. Therefore, it can be used to alter the surface characteristics of a host material without using any solvent [184].

The engineering of lactose carrier surfaces using the particle smoothing process resulted in significant differences in surface morphology when compared with the starting material. The mixing process has been proposed to decrease surface irregularities by filling FCA into surface flaws hence eliciting a relative smoothing of the lactose particle surface due to plastic deformation and/or a surface polishing effect by the FCA coating layer. This was measured by a significant reduction in surface area and roughness and was observed with AFM surface topography images [13, 22, 24].

Processed lactose carriers with FCAs have been investigated with different analytical techniques. Inverse gas chromatography (IGC) was used to determine total surface energy distributions [17]. Surface energies of excipient-blends prepared by high- and low-shear mixing have not been compared so far. Studies with atomic force microscopy (AFM) generated information about the surface properties and especially surface roughness of processed carriers in the past [13]. Nevertheless, a thorough mechanistic understanding of the role of FCA's in DPI formulations is still largely missing.

It has been recognized from previous work that there is a need to establish the nature and extent of carrier surface coatings, and for a detailed study of the relationship between the extent and nature of the coating and the particle interactions as well as bulk powder characteristics. This can be very difficult to achieve because of technological challenges of characterizing such thin coating layers on the surface of particles that can be in the range of only nanometers. Conventional techniques such as Raman spectroscopy penetrate the coating layer and measure both, the coating layer and the host particles. Time-of-flight secondary ion mass spectrometry (ToF-SIMS) is a highly sensitive analytical technique that provides chemical information regarding elemental, isotopic and molecular structure from the first few layers of small particles [24, 312]. Therefore, ToF-SIMS was used in this study to further investigate particle coating and MgSt distribution of carriers.

For evaluation of the *in vitro* aerosol performance of inhaled pharmaceutical products, the current state of the art is the use of cascade impaction [250], typically with chemical analysis using high performance liquid chromatography (HPLC), to characterize the aerodynamic particle size distribution (APSD) and fine particle fraction (FPF) of the drug. While highly quantitative for the total concentration of API delivered, this technique does not yield any information regarding the interactions of the various product components (active(s), excipients) with each other within the formulation. SPAMS is an analytical technique where the aerodynamic diameters and chemical compositions of many individual aerosol particles are determined in real-time. The SPAMS technique and its advantages have been published recently [30, 277]. SPAMS is a promising method to explore effects in DPI formulations due to the fact that the APSD of the total number of particles (excipient and API) in the formulation is determined simultaneously.

The fundamental attractive forces/mechanisms of interaction between particles in DPI formulations are classified as van der Waals, electrostatic and capillary forces [7, 196]. Techniques such as IGC, colloid probe and AFM enable the measurement of interparticulate or surface forces at the individual particle level, but due to the lack of understanding of the actual form of bodies in contact such as the contact area and coordination number, the exact description of the powder formulation and the correlation of measured forces with aerosol performance are still challenging. Besides the mentioned adhesion/cohesion forces, friction and mechanical interlocking also play important roles in power flow and deaggregation [197].

The aim of this study was to investigate the impact of the FCA MgSt on the mechanism of interaction and physico-chemical characteristics of the DPI carrier particles and the performance of active substances in pulmonary formulations using engineered excipient blends. A variety of analytical techniques, including for the first time SPAMS and ToF-SIMS, were employed. Blends with the cohesive drug fluticasone propionate (FP) [279] and the adhesive drug salmeterol xinafoate (SX) [225] were manufactured containing 0-10% (w/w) MgSt in the excipient-blend by high- and low-shear mixing. A formulation of FP or SX with untreated lactose (0% MgSt) was used as a reference. Particle size, morphology and surface properties were assessed and the aerosol performance in terms of APSD and FPF of the DPI formulations was evaluated with cascade impaction studies with the NGI and analyzed with SPAMS.

Materials and Methods

Materials

Micronized FP and SX were supplied by Sandoz. Inhalation grade lactose monohydrate (Respitose® ML001) was purchased from DFE Pharma (Netherlands) and inhalation grade magnesium stearate (MgSt) from Peter Greven (Germany).

DPI Formulation Preparation

Batches with a total amount of 50 g of powder (excipient and drug) were manufactured. For the high-shear excipient-blends, inhalation grade lactose and MgSt (0-10% w/w) were blended in a Collette MicroGral 2 L (GEA Pharma Systems, Switzerland) for 16 minutes at 1400 rpm. The low-shear excipient-blend was mixed for 16 min at 34 rpm in a Turbula® T2F mixer 2 L (Willy A. Bachofen AG, Switzerland). In both cases, excipient-blends were mixed together with the API in a Turbula mixer at 34 rpm for 16 min (low-shear blending method). The final powder was filled manually into size 3 Hydroxypropyl methylcellulose (HPMC) capsules (QualiCaps, Spain) containing a dosage strength of 200 mcg API per capsule. The FP capsules were stored at 25°C and 55% relative humidity for a period of 7 days prior to the experiments. The SX capsules were not conditioned because SX showed previously poor stability when exposed to temperature and humidity. Thus, the *in vitro* performance of SX is highly affected by the conditioning of the product [309].

The content uniformity of manufactured DPI capsules was measured by analyzing the quantity of active in 25 mg ± 0.1 mg samples. Drug content was analyzed by HPLC. Relative standard deviation between samples was calculated to assess the homogeneity of the different blends.

Scanning Electron Microscopy (SEM)

The particle morphology of the different powder blends was investigated using scanning electron microscopy (SEM, Zeiss Supra 40, Germany) at 6 keV. The samples were prepared by careful transfer onto double-adhesive carbon tape, and a thin gold layer was deposited on the sample surface using a Leica EM ACE600 (Leica, Germany) prior to imaging.

Time-of-flight Secondary Ion Mass Spectrometry (ToF-SIMS)

Time-of-flight secondary ion mass spectrometry (TOF.SIMS 5, ION-TOF, Germany) was used to detect the chemical composition of surfaces by scanning the sample with a focused ion beam of Bi^{3+} primary ions in spectrum mode using the ion beam with an extractor voltage of 10 kV. The area scanned was 500 x 500 micrometers. The samples were prepared on pieces of silicon wafers with dimensions of 10 x 10 mm. Double sided carbon tape was adhered to the silicon and covered with aluminum backed tape, with the adhesive side up. The powders were then spread over the surface and the excess shaken off. The samples were then fixed on to the ToF-SIMS plate and inserted into the ToF-SIMS vacuum chamber. Negative and positive spectra were measured in spectrum mode. Each sample was measured three times on different areas.

ToF-SIMS is a mass spectrometric technique that provides detailed information on the chemical composition of the uppermost monolayers of a surface. The Time-of-Flight detection system offers the parallel detection of all elements, isotopes, full molecules and molecular fragments present at the surface, with a high mass resolution and an ultra-high sensitivity, down to the ppm range. The acquisition of images can be achieved by scanning the relevant area with a lateral resolution in the range of up to 100 to 200 nm (theoretically) with a complete spectrum recorded at every pixel (256x256 pixels in our measurements) of the image. Layer-by-layer erosion is also possible, allowing the profiling of chemical species in the depth of the sample, with a depth resolution in the nanometer range.

The areas and m/z of the peaks used in determination of the relative amounts of magnesium (m/z 23.99) are given following the images. The relative amounts of magnesium stearate to lactose were calculated using all three fragments CH_3O^+, $C_2H_5O^+$ and $C_3H_5O_2^+$, which were present in the spectrum of lactose but not in the spectrum of magnesium stearate.

The relative amounts of magnesium were calculated from:

$$\frac{\text{Area Mg}}{(\text{Area Mg} + \text{Area of peak assigned to lactose})}$$

This gives a value of 1 when only magnesium stearate is present. Additionally, the spectra were normalized against total ion count.

Specific Surface Area

The specific surface area of the powders was determined by the BET method based on nitrogen adsorption using a Quadrasorb SI (Quantachrome Instruments, USA). Adsorption isotherms at P/P0: 0.01, 0.02, 0.03, 0.04, 0.05, 0.07, 0.1, 0.15, 0.2, 0.3, 0.4, 0.5, 0.6, 0.7, 0.8 and 0.9 were used.

Laser Light Diffraction Measurements

Laser light diffraction (LLD) analysis for particle size distribution (PSD) measurements was always performed using a Sympatec RODOS (Sympatec GmbH, Germany) dry dispersion system equipped with an R5 lens at 3bar.

Density Measurements

The density of the materials used in this study was determined with gas pycnometry (ULTRAPYC 1200e, Quantachrome Instruments, USA) according to the Pharmacopoeia Europea 8.0 (2.9.23)

DPI Analysis by Next Generation Impactor (NGI)

The deposition of the dry powder formulations was investigated using an NGI equipped with a pre-separator filled with 15 mL of solvent (Acetonitrile: Water: TFA, 58: 42: 0.1 v/v/v). All measurements were conducted at 55% RH

and ambient temperature (23 ± 2ºC). The cup trays of the impactor were coated with Brij® reagent (1% v/v solution of Glycerol in Ethanol). The capsules were actuated in a Breezhaler® inhalation device (Novartis, Switzerland) at a flow rate of 90 L/min for 2.7 sec (USP pressure drop of 4kPa). The amount of powder deposited on the different collection cups was recovered by extracting each cup with solvent. The remaining powder in the capsule, device, powder deposited in the throat and pre-separator was also collected. After dissolution of the particles, HPLC analysis was performed. In this study the mean of three individual determinations was taken for a given NGI result.

FP and SX were analyzed using HPLC coupled with an UV-detector. The samples were eluted with an isocratic method with Acetonitrile: Water: TFA (58: 42: 0.1 v/v/v) as mobile phase, through an ACT ACE 3 C18,100 × 4.6 mm, 3 µm column (ACE, UK). A wavelength of 225 nm was used for detecting FP and SX. The peaks eluted at approximately 7.1 min (FP) and 2.0 min (Salmeterol at 2.0 min; xinafoate at 2.9 min). The flow rate through the HPLC system was 1.5 mL/ min. Data acquisition was carried out with Chromeleon. (LOD: 0.01 ug/mL for both FP and SX; LOQ: 0.03 ug/mL for SX and 0.04 ug/mL for FP; R2 0.9995).

Single Particle Aerosol Mass Spectrometry (SPAMS) / DPI Testing by SPAMS

A detailed introduction into Single Particle Aerosol Mass Spectrometry is published in Morrical *et al.* [30].

A SPAMS 3.0 (Livermore Instruments, USA) was used for this study. The experimental setup of the SPAMS instrument and sample testing has been described earlier by Morrical *et al.* [30] and Jetzer *et al.* [248]. For the calibration of the SPAMS instrument in the region of 0.1-10 µm, polystyrene (PLS) microspheres (Thermo-Fisher Scientific, USA) were used. The dry powder formulations samples were acquired using a Breezhaler® inhalation device actuated via an induction port through a pre-separator into the relaxation chamber. The induction port was connected to a pre-separator (Copley Scientific, UK), which was filled with 15 mL of water and then connected to the 4L relaxation chamber. This assembly of pre-separator and relaxation chamber was then fitted to the SPAMS inlet. The primary purpose of the pre-separator was to filter out coarse lactose carrier particles (>10 µm) to prevent clogging of the SPAMS inlet interface. The sampling chamber allows for dilution of the particles and flow rate matching. The SPAMS interface deliberately size biases in favor of larger particles and this bias was not accounted for in this work. Nevertheless, even the biased aerodynamic particle size distribution (APSD) histograms can be informative given that they all have the same bias [248]. The actuation of the DPIs was made with a 2.7 seconds draw of air into the relaxation chamber, at a flow rate 90 L/min (i.e. 4 liters of air drawn). The same number of particles was analyzed for each sample run (ca. 10'000 individual particles each). SPAMS experiments were alternated with background blank runs for one minute each.

Preliminary experiments have been performed to investigate optimal parameters for pMDI and DPI measurements by SPAMS [30, 247, 277]. Both FP and SX have shown previously good absorbance at a wavelength of 248 nm [278]. Therefore, the desorption/ionization laser was set to fire at a wavelength at 248 nm. In the configuration being operated, the SPAMS was able to analyze up to 64 particles per second (laser repetition rate 64 Hz). The laser energy was maintained at around 12 mJ per pulse to obtain a high and consistent hit rate. It is important to note that the SPAMS interface is known to size bias in favor of larger particles and that that bias was not accounted for in this work [313].

Results and Discussion

General Physical Characterization

The PSD of the carrier has a significant influence on the performance of a DPI formulation, especially the fraction with a size below 10 µm that is counted as the "inhalable fraction". Typically more than 90 volume percent of the lactose carrier particles are within 50 and 200 µm. While only a small fraction has a size below 10 µm [12, 314]. Density, particle size data and specific surface area (BET) for all materials are given in Table 13.

Table 13: Materials used and measured key characteristics.

Material	Denotation	Density [g/cm³]	D10 [µm]	D50 [µm]	D90 [µm]	BET [m²/g]
Fluticasone propionate	FP	1.32	0.9	1.9	4.1	9.76
Salmeterol xinafoate	SX	1.11	0.7	1.4	2.9	6.99
Respitose® ML001	Lactose	1.53	6.6	57.8	170.3	0.63
Magnesium stearate	MgSt	1.05	1.6	6.1	21.3	16.61

In Figure 47 and Figure 48, high- and low-shear excipient-blends with differing MgSt-content and the lactose carrier itself are shown for comparison. With a MgSt-content up to 1%, the behavior of the PSD curves does not change significantly compared to the starting material. Adding 10% MgSt to the excipient mixture changed the shape of the curve: A significantly higher number of smaller particles in the range of 2-10 µm are present. The PSD curve is roughly trimodal with both applied blending methods for the 10% MgSt excipient-blends.

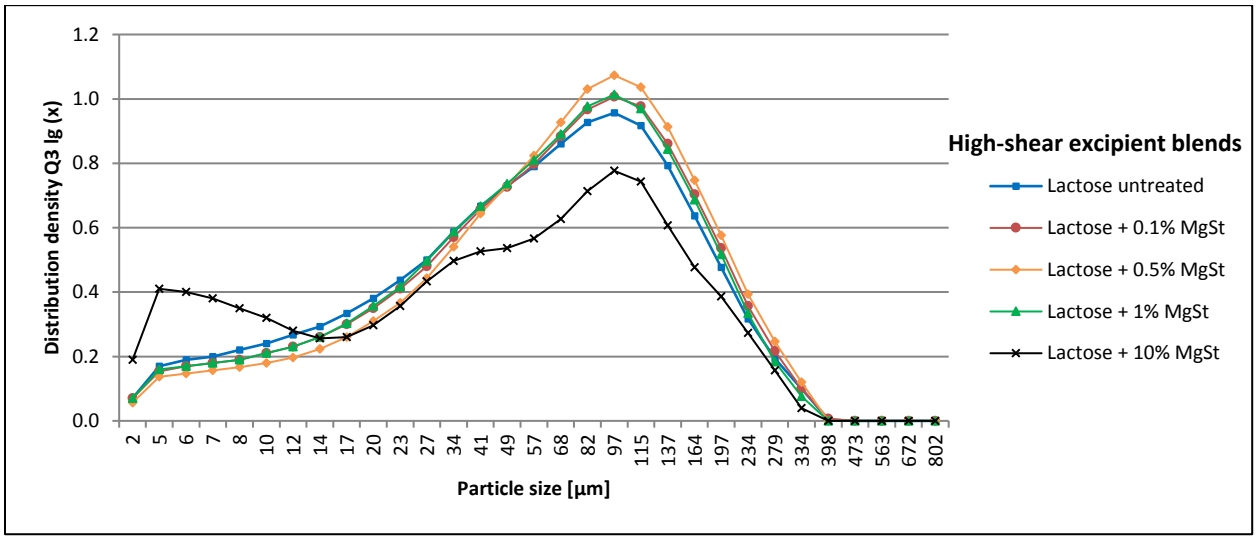

Figure 47: Particle size distribution of high-shear excipient-blends.

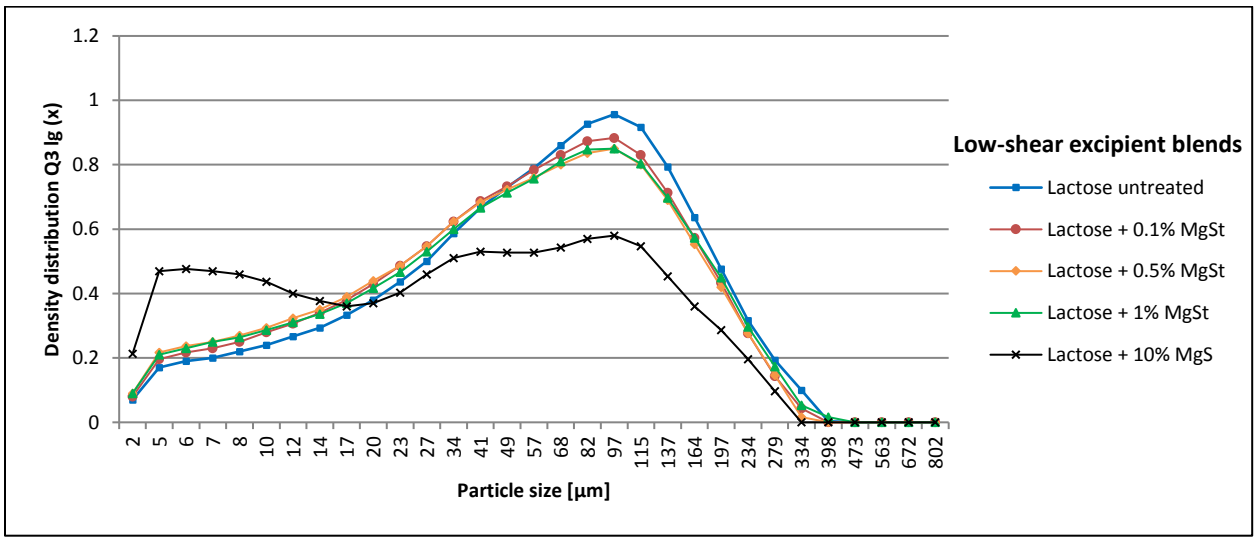

Figure 48: Particle size distribution of low-shear excipient-blends.

Characteristic parameters of PSD of processed excipient-blends are listed Table 14. While the x10, x50 and x90 values slightly increase for high-shear blends (except Lactose 10% MgSt), the values slightly decrease for low-shear blends both compared to lactose untreated (Table 13 and Table 14). These findings suggest that the high-shear mixing process is applying MgSt on the lactose carrier surface and therefore increasing the particle size. With an MgSt-content of 10%, the particle sizes are much lower for both used blending methods due to the introduction of a high number of small MgSt particles in the excipient-blend.

Table 14: Particle size distribution of the excipient-blends (mean, n=3).

High-shear	x10 [µm]	x50 [µm]	x90 [µm]	Low-shear	x10 [µm]	x50 [µm]	x90 [µm]
Lactose 0.1% MgSt	7.57	63.36	176.28	Lactose 0.1% MgSt	5.85	50.44	159.29
Lactose 0.5% MgSt	9.07	69.17	181.62	Lactose 0.5% MgSt	5.24	47.66	156.32
Lactose 1% MgSt	7.40	61.81	171.76	Lactose 1% MgSt	5.24	49.76	164.12
Lactose 10% MgSt	2.65	35.41	152.74	Lactose 10% MgSt	2.45	22.29	130.61

In order to examine changes in surface morphology of lactose before and after mixing with MgSt, scanning electron micrographs (SEM) were taken of all the powders. Representative SEM micrographs of the formulations are shown in Figure 49, Figure 50 and Figure 51.

The untreated lactose consists of large irregular shaped particles together with an amount of fine lactose particles. Some small particles were observed to adhere onto the surface of larger particles or to exist as agglomerates. Flat and smooth surfaces with sharp edges were clearly seen in SEM of untreated lactose. Pure MgSt particles were small (<20 µm size) and existed as multilayered flakes (Figure 49). When lactose was high-shear mixed with MgSt, the edges of larger particles became noticeably more rounded, and the characteristic MgSt flakes were not obviously visible (Figure 50). The SEM images of the excipient-blends containing a lower amount of MgSt (0.1-0.5%) were similar and did not differ from the untreated lactose. In contrast, the presence of small flakes and agglomerates were observed in both excipient-blends containing 1 and 10% MgSt, suggesting an excess of MgSt was present (arrows). The carrier particles seem to be well covered with fines, forming a thin layer on the carrier surface. In the 10% MgSt sample, the fine particle aggregates appear to be very dispersed and only loosely attached to the carrier particles. The surfaces of Lactose 0.5, 1 and 10% MgSt were visually rougher than the samples without MgSt (Figure 50). Interestingly, this is in strong contrast with what was observed with mechanofusion where the surface was significantly smoother after treatment [315].

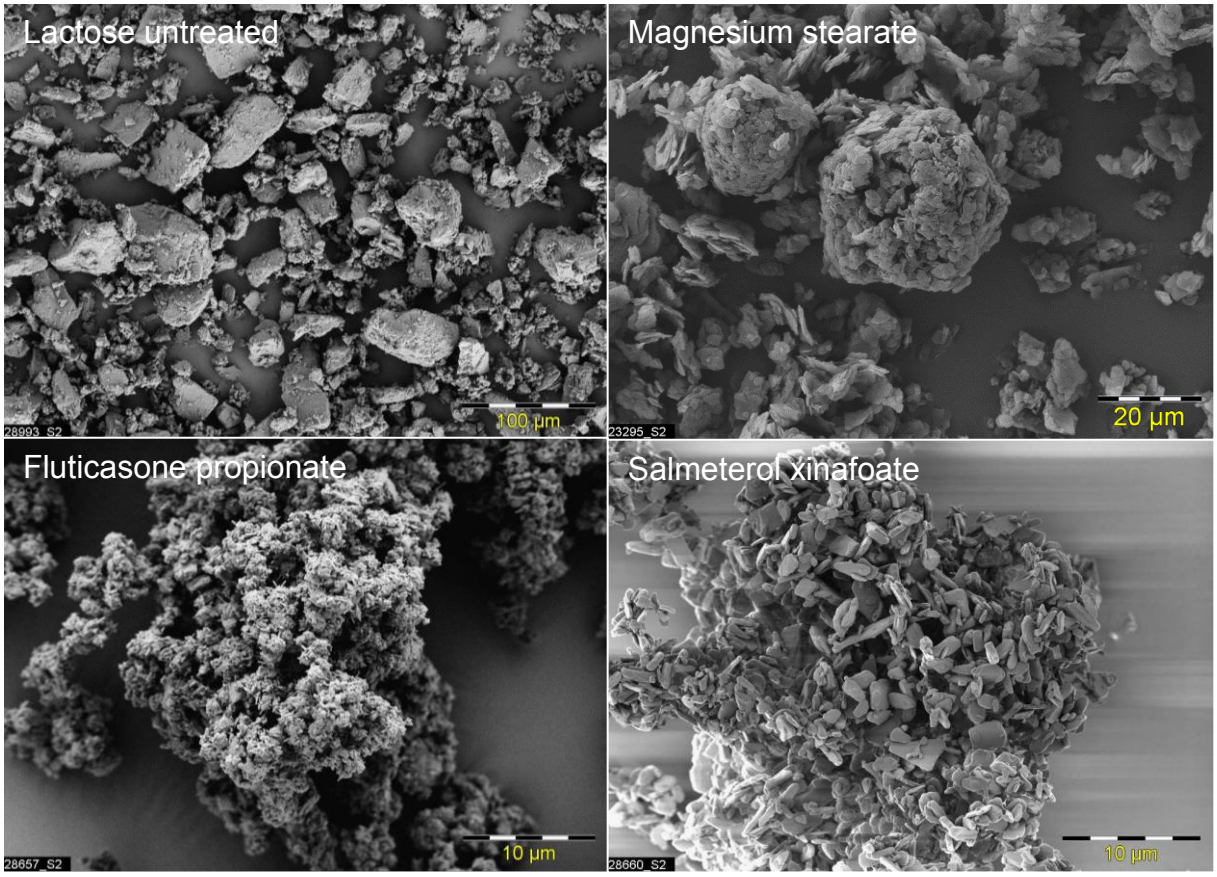

Figure 49: SEM images of raw materials untreated lactose, MgSt, FP and SX.

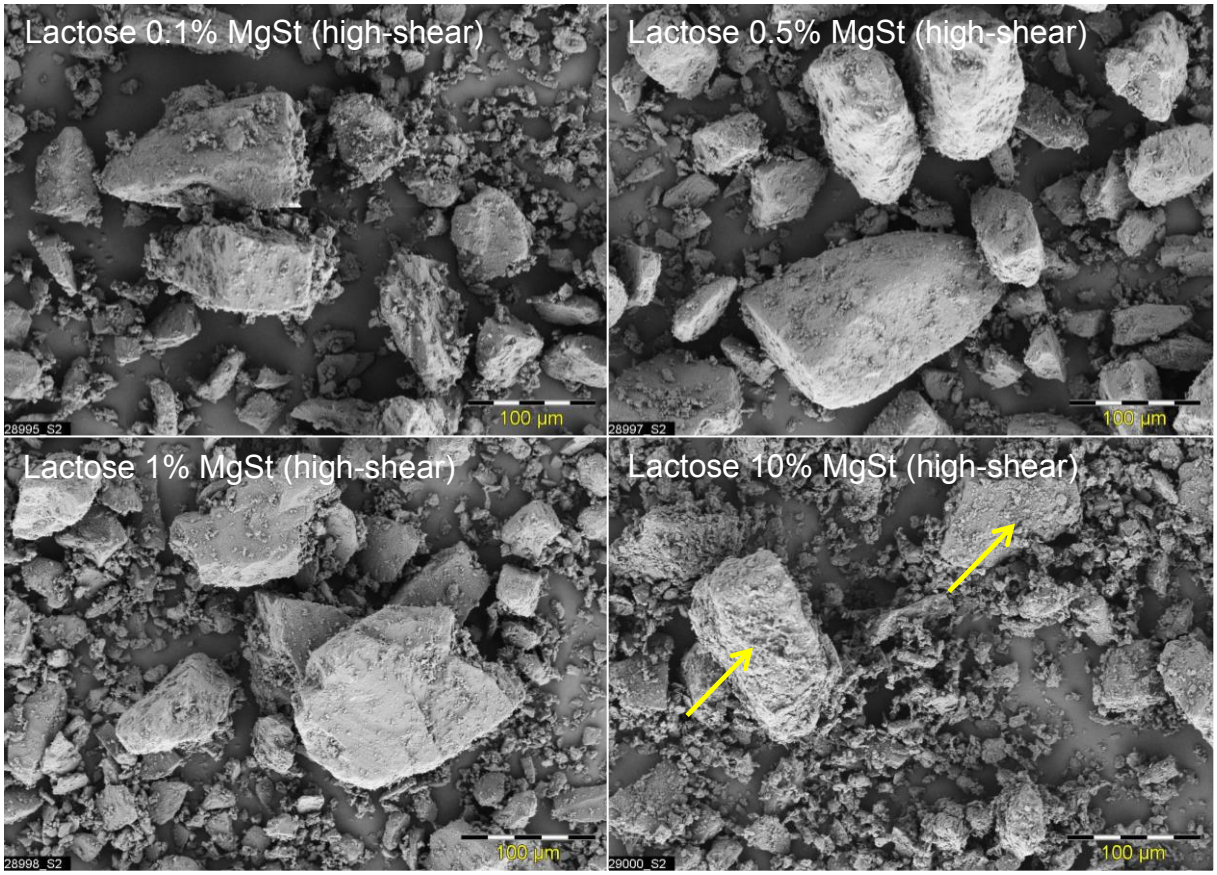

Figure 50: SEM images of high-shear excipient-blends.

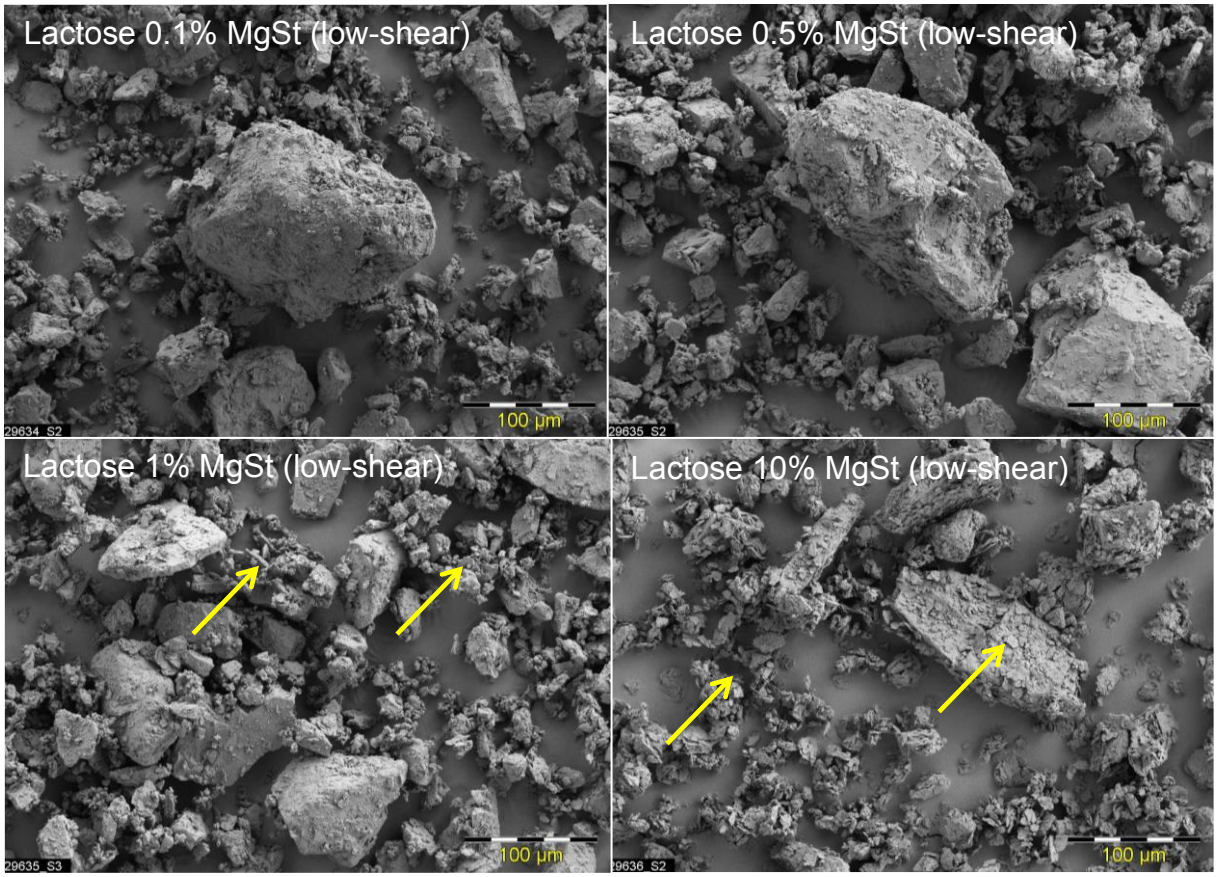

Figure 51: SEM images of low-shear excipient-blends.

In Figure 51, SEM images of the low-shear excipient-blends are shown. The edges of larger lactose particles did not change and characteristic MgSt flakes are clearly visible. In the excipient-blend containing 10% MgSt, the coverage of the carriers is patchy with aggregates of fine particles. A lot of larger particle agglomerates are visible (arrows).

Time-of-flight Secondary Ion Mass Spectrometry (ToF-SIMS) Measurements

The images were constructed from the spectra and cover an area of 500x500 µm. They show an overlay of the signal at m/z 23.99 assigned to Mg^+ in the magnesium stearate and the signal at m/z 73.04 assigned to $C_3H_5O_2^+$ in lactose. The reference samples (Lactose untreated and pure MgSt) give an indication of the residual signal detected at 23.99 for the lactose sample and at 73.04 for the magnesium stearate (Figure 52). The images constructed from the peak at 23.99 are shown in red and those from the peak at 73.04 are shown in green. For the untreated lactose sample, the signal mapping of $C_3H_5O_2^+$ was clearly observed (Figure 52). In contrast, there was no Mg^+-signal detected for the untreated lactose sample. This indicates that any Mg^+-signal detected for the processed excipient-blend sample, would come from the MgSt coating or MgSt agglomerates present.

The ToF-SIMS mapping of different signals on the various powder samples are shown in Figure 53. For the processed lactose samples with various MgSt content, the $C_3H_5O_2^+$ signals could still be observed to some extent (Figure 53). When the MgSt content was increased, the density of the $C_3H_5O_2^+$ signals (lactose) observed were relatively reduced while the density of the Mg-signals increased markedly. Regions that are red therefore represent positions where the coating of magnesium stearate is too thick to allow the lactose to be detected. Yellow regions show the presence of both lactose and magnesium stearate. Layer-by-layer erosion (profiling of depth of the sample) was not possible in the tested samples because the sample surface was too rough.

ToF-SIMS images showed ion signals for MgSt all over the measured area in the high-shear excipient-blends with high MgSt content (Figure 53). We conclude that MgSt must be evenly distributed on the lactose surface (overlay of MgSt and lactose) in a thin layer of MgSt that is covering the lactose surface. A fully coherent coverage may have been formed on the carrier surface, but it is possible that it is thinner in thickness than the ToF-SIMS penetration depth. Therefore, the lactose signal is still detected. While in the low-shear excipient-blend, MgSt agglomerates were detected by ToF-SIMS imaging as small intense spots (Figure 53). Low-shear blending did not induce any surface coating of the lactose with MgSt. The overlay of MgSt and lactose shows only some intense spots with ion signals indicating MgSt agglomerates.

With increasing MgSt-content in the high-shear excipient-blend, the relative amount on the lactose surface covered by MgSt increases (Table 15). Around 1% MgSt results in nearly full coverage (relative coverage 0.92) of the carrier. Interestingly Zhou *et al.* [24] investigated lactose coverage with X-ray Photoelectron Spectroscopy (XPS) in blends with MgSt manufactured by mechanofusion and were reaching much lower coverages (8.5% ± 0.2 for 0.1% MgSt-content; 75.0% ± 0.3 for 1% MgSt-content; 75.1% ± 0.1 for 5% MgSt-content) than were achieved in our formulations with the applied high-shear blending technique. The presence of MgSt as a coating layer on the lactose surface in the high-shear blend might change the interaction forces between API and lactose carrier substantially.

Table 15: Relative amounts of Magnesium in reference, high-shear and low-shear excipient-blend samples

Sample	**Mg/(Mg^+CH_3O)**	**Mg /($Mg^+C_2H_5O$)**	**Mg /($Mg^+C_3H_5O_2$)**
Lactose	0.0009±0.0002	0.0010±0.0002	0.0005±0.0001
MgSt	0.99±0.01	0.98±0.01	0.98±0.01
High-shear	**Mg/(Mg^+CH_3O)**	**Mg /($Mg^+C_2H_5O$)**	**Mg /($Mg^+C_3H_5O_2$)**
Lactose 0.1% MgSt	0.53 ± 0.01	0.54 ± 0.01	0.36 ± 0.01
Lactose 0.5% MgSt	0.80 ± 0.03	0.80 ± 0.03	0.68 ± 0.04
Lactose 1% MgSt	0.92 ± 0.002	0.91 ± 0.002	0.85 ± 0.006
Lactose 10% MgSt	0.97 ± 0.004	0.96 ± 0.003	0.94 ± 0.005
Low-shear	**Mg/(Mg^+CH_3O)**	**Mg /($Mg^+C_2H_5O$)**	**Mg /($Mg^+C_3H_5O_2$)**
Lactose 0.1% MgSt	0.011 ± 0.0005	0.012 ± 0.0006	0.006 ± 0.0004
Lactose 0.5% MgSt	0.11 ± 0.008	0.12 ± 0.008	0.08 ± 0.005
Lactose 1% MgSt	0.17 ± 0.009	0.19 ± 0.01	0.11 ± 0.007
Lactose 10% MgSt	0.44 ± 0.01	0.47 ± 0.009	0.30 ± 0.006

Lactose

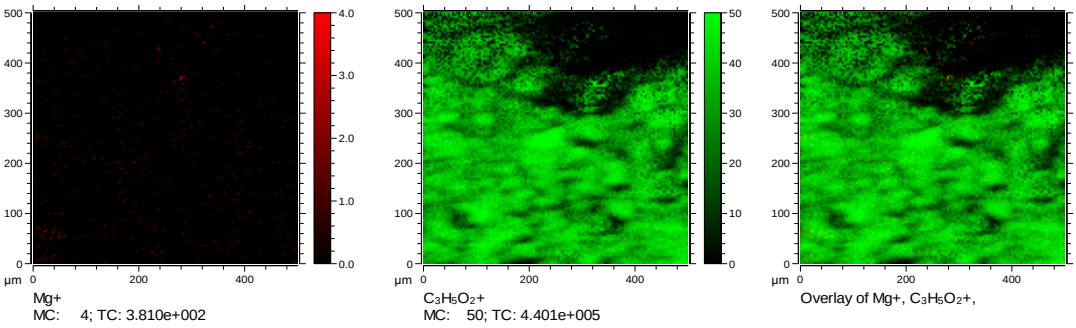

Magnesium stearate

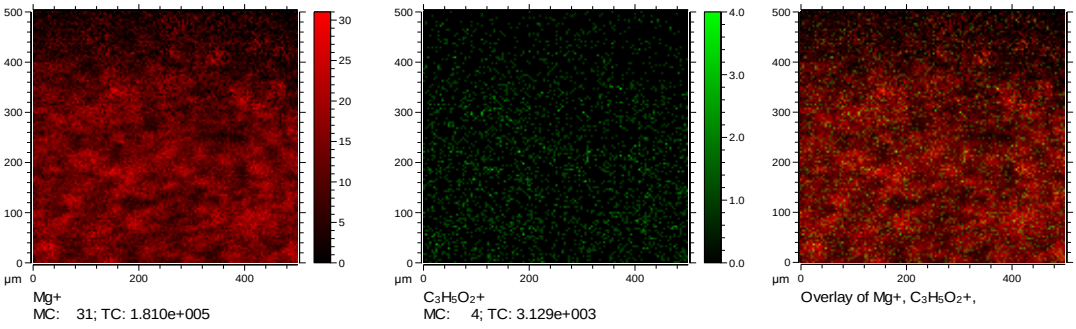

Figure 52: ToF-SIMS micrographs at scanning area of 500µm × 500µm for Lactose untreated (top) and pure magnesium stearate (bottom).

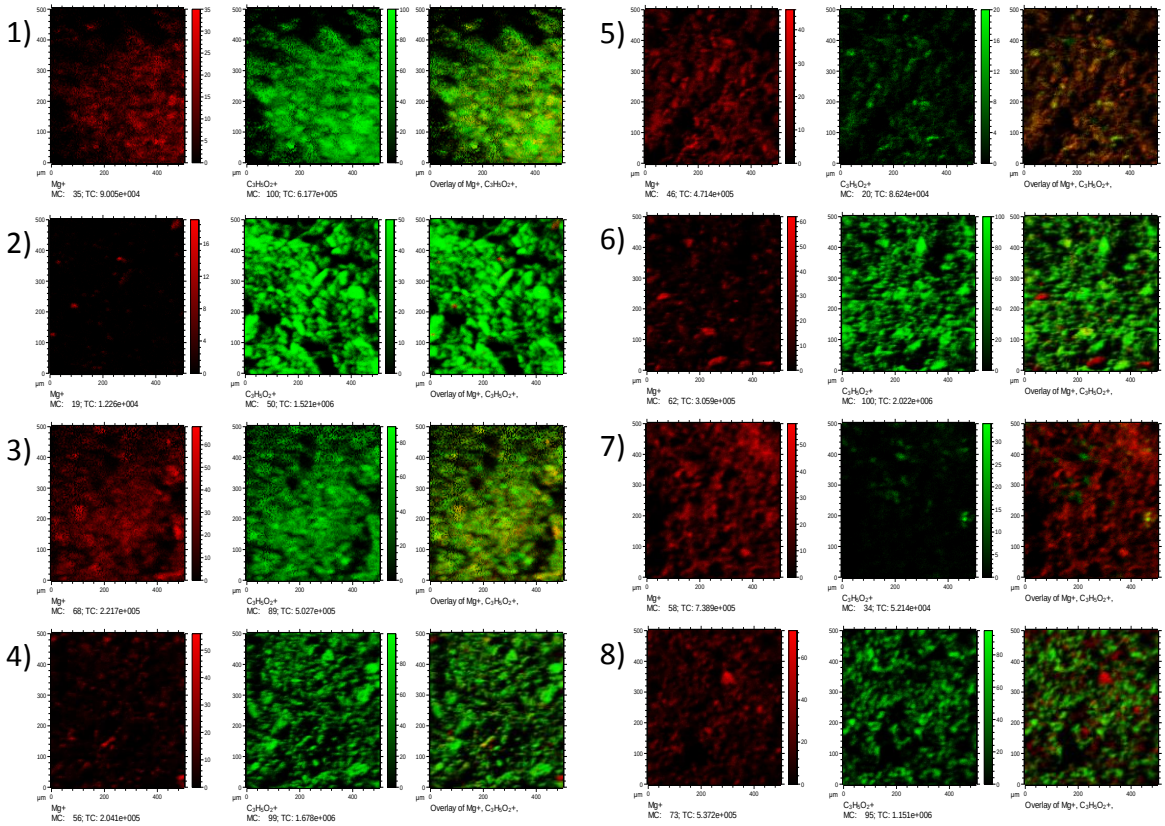

Figure 53: ToF-SIMS micrographs at scanning area of 500µm × 500µm for:
(1) Lactose 0.1% MgSt (high-shear) (5) Lactose 1% MgSt (high-shear)
(2) Lactose 0.1% MgSt (low-shear) (6) Lactose 1% MgSt (low-shear)
(3) Lactose 0.5% MgSt (high-shear) (7) Lactose 10% MgSt (high-shear)
(4) Lactose 0.5% MgSt (low-shear) (8) Lactose 10% MgSt (low-shear)

Aerosol Performance of DPI Formulations by SPAMS and NGI for FP blends

Figure 54 shows a comparison of SPAMS APSD histograms of total particles (API, fine lactose and MgSt) for three different FP blends with lactose untreated, lactose with 0.1 and 0.5% MgSt-content (high-shear), respectively. By adding MgSt to the formulation, the APSD profile shifts to a higher number of smaller particles with a higher number of particles in the size range from 0-1.7 µm diameter. By increasing the MgSt-content from 0.1 to 0.5% (w/w), the number of smaller particles increases even more and the size distribution shift is more pronounced.

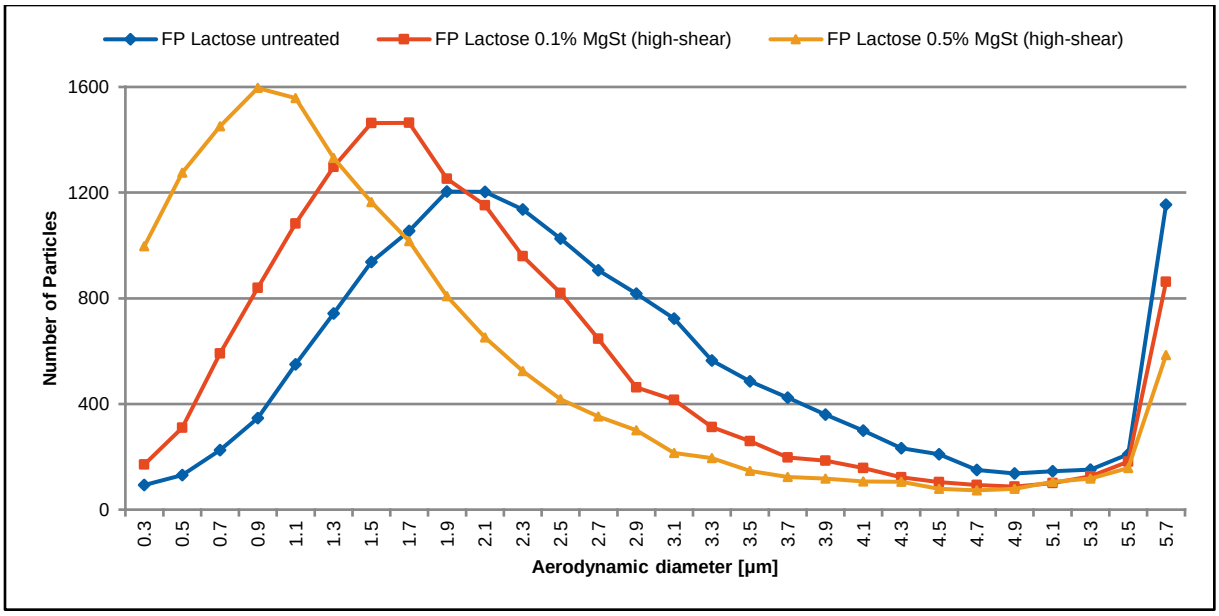

Figure 54: SPAMS Aerodynamic particle size distribution histogram of three FP blends with lactose untreated, 0.1 and 0.5% MgSt (high-shear), respectively. The plot shows the total number of particles measured (active substance FP and excipients).

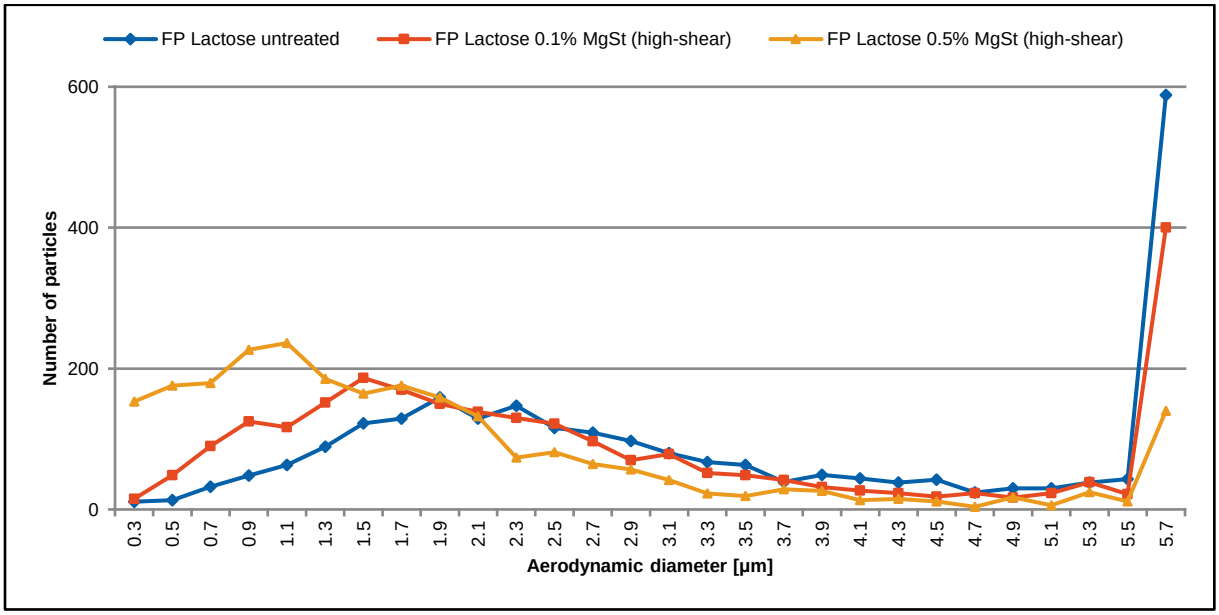

Figure 55: SPAMS Aerodynamic particle size distribution histogram of three FP blends with lactose untreated, 0.1 and 0.5% MgSt (high-shear), respectively. The plot shows the distribution of the active substance FP only. The size bins were scaled to the ratio of the hit rate in order to have a comparison between the different formulations.

The APSD histogram of particles containing FP in the two high-shear manufactured formulations and the reference formulation without MgSt is shown in Figure 55. The size bins in Figure 55 were scaled in order to compare the three formulations with each other. It can be seen that there is a significant increase in number of FP particles with a small particle size in the range from 0-1.7 µm for the formulations containing 0.1 and 0.5% MgSt, respectively. Interestingly, the same shift observed in the total number of particles (Figure 54) was also detected for the API FP following the

same pattern. SPAMS is indicating that the high-shear blends containing the FCA MgSt have a much higher dispersibility compared to the reference formulation without MgSt.

In Figure 56, a series of SPAMS APSD histograms of three FP blends is compared: two low-shear excipient-blends (0.1% and 0.5% MgSt) and the reference formulation without MgSt. It is clearly evident that there are significant differences between the high- and low-shear blends and also the reference formulation. While the APSD of the high-shear manufactured blend shifts to a higher number of smaller particles (0-1.7 µm), the APSD of the low-shear formulation seems to have no or a very slight shift to a larger particle size. A much lower number of particles with a size below 1.7 µm are present. The increase in number of particles in the region of 2.1 µm is probably due to MgSt agglomerates. The histogram of Figure 57 indicates that low-shear mixing of the excipient-blend does not increase the dispersibility of the manufactured FP formulation.

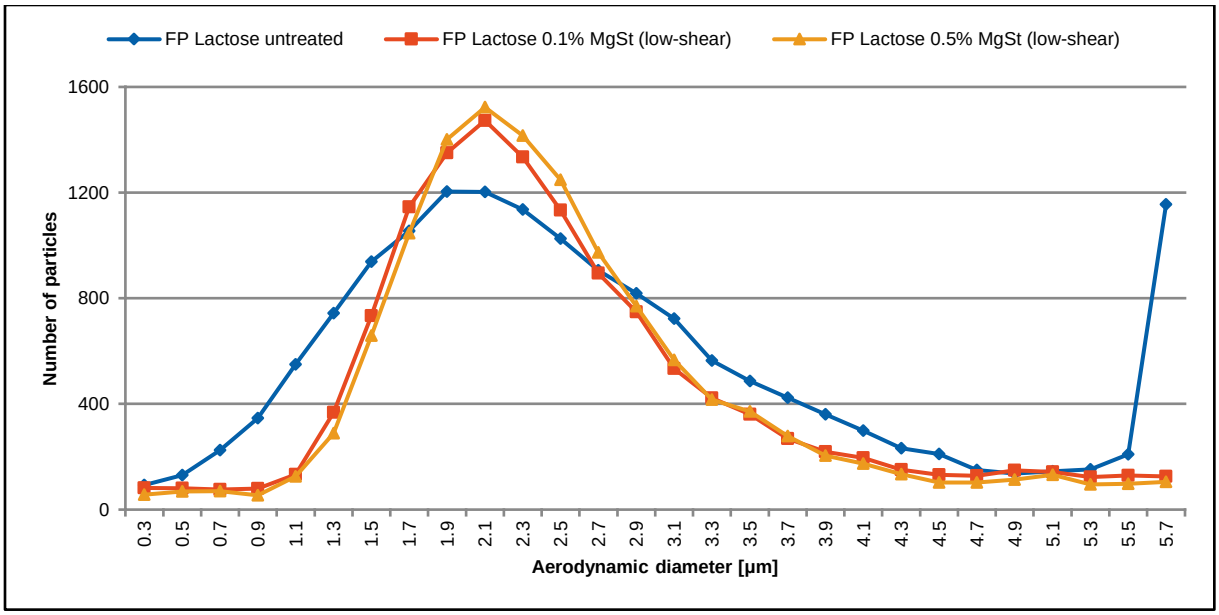

Figure 56: SPAMS Aerodynamic particle size distribution histogram of three FP blends with lactose untreated, 0.1 and 0.5% MgSt (low-shear), respectively. The plot shows the total number of particles measured (active substance FP and excipients).

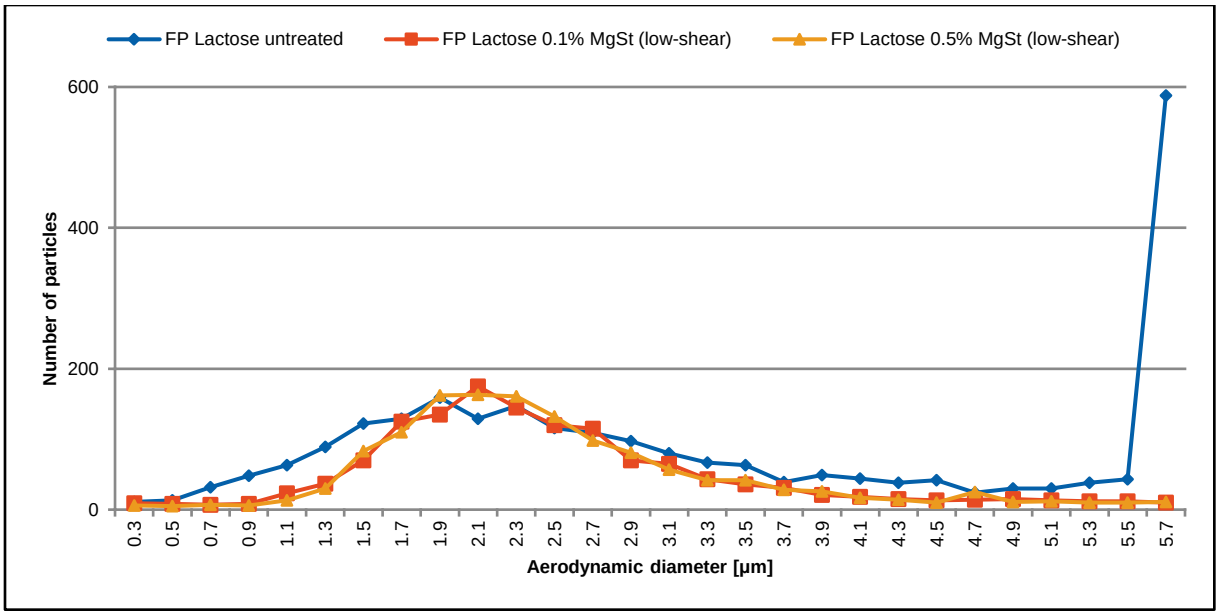

Figure 57: SPAMS Aerodynamic particle size distribution histogram of three FP blends with lactose untreated, 0.1 and 0.5% MgSt (low-shear), respectively. The plot shows the distribution of the active substance FP only. The size bins were scaled to the ratio of the hit rate in order to have a comparison between the different formulations.

Figure 58 shows NGI histograms of FP formulations. For the high-shear formulation of FP with 0.5% MgSt the NGI profile shows a decrease in drug deposited in the pre-separator compared to the reference formulation. There is a considerable increase in deposition of FP in NGI Cups 2-8 (cutoff 6.48-0.28 µm) for the high-shear formulation. While in the low-shear formulation there seems to be poor drug detachment from larger lactose carrier particles and therefore a higher deposition in the pre-separator. This results in lower performance. The drug detachment from the carrier is significantly different between the formulations manufactured with the two blending techniques.

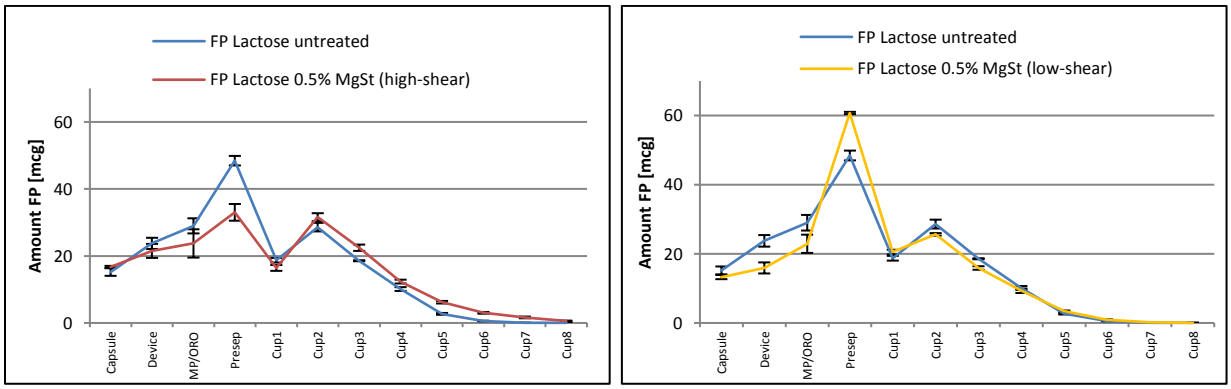

Figure 58: NGI profiles of FP formulations.

To further illustrate the impact of application of MgSt and high shear blending, the fine particle fraction (FPF, particles with a diameter <5 µm) of FP, calculated as a percentage of total recovery, is shown in Table 16. The FPF generally increases with the addition of MgSt for the high-shear blends. However, there seems to be a maximum or optimal amount around 0.5% MgSt for the FP high-shear formulation. Introducing more MgSt into the system beyond 0.5% did not further improve the performance of FP in terms of FPF. The tested formulations with an amount of 0.5% MgSt increased roughly 8% in FPF. This observation is in agreement with the theory of unsaturated "active sites" on the carrier [316]. The more MgSt is introduced into the system, the less interaction between large carrier particles and

drug. Therefore, the likelihood to form smaller agglomerates between drug and fine lactose is increased and the amount of liberated drug substance is higher. The FPF did not increase for the low-shear formulations at the MgSt concentrations evaluated. Only at a MgSt-content of 10%, the FPF increased slightly compared to lactose untreated. However, there is an excess of small carrier particles which could explain the increase in FPF (Table 14) [317].

Table 16: Fine particle fraction (% of declared content) of FP formulations obtained by NGI

High-shear	FPF [%]	StDev [%]	Low-shear	FPF	StDev [%]
FP Lactose untreated	24.4	0.2	FP Lactose untreated	24.4	0.2
FP Lactose 0.1% MgSt	26.3	0.2	FP Lactose 0.1% MgSt	22.0	1.2
FP Lactose 0.5% MgSt	32.2	0.8	FP Lactose 0.5% MgSt	22.3	0.5
FP Lactose 1% MgSt	29.5	1.2	FP Lactose 1% MgSt	23.6	1.0
FP Lactose 10% MgSt	32.5	0.6	FP Lactose 10% MgSt	26.1	1.3

Aerosol Performance of DPI Formulations by SPAMS and NGI for SX blends

In Figure 59 and Figure 61, a comparison of SPAMS APSD histograms of total particles (API, fine lactose and MgSt) for SX blends with lactose untreated, lactose with 0.1 and 0.5% MgSt-content are shown with high shear and low shear blending, respectively. By adding MgSt to the formulation with both, high- and low-shear mixing, the APSD profile shifts to a higher number of smaller particles similar to the effect in the FP high-shear formulations (Figure 54). A higher number of particles in the size range from 0-2.3 µm diameter are present. By increasing the MgSt-content from 0.1 to 0.5% (w/w), the number of smaller particles increases and the size distribution shift is more pronounced. Fewer particles with an aerodynamic diameter larger than 6.1 µm were detected in the SX high-shear formulations with SPAMS.

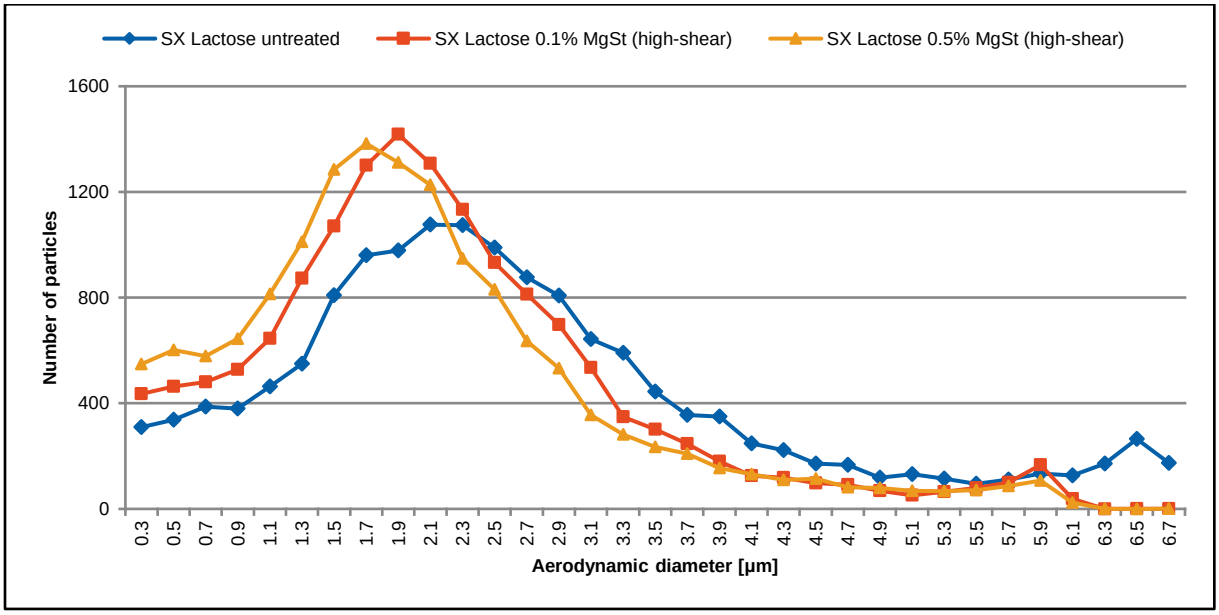

Figure 59: SPAMS Aerodynamic particle size distribution histogram of three SX blends with lactose untreated, 0.1 and 0.5% MgSt (high-shear), respectively. The plot shows the total number of particles measured (active substance SX and excipients).

The APSD histogram of SX particles only is shown in Figure 60. The size bins were scaled in order to compare the three formulations with each other on the same scale. It can be seen that there is a significant increase in number of SX particles with a small particle size in the range from 0-2.3 µm for the formulations containing 0.1 and 0.5% MgSt,

respectively. SPAMS data indicates that the high- and low-shear (Figure 62) manufactured SX blends containing the MgSt have a higher dispersibility compared to the reference formulation without MgSt.

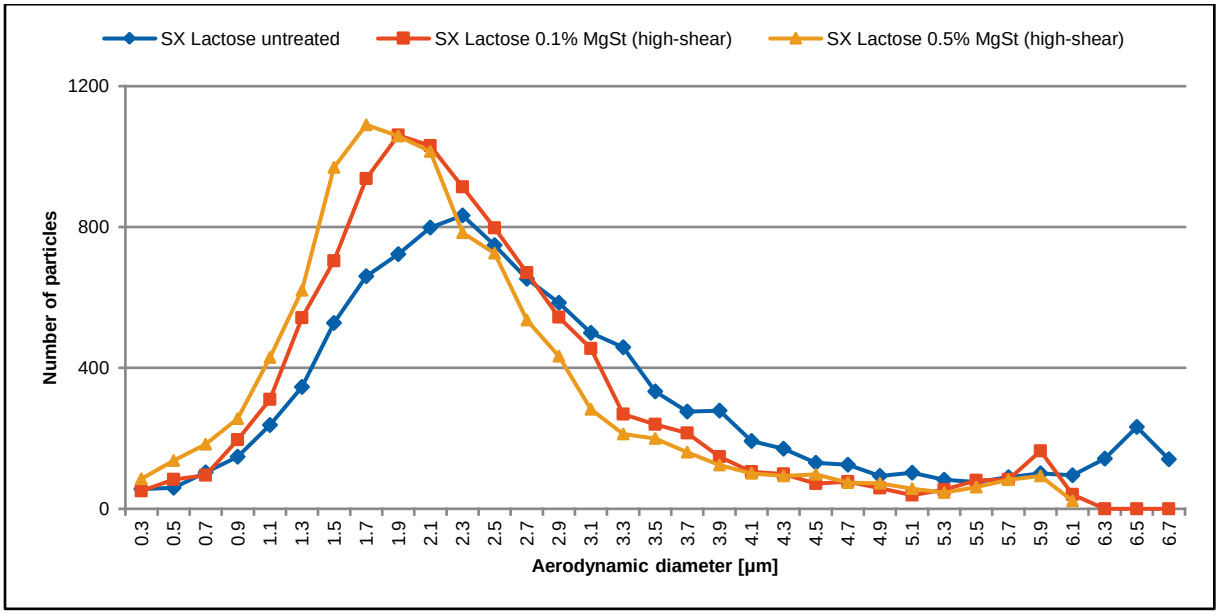

Figure 60: SPAMS Aerodynamic particle size distribution histogram of three SX blends with lactose untreated, 0.1 and 0.5% MgSt (high-shear), respectively. The plot shows the distribution of the active substance SX only. The size bins were scaled to the ratio of the hit rate in order to have a comparison between the different formulations.

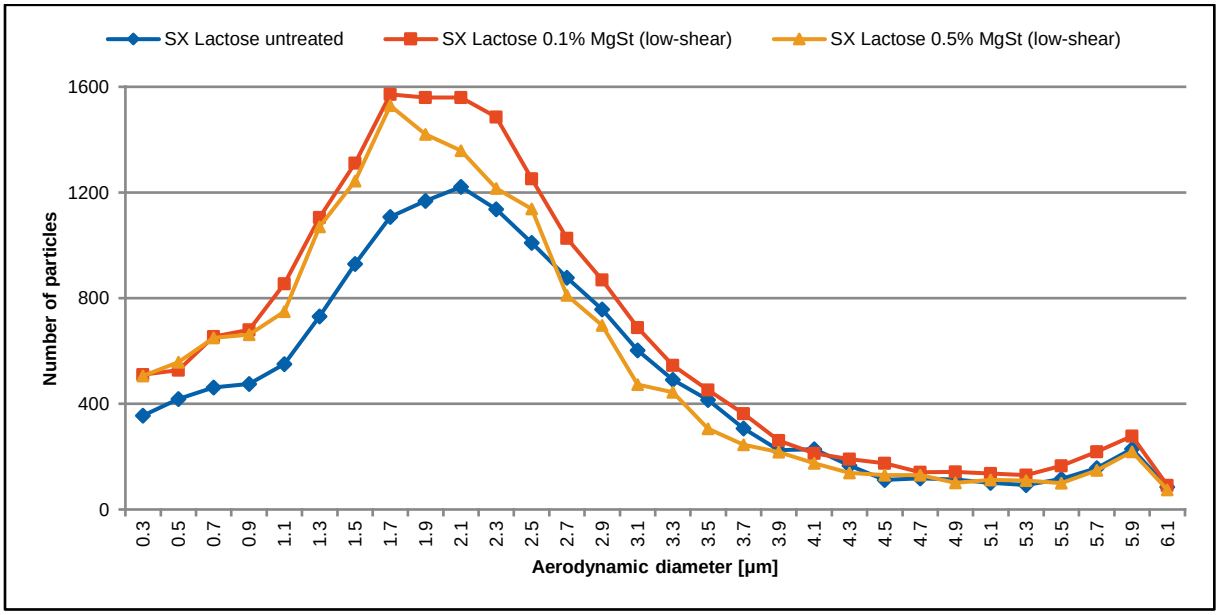

Figure 61: SPAMS Aerodynamic particle size distribution histogram of three SX blends with lactose untreated, 0.1 and 0.5% MgSt (low-shear), respectively. The plot shows the total number of particles measured (active substance SX and excipients).

Figure 62 shows the APSD histogram of SX low-shear formulations compared to the reference. Interestingly, the low-shear SX formulations show also a higher number of smaller SX particles (in the range from 0-1.9 µm), but this is not as pronounced as what is observed with the high shear blends where the increase in particles <1.5 µm is higher.

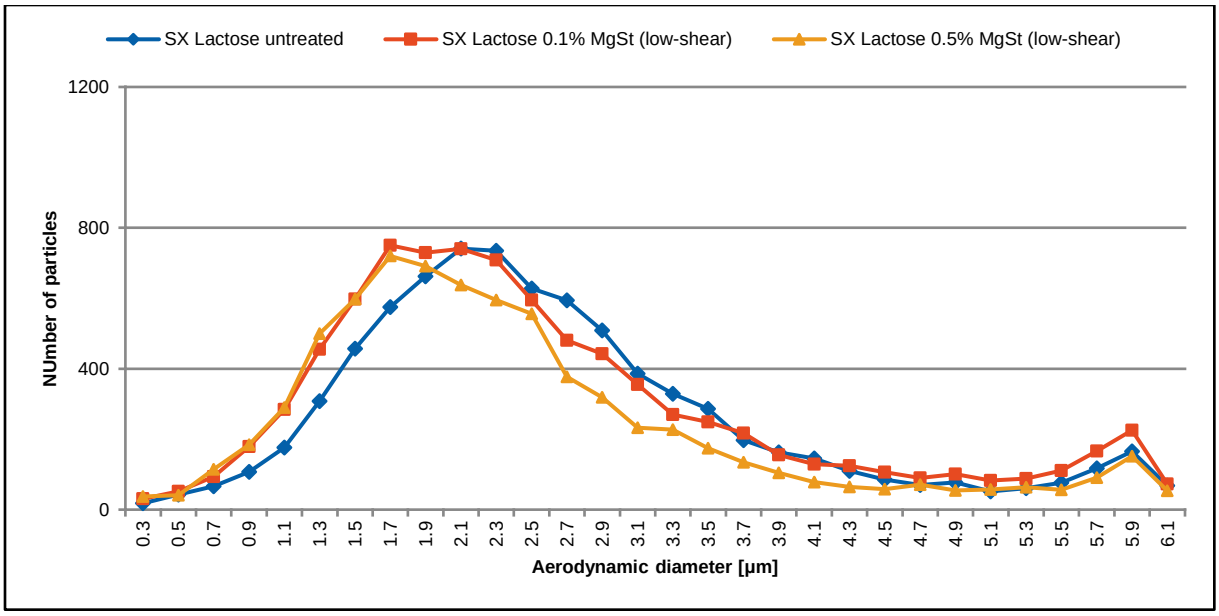

Figure 62: SPAMS Aerodynamic particle size distribution histogram of three SX blends with lactose untreated, 0.1 and 0.5% MgSt (low-shear), respectively. The plot shows the distribution of the active substance SX only. The size bins were scaled to the ratio of the hit rate in order to have a comparison between the different formulations.

In Figure 63, NGI APSD histograms of SX formulations are shown. Introducing MgSt in the formulation by high-shear mixing increased the deposition in NGI cups 3-8 for SX particles significantly. With MgSt present in the formulation, the deposition of SX in the pre-separator and Cups 1-2 is greatly decreased. A higher deposition in the device was observed for the high-shear formulations containing MgSt. This could be related to electrostatic forces built up during capsule spinning (triboelectrification) during actuation, as this has been observed in previous studies [318]. Adding more MgSt resulted in a further increase in the device deposition. The performance in terms of FPF for SX reached a maximum when 0.1% MgSt (w/w) was added by high-shear mixing in the excipient-blend (Table 17). A higher amount of MgSt did not further improve the performance of SX.

Surprisingly, the deposition of SX also increased when adding MgSt to the excipient-blend by low-shear mixing (Figure 63). The deposition significantly increased in NGI cups 3-6 for SX particles while the deposition was significantly decreased in the device, throat and pre-separator. High-shear mixing seemed to influence the deposition of SX also on the lowest NGI stages (Cups 6-8) while low-shear mixing the excipient-blends seemed to influence the deposition mainly in NGI Cups 3-5. This could be an indication that small agglomerates of fine excipient and drug are formed after actuation of the low-shear SX formulations.

We suggest that the adhesive compound SX seems to be rather loosely distributed in the blend and the cohesive FP is forming agglomerates with itself. Comparing the reference formulations of FP and SX, the performance of SX was already much higher than the one of FP (Table 16 and Table 17). The performance of SX was improved by MgSt independently of the blending method used. It can be hypothesized that SX is preferentially distributed on MgSt rather than on lactose and therefore the blending technique has a very limited influence on SX aerosol performance.

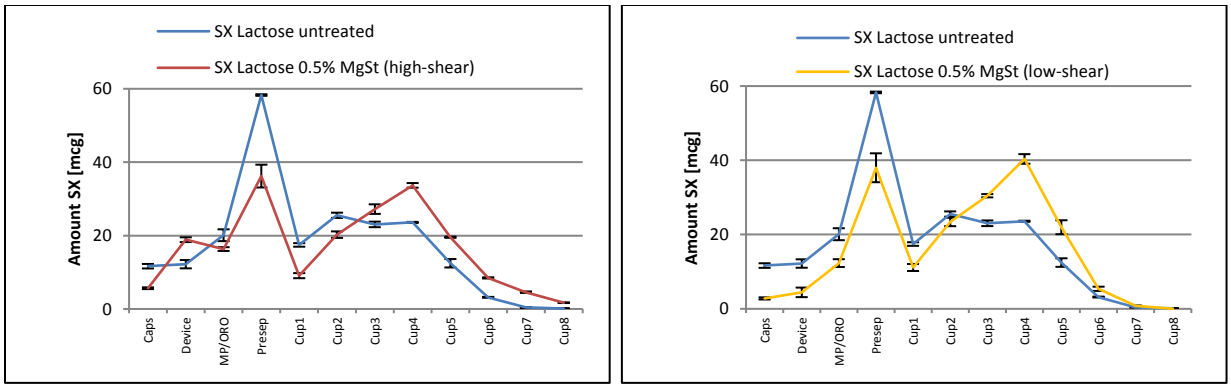

Figure 63: NGI profiles of SX formulations.

The FPF of the SX formulations is summarized in Table 17. The tested high-shear formulations with MgSt increased up to 18% in FPF. Interestingly, the FPF for the SX low-shear blends also increased with the amount of added MgSt. While the maximum in FPF was reached at a MgSt-content of 0.1% in the high-shear formulations, the maximum in FPF was reached at 0.5% MgSt in the low-shear formulations. A higher amount of MgSt in the low-shear formulation was necessary to increase the performance of SX in terms of FPF similar to the high-shear formulation. Too much MgSt seems to decrease the performance. Larger agglomerates of fine excipients and drug may be formed which deposit in the throat, pre-separator and upper NGI stages.

Table 17: Fine particle fraction (% of declared content) of SX formulations obtained by NGI

High-shear	FPF [%]	StDev [%]	Low-shear	FPF	StDev [%]
SX Lactose untreated	39.2	1.3	SX Lactose untreated	39.2	1.3
SX Lactose 0.1% MgSt	56.7	1.3	SX Lactose 0.1% MgSt	43.4	0.2
SX Lactose 0.5% MgSt	54.2	0.7	SX Lactose 0.5% MgSt	56.3	2.0
SX Lactose 1% MgSt	54.0	0.3	SX Lactose 1% MgSt	49.5	3.5
SX Lactose 10% MgSt	45.9	4.2	SX Lactose 10% MgSt	50.1	1.7

The results collected with SPAMS and NGI indicate that there is higher dispersibility of fine particles with an aerodynamic diameter below 5 µm when adding the FCA MgSt to the excipient blend by high-shear mixing. It has been observed from the SEM that the MgSt is modifying the lactose carrier surface. This modification is in such way that attractive forces, such as van der Waals or electrostatic forces, between drug and carrier and also between fine excipient and coarse excipient are reduced [319]. This leads to easier detachment of drug and also fine excipient from the coarse carrier. As a consequence, the amount of liberated drug substance increases [16].

The amount of MgSt added to the blend also played an important role in the DPI formulations. Introducing more MgSt into the system did not always result in a further increase of the aerosol performance in terms of FPF for the formulations (both high- and low-shear blends) although a higher amount of MgSt seems to cover more of the lactose surface area and should thus decreases interaction forces even more when applied on the lactose by high-shear mixing. The data suggests that the optimal amount of MgSt added by high-shear mixing was 0.5% for FP and 0.1% for SX. For the SX low-shear formulation 0.5% MgSt seemed to be optimal. This could be related to the different affinity of the APIs themselves to the lactose or MgSt. It can be hypothesized that above a certain concentration of MgSt in the excipient blend, different effects may influence the aerosol performance. Beyond a certain level of coverage on the carrier surface, there is no additional benefit to adding excess MgSt.

The drug-to-carrier interparticulate forces must be weak enough to allow substantial drug detachment during the inhalation process while strong enough to maintain powder blend homogeneity. Particle interactions and

aerosolization are prone to change when surface characteristics of the drug or carrier particles such as surface energy [320, 321], crystallinity [322, 323], hydrophobicity [311], coating with an FCA [23, 324, 325], additives [326, 327] or electrostatic behaviour [328], are changed. Reduced surface energy and low surface heterogeneity are often desired features for aerosol formulation optimization. In the case of our high-shear formulations there is a significant change of surface characteristics as the outermost surface consists more of MgSt and not of lactose anymore after the high-shear mixing process has been applied to the blend. The drug-to-carrier interaction has now changed from lactose-API to MgSt-API. Adding more MgSt by high-shear mixing seems to further weaken the interaction between drug and carrier. With a higher amount of MgSt added by high-shear blending, ToF-SIMS imaging detected a higher relative amount of MgSt and thus we conclude a higher surface coverage. This may result in a reduced surface energy and altered electrostatic behaviour. Measurements with IGC by Das *et al.* did explain that the dispersive surface energy of MgSt is significantly lower compared to lactose [17]. In the high-shear formulations, the carrier surface is more randomly covered with a thin coating layer of MgSt as it has been demonstrated with ToF-SIMS imaging. During powder mixing, drug particles are distributed between the surface of carrier and fines, forming weak agglomerates of drug and fines that can be dispersed and disaggregated easily during aerosolization as "soft-agglomerates" [1, 38]. Experiments using the SPAMS technology could show that high-shear blending of lactose carrier with MgSt improved the dispersibility of the manufactured FP and SX formulations.

Furthermore, the interparticulate forces can also change by altering physicochemical properties of drug or carrier particles such as size [226, 329], size distribution [230, 330], morphology [331-333], surface roughness [334], elastic/plastic deformity [335], drug/carrier ratio [316] and drug/fine ratio [179]. The addition of MgSt to the formulations resulted in apparent changes in particle size, size distribution, morphology, surface roughness and drug/fine ratio as can be seen in Table 14, Figure 47, Figure 48, Figure 50 and Figure 51. The particle size distribution is one of the determining factors for powder adhesion and resuspension, which will affect the powder processing and aerosolization. It may also influence the aerodynamics and particle deposition in the respiratory tract. The particle morphology may alter the true contact area and coordination number between particles. Improved aerosol performance can be related to smaller drug–carrier contact area. We hypothesize that the modification in surface roughness in our high-shear blends is also reducing the true contact area between drug and carrier and therefore we have an increased *in vitro* aerosol performance [13, 178]. In the high-shear formulations an excess of fine and very fine particles could be detected with SPAMS. Meanwhile, in the FP low-shear formulations, a much lower number of smaller particles were detected. It has been proposed that "high-energy active sites" exist on coarse lactose carrier particles [15, 167, 193, 307]. The drug/carrier ratio and drug/fines ratio may be involved in saturation of "active sites" on the particle surface and/or a redistribution of agglomerates, so that an optimum drug/carrier and drug/fine ratio exists. The addition of ternary fines such as MgSt or lactose preferentially binds to these "active sites", forcing the drug to the weaker binding site, thus drug particles are more easily liberated from the surface of the carrier particles after actuation. If this hypothesis is true, the "active sites" should be saturable, and the order of mixing of drug, carrier, and fines would result in performance difference [7, 176]. The "active site" theory could possibly explain the effects in the SX low-shear formulations and various competing effects such as the saturation of activated areas on the carrier surface or the formation of drug–fines agglomerates for easier lift-off could offer an explanation for the observed behaviour [21, 186, 193, 316]. The affinity between API and carrier is also substantially different for FP and SX. FP is a cohesive drug and tends to form agglomerates with itself while the adhesive drug SX is rather fine dispersed in the blend. This was observed in Figure 58 and Figure 63 where in the FP low-shear blend a high deposition in the pre-separator indicated the formation of larger agglomerates. While in the SX low-shear blend a much lower deposition in the pre-separator was observed and thus a higher deposition in the NGI stages.

Conclusions

The intensity of the blending technique is demonstrated in this work to affect the distribution of MgSt covering the lactose carrier. This covering/distribution was shown to significantly influence the *in vitro* aerosol performance (as evidenced in ToF-SIMS images). The underlying mechanism of particle interaction between API and the carrier seems

to be substantially different for high- and low-shear formulations. This provides the basis for a modification in particle interactions from drug-lactose to drug-MgSt (in high-shear) which then seems to be responsible for the improved performance (enhanced particle detachment from carrier due to lower interaction forces).

The blending method applied to pre-blend the excipients strongly impacts the APSD and FPF of FP. For SX, the important factor seemed to be the presence of MgSt in the blend since both blending techniques were nearly equally effective to increase the aerosol performance. SPAMS and NGI independently show an increase of the number of fines as result of the addition of MgSt by high-shear mixing, indicating a reduction of interaction between the actives and the lactose carrier particles. Low-shear mixing of the excipient-blend did not increase the performance of FP. However, low-shear mixing the excipient-blend did increase the FPF of the cohesive drug SX in our formulations. Nearly equal aerosol performances could be achieved for SX with both blending techniques applied to pre-blend the excipients. The aerosol performance of SX could be increased much more by adding MgSt compared to the performance of FP. This may be influenced by the properties of the APIs themselves and their interaction with the carrier surface (lactose or MgSt). The observed effects could possibly be explained with the "active site" and "soft-agglomerate" hypotheses.

Using NGI and SPAMS it is possible to distinguish changes in the formulation of DPI powders blended with different amounts of MgSt. The results from SPAMS can be correlated to NGI results. Valuable additional information in terms of dispersibility of fine particles in the formulations could also be obtained with SPAMS. SPAMS provides much finer particle resolutions compared to NGI cut-off stages (fine details of APSD). This gives a good understanding what happens with fine and very fine particles. Furthermore, SPAMS is also more sensitive for smaller particles down to 0.1um as with this technique the aerodynamic diameter of single particles is measured. Meanwhile the NGI relies on particle mass which is very low for fine particle sizes. In addition, SPAMS provides additional information on excipients and co-associations of particles in DPI formulations [248].

We hypothesize that other adhesive or cohesive APIs might show a similar behaviour in terms of *in vitro* aerosol performance as the model compounds used in this study when utilizing the proposed blending techniques. To confirm this further studies are necessary. This study yielded additional evidence for the mechanism of MgSt action in DPI formulations.

For future work it would be interesting to explore, if other FCAs can have a similar effect when using the excipient high-shear mixing method. There is high possibility for association of FP or SX (or both) with lactose and/or MgSt and future work would involve development of techniques that could further differentiate and identify the particles generated. Using an upgraded SPAMS setup with a desorption and ionization laser firing at a different wavelength, SPAMS could potentially detect co-associations not only between APIs, but also between API and excipients (lactose and FCA).

Acknowledgements

The authors would like to thank D. Fergenson (Livermore Instruments Inc., USA) for technical support with the SPAMS instrument and R. Crockett (EMPA, Switzerland) for ToF-SIMS imaging. The authors are grateful to B. Haeberlin, T. Storm, N. Silva and R. Guchardi for fruitful discussions and valuable scientific input. This work was funded by Novartis Pharma AG's internal research funds.

5. Investigation of Electrostatic Behavior of Dry Powder Inhaled Model Formulations

Jetzer et al. ***submitted to Journal of Pharmaceutical Sciences (November 2018)***

Abstract

The accumulation of electrostatic charge on drug particles and excipient powders arising from interparticulate collisions or contacts with other surfaces can lead to agglomeration and adhesion problems during the manufacturing process and application of dry powder inhaler (DPI) formulations. The objective of the study was to investigate the role of triboelectrification to better understand the influence of electrostatic charge on the performance of DPIs with two capsule based devices constructed to be dimensionally the same but with different materials. Another goal was to investigate strategies to reduce electrostatic charge build up during the manufacturing process and study the processes involved in this phenomenon. Electrostatic charge measurements showed that there is a significant difference in electrostatic charge generated between tested formulations and devices. This affects particle detachment from carrier and thus significantly impacts aerosol performance. Conditioning fluticasone DPI capsules at certain temperature and humidity conditions reduced electrostatic charges acquired during manufacturing. Conditioning salmeterol DPI capsules at same conditions seemed disadvantageous for their aerosol performance due to increasing capillary forces and solid bridge formation due to water absorption. The presented results provide increased knowledge and understanding of the role of electrostatic forces in influencing DPI formulation performance.

Introduction

Dry powder inhalers (DPIs) are well established for delivering pharmaceutical aerosols to the lungs. They commonly consist of coarser carrier particles (usually α-Lactose monohydrate; >30 µm) and micronized drug particles (<5 µm) [7]. The addition of a carrier particle has the effect of improving the respirable fraction through the prevention of agglomeration of cohesive active pharmaceutical ingredients (APIs) and improving powder flowability, which facilitates metering and drug aerosol formation and uniform filling [3]. To reach the deeper parts of the lung, the small drug particles have to detach from the carrier particles [4]. The fundamental attractive forces/mechanisms of interaction between drug and carrier particles in DPI formulations can be summarized as van der Waals, electrostatic and capillary forces [7, 196]. Besides the mentioned adhesion/cohesion forces, friction and mechanical interlocking also play important roles in powder flow and deaggregation [197]. The drug-to-carrier interparticulate forces must be weak enough to allow substantial drug detachment during the inhalation/aerosolization process while strong enough to maintain powder blend homogeneity. The performance of DPI formulations is therefore a function of the relative magnitudes of cohesive (drug–drug) and adhesive (drug–excipient) interparticulate forces. Particle interactions and aerosolization are prone to change when surface characteristics of the drug or carrier particles such as surface energy [320, 321], crystallinity [322, 323], hydrophobicity [336], coating with a force control agent (FCA) [14, 23, 24], additives [20, 195] or electrostatic charge [337], are changed.

The accumulation of electrostatic charge in DPI particles can occur during formulation preparation, when the API is sieved and blended with coarser carrier particles, and during processing, when the formulation may be transported or stored, filled into capsules or blister strips or transferred to a powder reservoir device. During these different manufacturing processes as particles are disturbed and agitated they undergo collisions with themselves and the surfaces with which they come into contact. During such collisions particles will become charged via the mechanism of triboelectrification, which may result in a bipolar charge distribution [206, 207]. Since triboelectrification arises from interactions between surfaces, the composition of equipment surfaces will directly affect both the polarity and magnitude of particle tribocharging. This is due to the fact that different materials have different abilities to transfer electrons from or to a surface depending on their relative abilities to donate or accept electrons. Therefore, interactions

between particles and different material surfaces may result in different charge levels and polarity in the powder [199]. This can potentially affect the physical structure of the blend and result in processing problems such as adhesion to container surfaces, agglomeration, poor flow behavior, reduced API recovery, loss of content uniformity and manual handling difficulties [208]. The presence of charge on a DPI formulation, which may not decay quickly with time, can result in variable formulation performance.

To achieve a tailored API particle size (<5 μm) for a successful delivery to the lungs requires secondary processing of primary API crystals using highly energetic comminution techniques, such as air-jet micronization [338]. Although an accumulation of electrostatic charge on APIs during micronization is not commonly reported in literature, it is a well-known issue observed in industrial manufacturing sites. The impact and breaking apart of the API crystals within the mill during micronization and subsequent transfer to a storage container results in a high level of static charge build up on the API particles, making them difficult to handle and process [143].

In addition to a build-up of electrostatic charge during manufacturing and processing, DPI formulations also undergo triboelectrification upon aerosolization within an inhaler device. During drug dispersion in a DPI, interactions between the powder, air turbulence and inhaler device surface build up electrostatic charge in the aerosol cloud and along the inner walls of the device itself, which are made primarily from hard, insulative, plastics. Particles deagglomerate from each other, fluidize and enter the air stream. The particles circulate within the internal cavity of the inhaler where they also undergo numerous interparticulate collisions and collisions with the inner surfaces of the device. Modelling with computational fluid dynamics by Shur et al. reported that the velocity of the airstream travelling through the device can influence the particle impact velocities and frequency that govern the extent of triboelectrification [339]. Other factors influencing the extent of electrostatic charge during DPI aerosolization include; the deaggregation mechanism of the device, device material, capsule material, physico-chemical and electrical properties of the particles, humidity and temperature [205, 209]. The resultant electrostatic interactions between the particles may affect the extent of deaggregation of the API from the carrier and also the attraction to and deposition of drug on the walls of the device which in turn will affect the DPI performance. The group of Byron et al. investigated the net charge of pharmaceutical aerosols before and after aerosolization with a Faraday-pail [189]. Studies using an electrical low-pressure impactor (ELPI) provided the measurement of charge in various particle size fractions of the aerosol [318]. O' Callaghan et al. reported evidence that the static charge generated on plastic aerosol devices resulted in significant drug retention within the device [340, 341]. All these studies showed that many types of DPI aerosols carry a significant amount of electrostatic charge that may affect *in vivo* deposition of fine aerosol particles in the lungs [9, 342].

Interparticluate forces can vary within different temperature and relative humidity (RH) settings or storage duration depending on the material properties of the product. The *in vitro* aerosol performance or drug dispersion changes during storage or can therefore be modified through conditioning of the DPI capsules. A number of previous studies investigated the influence of storage humidity on the dispersion of DPI formulations [309, 343-345].

Extensive research has been conducted on aerosol characteristics of DPIs such as particle size and mass output, but their electrostatic properties have not been studied comprehensively up to date [199, 209, 337, 346]. This study aims to better understand the influence of electrostatic charge on the performance of DPI formulations. The objective of the study was to investigate the electrostatic behavior of different custom manufactured DPI formulations with two identical devices constructed of different materials; plastic and metal. A custom made dynamic electrostatic charge measurement device (flow-through Faraday pail) and an electrostatic charge decay meter were used to analyze the electrostatic properties of the DPI formulations. Another goal was to investigate strategies to reduce electrostatic charge build up during the manufacturing process and study the processes involved in this phenomenon.

A standard inhalation device made of Acrylonitrile butadiene styrene (ABS) plastic and a custom inhalation device made of titanium were used to compare device material properties and simulate a state where presumably less electrostatic charge is built up in the metal device due its being a conductive material with less propensity to tribocharge. The radical change in materials was done to generate insights in electrostatic charge generation during

capsule spinning and aerosolization in the inhalation device (i.e. unit dose capsule inhaler), its dependence on the material properties of the device and its effect on the aerosol performance. Furthermore, several formulation process related electrostatic effects on *in vitro* aerosol performance (such as: two different APIs, presence of a force control agent (magnesium stearate), blending method and powder conditioning/storage) have been examined.

The results of this study are expected to provide a valuable insight into how changes of material properties during storage and aerosolization can affect electrostatic particle interactions of drug-carrier and drug-device, and consequently the *in vitro* aerosol performance of carrier-based DPI formulations.

Materials and Methods

Micronized fluticasone propionate (FP) and salmeterol xinafoate (SX) were supplied by Sandoz. Inhalation grade lactose monohydrate (Respitose® ML001) was purchased from DFE Pharma (Netherlands) and inhalation grade magnesium stearate (MgSt) from Peter Greven (Germany). Density, particle size data and specific surface area (SSA; Brunauer-Emmett-Teller theory) for all materials are given in Table 18.

Table 18: Materials used in this study and measured key characteristics.

Material	Denotation	Density [g/cm^3]	D10 [µm]	D50 [µm]	D90 [µm]	SSA [m^2/g]
Fluticasone propionate	FP	1.32	0.9	1.9	4.1	9.76
Salmeterol xinafoate	SX	1.11	0.7	1.4	2.9	6.99
Respitose® ML001	Lactose	1.53	6.6	57.8	170.3	0.63
Magnesium stearate	MgSt	1.05	1.6	6.1	21.3	16.61

Specific Surface Area

The specific surface area (SSA) of the powders was determined by the BET method (Brunauer-Emmett-Teller theory) based on nitrogen adsorption using a Quadrasorb SI (Quantachrome Instruments, USA). Adsorption isotherms at P/P_0: 0.01, 0.02, 0.03, 0.04, 0.05, 0.07, 0.1, 0.15, 0.2, 0.3, 0.4, 0.5, 0.6, 0.7, 0.8 and 0.9 were used.

Laser Light Diffraction Measurements

Laser light diffraction (LLD) analysis for particle size distribution (PSD) measurements was always performed using a Sympatec RODOS (Sympatec GmbH, Germany) dry dispersion system equipped with an R5 lens at 3bar.

Density Measurements

The density of the materials used in this study was determined with gas pycnometry (ULTRAPYC 1200e, Quantachrome Instruments, USA) according to the Pharmacopoeia Europea 8.0 (2.9.23)

DPI Formulation Preparation

Batches with a total amount of 50 g of powder (excipient and drug) were manufactured. For the high-shear excipient-blend, inhalation grade lactose and MgSt (0.5% w/w) was blended in a Collette MicroGral 2 L (GEA Pharma Systems, Switzerland) for 16 min at 1400 rpm. The low-shear excipient-blend was mixed for 16 min at 34 rpm in a Turbula® T2F mixer 2 L (Willy A. Bachofen AG, Switzerland). In both cases, excipient-blends together with the API were sieved and then mixed in a Turbula mixer at 34 rpm for 16 min (low-shear blending method). The final powder was filled manually (25 mg per capsule) into size 3 hydroxypropyl methylcellulose capsules (HPMC, QualiCaps, Spain) containing a dosage strength of 200 mcg API per capsule. All formulation manufacturing, processing and testing parameters are given in Table 19.

The content uniformity of manufactured DPI capsules was measured by analyzing the quantity of active in 25 ± 0.1 mg samples. Drug content was analyzed by high performance liquid chromatography (HPLC). Relative standard deviation between samples was calculated to assess the homogeneity of the different blends.

Table 19: DPI formulation manufacturing parameters used in this study.

	Pre-blending Excipient-blend	Blending with API	Filling	Conditioning	Actuation/Testing
High-shear formulations	Lactose + MgSt (high-shear)	Excipient-blend + FP or SX (low-shear)	HPMC Capsules (by hand)	Not conditioned (tested immediately after manufacturing and filling)	Standard ABS plastic device
				Conditioned at 25°C, 55% RH for 7 days	Custom made titanium device
Low-shear formulations	Lactose + MgSt (low-shear)	Excipient-blend + FP or SX (low-shear)	HPMC Capsules (by hand)	Not conditioned (tested immediately after manufacturing and filling)	Standard ABS plastic device
				Conditioned at 25°C, 55% RH for 7 days	Custom made titanium device

DPI Capsule Conditioning

Capsules were either not conditioned (tested immediately after manufacturing and filling) or stored in a clima chamber (CTS Clima chamber QK 10/660 EI, CTS-QS-Technik AG, Switzerland) chamber at 25°C and 55% relative humidity (RH) for a period of 7 days prior to the experiments for conditioning (Table 19). Previous studies have been performed to investigate optimal parameters for DPI capsule storage. Capsules were kept in open petri dishes.

Inhaler Devices used in this Study

A standard capsule based inhalation device inhalation device made of ABS plastic and a custom made inhalation device made of pure titanium with the exact same dimensions were used to compare device material properties (titanium device Figure 64 left).

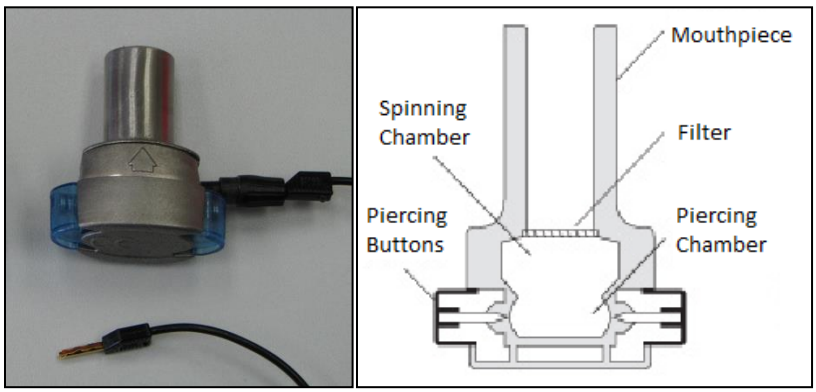

Figure 64: Left: Custom made (capsule based) inhalation device made of titanium with grounding wire. Right: Schematic of a standard capsule based inhalation device made of ABS plastic.

DPI Analysis by Next Generation Impactor (NGI)

The deposition of the dry powder formulations was investigated using an NGI equipped with a pre-separator filled with 15 mL of solvent (Acetonitrile: Water: TFA, 58: 42: 0.1 v/v/v). All measurements were conducted at 55% RH and ambient temperature (23 ± 2ºC). The cup trays of the impactor were coated with Brij® reagent (1% v/v solution of Glycerol in Ethanol). The capsules were actuated either in a standard plastic inhalation device or in a grounded titanium inhalation device at a flow rate of 90 L/min for 2.7 sec. The amount of powder deposited on the different collection cups was recovered by extracting each cup with solvent. The remaining powder in the capsule, device, powder deposited in the throat and pre-separator was also collected. After dissolution of the particles, HPLC analysis was performed. In this study the mean of three individual determinations was taken for a given NGI result.

FP and SX were analyzed using HPLC coupled with an UV-detector. The samples were eluted with an isocratic method with Acetonitrile: Water: TFA (58: 42: 0.1 v/v/v) as mobile phase, through an ACT ACE 3 C18,100 × 4.6 mm, 3 µm column (ACE, UK). A wavelength of 225 nm was used for detecting FP and SX. The peaks eluted at approximately 2.0 min for Salmeterol, xinafoate at 2.9 min and FP at 7.1 min. The flow rate through the HPLC system was 1.5 mL/ min. Data acquisition was carried out with Chromeleon.

Electrostatic Charge Decay of Powders

Electrostatic properties of powders were characterized using a charge decay time analyzer (JCI155v5, Chilworth Technology Ltd., UK). Samples (ca. 2g) were placed in the sample holder to form an even layer. A positive corona discharge of 9.0 kV was applied to the sample for a duration of 0.02 s. The data analysis was commenced at 0.07 s after the corona discharge, and the rate of charge decay was measured until 10% of the initial charge was reached. Five measurements were taken for each sample at 55% RH and ambient temperature (23 ± 2ºC).

Dynamic Emitted Electrostatic Charge (DEEC) Measurement

Dynamic emitted electrostatic charge (DEEC) measurements were performed using an in-house designed dynamic Faraday cage with an isolated mesh screen inside that is isolated from external fields (Figure 65). Actuated particles fly through the screen and impart a charge that is detected by a JCI 178 charge measuring unit electrometer (Chilworth JCI 178 Charge Measurement Device) to record the electrostatic charge that the powder generated on the mesh screen. The DEEC device was connected to a vacuum pump (Copley Scientific, USA). Five Capsules of each formulation were actuated in each device at a flow rate of 90 L/min for 2.7 sec and taken as a DEEC result. The measurements were performed at 55% RH and ambient temperature (23 ± 2ºC). A diagram and image of the experimental setup of the dynamic Faraday cage is shown in Figure 65.

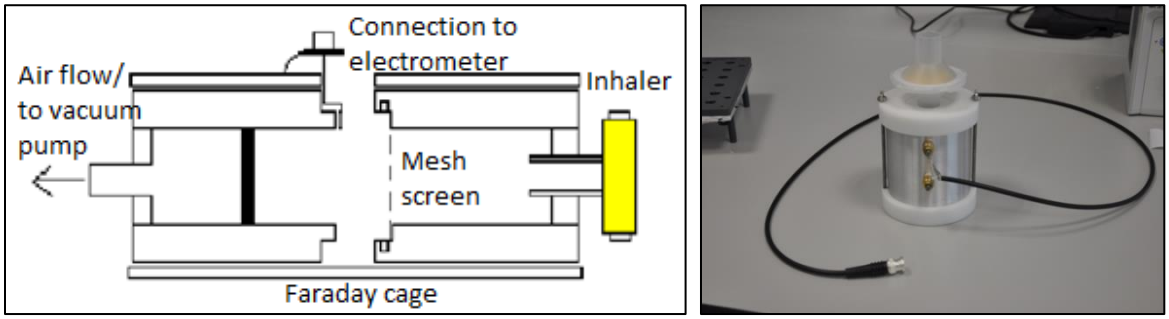

Figure 65: Schematic and photo of flow through Faraday pail for the measurement of the electrostatic emitted dose of DPI formulations.

Dynamic vapor sorption (DVS)

Dynamic vapor sorption (DVS) was used to assess the moisture sorption characteristics of the raw materials. Sorption profiles were determined using a DVS (Surface Measurement Systems Ltd., UK). Approximately 50mg of sample was weighed into the sample cell and subjected to a 0–95% relative humidity (RH) sorption cycle, over 10% (RH) increments. Equilibrium sorption at each humidity was determined by a change in mass to time ratio of ≥0.001 dm/dt.

Results and Discussion

Moisture Sorption Characteristics of the Raw Materials

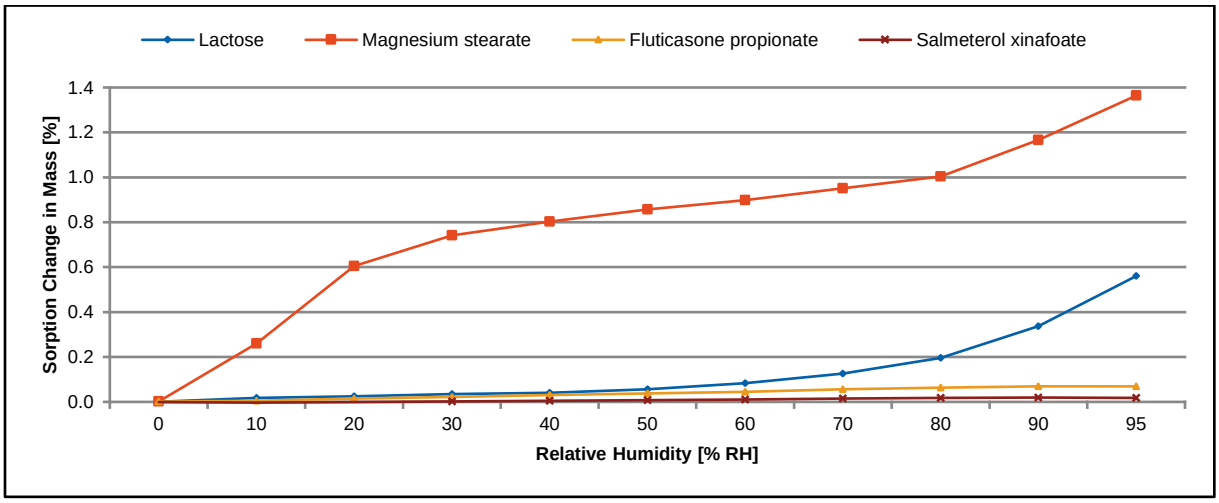

Figure 66: Dynamic vapor sorption profiles for pure lactose, pure magnesium stearate, fluticasone propionate and salmeterol xinafoate.

Representative moisture sorption isotherms for all raw materials are shown in Figure 66. A clear difference in moisture sorption for magnesium stearate and the other three materials was observed. The water sorption isotherm for magnesium stearate follows a sigmoidal class L3 curve, suggesting multilayer water sorption onto the surface [347]. Magnesium stearate seems to take up around 8-10x the amount of moisture compared to the other materials. Lactose, FP and SX do not seem to take up a significant amount of moisture below 65% of relative humidity.

Charge Accumulation by Corona Charging: Maximum Electrostatic Potential

Corona discharge has been used extensively as a method for assessing the electrostatic properties of various materials ranging from thin films [348] and fibers [349] to polymers [350] and powders [351]. The technique is believed to provide results comparable with tribocharging experiments [207, 352].

To assess the charging behavior of each material, the maximum electrostatic potential (V_{max}) of each powder was measured. The maximum charge provides an indication of the ability of the powder to become electrostatically charged under specific applied corona charging conditions. Figure 67 shows the maximum surface potential detected (V_{max}) for each tested sample.

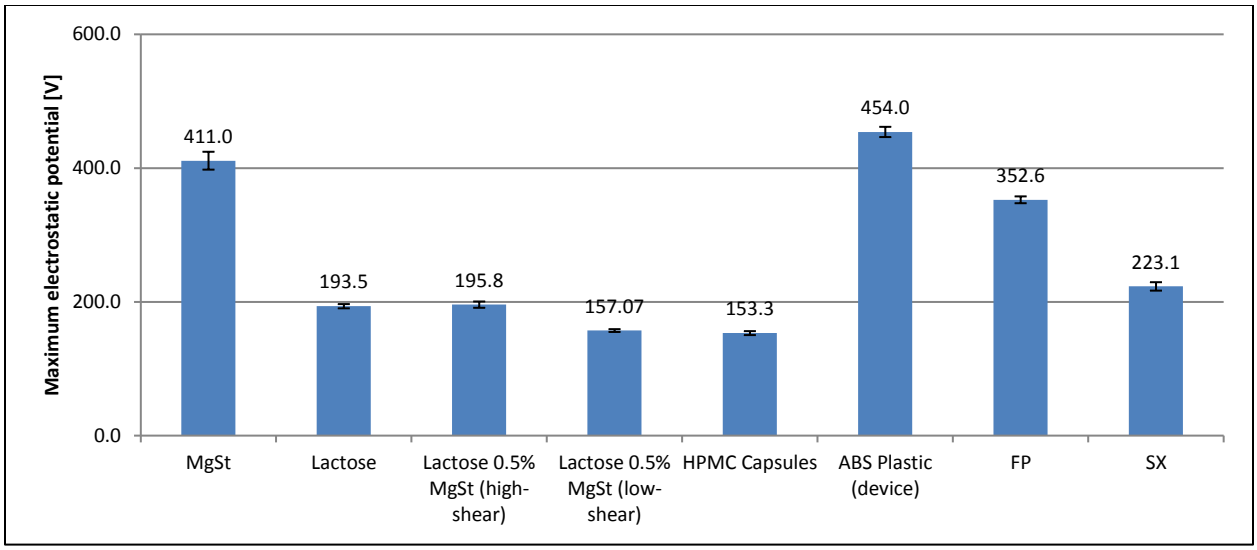

Figure 67: Maximum electrostatic potential (V_{max}) of different powders and materials used in this study charged by positive corona discharge (22°C, 50%RH; n=5 ±SD).

As shown in Figure 67, each sample accumulated a distinct level of charge under the same conditions. The ABS plastic, pure MgSt and FP acquired the highest overall charge while SX, HPMC capsules, pure lactose and the mixed excipient-blends containing MgSt acquired much lower overall charge. It should be noted, that HPMC and lactose contain similar structures.

The ability of FP to charge was in the range of approximately 352 V while SX charged up much lower at only a V_{max} of around 223 V. The ability of electrostatic charging of SX was therefore closer to that of lactose (V_{max} 193 V). Figure 67 could potentially indicate that the SX would likely tribocharge much less than the FP at selected experimental conditions.

The tested samples can be ranked in a corona charge holding series in the order of increasing ability to accumulate and hold charge as follows:

ABS Plastic > MgSt > FP > SX > high-shear excipient blend > Lactose > low-shear excipient blend > HPMC Capsules

A recent study by Biegaj and coworkers indicated that the electrostatic properties are directly related to the surface functional group chemistry, with hydrophobic and electronegative groups accumulating greater quantities of charge than hydrophilic groups. Florine-rich surfaces, such as fluticasone accumulate much greater charge upon tribocharging than hydroxyl-rich surfaces as for example in salmeterol [207]. This seems to be in line with the findings in the present study.

Interestingly, the ABS plastic shows a very high propensity to build up electrostatic charge, although it is commonly used as a material for medical inhaler devices. This material is highly insulative and therefore completely non-conductive. The volume resistivity of ABS plastic is $>10^{16}$ Ohm.cm; below 10^5 Ohm.cm a material is considered as conductive; above 10^9 Ohm.cm a material is considered as an electrical insulator [353]. The volume resistivity of lactose is 10^4 Ohm.cm, and the resistivity of HPMC is approximately 10^6 Ohm.cm. This indicates that both materials are at least somewhat conductive. In contrary, pure MgSt is known to be very hydrophobic and can accumulate very high amounts of electrostatic charge, similar to ABS plastic, which suggests a high volume resistivity. However, its volume resistivity is not known in literature.

Electrostatic Charge Decay

An electrostatic charge decay test unit was used to characterize and compare the charge decay kinetics of the formulation components (FP, SX, lactose, MgSt, HPMC capsules and device material) under controlled laboratory conditions of 22°C and 50% RH following application of a constant corona charge voltage of 9kV across each test sample. The charge decay results are shown in Figure 68.

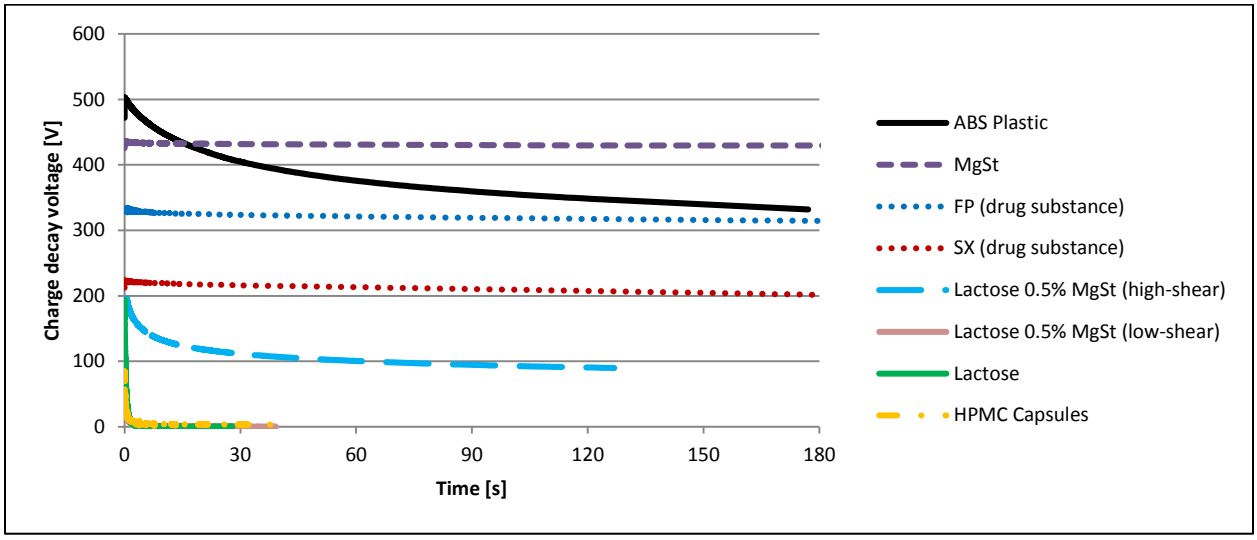

Figure 68: Comparison of charge decay curves (at 22°C, 50% RH) for materials used in this study.

It can be concluded from Figure 68 that MgSt, FP and SX are uniquely placed with respect to charge retention relative to the other formulation components. They all dissipate the charge extremely slowly. However, it should be noted, that the SX dissipates faster than FP and MgSt and furthermore, it accumulates a much lower amount of charge. In contrast, the charge decay of lactose, the lactose-MgSt low-shear excipient blend and HPMC capsules is extremely fast within only a few seconds (to 0 V).

As expected, the decay kinetics behavior of the lactose-MgSt high-shear excipient-blend is dominated by the presence of MgSt on the lactose surface. As demonstrated in previous work, the magnesium stearate is not coating surface of the lactose particles in the low-shear blend [146], the surface mainly consists of lactose, and the electrostatic charge can be distributed and dissipated much faster through the lactose.

The device material (ABS plastic) dissipates charge quite slowly compared to lactose and HPMC capsules and is comparable to the MgSt and FP. The ABS plastic reaches the overall highest charge potential of all tested samples.

The results suggest that any residual charge related performance issues of the drug product would originate mainly from the drug substance, MgSt or device material. Lactose and HPMC Capsules dissipate the charge extremely fast.

Although it has been described earlier that corona discharge has been used extensively as a method for assessing the electrostatic properties of various materials and the technique is believed to provide results comparable with tribocharging experiments, there are still some unknown variables and differences that cannot be simply explained. It is important to note that during tribocharging much lower electrostatic charges are generated as compared to corona charging [207]. When using corona charging for these measurements, a constant positive corona discharge of 9.0 kV was applied to the sample for a duration of 0.02 seconds. These measurements are very useful for characterizing the raw materials when they are used to predict tribocharging. Additional factors should also be considered such as material against which the powder is in frictional contact with and also the duration of the tribocharging event.

Influence of Relative Humidity on Electrostatic Charge Decay Rate

Triboelectrification is considered as a surface phenomenon and can therefore be influenced by several external parameters such as for example temperature and relative humidity [354]. Typically, higher moisture content in the surrounding environment results in a reduction in the absolute charge generated during the tribocharging process [355, 356] but it also will have an impact on how long a charge can remain on a surface before being neutralized. This can then have an impact on how long a charged powder will remain charged, depending on the environmental conditions. Experiments were conducted on the different blends in this study looking at the charge decay rate as a function of relative humidity (%RH) to gain understanding about the role %RH plays in charge decay rates that could impact aerosol performance.

Figure 69 illustrates the decay time required for the charge to decrease to 10% ($t_{1/10}$) of its initial level, for the samples tested with a corona discharge of 9.0 kV. This data quantifies how quickly powder surfaces lose charge when subjected to a corona charging method.

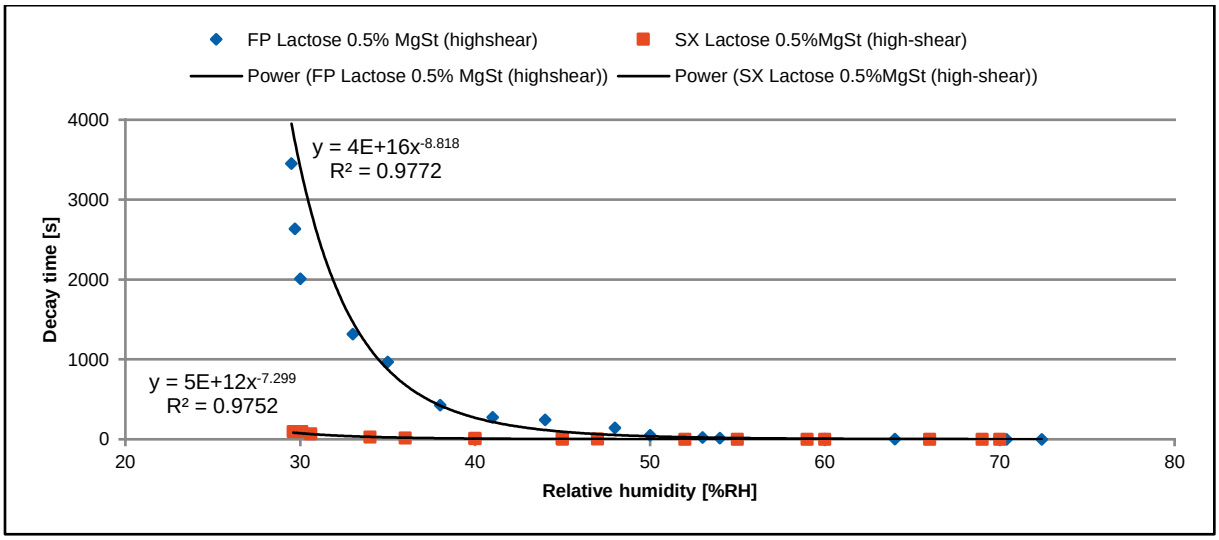

Figure 69: Charge decay of FP and SX Lactose 0.5% MgSt (high-shear) formulations at different relative humidity levels as a result of negative corona discharge (average n=3).

In general, an increase in relative humidity resulted in a decrease in the charge relaxation times for all samples tested using a corona discharge method. This general observation agrees with previously published data on the effect of humidity on charge decay kinetics [356, 357]. However, there is a significant difference in charge decay time highly depending on the API in the formulation. As seen in Figure 69, the fluticasone formulation exhibited much slower charge decay kinetics below relative humidity of 50% RH, while the charge on the salmeterol formulation still dissipated very fast (less than 100 sec) even down to 30% RH. This observation also seems to be in line with previous investigations that electrostatic properties of powders are directly related to the surface functional group chemistry of the sample measured [207]. Both the fluticasone and salmeterol formulations have very rapid charge decay kinetics above 50% RH. The charge decay times for different surfaces became more similar and therefore the surface chemistry itself became less pronounced at higher humidity levels. Interestingly, the excipient-blend for both formulations was manufactured with a high-shear blending method to apply a thin MgSt coating on the lactose surface [146], but the charge decay kinetics seemed to be mainly dominated by the API properties and not by the excipient-blend, which was not entirely expected as MgSt on its own showed very slow charge decay kinetics and a high propensity to accumulate electrostatic charge previously in Figure 67 and Figure 68.

It has been previously discussed in literature that charge relaxation properties could not only be dependent on the existing surface moisture but could also be a function of the interactions with water and ions present in the surrounding environment. An overall reduction in electrostatic charge by moisture is also associated with a lowering in surface resistivity, because of water molecules physically adsorbing on the surface. More specifically, the presence and adsorption of $[OH(H2O)_n]^-$ and $[H(H2O)_n]^+$ ions on the surface have been identified to contribute towards a reduction of charge [358]. A preferential adsorption of either type of water ion, depending on the surface type, has been observed by Burgo et al. [359]. This indicates indeed, that water plays an important role as a source and sink of ions in the surface electrostatic phenomenon [359-361].

Electrostatic Behavior and In Vitro Aerosol Performance of FP DPI Formulations

For DPI formulations two main causes can lead to a build-up of electrostatic charge: (A) the manufacturing process (micronization, sieving, mixing, filling, transport and storage) and (B) the actuation of the device (tribocharging during aerosolization process). For capsule based DPIs, the electrostatic forces present or acquired on drug and excipient powders during the manufacturing process or capsule spinning in the inhaler device can cause agglomeration with other particles, reduced deagglomeration of drug particles from carrier or adhesion of particles to device surfaces with a resulting impact on dispersion properties of DPI products. The formulation and/or its components can be electrostatically charged during the various API and final product manufacturing process steps, leading to a change in the electrostatic forces between particles and surfaces and potentially resulting in a higher retention of the powdered formulation on the capsule itself and device surfaces when tested shortly after manufacture. As the charge decays, the electrostatic forces within the formulation decline resulting in an increased dispersion efficiency of the formulation upon actuation from the delivery system.

It would be expected that triboelectric charging during device actuation is highly dependent on the type of material the particles are undergoing frictional contact with. Measurements of triboelectric charging of the powder plume expelled from the inhaler were performed to assess the electrostatic behavior of model powders and DPI formulations and the potential influence of charge on aerosol performance (FPF). Dynamic electrostatic charge measurements were performed with a custom made device described in the methods section. Measurements for pure lactose and pure MgSt are shown in Figure 70. Using a standard plastic device made of ABS plastic, emitted pure lactose particles are charged slightly negative/close to zero (capsule filled with pure lactose) while pure MgSt particles are charged strongly positively (capsule filled with pure MgSt). When changing the device type to a grounded titanium device, pure lactose changed from slightly negative charge to positive while MgSt remained positively charged.

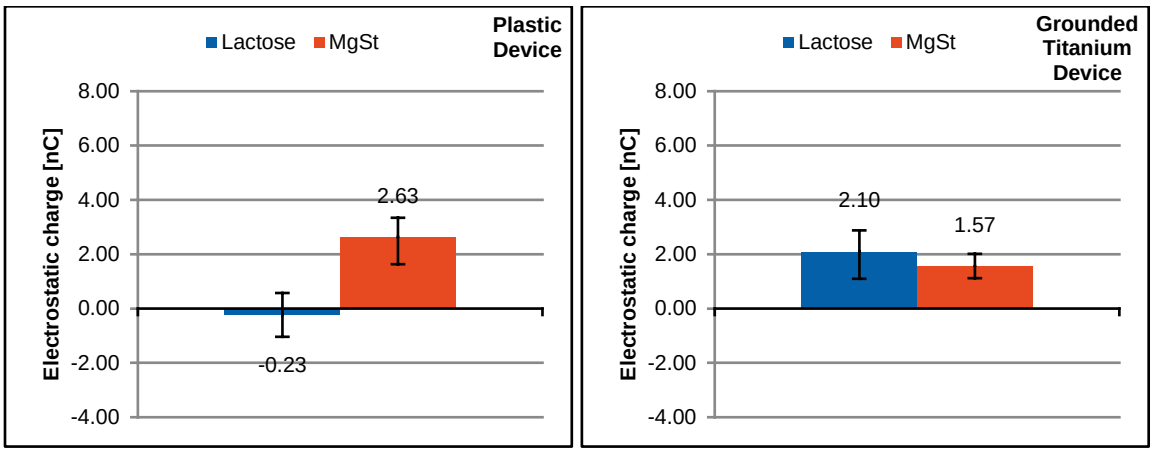

Figure 70: Dynamic charge measurement of pure lactose and pure MgSt with standard ABS plastic device (left) and grounded titanium device (right).

Measurements of the dynamic emitted electrostatic charge (DEEC) showed significant differences between the various FP formulations tested with a standard ABS plastic device (Figure 71 and Table 20). The FP is again to have a very high propensity for acquiring and retaining electrostatic charge as determined from its maximum acquired potential (V_{max}) and charge decay measurements.

In an attempt to reduce electrostatic charge acquired during the powder manufacturing process to optimize aerosol performance, capsules were conditioned at 25°C and 55% RH in order to dissipate the charge. In general, an increase in relative humidity resulted in a significant decrease in the dynamic electrostatic charge for all of the samples tested in this study. This general observation agrees with our data and previously published data on the effect of humidity on charge decay kinetics [205, 207]. For all tested FP formulations, the measured charge was significantly lower (closer to zero) after the conditioning step (tested with the standard ABS plastic device). A strong relative difference (Δ) in the range of 1-2 nC was measured between conditioned and not-conditioned FP DPI capsules with the unconditioned capsules generating higher electrostatic charges when using a standard plastic device (Table 20 and Figure 71). However, no significant effect before and after conditioning could be detected when using the titanium device. Table 20 shows that the effect of humidity on charge decay rate is different for different powder formulations.

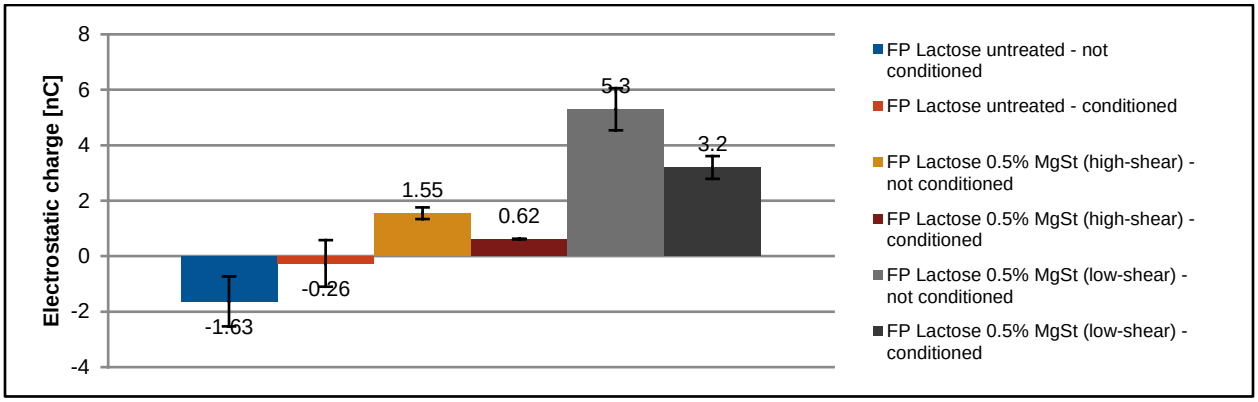

Figure 71: Dynamic electrostatic charge measurement with standard ABS plastic device for FP formulations before and after conditioning (n=5 capsules shot ±SD).

The results in Figure 71 show that the addition of MgSt to a FP lactose formulation changes the overall polarity of the powder with low-shear mixing having a positive and high charge upon actuation. This might be because with low-shear MgSt is still present as discrete particles in the formulation, which will charge up during tribocharging. Since MgSt is an electrical insulator and is not in direct contact with conductive surfaces and has minimal contact surface with the lactose and API particles it will therefore strongly retain charge (based on slow charge decay measured for pure MgSt, Figure 68). However, when applied through high-shear blending [146], the thin layer of MgSt (<10 nm) is in direct contact with lactose, which could act as an effective sink (based on the rapid charge decay measured for lactose, Figure 68) for the charge, thus lowering the overall impact of having MgSt in the formulation. Values in a similar range have been measured by Byron and coworkers for the APIs budesonide and salbutamol sulfate using similar measuring techniques [189].

Table 20: DEEC measurement of FP formulations before and after conditioning (n=5 ± SD).

Formulation	ABS plastic device			Titanium device		
	Charge [nC]	SD	Δ	Charge [nC]	SD	Δ
FP Lactose untreated - not conditioned	-1.63	0.9		2.85	0.66	
FP Lactose untreated - conditioned	-0.26	0.84	1.37	2.58	0.64	0.27
FP Lactose 0.5% MgSt (high-shear) - not conditioned	1.55	0.21		0.68	0.28	
FP Lactose 0.5% MgSt (high-shear) - conditioned	0.62	0.01	0.93	0.8	0.22	0.12
FP Lactose 0.5% MgSt (low-shear) - not conditioned	5.3	0.76		3.09	0.23	
FP Lactose 0.5% MgSt (low-shear) -conditioned	3.2	0.41	2.1	2.75	0.35	0.34

Many of the theoretical models developed to describe charge transfer and triboelectrification assume that charged species are only transferred from one material to another resulting in a unipolar charge distribution for each material present during the contact [362]. But during the manufacture of respiratory drug products, particles will undergo multiple collisions with many different types of materials such as stainless steel (equipment for micronizing and blending), gelatin or hydroxypropylmethyl cellulose (HPMC) used for capsules and plastic and/or metal components of the inhaler. Excipient-excipient, excipient-API and API-API collisions will also lead to charge transfer [363]. While the overall net charge of the powder will remain constant, due to the different types of collisions involved some particles will become positively charged and some will become negatively charged, resulting in a bipolar charge distribution within the powder where the particles will be both positively and negatively charged at the same time. Furthermore, different particle sizes will charge differently. [364].This can be difficult to assess accurately using conventional methods of measuring net charge as net charge only provides a sum of the positive and negative charges present [365, 366]. Bipolar charge can be measured using an electrical low pressure impactor (ELPI). Since the MgSt prefers to charge positively and the FP prefers to charge negatively, it may also be possible that the overall charge of such a formulation is neutral (or close to zero) and this could then be advantageous for powder dispersion mechanics and thus aerosol performance. The bipolar charge then depends on multiple factors, such as the number of particles involved, their size and identity.

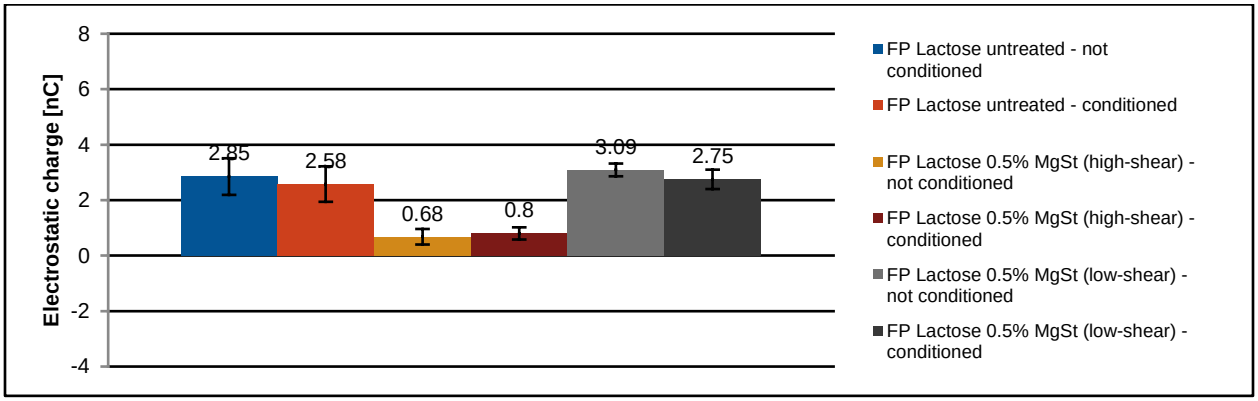

Figure 72: Dynamic electrostatic charge measurement with grounded titanium device for FP formulations before and after conditioning (n=5 capsules shot ±SD).

Measuring the dynamic electrostatic charge using the titanium device shows a reduction in electrostatic charge compared to the standard plastic device for both the high- and low-shear blends containing MgSt in the non-conditioned state. Furthermore, there was no more significant difference detected before and after conditioning for all FP formulations (Figure 72). Interestingly, the charge generated using the titanium device for the blends containing MgSt (conditioned and not-conditioned) were at the same levels as the electrostatic charge levels generated for the same formulations using the standard plastic device with conditioned capsules.

For the FP Lactose untreated formulation there was a shift from negative to positive overall charge with the difference in device contact material (ABS plastic-titan). An important aspect in addition to the magnitude of the charge seems to be the polarity of the electrostatic net charge generated. Negative charge has been described in literature to decay much slower than positive electrostatic charge [359]. (Small) Negative electrostatic charge also seems to be disadvantageous for aerosol performance (FP Lactose untreated). Furthermore, generating high positive electrostatic charge also results in lower aerosol performance (Figure 73).

Comparing the electrostatic charge built up in the two tested devices, it was detected that there is a lower amount of electrostatic charge generated when actuating the capsule in the grounded titanium device. This difference in charge indicates that a significant amount of charge in the powder is from triboelectrification in the device itself. A significant amount of electrostatic charge is also depending on the materials in the formulation. Another interesting finding was also that there was no longer a significant difference in electrostatic charge between conditioned and un-conditioned samples when using the grounded titanium device (Δ relative difference). These findings seem to be in line with what Elajnaf and coworkers concluded that the effect of humidity on charge decay kinetics can be further affected by the nature of the contacting surface, as differing extents of charge reduction could be observed when the same powder interacted with metal or plastic surfaces [355].

Assuming that a significant amount of electrostatic charge is generated due to tribocharging in the device upon aerosolization of the formulation and not during formulation manufacturing at least for FP, then another hypothesis for the increase in aerosol performance could also be that adding moisture by conditioning the DPI capsules is modifying (decreasing) the way in which tribocharging occurs in the device. An overall reduction in electrostatic charge by moisture is associated with a lower surface resistivity, because of water molecules adsorbing on the surface [358, 359]. This would mean that less tribocharging can be occurring after conditioning of the capsules due to the presence of moisture in the formulation and capsule shell. In contrast to the standard ABS plastic device, the grounded titanium device presumably only generates low amounts of tribocharging, and the difference in electrostatic charge before and after conditioning of the DPI capsules might be negligible as the moisture effect is almost irrelevant.

Comparing the dynamic electrostatic measurements for FP to the *in vitro* aerosol performance determined with cascade impaction testing (Figure 73) it seems evident that the electrostatic behavior has a considerable influence on the performance for the FP formulations tested in this study. After conditioning the capsules at given conditions, the *in vitro* aerosol performance was improved in all tested FP formulations when using a plastic device.

The impact of the observed electrostatic effects on the *in vitro* aerosol performance in terms of fine particle fraction (FPF, % of declared content) of the fluticasone formulations after manufacturing and after storage for seven days under controlled conditions at 25°C and 55% RH are given in Figure 73.

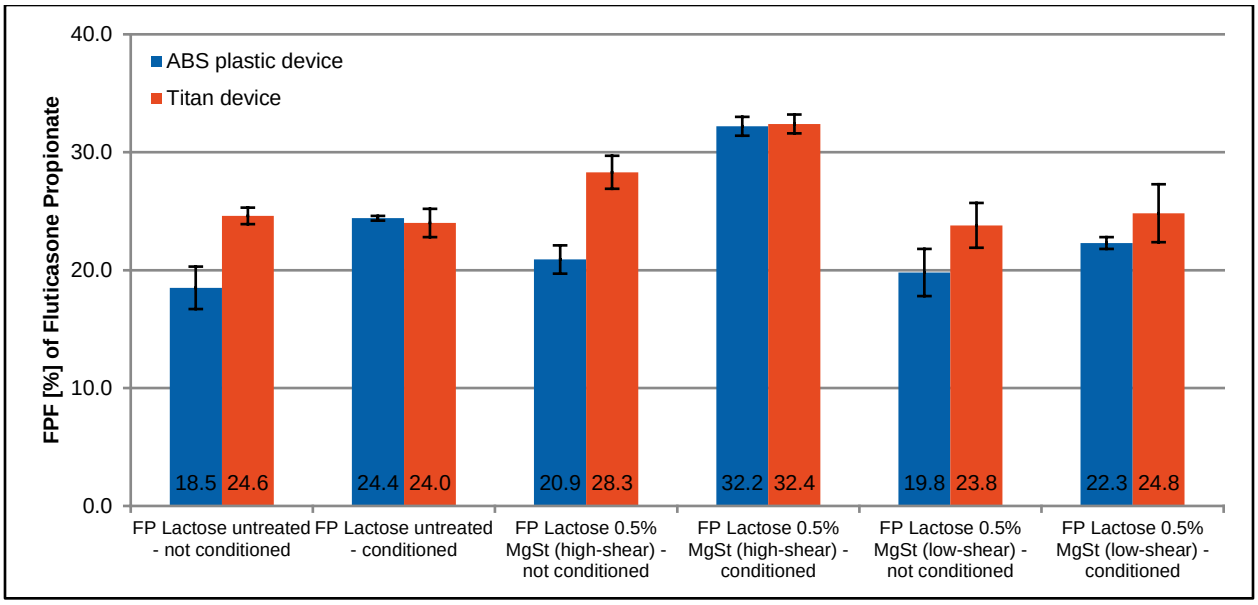

Figure 73: Fine Particle Fraction (FPF; % of declared content; ± SD) of Fluticasone Propionate DPI formulations before and after conditioning at 25°C/55% RH for 7 days obtained by NGI (n=3 capsules).

A consistent and reproducible change in FPF was observed before and after conditioning of the FP DPI capsules. In vitro data show that a significant increase in performance was determined for the fluticasone formulations when actuating with an ABS plastic device for unconditioned DPI formulations. The FP formulations increased about 6% (abs.) (Lactose untreated), 11% (Lactose 0.5% MgSt high-shear) and 3% (Lactose 0.5% MgSt low-shear) in FPF after conditioning of 7 days using the ABS plastic device. Interestingly, no significant difference was observed before and after conditioning when actuating the FP capsules with the grounded titanium device. These observations for the plastic device go in hand with a significant reduction of electrostatic charge (Δ) as can be seen from Table 20, Figure 71 and Figure 72. The titanium device showed no change from unconditioned to conditioned and this can reflect the lack of change in FPF.

Figure 74 and Figure 75 show plots of the electrostatic charge (determined from the dynamic charge measurement) against fine particle fraction (determined by NGI measurement) of fluticasone formulations before and after conditioning. The measurements for Figure 74 were obtained with the ABS plastic device while for Figure 75 the titanium device was used. It can be clearly seen that the tested formulations exhibiting a total electrostatic charge < ±1 nC results in higher *in vitro* aerosol performances. In Figure 75 it can also be seen that the presence of MgSt and the use of the high-shear blending technique results in lower electrostatic charge and higher aerosol performance. Overall, the electrostatic charging behavior for the fluticasone formulations using the titanium device seems to be also less variable compared to the ABS plastic device (Figure 74). One thing that seems to apparent from Figure 11 is that the overall polarity of the powder is significant and that less negative charge seems to be more detrimental to in vitro performance than the equivalent positive charge for FP formulations.

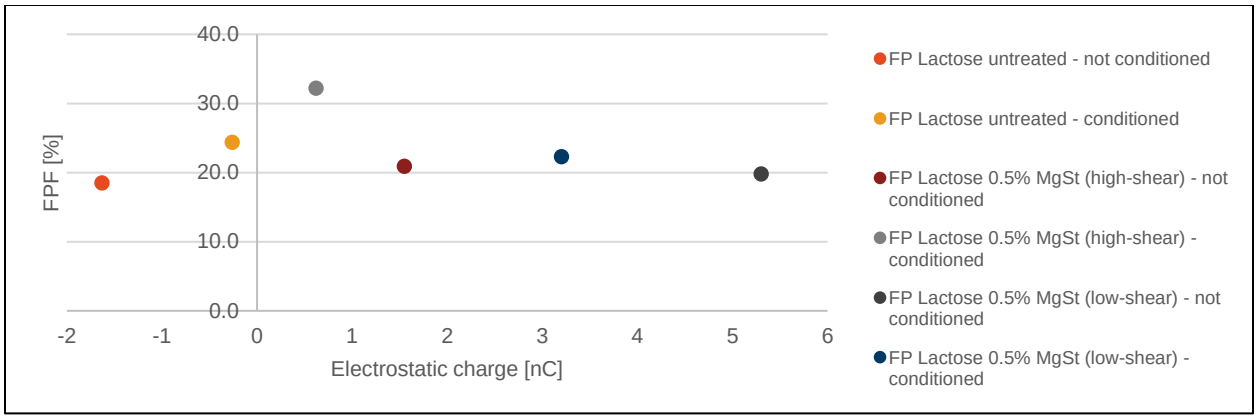

Figure 74: Electrostatic charge vs. fine particle fraction of fluticasone propionate tested with an ABS plastic inhalation device (before and after conditioning).

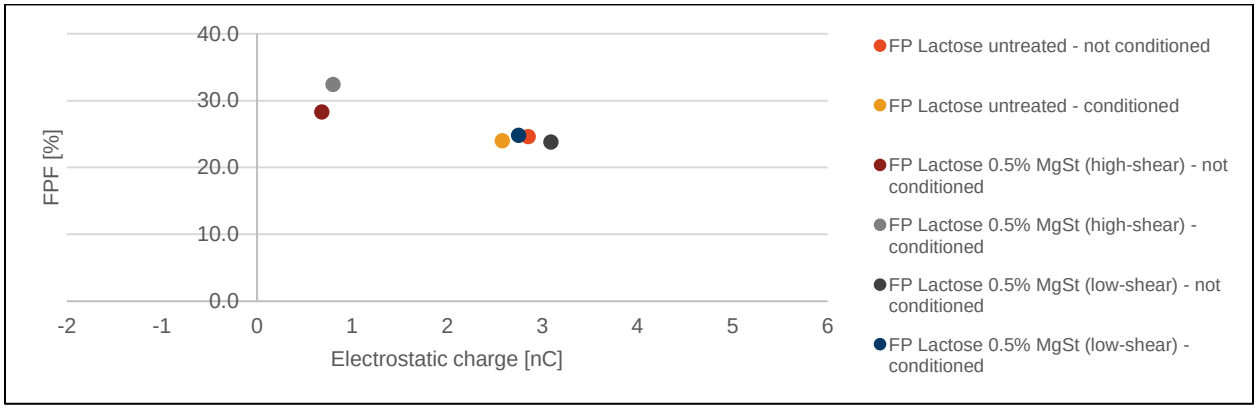

Figure 75: Electrostatic charge vs. fine particle fraction of fluticasone propionate tested with a titanium inhalation device (before and after conditioning).

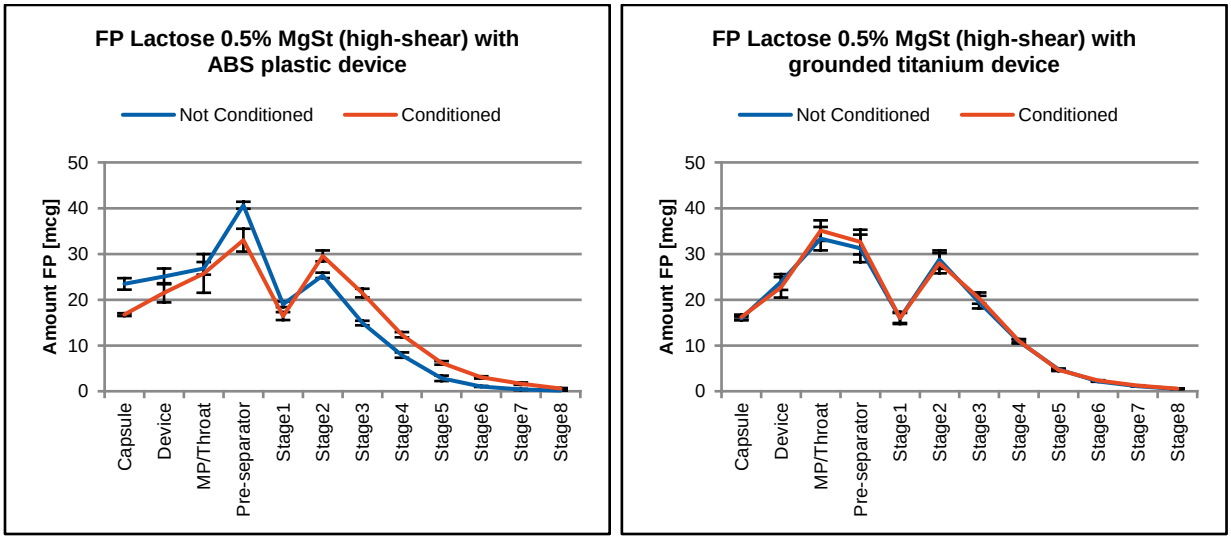

Figure 76: Aerodynamic particle size distribution of fluticasone high-shear formulations before and after conditioning (25°C/55% RH for 7 days) obtained with NGI (APSD; average n=3 capsules ± SD). Actuation with standard ABS plastic device (left) and grounded titanium device (right).

Figure 76 shows the NGI APSD histograms for the FP Lactose 0.5% MgSt (high-shear) formulation before and after conditioning using either the plastic device or the grounded titanium device. It could be determined that there was no difference in the APSD profile before and after the conditioning period when using the grounded titanium device. However, there were apparent differences measured when using a plastic device. A significant reduction in drug deposition was observed in the capsule, inhaler device and pre-separator. This resulted in a large shift to smaller particle size and better drug detachment from larger carrier. The deposition in NGI stages 2-8 was significantly increased.

The blending technique also seems to have an impact on the interparticulate electrostatic forces. High-shear blending of MgSt seems to modify the carrier surface so that electrostatic forces, between drug and carrier and also between fine excipient and coarse excipient, are much reduced as witnessed by the increase in fine particles observed for FP with NGI (Figure 73). The modification of particle interaction from drug-lactose to drug-MgSt (in high-shear) seems to be responsible for the improved performance (enhanced particle detachment from carrier due to lower interaction forces). Low-shear blends with FP seem to have a reduced drug detachment, even after conditioning, from the carrier due to high interactive forces such as van der Waals or capillary forces (non-electrostatic forces) and also electrostatic forces (as witnessed in this study) and therefore a lower FPF.

Electrostatic Behavior and In Vitro Aerosol Performance of SX DPI Formulations

Measurements of the dynamic emitted electrostatic charge (DEEC) for the SX formulations are shown in Figure 77 (ABS plastic device), Figure 78 (grounded titanium device) and Table 21. All tested SX formulations seemed to exhibit weak electrostatic forces. SX does not have the same propensity to charge as FP and in fact seems to dissipate electrostatic charge relatively effectively. This was observed as SX had quite a low propensity for acquiring electrostatic charge as determined from its maximum acquired potential (V_{max}) around only 220 V as compared to the highly electrostatic compound FP around 350 V. Furthermore, there was no difference in dynamic emitted electrostatic charge detected before and after conditioning ($p>0.05$) of the SX DPI formulations when using the plastic device (Table 21).

Measuring the dynamic electrostatic charge using the titanium device shows a shift from positive to negative overall charge for the MgSt-blends with the difference in device contact material. Interestingly, there was also no significant ($p>0.05$) change between conditioned and un-conditioned samples (Δ relative difference). All formulations tested with the plastic had a dynamic electrostatic charge around +1.1nC. Using the grounded titanium device, the formulations containing MgSt exhibited an average dynamic charge around -1.4nC while the Lactose formulation had an average dynamic charge around +1.3nC. The conditioning step did not seem to influence the electrostatic charging behavior of SX (relative difference Δ in the range of 0.02 nC after conditioning).

All three SX formulations exhibited a relatively high *in vitro* aerosol performance (as compared to the highly electrostatic FP) as could be verified with NGI (Figure 73). This could also be attributed to the weak electrostatic interaction forces measured in the SX formulations.

Table 21: DEEC measurement of SX formulations before and after conditioning (n=5 ± SD).

	ABS plastic device			**Titanium device**		
Formulation	Charge [nC]	SD	Δ	Charge [nC]	SD	Δ
SX Lactose untreated - not conditioned	1.08	0.21		1.54	0.45	
SX Lactose untreated - conditioned	1.06	0.34	0.02	1.15	0.32	0.39
SX Lactose 0.5% MgSt (high-shear) - not conditioned	1.11	0.39		-1.55	0.36	
SX Lactose 0.5% MgSt (high-shear) - conditioned	1.08	0.6	0.03	-1.22	0.16	0.33
SX Lactose 0.5% MgSt (low-shear) - not conditioned	1.15	0.21		-1.36	0.31	
SX Lactose 0.5% MgSt (low-shear) - conditioned	1.14	0.18	0.01	-1.36	0.66	0

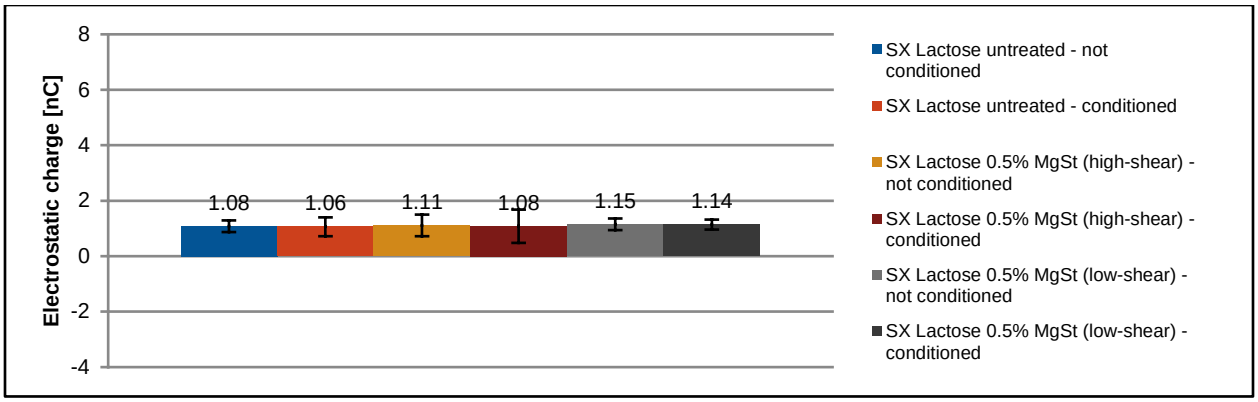

Figure 77: Dynamic electrostatic charge measurement with ABS plastic device for SX formulations before and after conditioning (n=5 capsules shot ±SD).

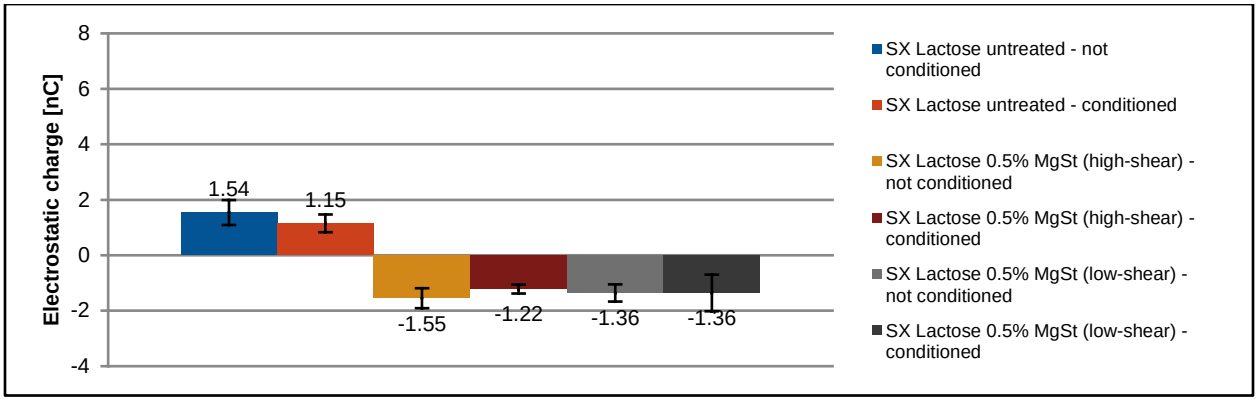

Figure 78: Dynamic electrostatic charge measurement with grounded titanium device for SX formulations before and after conditioning (n=5 capsules shot ±SD).

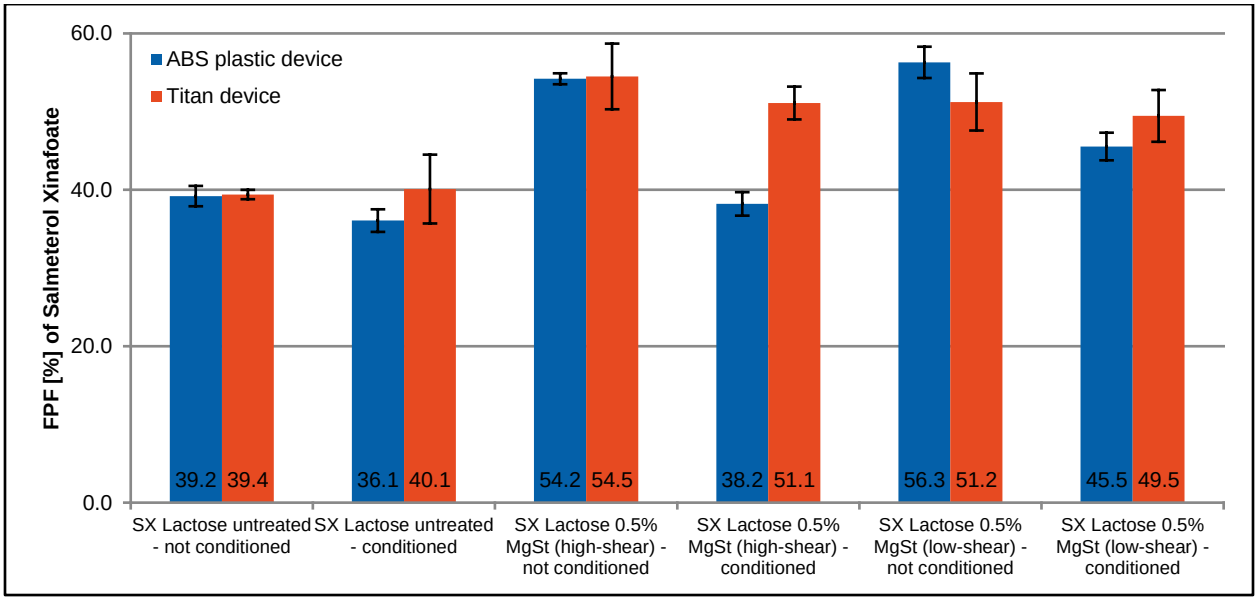

Figure 79: Fine Particle Fraction (FPF; % of declared content; ± SD) of Salmeterol Xinafoate DPI formulations before and after conditioning at 25°C/55% RH for 7 days obtained by NGI (n=3 capsules).

In vitro aerosol performance data show that storage at the conditions used did affect the FPF of salmeterol with a considerable decrease after storage. The SX formulations decreased around 3% (Lactose untreated), 16% (Lactose 0.5% MgSt high-shear) and 11% (Lactose 0.5% MgSt low-shear) in FPF when conditioned at 25°C and 55% RH for 7 days and actuated with a plastic inhaler device. This is in stark contrast to the FP formulations, where a significant increase in performance was observed after storage when actuating the FP capsules with the ABS plastic device. The decrease in aerosol performance for SX formulations using a plastic device was determined to be much more pronounced if MgSt was present in the formulation. The decrease of 3% in performance for the SX Lactose untreated formulation seems to be negligible. This might be due to the ability of MgSt to take up a much higher amount of moisture than the other formulation components (Figure 66). A hypothesis could be that due to a higher water uptake there is an increased likelihood to form water bridges in these formulations. Further studies are necessary to learn more about this phenomenon.

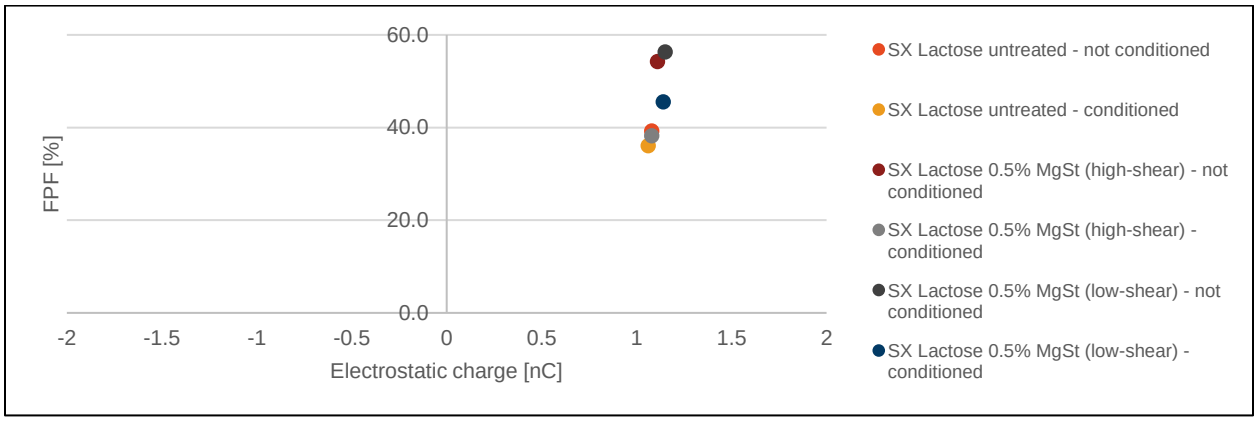

Figure 80: Electrostatic charge vs. fine particle fraction of salmeterol xinafoate tested with an ABS plastic inhalation device (before and after conditioning).

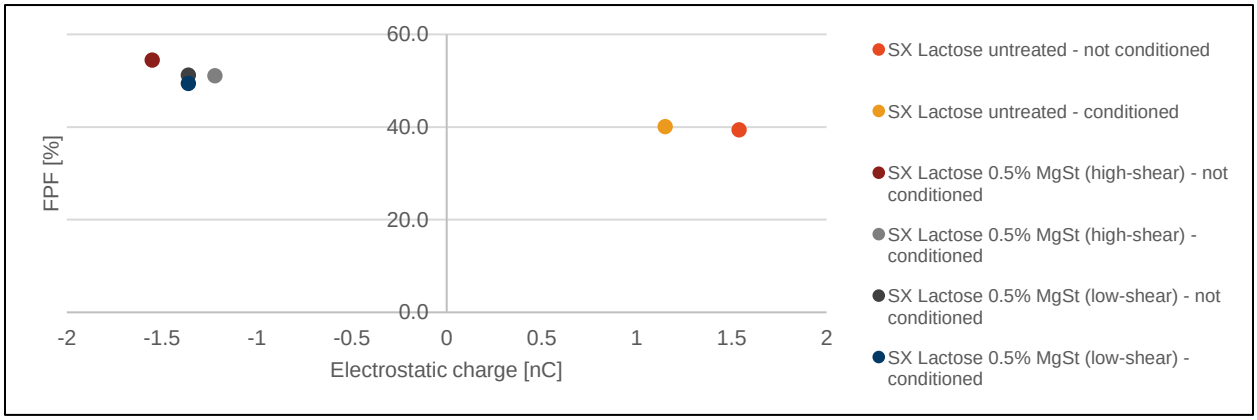

Figure 81: Electrostatic charge vs. fine particle fraction of salmeterol xinafoate tested with a titanium inhalation device (before and after conditioning).

Figure 80 and Figure 81 show plots of the electrostatic charge (determined from the dynamic charge measurement) against fine particle fraction (determined by NGI measurement) of salmeterol formulations before and after conditioning. The measurements for Figure 74 were obtained with the ABS plastic device while for Figure 75 the titanium device was used. The amount of electrostatic charge built-up using an ABS plastic device does not seem to differ between the tested salmeterol formulations as can be seen in Figure 80. The *in vitro* aerosol performance seems to be more dependent on the presence of MgSt in the formulation and on humidity exposure rather than on electrostatic

charge. Overall, only lower amounts of electrostatic charge in the range of +/-1.5 nC were measured for SX formulations. From the results in Figure 81, it seems that the addition of MgSt results in a negative charge relative to contact with titanium device material in presence of salmeterol.

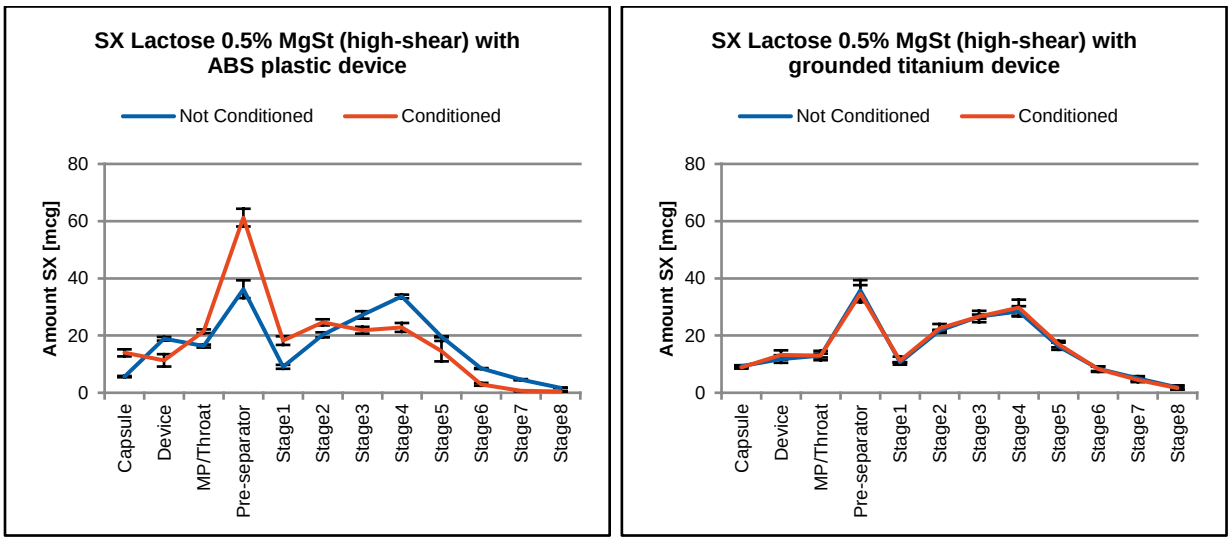

Figure 82: Aerodynamic particle size distribution of salmeterol low-shear formulations before and after conditioning (25°C/55% RH for 7 days) obtained with NGI (APSD; average n=3 capsules ± SD). Actuation with standard ABS plastic device (left) and grounded titanium device (right).

Figure 82 shows the NGI APSD histograms for the SX Lactose 0.5% MgSt (high-shear) formulation before and after conditioning using either the standard plastic device or the grounded titanium device. It could be determined that there was no significant ($p>0.05$) difference in the APSD profile before and after the conditioning period when using the grounded titanium device. Similar to the FP formulation in Figure 76 there were apparent differences measured when using a plastic device. However, a significant reduction in drug deposition was observed in NGI stages, while the deposition in the capsule, mouthpiece/throat and pre-separator was significantly increased. The conditioning period resulted in a shift to larger particle size and decreased drug deagglomeration from carrier.

Hygroscopicity is the intrinsic tendency of a material to take on moisture from its surroundings. It is affected by the crystallinity of the material and the particle morphology. Hygroscopic drugs such as SX present a greater risk of physical and chemical instability while more lipophilic APIs such as FP are expected to have only a very limited water uptake [367]. Moisture uptake and loss due to changes in relative humidity can result in local dissolution and recrystallization of the API, leading to irreversible aggregation through solid bridge formation [8], which can negatively influence aerosol generation and thus decrease lung deposition [343]. This water uptake can alter adhesive and cohesive properties or even increase particle size substantially. Hygroscopic growth has implications for the equilibrium moisture content of the particles in the dosage form prior to aerosol generation and it can cause chemical or physical instability of the product in some cases [368]. A number of excipients can modify the hygroscopic properties of a drug. Previous studies have also evaluated the influence of storage humidity on the dispersion of DPI formulations [309, 369, 370]. Young et al. observed that the fine particle fraction (FPF) of some APIs decreased at elevated humidity while other APIs exhibited an increased *in vitro* aerosol performance when stored at different humidity conditions [370].

Currently it is not fully understood why there is no drop in performance for the conditioned SX formulations with MgSt when using the titanium device. In this study it could be demonstrated that the dynamic emitted electrostatic charge is different depending on the device material. Although both the ABS plastic and titanium device have the exact same dimensions, it was observed that the surface of the titanium device is much rougher compared to the

smooth surface of the injection molded ABS plastic device. Further studies are necessary to investigate an effect of device surface roughness on drug deagglomeration and particle-particle or particle-wall collisions. A difference in device surface roughness might lead to different spinning properties (e.g. turbulence) due to a presumably smaller contact area of capsule and device surface.

Conclusions

The results of the present study highlight that electrostatic forces and interactions play a significant role in dry powder inhaled formulations. Large differences in the electrostatic charging behavior were observed. Fluticasone propionate seems to have a high propensity to electrostatically charge, while salmeterol xinafoate only showed a negligible electrostatic charging behavior. FP drug particles tend to acquire and carry much higher electrostatic charges compared to SX particles and excipients (with the exception of pure MgSt). APIs may also possess a larger variety of elements, including halogen containing functionalities such as in FP. Therefore they may be more electrically resistive, which makes them more prone to acquiring charge. This ability of acquiring large charges could be potentially magnified even further when coupled with typically small particle sizes of APIs, as these tend to accept greater charges compared with large particles. Most of the common excipients used in DPI formulations, such as lactose monohydrate, possess hydroxyl groups on the surface and do not experience significant charge accumulation. Other formulation components like the HPMC capsules did not charge significantly in comparison to other excipients such as MgSt.

DPI formulation conditioning at certain temperature and humidity levels can be used to reduce electrostatic charges built up during the manufacturing process. This could be demonstrated by measuring the dynamic charge before and after storage of FP formulations. This process is highly dependent on the propensity of the API to accumulate electrostatic charge. APIs that have a low propensity to build up electrostatic charge, such as salmeterol xinafoate, may not benefit from this conditioning process. In fact, for SX, a conditioning step and exposing the drug product to humidity was found to be disadvantageous in terms of aerosol performance. Capillary interactions seemed to lead to agglomeration and poor drug dispersion. Another hypothesis might be that conditioned DPI capsules are simply tribocharging less because they contain a higher amount of moisture. An overall reduction in electrostatic charge by moisture is associated with a lowering in surface resistivity, because of water molecules adsorbing on the surface. This would mean that less tribocharging can be generated after conditioning of the capsules due to the presence of moisture in the formulation. Since this study did not evaluate the performance of the formulations after prolonged storage, the impact of any change generated during the manufacture of DPIs during stability has yet to be evaluated, with obvious simplications for any shelf-life.

Device material also seemed to be an important factor for DPI performance. ABS plastic, which is commonly used as material for medical inhaler devices, showed a very high propensity to build up electrostatic charge. Its bulk resistivity and insulative properties are well known in literature. Measuring the dynamic charge when using a grounded titanium device showed that less triboelectric charge was built up during the aerosolization process for FP capsules which in turn resulted in higher aerosol performance. SX capsules generated only low amounts of electrostatic charge independently of the device material.

Acknowledgements

The authors are grateful to S. Edge and M. Schneider for fruitful discussions and inputs to this manuscript. This work was funded by Novartis Pharma AG's internal research funds.

CHAPTER 3: UNPUBLISHED DATA

1. Detection of Particle Co-associations using Raman Microscopy

The combination of the long-acting β2-agonists and inhaled corticosteroids has shown enhanced efficacy compared with concurrent administration of the two drug classes from individual inhalers at the same dose. A possible explanation for this increased effect is a higher degree of co-deposition of the two drugs from the combination inhaler compared with the component drugs administered separately [38, 101, 106, 256, 263].

The goal of this project was to use Raman laser spectroscopy, a technique capable of identifying individual drug particles, together with the nearest neighbor function methodology, to determine whether there is any co-association between drug particles. Raman laser spectroscopy was applied to particles deposited on the stages of a Next Generation Impactor (NGI). This method is capable of identifying individual drug particles and presents images where particles are color coded. Previously this technique has been shown to highlight deposition of beclomethasone and salbutamol from a Ventide® metered dose inhaler in a study by Fraser Steele *et al.* [371]. The ratios of salbutamol-beclomethasone identified by Raman spectroscopy were found to be similar to that of the quantified amounts, but an assessment of co-deposition was not made. A similar approach has also been used by the group of Theophilus *et al.* to analyze a Seretide® MDI formulation. Concurrent samples of salmeterol xinafoate and fluticasone propionate were taken from stage 4 of an Andersen Cascade Impactor. This plate was considered to represent the dose delivered to the central airways [270].

However, after preliminary tests using commercial and proprietary model DPI formulations (data not shown) it was concluded that the particle concentration on the impactor stage was too high (even after actuating only one capsule) and it was impossible to disambiguate whether particle co-associations were formed before (during manufacturing, aerosolization or in the aerosol cloud) or upon particle impaction on the plate. The sampling method was likely to bias the results. Collecting a sample on stage 4 of the NGI at particle concentrations similar to those reported is expected to result in powder piles accumulating under the nozzles on the impactor stage (Figure 83).

Figure 83: NGI collection cups with characteristic deposition pattern after actuation of a DPI formulation.

Therefore, determining the chemical composition of individual particles with a technique measuring particles in an aerosol cloud in real-time such as SPAMS should yield more definitive data [248]. Nevertheless, drug particles from combination inhalers could still be deposited individually at the same location in the lungs and exhibit their complementary effects.

2. Determination of the Carrier Surface Coverage with Magnesium Stearate using Raman Microscopy

It has been recognized from previous work that there is a need to establish the nature and extent of carrier surface coatings, and for a detailed study of the relationship between the extent and nature of the coating and the particle interactions as well as bulk powder characteristics. This can be very difficult to achieve because of technological challenges of characterizing such thin coating layers on the surface of particles that can be in the range of only nanometers. Conventional techniques such as Raman spectroscopy penetrate the coating layer and measure both, the coating layer and the host particles (see Figure 84). Time-of-flight secondary ion mass spectrometry (ToF-SIMS) is a highly sensitive analytical technique that provides chemical information regarding elemental, isotopic and molecular structure from the first few layers of small particles [24, 312]. Therefore, ToF-SIMS was used in this study to further investigate particle coating and MgSt distribution of carriers.

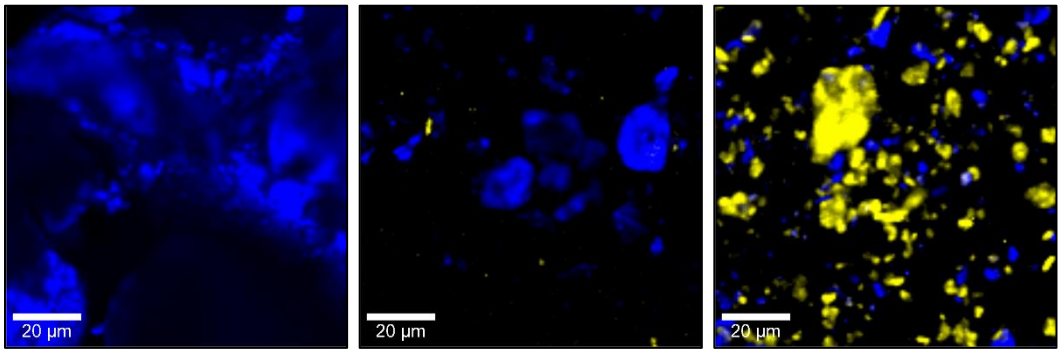

Figure 84: Raman spectroscopy micrographs of excipient-blend mixtures. Left: Lactose 0.5% MgSt (high-shear); Middle: Lactose 5% MgSt (high-shear); Right: Lactose 10% MgSt (high-shear). Color codes: Blue = Lactose; Yellow = MgSt.

3. Combination Dry Powder Inhalation Formulations of Fluticasone Propionate and Salmeterol Xinafoate

The guidelines for the treatment of patients with COPD (GOLD) mention the use of long-acting beta2-receptor agonists (LABA) in combination with inhaled corticosteroids (ICS) whenever the patient's treatment with ICS alone is insufficient. In this manner, the two fundamental processes of the disease can be addressed simultaneously (bronchoconstriction and inflammation). The co-administration of ICS/LABA for chronic obstructive pulmonary disease has resulted in reduced mortality compared to either drug administered alone. It was discovered that the co-administration of the two types of drugs in the same formulation resulted not only in increased patient convenience, but also showed improved β2-adrenoceptor and glucocorticoid receptor function, as well as a reduction in inflammation due to the synergistic effects [101, 106]. For this effect to occur, both drugs need to be present on the same cell in the airways. It has been shown to reduce exacerbations, hospitalization, emergency department visits and health care costs [372, 373]. A possible explanation for this increased effect is a higher degree of co-deposition of the two drugs from the combination inhaler compared with the respective drugs administered separately. Administration of the two drugs via the same inhaler would lead to an increased likelihood of co-deposition compared with the administration via two separate inhalers. This is because natural variation in inspiratory maneuvers, causing different deposition patterns within the lung between inhalations from two separate inhalers, is avoided when both drugs are delivered in a single breath. It is possible that the opportunity for synergistic action is further enhanced in the combination formulation by co-deposition of FP and SX particles in the airways as a result of particle co-association during the manufacturing process or aerosolization event [248].

Several combination product development programs are currently underway. Additionally, there is a great interest in the development of 'generic' combination inhalers combining for example corticosteroids with long-acting β2-agonists such as in Advair® Diskus® (SX with FP). The equivalence of two products is usually assessed *in vitro*, by comparing drug deposition using parameters such as the mass median aerodynamic diameter (MMAD), geometric standard deviation (GSD), fine particle dose (FPD) and fine particle fraction (FPF) (FPD and FPF are often defined as the amount or proportion of particles with an aerodynamic diameter <5 μm). However, it is currently thought that changes to the particle size distribution within the range of 1–5 μm may affect the drug's site of deposition within the lungs, and thus possibly producing significant clinical differences. *In vitro*, this may be assessed by comparing drug deposition within a multi-stage cascade impactor on a stage-by-stage basis. Guidance by the European Medicines Agency (EMEA) has been introduced defining a step-wise approach to demonstrating bioequivalence between different inhalation products [374, 375]. The 'innovator' and the 'generic' product must be equivalent (within ± 15%) when tested at all flow rates with respect to all individual stage depositions or at least 4 justified grouped stages [263]. Only limited work has been done up to date investigating drug deposition when aerosolized from combination versus single-active formulation. Despite the potential similarities in FPD and FPF values between the single-active and combination products, difference in stage-by-stage deposition may be found which might explain the reported clinical differences between the two types of products.

The aim of this study was to investigate the particle detachment from carrier, dispersion mechanisms and particle co-associations of active pharmaceutical ingredients (APIs) in model combination products. Up to the present, only limited assessments have been carried out on the nature of particle of the delivered dose emitted from the device. Another goal of this work was to compare the *in vitro* aerosol performance and stage-by-stage deposition of dry powder inhaled formulations aerosolized from single-active FP and SX with the respective FP–SX combination formulations.

3.1 In Vitro Aerosol Performance of Combination DPI Formulations by NGI

A detailed study of the influence and mechanism of the force control agent magnesium stearate in FP and SX mono DPI formulations can be found in Jetzer *et al.* [146].

In Figure 85, the *in vitro* aerosol performance in terms of fine particle fraction (FPF) of three FP-SX combination DPI formulations is shown. Figure 86 shows the FPF of the respective FP and SX mono DPI formulations. Co-formulation of the two active ingredients in lactose monohydrate dry powder blends lead to substantial changes in aerosol performance (FPF) and the APSD profiles of the active ingredients compared to their mono formulations. When comparing mono and combination formulations, it can be seen that the combination of FP and SX in the same DPI formulation resulted in an increase of approximately 10% in FPF for SX compared to their *in vitro* performance administered alone. Meanwhile the FPF of FP did not change. Adding 0.5 % MgSt to the combination formulation by high-shear mixing further increased the FPF of SX for about 8% and also increased the FPF of FP (around 11% compared to lactose untreated). Adding 0.5% MgSt to the combination formulation by low-shear mixing did not influence the performance of FP, however it did increase the performance of SX. While these effects are well understood from a pharmaceutical process development point of view, there is only limited mechanistic understanding of what physical processes and interactions between the particles are responsible for phenomena such as compound/compound interactions (particle co-associations) in a formulation.

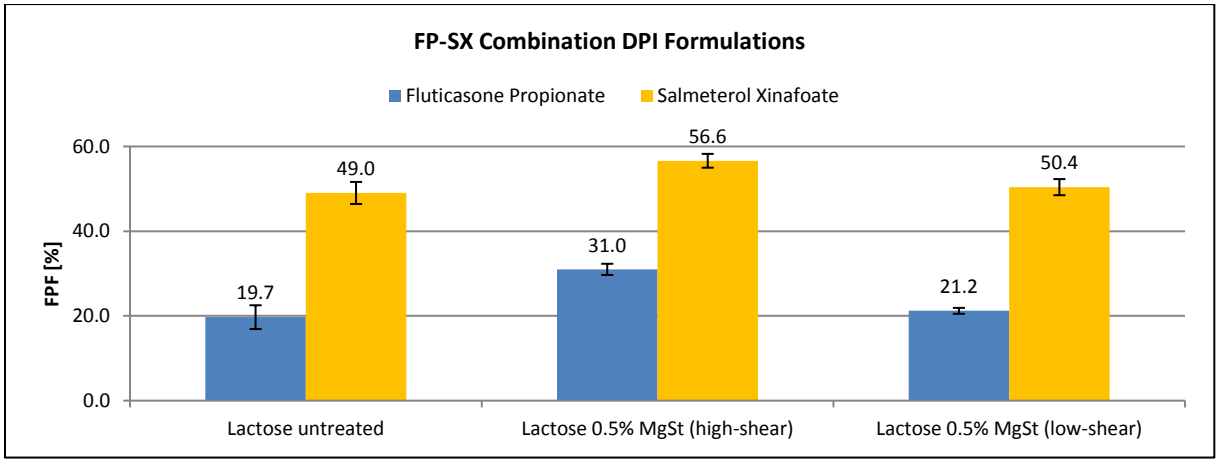

Figure 85: Fine Particle Fraction of the tested FP-SX Combination DPI Formulations obtained by NGI (n=3 DPI actuations; error bars represent one standard deviation). Capsules were not conditioned.

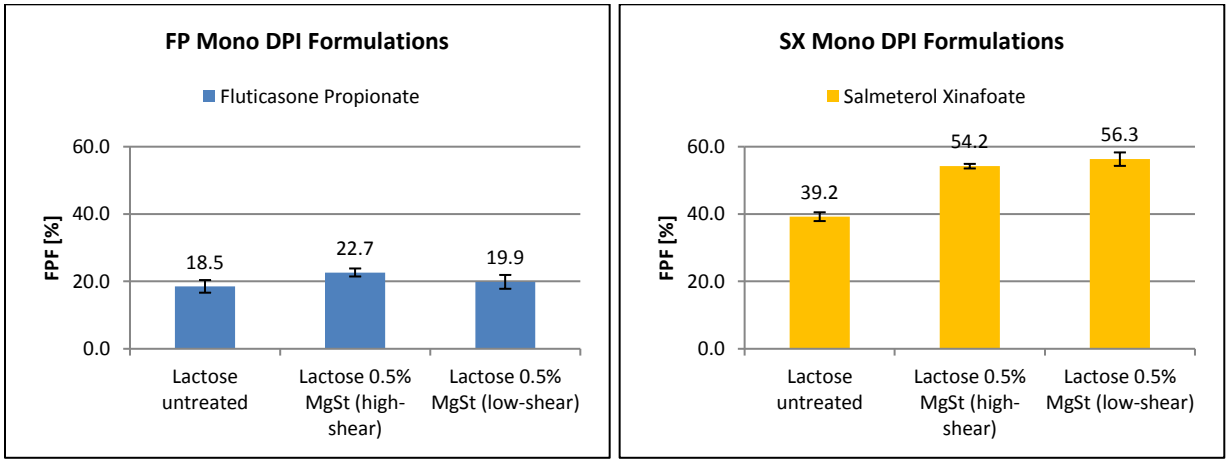

Figure 86: Fine Particle Fraction of the tested FP and SX mono DPI Formulations obtained by NGI (n=3 DPI actuations; error bars represent one standard deviation). Capsules were not conditioned.

Figure 87-Figure 90 show the NGI stage-by-stage profiles from the FP-SX mono and combination formulations. It is clearly evident that there are significant differences between the particle depositions in the various stages of the formulations with differing blending technique. Both drugs FP and SX, show a significant increase in deposition of fine particles in the impactor stages (NGI Cup 2 to Cup 8) when adding MgSt to the excipient-blend by high-shear

mixing as well as a significant decrease in drug deposition in the pre-separator. This suggests better detachment from coarse carrier resulting in a higher deposition in the NGI stages (and hence a higher FPF). The plots show significant differences between mono and combination formulations.

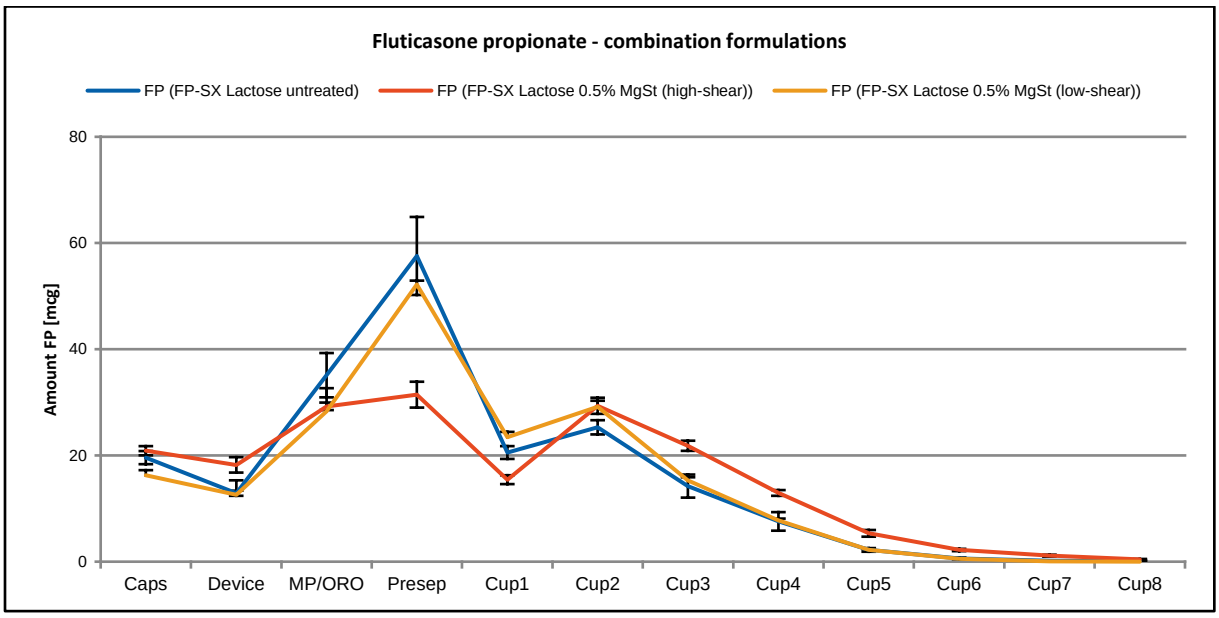

Figure 87: NGI profiles of FP in FP-SX combination DPI formulations (n=9 capsules actuated; error bars represent one standard deviation).

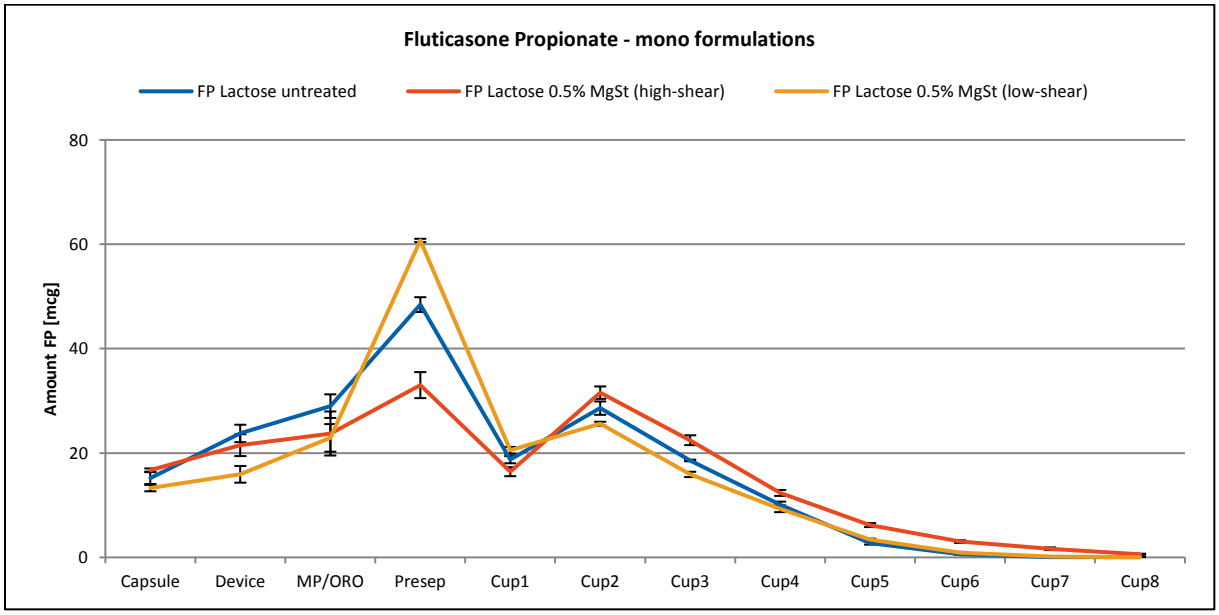

Figure 88: NGI profiles of FP mono DPI formulations (n=9 capsules actuated; error bars represent one standard deviation).

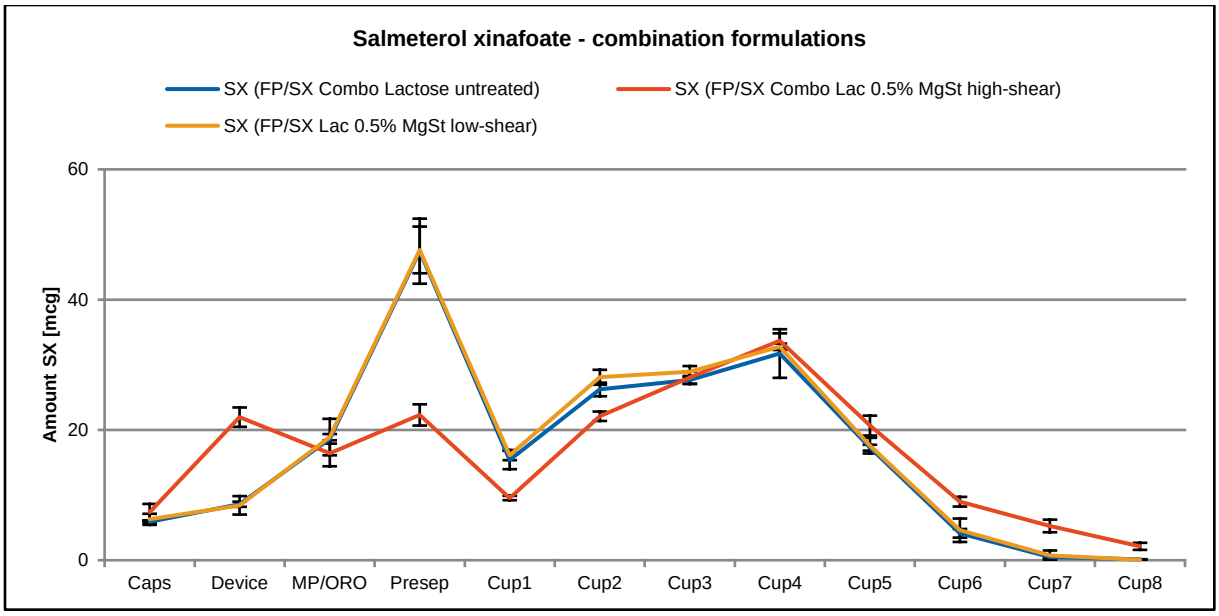

Figure 89: NGI profiles of SX in FP-SX combination DPI formulations (n=9 capsules actuated; error bars represent one standard deviation).

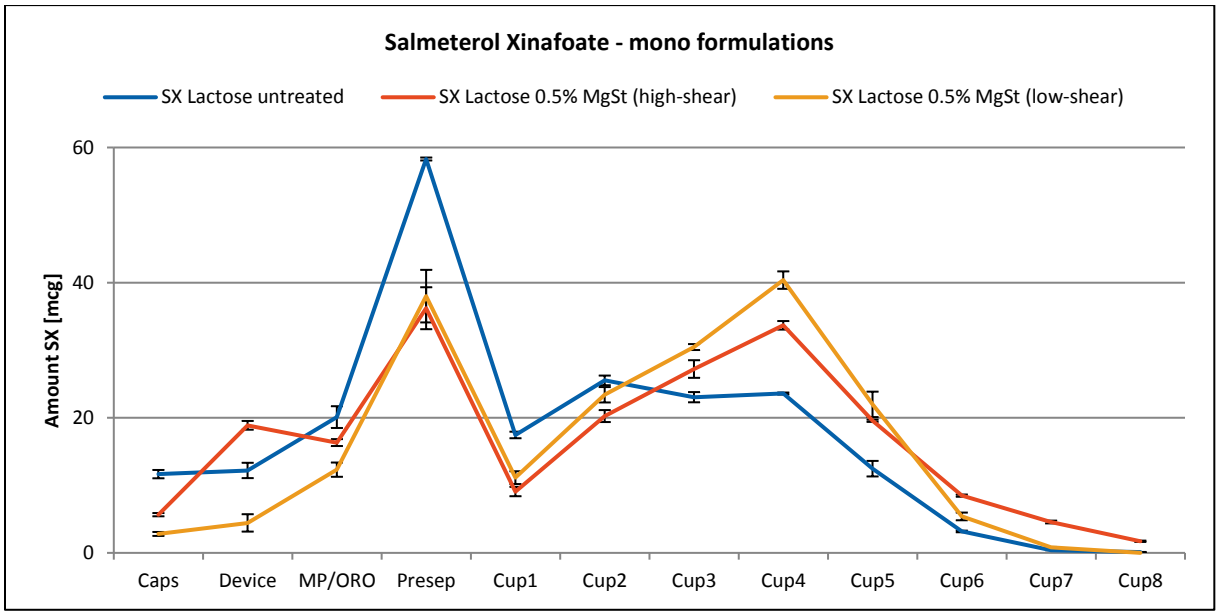

Figure 90: NGI profiles of SX mono DPI formulations (n=9 capsules actuated; error bars represent one standard deviation).

The Mass Median Aerodynamic Diameter (MMAD) and Geometric Standard Deviation (GSD) measurements of the aerodynamic particle size distributions of all FP-SX formulations are shown in Table 22. Interestingly, the MMADs of both FP and SX in the mono products were detected to be larger than the ones in the combination products (for both, lactose untreated and high-shear formulations). While there was no difference in MMAD between mono and combination formulations for the low-shear blends. The MMAD for the high-shear combination formulation was detected to be the smallest. It is important to note that even though significant differences in MMAD for these formulations were measured using the standard pharmacopoeial methodology, this does not necessarily mean they

will have significant differences with respect to regional deposition, since their median values may be considered similar (ca. 3–4 µm).

Table 22: Mass Median Aerodynamic Diameter (MMAD) and Geometric Standard Deviation (GSD) of the FP and SX mono and combination Formulations calculated from NGI.

	MMAD (µm)		GSD	
MONO DPI PRODUCTS	**FP**	**SX**	**FP**	**SX**
Lactose untreated	4.71	2.97	1.84	2.23
FP and SX Lactose 0.5% MgSt (high-shear)	4.33	2.13	1.93	2.13
FP and SX Lactose 0.5% MgSt (low-shear)	4.71	2.34	1.80	2.04
	MMAD (µm)		**GSD**	
COMBINATION DPI PRODUCTS	**FP**	**SX**	**FP**	**SX**
FP-SX Lactose untreated	4.58	2.67	1.87	2.12
FP-SX Lactose 0.5% MgSt (high-shear)	3.58	2.12	1.89	2.15
FP-SX Lactose 0.5% MgSt (low-shear)	4.70	2.69	1.83	2.12

3.2 In Vitro Aerosol Performance of Combination DPI Formulations by SPAMS

The hitrate for the combination products was at 64% for FP-SX Lactose untreated, 36% for FP-SX Lactose 0.5% MgSt (high-shear) and 54% for FP-SX Lactose 0.5% MgSt (low-shear). The hit rate for the different formulations can depend on several factors as described by Jetzer *et al.* [248, 249]. Excipients in a formulation, such as lactose and/or MgSt, will significantly decrease the hit rate.

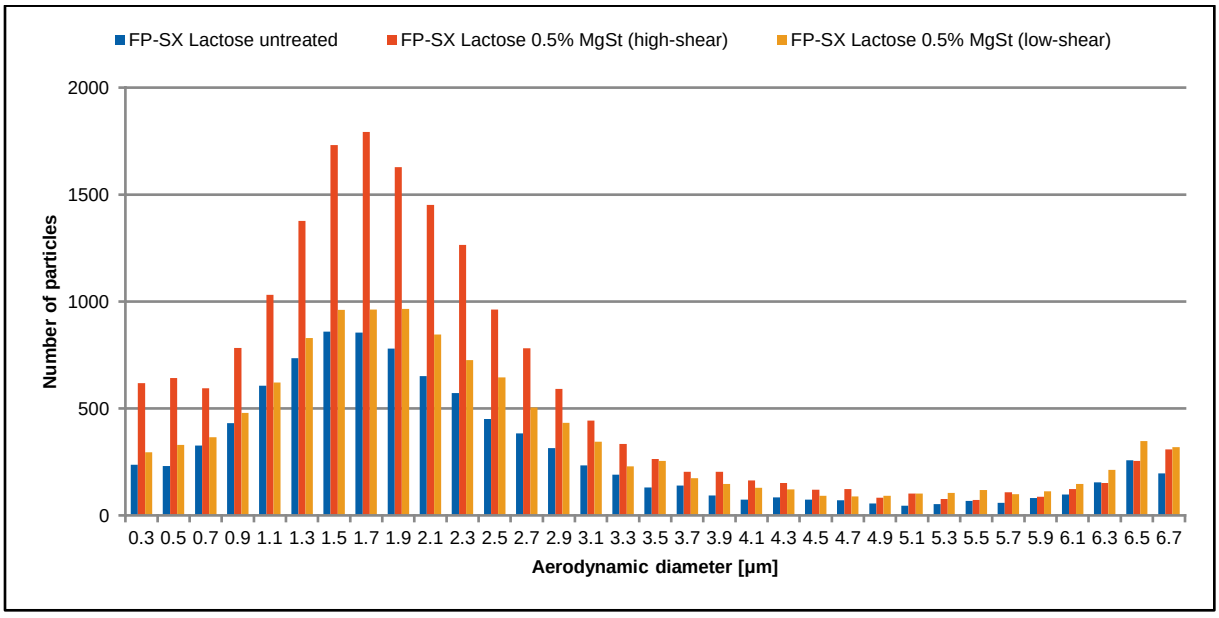

Figure 91: Aerodynamic particle size distribution of FP-SX Combination formulations obtained by SPAMS (n=3 DPI actuations). The plot shows the distribution of total particles (API + excipients). The bars in this plot are normalized with the hitrate of each formulation.

Figure 91 shows a comparison of SPAMS APSD histograms of total particles (API, fine lactose and fine MgSt) for FP-SX combination formulations. By adding MgSt to the formulation by high-shear mixing, the APSD profile increases to a much higher number of smaller particles in the size range from 0-3.9 µm diameter. The high-shear mixing process used in this study seems to lead to comminution of larger MgSt agglomerates to (very) fine MgSt particles. Therefore, a much higher number of particles is present compared to the reference formulation. While in the

low-shear mixing process, not enough shear forces to break the agglomerates are applied to the blend. Only a very small increase in number of particles in the region of 1.5-3.7 µm can be seen due to the addition of MgSt (Figure 91).

The Median Aerodynamic Diameter (MAD) measurements of the aerodynamic particle size distributions of processed and unprocessed FP-SX formulations are shown in Table 23. Generally, the MADs for the low-shear formulation were detected to be coarser than those from the high-shear formulations. Therefore it was concluded that there may be an agglomeration of API and excipient (possible MgSt). The MAD for the high-shear combination product was determined to be the smallest. These findings would explain the increased performance of this particular formulation.

Table 23: Median aerodynamic diameter (MAD) calculated from the FP-SX combination DPI products measured by SPAMS.

MAD [um]	Total	FPSX	FP	SX	Unassigned
FP-SX Lactose untreated	1.89	2.32	2.40	1.71	1.90
FP-SX Lactose 0.5% MgSt (high-shear)	2.03	2.26	2.12	1.89	2.13
FP-SX Lactose 0.5% MgSt (low-shear)	2.05	2.46	2.44	1.90	2.27

The particle co-associations and interactions in combination products may influence the ratio and MAD of the APIs in a formulation. It is possible that a certain particle size of each API preferentially forms heterogeneous agglomerates as reported by Jetzer *et al.* [248]. Because DPI formulations also contain excipients such as lactose, it seems likely that pure particles (FP or SX) and co-associated particles (FPSX) are made of agglomerates of API and excipient, resulting in larger particle size.

Figure 92-Figure 94 show the APSD of APIs in FP-SX Lactose untreated, FP-SX Lactose 0.5% MgSt (high-shear) and FP-SX Lactose 0.5% MgSt (low-shear) combination formulations, respectively. Both, mono API particles and co-associated API particles are plotted. The APSD histograms show the fractionation of the "hit" particles. The collected data demonstrates that a considerable fraction of all particles emitted contained both APIs in co-association (25-33%). Due to the dosage strength of 200/200 mcg and given the much smaller particle size of SX compared to FP used in this study (Jetzer *et al.* [146]), many more SX particles are present in the formulations. A higher number of pure SX particles (about 58-66%) were detected than pure FP particles (7-9%). Only a very small fraction of particles (< 2%) could not be identified, most likely due to insufficient ionization.

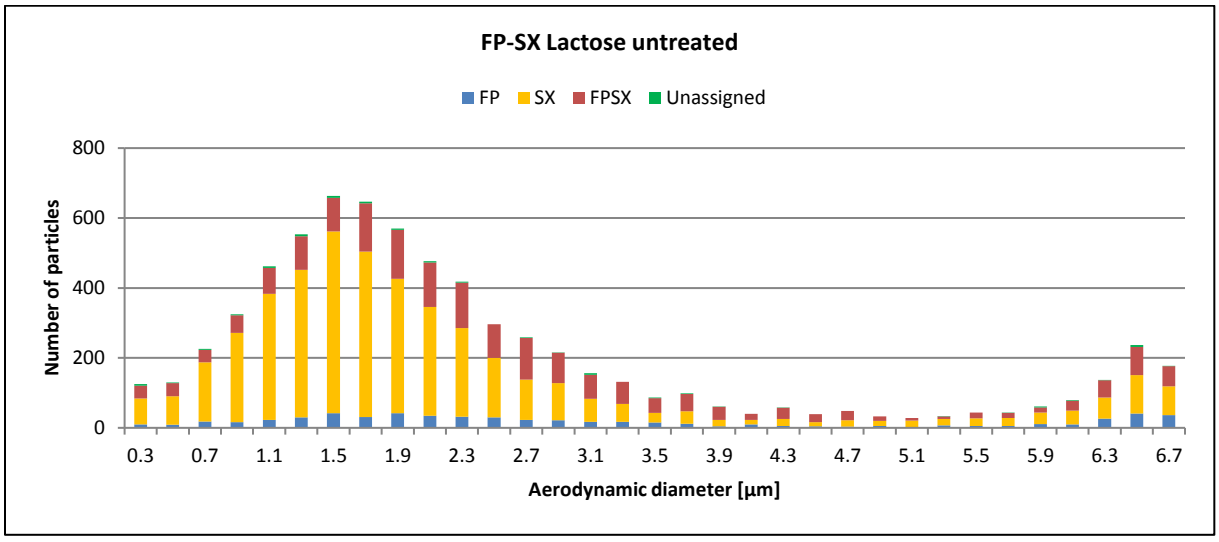

Figure 92: Aerodynamic particle size distribution of FP-SX Lactose untreated obtained by SPAMS (n=3 capsule actuations; error bars represent one standard deviation). The plot shows the distribution of number of particle co-associations (FPSX), pure FP, pure SX and unassigned particles. The bars in this plot are normalized with the hitrate of the tested formulation.

In the reference formulation (FP-SX Lactose untreated), 28% of all hit particles contained FP and SX in co-association as can be seen in Figure 7. A majority of FP particles (81%) also contained SX.

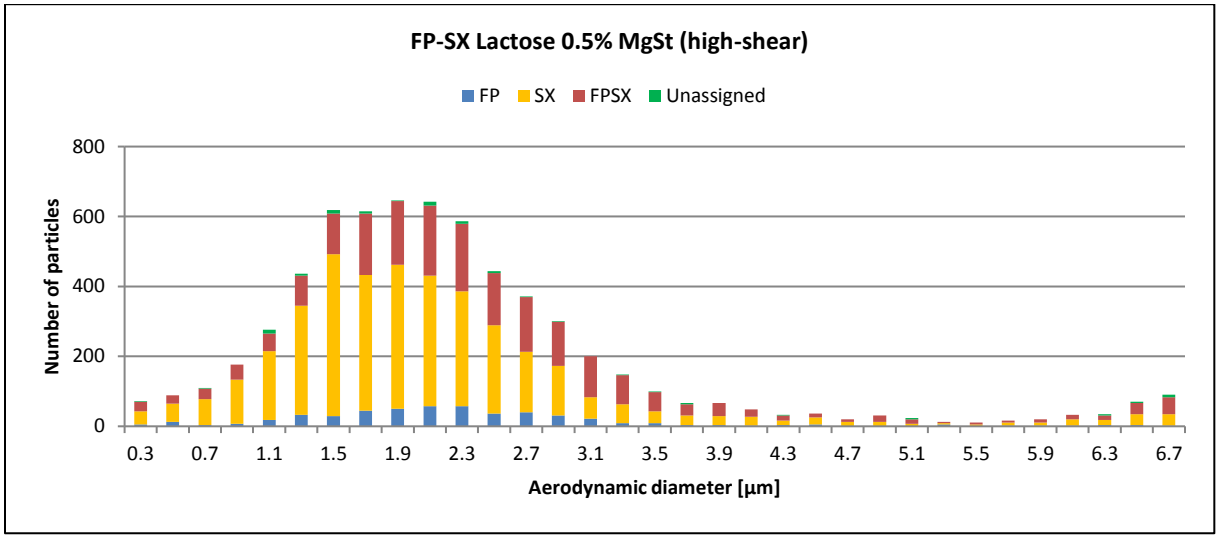

Figure 93: Aerodynamic particle size distribution of FP-SX Lactose 0.5% MgSt (high-shear) obtained by SPAMS (n=3 capsule actuations; error bars represent one standard deviation). The plot shows the distribution of number of particle co-associations (FPSX), pure FP, pure SX and unassigned particles. The bars in this plot are normalized with the hitrate of the tested formulation.

In the FP-SX Lactose 0.5% MgSt (high-shear) formulation the highest percentage of particle co-associations of FP-SX (33%) were detected. A lower number of smaller particles (0.3-1.5 µm) were detected compared to the reference and low-shear formulations. This is most likely a result of the fine particles forming particle co-associations which results then in the higher number of particles in the range from 1.9-3.1 µm. Also, a much lower number of particles in the range from 5.5-6.7 µm were measured.

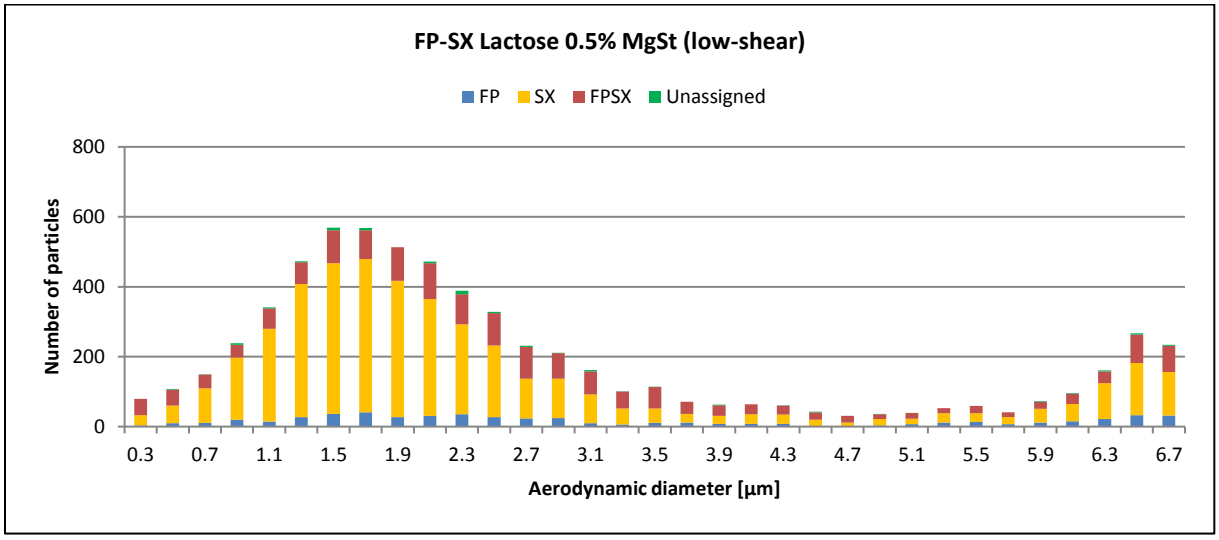

Figure 94: Aerodynamic particle size distribution of FP-SX Lactose 0.5% MgSt (low-shear) obtained by SPAMS (n=3 capsule actuations; error bars represent one standard deviation). The plot shows the distribution of number of particle co-associations (FPSX), pure FP, pure SX and unassigned particles. The bars in this plot are normalized with the hitrate of the tested formulation.

Figure 95 shows the overlay of co-associated particles of FP-SX in the combination products (Lactose untreated, Lactose 0.5% MgSt (high-shear) and Lactose 0.5% MgSt (low-shear). A much higher number of FP-SX co-associated particles are present in the Lactose 0.5% MgSt (high-shear) formulation with the highest number of particles in the range of 1.7-3.3 µm. Also the MAD for the three formulations seems to be quite different.

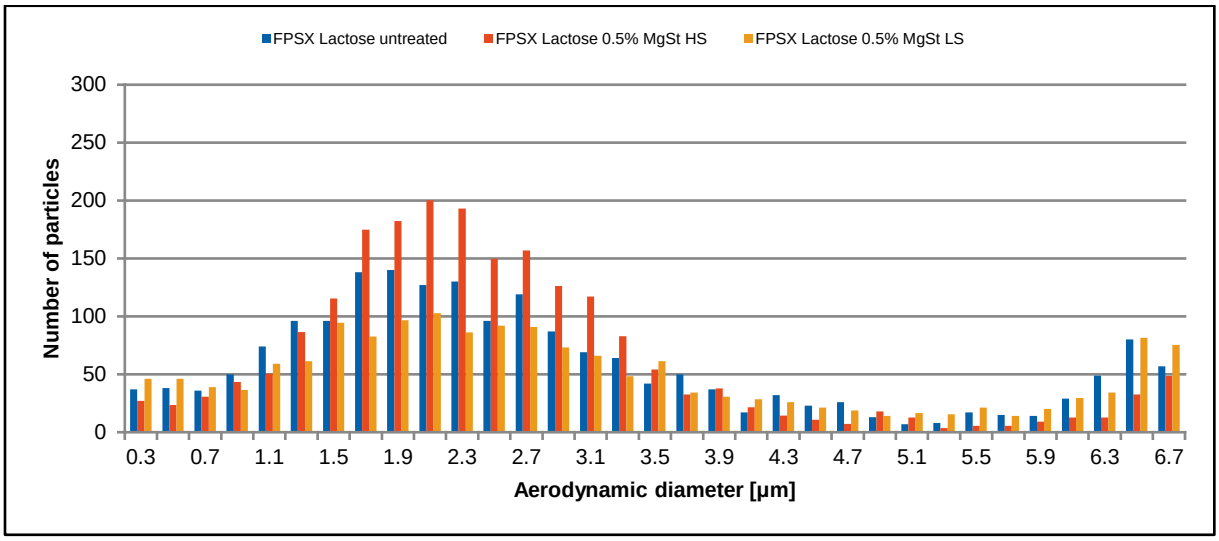

Figure 95: Overlay of aerodynamic particle size distribution of co-associated particles of FP-SX in the combination products (Lactose untreated, Lactose 0.5% MgSt (high-shear) and Lactose 0.5% MgSt (low-shear)). The bars in this plot are normalized with the hitrate of the tested formulation.

MADs determined by SPAMS for co-associated particles of FP and SX were found to be slightly different in the tested combination formulations (Table 23 and Figure 95). Interestingly, the MAD was detected the smallest for the FPSX Lactose 0.5% MgSt (high-shear) formulation with 2.26 µm while 2.32 and 2.46 µm for the Lactose untreated and low-shear formulation, respectively.

Adding 0.5% MgSt by high-shear mixing to the excipient-blend increased the number of particle co-associations about 5% compared to the reference formulation without MgSt. Low-shear mixing of the lactose-MgSt excipient-blend did not influence the ratio of particle co-associations in the tested formulations. The combination of FP and SX in one formulation resulted in an enhanced *in vitro* aerosol performance compared to either drug tested as mono formulation. The addition of MgSt by high-shear mixing to the excipient-blend could further increase the performance of the combination DPI products to some extent. Adding MgSt by low-shear mixing did not alter the aerosol performance compared to no MgSt in the formulation.

Table 24: Percentage of individual particles measured in the formulations (10'240 particles per run).

[%]	FPSX	FP	SX	Unassigned
FP-SX Lactose untreated	27.5	8.6	62.9	1.0
FP-SX Lactose 0.5% MgSt (high-shear)	32.6	7.8	58.1	1.5
FP-SX Lactose 0.5% MgSt (low-shear)	25.8	8.6	64.5	1.1

Looking at the aerosol populations in their entireties, significant levels of API particle co-associations were detected in all tested combination products (Table 24). Around 33% of all particles in FP-SX Lactose 0.5% MgSt (high-shear) were found to contain both APIs. A significantly lower percentage of pure SX particles (58%) were measured in this particular formulation. The levels of particle co-association of FP and SX in the other tested formulations did not

differ much. Low-shear mixing the excipient-blend did not seem to affect the number of drug particle co-associations in the tested formulations.

Table 25: Percentage distribution of total FP and SX in the formulations in co-associated or pure state in the tested combination products.

[%]	FP-SX Lactose untreated	FP-SX Lactose 0.5% MgSt (high-shear)	FP-SX Lactose 0.5% MgSt (low-shear)
FP co-associated	76	81	75
SX co-associated	30	36	29
FP pure	24	19	25
SX pure	70	64	71

Most of the FP (around 80%) was detected to be in co-association with SX. While still a very large fraction (around 70%) of SX was found to be made of pure particles. A possible explanation for this effect is the dosage strength and particle size distribution of the raw materials (FP and SX). The SX was much finer than the FP. Therefore many more SX particles overall are present in the formulations.

The deposition of FP and SX from single-active versus combination formulations on an NGI stage-by-stage basis was determined to be significantly different. Both APIs in the combination products appear to affect the deposition of each other. Concentration-related trends may be observed when expanding this study with different dosage strengths of FP and SX. However, no firm conclusions can be drawn to date why such differences in drug deposition are happening in the combination formulations. More studies are necessary to investigate important factors such as the particle size distributions of the two drugs, the effect of dosage strength, particle interactions and the drug-carrier interaction area and cohesive-adhesive balance on *in vitro* aerosol performance of combination DPI formulations.

CHAPTER 4: GENERAL CONCLUSIONS

For many decades DPI products have been successfully developed using a variety of formulation strategies including drug-only or powder mixture approaches containing only one single excipient (alpha lactose monohydrate). Single excipient based formulations continue to be used in approved commercial DPI products today. Novel dual excipient formulation strategies containing ternary materials such as the force control agent magnesium stearate are now considered to be a somewhat standard formulation approach as witnessed in the latest DPI product approvals. Scientific literature is claiming that the addition of magnesium stearate may improve the fine particle dose performance characteristics of DPI formulations [189-191].

The understanding of the particle-particle interactions and determination of DPI formulation *in vitro* aerosol performance are key requirements for the rational and effective research and development of novel formulations. The present thesis aimed at improving the mechanistic understanding of particle interactions in engineered dry powder inhaled formulations (adhesive mixtures) using advanced analytical tools such as single particle aerosol mass spectrometry (SPAMS).

The SPAMS technique was identified to be able to distinguish small changes in DPI and pMDI formulations. A range of model formulations blended with different amounts of the force control agent magnesium stearate with various APIs was successfully investigated. Valuable reproducible additional information in terms of dispersibility of fine particles in the formulations could also be obtained with SPAMS. The SPAMS instrument sizes emitted particles from an inhaler in the size range from ca. 0-10 µm. This means that also information about fine excipients (e. g. lactose fines or force control agents) in the tested formulation is generated and can therefore be evaluated for a better understanding of the product.

The development of a precise, accurate, robust analytical test methodology is a key part in the development and quality control of inhalation drug products. SPAMS as an additional or alternative technique to the current compendial cascade impaction test methods should meet all these goals and also the comparability of its measurements must be demonstrated (as well as repeatability and reproducibility [247]). The aerodynamic particle size distribution profiles (APSD) of pMDI and DPI products were obtained using SPAMS and then compared to those obtained by the Aerodynamic Particle Sizer and NGI. In addition, the transmission efficiency of SPAMS as well as potential size bias of APSD measurements that might result from a size dependent transmission profile were evaluated. This study demonstrated the application of SPAMS for the analysis of pharmaceutical aerosols in real-time for semi-quantitative analysis. It could be shown that the SPAMS can generate useful APSD measurements for both pMDI and DPI products. The APSD results generated using SPAMS can be transformed and compared to APSD data generated using cascade impactors. However, a consistent anomaly of particle transmission in the SPAMS in the region of 2-3 µm was found.

Measurements of the commercially available combination pMDI and DPI products Seretide® and Advair® Diskus® using the SPAMS technique showed that a significant fraction of the emitted drug particles fluticasone propionate and salmeterol xinafoate can form co-associated particles with other APIs (and maybe excipients) in the same formulation. Unique mass spectral fragmentation patterns can be recognized and assigned for each API using the SPAMS data analysis software. SPAMS also revealed which particle size fractions are most likely forming these co-associations. Measurements with SPAMS have demonstrated that particle co-associations between drug product components can be evaluated in a way that is inaccessible via cascade impaction techniques. A deeper understanding about product performance and particle interactions can be gained, providing valuable information for combination products. Using SPAMS it could be demonstrated that the degree of particle co-association can be manipulated by the choice of formulation and manufacturing approach for DPIs. It is possible that in the manufacturing process drugs or carrier can be processed together with a force control agent such as magnesium stearate to improve dispersion mechanics. A possible explanation may be that the drug or the carrier receive an MgSt-coating that would prevent the co-association or agglomeration of the particles and moreover facilitate detachment from carrier. This results in high in-vitro

performance (and furthermore very high extra fine particle fraction of particles <2 µm) and a relatively fine APSD profile compared to products not engineered in this way.

The choice and intensity of the blending technique of the excipient mixture was found to affect the distribution of the force control agent magnesium stearate covering the lactose carrier. This covering/distribution was shown to significantly influence the *in vitro* aerosol performance (as evidenced using the ToF-SIMS technique). The underlying mechanism of particle interaction between API and the carrier seems to be substantially different for high- and low-shear formulations. This provides the basis for a modification in particle interactions from drug-lactose to drug-MgSt (in high-shear) which then seems to be responsible for the improved performance (enhanced particle detachment from carrier due to lower interaction forces). SPAMS and NGI techniques independently showed an increase of the number of fines as result of the addition of MgSt by high-shear mixing, indicating a reduction of interaction between the actives and the lactose carrier particles. Low-shear mixing of the excipient-blend did not increase the performance of FP. However, low-shear mixing the excipient-blend did increase the FPF of the adhesive drug SX in our formulations. Nearly equal aerosol performances could be achieved for SX with both blending techniques applied to pre-blend the excipients. The aerosol performance of SX could be increased much more by adding MgSt compared to the performance of FP.

In carrier based mixtures for inhalation a proper balance has to be obtained between the stability of the blend during storage and handling, and dispersibility during inhalation. This requires control of the interparticulate forces in the mixture in order to prevent segregation on the one hand and insufficient dispersion of drug particles in the required aerodynamic size distribution from the blend on the other. Storage and conditioning of DPI capsules at controlled temperature and humidity levels showed to have a significant effect on the separation of drug and carrier particles. Significant differences were observed between adhesive and cohesive model compounds (with respect to lactose). The present study highlights that electrostatic forces and interactions play a key role in dry powder inhaled formulations. Large differences in the electrostatic charging behavior were observed. Fluticasone propionate seems to have a high propensity to electrostatic charging, while salmeterol xinafoate only showed a negligible electrostatic charging behavior. Most of the common excipients used in DPI formulations, such as lactose monohydrate, do not seem to experience significant charge accumulation. Other formulation components like the HPMC capsules did not charge significantly in comparison to other excipients such as MgSt. Conditioning of certain APIs was found to be helpful to dissipate electrostatic charge which in turn increased aerosol performance. Significant differences were also observed when using different device materials: the standard inhaler device made of ABS plastic showed to generate a high amount of tribocharge while a grounded titanium device (made of pure titanium; with same dimensions) showed to build up lower electrostatic charges.

The effects of DPI formulation variables on drug dispersion performance can be explained by changes in three overall factors: (1) The size distribution of the drug particles (including drug/drug and drug/fine-lactose agglomerates or degree of particle co-associations) as they detach from the carrier surface; (2) The interaction forces between drug and carrier; (3) The properties of the APIs (e. g. physico-chemical properties, ability to tribocharge, behavior when exposed to temperature or humidity, cohesive/adhesive balance with respect to the carrier).

In summary, this thesis combines improvements to the analytical methodologies such as SPAMS with the systematic investigation of dry powder inhalation drug product formulations to advance the understanding of *in vitro* aerosol characteristics of formulations at a fundamental mechanistic level. It also highlights the relevance of electrostatic forces in DPI formulation *in vitro* aerosol performance. The improved conception of the interplay between variables in the formulation and dispersion mechanics of adhesive mixtures resulting from this thesis may stimulate the effective implementation of quality by design approaches to dry powder inhalation product development. In addition, it may facilitate and speed up the development of generic or more efficiently dispersing products with the advantage to lower the dosage strength and ultimately reduce unwanted side effects for patients.

CHAPTER 5: FUTURE OUTLOOK

One of the most important goals for the further development of dry powder inhalation should be the improvement of efficacy of such inhalers. Despite of a gradual increase in the total lung deposition over the past decades from less than 10% (!) to 20-40% for currently marketed inhalers, still less than half of the dose becomes available to the site of action (or site of absorption). In general, the performance of a DPI system can be improved by establishing a better balance between the three types of forces shown in Figure 96: (a) interparticulate forces in the powder formulation, (b) dispersion forces generated in the DPI and (c) deposition forces in the respiratory tract [137, 138].

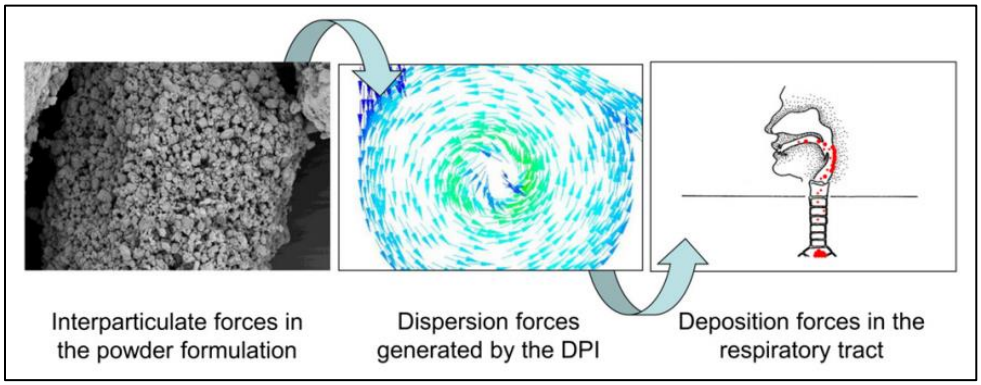

Figure 96: Desired balance for optimal DPI therapy between the interparticulate forces in the powder formulation, the dispersion forces generated by the inhaler device and the deposition forces in the respiratory tract during inhalation. Adapted from [138].

In DPI formulation research and development, several challenges still remain despite many years of effort put in the understanding of mechanisms of powder dispersion. For adhesive mixtures some relevant variables, like moisture content or roughness have extensively been described, but there is insufficient knowledge of the mixture properties and the processes occurring during the mixing process that affect the final performance of the mixture. The extent to which particles de- and re-agglomerate and distribute over the carrier surface and to which the interparticulate forces are increased by inertial and frictional forces during blending are difficult to measure and require the introduction of new techniques.

Most studies in the literature investigate and discuss the understanding and controlling of the factors that determine the interparticulate forces in dry powder formulations. They aim to improve the dispersion of the powder during inhalation [6, 8, 136, 172, 228, 309, 310, 317, 324, 332, 376]. The inhaler design as an important factor in powder dispersion has mostly been neglected in many studies until just recently [377, 378]. So far, most studies still focus on studying the performance of existing devices or investigating the effect of small design modifications thereon [339, 379-381] as well as understanding the mechanisms of powder dispersion [382-384]. The design of new inhaler technology is hardly studied. Peer reviewed publications dealing with computational fluid dynamics-assisted new DPI developments are still quite rare although most pharmaceutical companies make use of this technique by now. With the availability of such new techniques in combination with an increased understanding of the mechanisms of powder dispersion, better integrated device-formulation development becomes possible. One of the challenges is to design optimally tuned combinations of the powder formulation and the dispersion principle. In this respect it is highly regrettable that still many consultancy agents or plastic manufacturers continue developing inhaler concepts for the market, initially not knowing for which types of formulation these concepts will be used. Part of the newly developed devices, or existing devices used for new powder formulations are still low resistance capsule based DPIs [111, 129, 133, 163, 385, 386]. This has the disadvantage that powder properties need to be optimized with respect to both emptying of the capsules and good dispersion. If the drug formulation is an adhesive mixture, the carrier material providing best flow properties for discharge of the capsules may not always be the first choice from a dispersion point of view.

Cascade impaction testing requires mastery of a complex technique before consistent results can be achieved. NGI-testing results in a large demand on resources in terms of laboratory personnel and solvents, the measurements are very time-consuming and results are typically returned days or even weeks later [29, 30]. There is, therefore, high interest in the development and routine use of more rapid techniques that might have particular application for routine product quality testing as well as in product development applications in which many similar impactor measurements are often necessary [31]. The SPAMS technique is an attractive additional technique in the field of pharmaceutical aerosol analysis and complementary to the current standard of impactor/HPLC-analysis. The results of this thesis indicate that the SPAMS technique is very well able to distinguish between small changes in the formulation of various DPI powders (and also pMDIs). The results from SPAMS can be correlated to NGI results. Valuable additional information in terms of dispersibility of fine particles in the formulations can also be obtained with SPAMS. SPAMS provides much finer particle resolutions compared to NGI cut-off stages (fine details of APSD). It is also more sensitive for smaller particles down to 0.1 μm as with this technique the aerodynamic diameter of single particles is measured. Meanwhile the NGI relies on particle mass which is very low for fine particle sizes. In addition, SPAMS also may be used to investigate the nature of API particulates and provide feedback control for the level of particle co-association (API-API or API-excipient) in early-phase development of inhaled products [248].

The Analysis of organic compounds in aerosol particles using real-time single particle techniques is difficult because of the extensive fragmentation that occurs in the laser desorption/ionization step [243]. The current setup of the SPAMS 3.0 instrument contains a one-step desorption/ionization excimer laser using a krypton-fluoride gas mixture (KrF) firing at a wavelength of 248 nm [246]. In an effort to avoid extensive fragmentation and make the identification of the analyte compounds easier, a modification to the SPAMS to allow for a two-step laser desorption/ionization would potentially make identification of analytes less problematic than the current single laser system. Such an upgrade to the SPAMS instrument would be highly valuable for the analysis of pharmaceutical aerosols. An upgraded SPAMS with separate desorption and ionization lasers firing at a different wavelength could potentially detect co-associations not only between APIs, but also between API and excipients (lactose or force control agents) in the future if an appropriate ionization wavelength were selected (for example 193 nm using an argon-fluoride (ArF) gas mixture) [283]. This might shed more light on particle dispersion mechanisms of complex DPI systems.

For the development of generic versions of established DPI or pMDI products, the SPAMS technique might help generic drugmakers to better analyze and characterize innovator products with regards to dispersion mechanics, particle interactions and co-associations in the formulation. Such an approach might also speed up the development of generic drugs and therefore ultimately reduce costs for the pharmaceutical industry, patients and healthcare systems. Several generic versions of for example Advair® Diskus®/Seretide® are currently under development [387].

Additional future work would be to explore, if other force control agents than magnesium stearate can have a similar effect when using the excipient high- or low-shear mixing method. Alternate blending or coating techniques could be explored to apply such a force control agent on the carrier surface. Another attractive area of research could also be to further probe the treatment of drug particles instead of processing only the carrier particles. In this way, the degree of drug-drug/drug-excipient particle co-association could be controlled. This would enable to target the different regions of the human lung by controlling (if a co-association is desired) or even preventing such a formation of agglomerates. Such a formulation approach would potentially result in very high *in vitro* aerosol performance and therefore ultimately might lead to high lung deposition in patients. Combined with a two-step laser desorption/ionization SPAMS system this could provide more insight into particle deagglomeration and dispersion mechanics in dry powder inhaled formulations of adhesive mixtures.

Although product development focuses on minimizing variability across all aspects of the product, it is also important to understand there is an inherent variability among patients, who differ both in their oropharyngeal and airway anatomies and in their breathing profiles. Overcoming this variability is a key challenge in inhaled product development. Differences in lung deposition because of anatomical variability can be addressed through design of powder and device combinations that enable aerosols that largely bypass the mouth and throat.

CHAPTER 6: REFERENCES

1. Crompton GK: **Dry powder inhalers: advantages and limitations.** *J Aerosol Med* 1991, **4:**151-156.
2. Krüger P, Ehrlein B, Zier M, Greguletz R: **Inspiratory flow resistance of marketed dry powder inhalers (DPI).** *European Respiratory Journal* 2014, **44**.
3. Labiris NR, Dolovich MB: **Pulmonary drug delivery. Part I: physiological factors affecting therapeutic effectiveness of aerosolized medications.** *British journal of clinical pharmacology* 2003, **56:**588-599.
4. Labiris NR, Dolovich MB: **Pulmonary drug delivery. Part II: the role of inhalant delivery devices and drug formulations in therapeutic effectiveness of aerosolized medications.** *British journal of clinical pharmacology* 2003, **56:**600-612.
5. Vanbever R, Mintzes JD, Wang J, Nice J, Chen D, Batycky R, Langer R, Edwards DA: **Formulation and physical characterization of large porous particles for inhalation.** *Pharm Res* 1999, **16:**1735-1742.
6. Telko MJ, Hickey AJ: **Dry powder inhaler formulation.** *Respir Care* 2005, **50:**1209-1227.
7. Xu Z, Mansour HM, Hickey AJ: **Particle Interactions in Dry Powder Inhaler Unit Processes: A Review.** *Journal of Adhesion Science and Technology* 2012, **25:**451-482.
8. Dunbar CA, Hickey AJ, P H: **Dispersion and characterization of pharmaceutical dry powder aerosols.** *KONA Powder Part J* 1998, **16:**7-45.
9. Young PM, Sung A, Traini D, Kwok P, Chiou H, Chan HK: **Influence of humidity on the electrostatic charge and aerosol performance of dry powder inhaler carrier based systems.** *Pharm Res* 2007, **24:**963-970.
10. Chow AH, Tong HH, Chattopadhyay P, Shekunov BY: **Particle engineering for pulmonary drug delivery.** *Pharm Res* 2007, **24:**411-437.
11. Voss A, Finlay WH: **Deagglomeration of dry powder pharmaceutical aerosols.** *Int J Pharm* 2002, **248:**39-50.
12. Jones MD, Price R: **The influence of fine excipient particles on the performance of carrier-based dry powder inhalation formulations.** *Pharm Res* 2006, **23:**1665-1674.
13. Ferrari F, Cocconi D, Bettini R, Giordano F, Santi P, Tobyn M, Price R, Young P, Caramella C, Colombo P: **The surface roughness of lactose particles can be modulated by wet-smoothing using a high-shear mixer.** *AAPS PharmSciTech* 2004, **5:**69-74.
14. Begat P, Morton DA, Shur J, Kippax P, Staniforth JN, Price R: **The role of force control agents in high-dose dry powder inhaler formulations.** *J Pharm Sci* 2009, **98:**2770-2783.
15. Thalberg K, Aslund S, Skogevall M, Andersson P: **Dispersibility of lactose fines as compared to API in dry powders for inhalation.** *Int J Pharm* 2016, **504:**27-38.
16. Guchardi R, Frei M, John E, Kaerger JS: **Influence of fine lactose and magnesium stearate on low dose dry powder inhaler formulations.** *Int J Pharm* 2008, **348:**10-17.
17. Das SC, Zhou Q, Morton DA, Larson I, Stewart PJ: **Use of surface energy distributions by inverse gas chromatography to understand mechanofusion processing and functionality of lactose coated with magnesium stearate.** *Eur J Pharm Sci* 2011, **43:**325-333.
18. Jetzer M, Morrical BD, Schneider M, Imanidis G: **Investigating the Effect of the Force Control Agent Magnesium Stearate in Fluticasone Propionate Dry Powder Inhaled Formulations with Single Particle Aerosol Mass Spectrometry (SPAMS).** *DDL27 Edinburgh* 2016.
19. Shur J, Price R, Lewis D, Young PM, Woollam G, Singh D, Edge S: **From single excipients to dual excipient platforms in dry powder inhaler products.** *Int J Pharm* 2016, **514:**374-383.
20. Kinnunen H, Hebbink G, Peters H, Huck D, Makein L, Price R: **Extrinsic lactose fines improve dry powder inhaler formulation performance of a cohesive batch of budesonide via agglomerate formation and consequential co-deposition.** *Int J Pharm* 2015, **478:**53-59.
21. Louey MD, Stewart PJ: **Particle interactions involved in aerosol dispersion of ternary interactive mixtures.** *Pharm Res* 2002, **19:**1524-1531.
22. Singh DJ, Jain RR, Soni PS, Abdul S, Darshana H, Gaikwad RV, Menon MD: **Preparation and Evaluation of Surface Modified Lactose Particles for Improved Performance of Fluticasone Propionate Dry Powder Inhaler.** *J Aerosol Med Pulm Drug Deliv* 2015, **28:**254-267.
23. Begat P, Price R, Harris H, Morton DA, Staniforth JN: **The influence of force control agents on the cohesive-adhesive balance in dry powder inhaler formulations.** *KONA Powder and Particle Journal* 2005, **23:**109-121.

24. Zhou QT, Qu L, Gengenbach T, Denman JA, Larson I, Stewart PJ, Morton DA: **Investigation of the extent of surface coating via mechanofusion with varying additive levels and the influences on bulk powder flow properties.** *Int J Pharm* 2011, **413:**36-43.
25. Pfeffer R, Dave RN, Wei DG, Ramlakhan M: **Synthesis of engineered particulates with tailored properties using dry particle coating.** *Powder Technology* 2001, **117:**40-67.
26. Marple VA, Olson BA, Santhanakrishnan K, Roberts DL, Mitchell JP, Hudson-Curtis BL: **Next generation pharmaceutical impactor: a new impactor for pharmaceutical inhaler testing. Part III. extension of archival calibration to 15 L/min.** *J Aerosol Med* 2004, **17:**335-343.
27. Marple VA, Olson BA, Santhanakrishnan K, Mitchell JP, Murray SC, Hudson-Curtis BL: **Next generation pharmaceutical impactor (a new impactor for pharmaceutical inhaler testing). Part II: Archival calibration.** *J Aerosol Med* 2003, **16:**301-324.
28. Marple VA, Roberts DL, Romay FJ, Miller NC, Truman KG, Holroyd MJ, Mitchell JP, Hochrainer D: **Next generation pharmaceutical impactor (A new impactor for pharmaceutical inhaler testing). Part I: Design.** *Journal of Aerosol Medicine-Deposition Clearance and Effects in the Lung* 2003, **16:**283-299.
29. Christopher D, Curry P, Doub B, Furnkranz K, Lavery M, Lin K, Lyapustina S, Mitchell J, Rogers B, Strickland H, et al: **Considerations for the development and practice of cascade impaction testing, including a mass balance failure investigation tree.** *J Aerosol Med* 2003, **16:**235-247.
30. Morrical BD, Balaxi M, Fergenson D: **The on-line analysis of aerosol-delivered pharmaceuticals via single particle aerosol mass spectrometry.** *International Journal of Pharmaceutics* 2015, **489:**11-17.
31. Bonam M, Christopher D, Cipolla D, Donovan B, Goodwin D, Holmes S, Lyapustina S, Mitchell J, Nichols S, Pettersson G, et al: **Minimizing Variability of Cascade Impaction Measurements in Inhalers and Nebulizers.** *AAPS PharmSciTech* 2008, **9:**404-413.
32. Prather KA, Nordmeyer T, Salt K: **Real-Time Characterization of Individual Aerosol Particles Using Time-of-Flight Mass Spectrometry.** 1994, **66:**1403-1407.
33. Su YX, Sipin MF, Furutani H, Prather KA: **Development and characterization of an aerosol time-of-flight mass spectrometer with increased detection efficiency.** *Analytical Chemistry* 2004, **76:**712-719.
34. Lipson DA, Barnacle H, Birk R, Brealey N, Locantore N, Lomas DA, Ludwig-Sengpiel A, Mohindra R, Tabberer M, Zhu CQ, Pascoe SJ: **FULFIL Trial: Once-Daily Triple Therapy for Patients with Chronic Obstructive Pulmonary Disease.** *Am J Respir Crit Care Med* 2017, **196:**438-446.
35. Buttini F, Brambilla G, Copelli D, Sisti V, Balducci AG, Bettini R, Pasquali I: **Effect of Flow Rate on In Vitro Aerodynamic Performance of NEXThaler((R)) in Comparison with Diskus((R)) and Turbohaler((R)) Dry Powder Inhalers.** *J Aerosol Med Pulm Drug Deliv* 2016, **29:**167-178.
36. Corradi M, Chrystyn H, Cosio BG, Pirozynski M, Loukides S, Louis R, Spinola M, Usmani OS: **NEXThaler, an innovative dry powder inhaler delivering an extrafine fixed combination of beclometasone and formoterol to treat large and small airways in asthma.** *Expert Opin Drug Deliv* 2014, **11:**1497-1506.
37. New A, Prime D, Zomer S, Elder D, Donovan R, Freney E: **Detection and assessment of co-association in inhalable drug particles using aerosol time-of-flight mass spectrometry.** *Rapid Commun Mass Spectrom* 2008, **22:**3873-3882.
38. Haghi M, Traini D, Postma DS, Bebawy M, Young PM: **Fluticasone uptake across Calu-3 cells is mediated by salmeterol when deposited as a combination powder inhaler.** *Respirology* 2013, **18:**1197-1201.
39. Ambrosino N, Paggiaro P: **The management of asthma and chronic obstructive pulmonary disease: current status and future perspectives.** *Expert Rev Respir Med* 2012, **6:**117-127.
40. Adjei A, Gupta P: **Pulmonary delivery of therapeutic peptides and proteins.** *Journal of Controlled Release* 1994, **29:**361-373.
41. Grossman J: **The evolution of inhaler technology.** *J Asthma* 1994, **31:**55-64.
42. Rau JL: **The inhalation of drugs: advantages and problems.** *Respir Care* 2005, **50:**367-382.
43. Stein SW, Thiel CG: **The History of Therapeutic Aerosols: A Chronological Review.** *Journal of Aerosol Medicine and Pulmonary Drug Delivery* 2017, **30:**20-41.
44. Cochrane MG, Bala MV, Downs KE, Mauskopf J, Ben-Joseph RH: **Inhaled corticosteroids for asthma therapy: patient compliance, devices, and inhalation technique.** *Chest* 2000, **117:**542-550.
45. Islam N, Cleary MJ: **Developing an efficient and reliable dry powder inhaler for pulmonary drug delivery--a review for multidisciplinary researchers.** *Medical engineering & physics* 2012, **34:**409-427.
46. Wijkstra PJ, van der Mark TW, Boezen M, van Altena R, Postma DS, Koeter GH: **Peak inspiratory mouth pressure in healthy subjects and in patients with COPD.** *Chest* 1995, **107:**652-656.

47. Kanabuchi K, Kondo T, Tanigaki T, Tajiri S, Hayama N, Takahari Y, Iwao K: **Minimal inspiratory flow from dry powder inhalers according to a biphasic model of pressure vs. flow relationship.** *Tokai J Exp Clin Med* 2011, **36:**1-4.
48. Sarinas PS, Robinson TE, Clark AR, Canfield J, Jr., Chitkara RK, Fick RB, Jr.: **Inspiratory flow rate and dynamic lung function in cystic fibrosis and chronic obstructive lung diseases.** *Chest* 1998, **114:**988-992.
49. ER. W: **Morphometry of the human lung.** *Springer Verlag Berlin* 1963**:**151.
50. AJ. H: **Inhalation aerosols: Physical and biological basis for therapy.** *New York, Marcel Dekker, Inc* 1996.
51. Levitzky MG: **Chapter 1. Function and Structure of the Respiratory System.** In *Pulmonary Physiology, 8e.* New York, NY: The McGraw-Hill Companies; 2013
52. Byron PR, Patton JS: **Drug delivery via the respiratory tract.** *J Aerosol Med* 1994, **7:**49-75.
53. Rees PJ, Clark TJ, Moren F: **The importance of particle size in response to inhaled bronchodilators.** *Eur J Respir Dis Suppl* 1982, **119:**73-78.
54. Byron PR: **Prediction of drug residence times in regions of the human respiratory tract following aerosol inhalation.** *J Pharm Sci* 1986, **75:**433-438.
55. Ward AJ, Kassem N, Evans JM, Moxham J, Ganderton D: **A clinically relevant modification to existing inhaler therapy.** *Respir Med* 1992, **86:**237-241.
56. Timsina MP, Martin GP, Marriott C, Ganderton D, Yianneskis M: **Drug-Delivery to the Respiratory-Tract Using Dry Powder Inhalers.** *International Journal of Pharmaceutics* 1994, **101:**1-13.
57. Suarez S, Hickey AJ: **Drug properties affecting aerosol behavior.** *Respir Care* 2000, **45:**652-666.
58. Edwards DA, Hanes J, Caponetti G, Hrkach J, Ben-Jebria A, Eskew ML, Mintzes J, Deaver D, Lotan N, Langer R: **Large porous particles for pulmonary drug delivery.** *Science* 1997, **276:**1868-1871.
59. Ben-Jebria A, Chen D, Eskew ML, Vanbever R, Langer R, Edwards DA: **Large porous particles for sustained protection from carbachol-induced bronchoconstriction in guinea pigs.** *Pharm Res* 1999, **16:**555-561.
60. Dunbar C, Scheuch G, Sommerer K, DeLong M, Verma A, Batycky R: **In vitro and in vivo dose delivery characteristics of large porous particles for inhalation.** *Int J Pharm* 2002, **245:**179-189.
61. JE. A: **Physical properties and mechanisms of deposition of aerosols.** *Aerosols and the Lung: Clinical and Experimental Aspects* 1984**:**49.
62. NA. F: **The Mechanics of Aerosols.** *Elmsford, NY: Pergamon Press* 1964.
63. Hinds W: **Aerosol Technology: Properties, Behavior, and Measurement of Airborne Particles, 2nd Edition.** *Aerosol Technology* 1999**:**191-192.
64. **Encyclopaedia of Occupational Health and Safety, 4th Edition, Chapter 10 Respiratory System.**
65. Patton JS: **Mechanisms of macromolecule absorption by the lungs.** *Advanced Drug Delivery Reviews* 1996, **19:**3-36.
66. Wiedmann TS, Bhatia R, Wattenberg LW: **Drug solubilization in lung surfactant.** *J Control Release* 2000, **65:**43-47.
67. Olsson B, Bondesson E, Borgström L, Edsbäcker S, Eirefelt S, Ekelund K, Gustavsson L, Hegelund-Myrbäck T: **Pulmonary Drug Metabolism, Clearance, and Absorption.** In *Controlled Pulmonary Drug Delivery.* Edited by Smyth HDC, Hickey AJ. New York, NY: Springer New York; 2011: 21-50
68. Tronde A, Norden B, Marchner H, Wendel AK, Lennernas H, Bengtsson UH: **Pulmonary absorption rate and bioavailability of drugs in vivo in rats: structure-absorption relationships and physicochemical profiling of inhaled drugs.** *J Pharm Sci* 2003, **92:**1216-1233.
69. Fischer H, Widdicombe JH: **Mechanisms of acid and base secretion by the airway epithelium.** *J Membr Biol* 2006, **211:**139-150.
70. Boat TF, Cheng PW: **Biochemistry of airway mucus secretions.** *Fed Proc* 1980, **39:**3067-3074.
71. Pham S, Wiedmann TS: **Note: dissolution of aerosol particles of budesonide in Survanta, a model lung surfactant.** *J Pharm Sci* 2001, **90:**98-104.
72. Eljamal M, Nagarajan S, Patton JS: **In Situ and in Vivo Methods for Pulmonary Delivery.** In *Models for Assessing Drug Absorption and Metabolism.* Edited by Borchardt RT, Smith PL, Wilson G. Boston, MA: Springer US; 1996: 361-374
73. Yu LX, Lipka E, Crison JR, Amidon GL: **Transport approaches to the biopharmaceutical design of oral drug delivery systems: prediction of intestinal absorption.** *Adv Drug Deliv Rev* 1996, **19:**359-376.
74. Gray V, J. Hickey A, Balmer P, Davies N, Dunbar C, S. Foster T, L. Olsson B, Sakagami M, P. Shah V, J. Smurthwaite M, et al: *The Inhalation Ad Hoc Advisory Panel for the USP Performance Tests of Inhalation Dosage Forms.* 2008.

75. Riley T, Christopher D, Arp J, Casazza A, Colombani A, Cooper A, Dey M, Maas J, Mitchell J, Reiners M, et al: **Challenges with developing in vitro dissolution tests for orally inhaled products (OIPs).** *AAPS PharmSciTech* 2012, **13:**978-989.
76. Rohrschneider M, Bhagwat S, Krampe R, Michler V, Breitkreutz J, Hochhaus G: **Evaluation of the Transwell System for Characterization of Dissolution Behavior of Inhalation Drugs: Effects of Membrane and Surfactant.** *Molecular Pharmaceutics* 2015, **12:**2618-2624.
77. Edsbacker S, Wollmer P, Selroos O, Borgstrom L, Olsson B, Ingelf J: **Do airway clearance mechanisms influence the local and systemic effects of inhaled corticosteroids?** *Pulm Pharmacol Ther* 2008, **21:**247-258.
78. Smaldone GC, Perry RJ, Bennett WD, Messina MS, Zwang J, Ilowite J: **Interpretation of "24 Hour Lung Retention" in Studies of Mucociliary Clearance.** *Journal of Aerosol Medicine* 1988, **1:**11-20.
79. Houtmeyers E, Gosselink R, Gayan-Ramirez G, Decramer M: **Regulation of mucociliary clearance in health and disease.** *Eur Respir J* 1999, **13:**1177-1188.
80. Summers QA: **Inhaled drugs and the lung.** *Clin Exp Allergy* 1991, **21:**259-268.
81. Folkesson HG, Matthay MA, Westrom BR, Kim KJ, Karlsson BW, Hastings RH: **Alveolar epithelial clearance of protein.** *J Appl Physiol (1985)* 1996, **80:**1431-1445.
82. Martonen TB: **Mathematical model for the selective deposition of inhaled pharmaceuticals.** *J Pharm Sci* 1993, **82:**1191-1199.
83. Folkesson HG, Westrom BR, Karlsson BW: **Permeability of the respiratory tract to different-sized macromolecules after intratracheal instillation in young and adult rats.** *Acta Physiol Scand* 1990, **139:**347-354.
84. Krishna DR, Klotz U: **Extrahepatic metabolism of drugs in humans.** *Clin Pharmacokinet* 1994, **26:**144-160.
85. Upton RN, Doolette DJ: **Kinetic aspects of drug disposition in the lungs.** *Clin Exp Pharmacol Physiol* 1999, **26:**381-391.
86. Dahl AR, Lewis JL: **Respiratory tract uptake of inhalants and metabolism of xenobiotics.** *Annu Rev Pharmacol Toxicol* 1993, **33:**383-407.
87. Muralidharan P, Hayes D, Mansour HM: **Dry powder inhalers in COPD, lung inflammation and pulmonary infections.** *Expert Opinion on Drug Delivery* 2015, **12:**947-962.
88. Cipolla D, Blanchard J, Gonda I: **Development of Liposomal Ciprofloxacin to Treat Lung Infections.** *Pharmaceutics* 2016, **8**.
89. Rietscher R, Schroder M, Janke J, Czaplewska J, Gottschaldt M, Scherliess R, Hanefeld A, Schubert US, Schneider M, Knolle PA, Lehr CM: **Antigen delivery via hydrophilic PEG-b-PAGE-b-PLGA nanoparticles boosts vaccination induced T cell immunity.** *Eur J Pharm Biopharm* 2016, **102:**20-31.
90. LiCalsi C, Christensen T, Bennett JV, Phillips E, Witham C: **Dry powder inhalation as a potential delivery method for vaccines.** *Vaccine* 1999, **17:**1796-1803.
91. Al-Tabakha MM: **Future prospect of insulin inhalation for diabetic patients: The case of Afrezza versus Exubera.** *J Control Release* 2015, **215:**25-38.
92. Nassar YS, Ibrahim M, Salman AG, Elgohary TS: **Inhaled ceftazidime and amikacin versus inhaled colistin in the treatment of gram negative ventilator associated pneumonia.** *Intensive Care Medicine Experimental* 2015, **3:**A380.
93. Murdoch JR, Lloyd CM: **Chronic inflammation and asthma.** *Mutation Research* 2010, **690:**24-39.
94. Rabe KF, Hurd S, Anzueto A, Barnes PJ, Buist SA, Calverley P, Fukuchi Y, Jenkins C, Rodriguez-Roisin R, van Weel C, Zielinski J: **Global strategy for the diagnosis, management, and prevention of chronic obstructive pulmonary disease: GOLD executive summary.** *Am J Respir Crit Care Med* 2007, **176:**532-555.
95. **Standards for the diagnosis and care of patients with chronic obstructive pulmonary disease (COPD) and asthma. This official statement of the American Thoracic Society was adopted by the ATS Board of Directors, November 1986.** *Am Rev Respir Dis* 1987, **136:**225-244.
96. Greening AP, Ind PW, Northfield M, Shaw G: **Added salmeterol versus higher-dose corticosteroid in asthma patients with symptoms on existing inhaled corticosteroid. Allen & Hanburys Limited UK Study Group.** *Lancet* 1994, **344:**219-224.
97. Canadian Agency for D, Technologies in H: **Long-Acting Beta(2)-Agonist and Inhaled Corticosteroid Combination Therapy for Adult Persistent Asthma: Systematic Review of Clinical Outcomes and Economic Evaluation.** *CADTH Technology Overviews* 2010, **1:**e0120.

98. Bateman ED, Bantje TA, Joao Gomes M, Toumbis MG, Huber RM, Naya I, Eliraz A: **Combination therapy with single inhaler budesonide/formoterol compared with high dose of fluticasone propionate alone in patients with moderate persistent asthma.** *Am J Respir Med* 2003, **2:**275-281.
99. Athanazio R: **Airway disease: similarities and differences between asthma, COPD and bronchiectasis.** *Clinics* 2012, **67:**1335-1343.
100. Bateman ED, Hurd SS, Barnes PJ, Bousquet J, Drazen JM, FitzGerald M, Gibson P, Ohta K, O'Byrne P, Pedersen SE, et al: **Global strategy for asthma management and prevention: GINA executive summary.** *Eur Respir J* 2008, **31:**143-178.
101. Barnes PJ: **Scientific rationale for inhaled combination therapy with long-acting beta2-agonists and corticosteroids.** *Eur Respir J* 2002, **19:**182-191.
102. Holgate ST, Polosa R: **Treatment strategies for allergy and asthma.** *Nat Rev Immunol* 2008, **8:**218-230.
103. Cazzola M, Page CP, Calzetta L, Matera MG: **Pharmacology and therapeutics of bronchodilators.** *Pharmacol Rev* 2012, **64:**450-504.
104. Barnes PJ, Stockley RA: **COPD: current therapeutic interventions and future approaches.** *Eur Respir J* 2005, **25:**1084-1106.
105. Buhl R, Banerji D: **Profile of glycopyrronium for once-daily treatment of moderate-to-severe COPD.** *International Journal of Chronic Obstructive Pulmonary Disease* 2012, **7:**729-741.
106. Miller-Larsson A, Selroos O: **Advances in asthma and COPD treatment: combination therapy with inhaled corticosteroids and long-acting beta 2-agonists.** *Curr Pharm Des* 2006, **12:**3261-3279.
107. Nelson HS, Chapman KR, Pyke SD, Johnson M, Pritchard JN: **Enhanced synergy between fluticasone propionate and salmeterol inhaled from a single inhaler versus separate inhalers.** *Journal of Allergy and Clinical Immunology* 2003, **112:**29-36.
108. Ducharme FM, Ni Chroinin M, Greenstone I, Lasserson TJ: **Addition of long-acting beta2-agonists to inhaled corticosteroids versus same dose inhaled corticosteroids for chronic asthma in adults and children.** *The Cochrane database of systematic reviews* 2010**:**CD005535-CD005535.
109. Cazzola M, Matera MG: **Triple combinations in chronic obstructive pulmonary disease - is three better than two?** *Expert Opin Pharmacother* 2014, **15:**2475-2478.
110. Stein SW, Sheth P, Hodson PD, Myrdal PB: **Advances in Metered Dose Inhaler Technology: Hardware Development.** *AAPS PharmSciTech* 2014, **15:**326-338.
111. Hess DR: **Aerosol delivery devices in the treatment of asthma.** *Respir Care* 2008, **53:**699-723; discussion 723-695.
112. Hess DR: **Nebulizers: principles and performance.** *Respir Care* 2000, **45:**609-622.
113. Tiwari G, Tiwari R, Sriwastawa B, Bhati L, Pandey S, Pandey P, Bannerjee SK: **Drug delivery systems: An updated review.** *Int J Pharm Investig* 2012, **2:**2-11.
114. Terzano C: **Pressurized metered dose inhalers and add-on devices.** *Pulmonary pharmacology & therapeutics* 2001, **14:**351-366.
115. Bell J, Newman S: **The rejuvenated pressurised metered dose inhaler.** *Expert Opinion on Drug Delivery* 2007, **4:**215-234.
116. Pitcairn G, Reader S, Pavia D, Newman S: **Deposition of corticosteroid aerosol in the human lung by Respimat Soft Mist inhaler compared to deposition by metered dose inhaler or by Turbuhaler dry powder inhaler.** *J Aerosol Med* 2005, **18:**264-272.
117. Dalby R, Spallek M, Voshaar T: **A review of the development of Respimat Soft Mist Inhaler.** *Int J Pharm* 2004, **283:**1-9.
118. McDonald KJ, Martin GP: **Transition to CFC-free metered dose inhalers--into the new millennium.** *Int J Pharm* 2000, **201:**89-107.
119. Newman SP: **Drug delivery to the lungs from dry powder inhalers.** *Current Opinion in Pulmonary Medicine* 2003, **9:**S17-S20.
120. Hickey AJ, Mansour HM, Telko MJ, Xu Z, Smyth HDC, Mulder T, McLean R, Langridge J, Papadopoulos D: **Physical characterization of component particles included in dry powder inhalers. I. Strategy review and static characteristics.** *Journal of Pharmaceutical Sciences* 2007, **96:**1282-1301.
121. Hirst PH, Newman SP, Clark DA, Hertog MGL: **Lung deposition of budesonide from the novel dry powder inhaler AirmaxTM.** *Respiratory Medicine* 2002, **96:**389-396.
122. Newman SP, Hollingworth A, Clark AR: **Effect of different modes of inhalation on drug delivery from a dry powder inhaler.** *International Journal of Pharmaceutics* 1994, **102:**127-132.
123. Cegla UH: **Pressure and inspiratory flow characteristics of dry powder inhalers.** *Respir Med* 2004, **98 Suppl A:**S22-28.

124. Dunbar CA, Morgan B, Van Oort M, Hickey AJ: **A comparison of dry powder inhaler dose delivery characteristics using a power criterion.** *PDA J Pharm Sci Technol* 2000, **54:**478-484.
125. Zeng XM, Martin GP, Marriott C, Pritchard J: **The influence of carrier morphology on drug delivery by dry powder inhalers.** *International Journal of Pharmaceutics* 2000, **200:**93-106.
126. Clark AR, Hollingworth AM: **The relationship between powder inhaler resistance and peak inspiratory conditions in healthy volunteers--implications for in vitro testing.** *J Aerosol Med* 1993, **6:**99-110.
127. Tiddens HA, Geller DE, Challoner P, Speirs RJ, Kesser KC, Overbeek SE, Humble D, Shrewsbury SB, Standaert TA: **Effect of dry powder inhaler resistance on the inspiratory flow rates and volumes of cystic fibrosis patients of six years and older.** *J Aerosol Med* 2006, **19:**456-465.
128. Feddah MR, Brown KF, Gipps EM, Davies NM: **In-vitro characterisation of metered dose inhaler versus dry powder inhaler glucocorticoid products: influence of inspiratory flow rates.** *J Pharm Pharm Sci* 2000, **3:**318-324.
129. Berkenfeld K, Lamprecht A, McConville JT: **Devices for Dry Powder Drug Delivery to the Lung.** *AAPS PharmSciTech* 2015, **16:**479-490.
130. Maltz D, Paboojian S: **Device engineering insights into TOBI Podhaler: a development case study of high efficient powder delivery to cystic fibrosis patients.** *RDD Europe 2011* 2011, **In: Dalby RN, Byron PR, Peart J, Suman JD, Young PM, editors. Proceedings of RDD Europe 2011. River Grove: Davis Healthcare International Publication:** 55–65.
131. Basheti IA, Bosnic-Anticevich SZ, Armour CL, Reddel HK: **Checklists for powder inhaler technique: a review and recommendations.** *Respir Care* 2014, **59:**1140-1154.
132. Olsson M, Trofast E: **Dry powder inhaler.** Astra Zeneca: US Patent US20070107721A1; 2004.
133. Chan JG, Wong J, Zhou QT, Leung SS, Chan HK: **Advances in device and formulation technologies for pulmonary drug delivery.** *AAPS PharmSciTech* 2014, **15:**882-897.
134. Weers JG, Miller DP: **Formulation Design of Dry Powders for Inhalation.** *Journal of Pharmaceutical Sciences* 2015, **104:**3259-3288.
135. Xu Z, Mansour HM, Hickey AJ: **Particle Interactions in Dry Powder Inhaler Unit Processes: A Review.** *Journal of Adhesion Science and Technology* 2011, **25:**451-482.
136. de Boer AH, Dickhoff BH, Hagedoorn P, Gjaltema D, Goede J, Lambregts D, Frijlink HW: **A critical evaluation of the relevant parameters for drug redispersion from adhesive mixtures during inhalation.** *Int J Pharm* 2005, **294:**173-184.
137. de Boer AH, Hagedoorn P, Hoppentocht M, Buttini F, Grasmeijer F, Frijlink HW: **Dry powder inhalation: past, present and future.** *Expert Opin Drug Deliv* 2017, **14:**499-512.
138. Hoppentocht M, Hagedoorn P, Frijlink HW, de Boer AH: **Technological and practical challenges of dry powder inhalers and formulations.** *Adv Drug Deliv Rev* 2014, **75:**18-31.
139. Dolovich MA: **Influence of inspiratory flow rate, particle size, and airway caliber on aerosolized drug delivery to the lung.** *Respir Care* 2000, **45:**597-608.
140. De Backer W, Devolder A, Poli G, Acerbi D, Monno R, Herpich C, Sommerer K, Meyer T, Mariotti F: **Lung deposition of BDP/formoterol HFA pMDI in healthy volunteers, asthmatic, and COPD patients.** *J Aerosol Med Pulm Drug Deliv* 2010, **23:**137-148.
141. Usmani OS, Biddiscombe MF, Barnes PJ: **Regional lung deposition and bronchodilator response as a function of beta2-agonist particle size.** *Am J Respir Crit Care Med* 2005, **172:**1497-1504.
142. Gaisford S, Dennison M, Tawfik M, Jones MD: **Following mechanical activation of salbutamol sulphate during ball-milling with isothermal calorimetry.** *International Journal of Pharmaceutics* 2010, **393:**75-79.
143. Depasquale R, Lee SL, Saluja B, Shur J, Price R: **The influence of secondary processing on the structural relaxation dynamics of fluticasone propionate.** *AAPS PharmSciTech* 2015, **16:**589-600.
144. Larhrib H, Martin GP, Marriott C, Prime D: **The influence of carrier and drug morphology on drug delivery from dry powder formulations.** *Int J Pharm* 2003, **257:**283-296.
145. Saleem IY, Smyth HDC: **Micronization of a Soft Material: Air-Jet and Micro-Ball Milling.** *AAPS PharmSciTech* 2010, **11:**1642-1649.
146. Jetzer M, Schneider M, Morrical B, Imanidis G: **Investigations on the Mechanism of Magnesium Stearate to Modify Aerosol Performance in Dry Powder Inhaled Formulations.** *J Pharm Sci* 2017.
147. Maa Y-F, Nguyen P-A, Sweeney T, Shire SJ, Hsu CC: **Protein Inhalation Powders: Spray Drying vs Spray Freeze Drying.** *Pharmaceutical Research* 1999, **16:**249-254.
148. Sweeney LG, Wang Z, Loebenberg R, Wong JP, Lange CF, Finlay WH: **Spray-freeze-dried liposomal ciprofloxacin powder for inhaled aerosol drug delivery.** *Int J Pharm* 2005, **305:**180-185.

149. Costantino HR, Firouzabadian L, Wu C, Carrasquillo KG, Griebenow K, Zale SE, Tracy MA: **Protein spray freeze drying. 2. Effect of formulation variables on particle size and stability.** *Journal of Pharmaceutical Sciences*, **91:**388-395.
150. Costantino HR, Firouzabadian L, Hogeland K, Wu C, Beganski C, Carrasquillo KG, Córdova M, Griebenow K, Zale SE, Tracy MA: **Protein Spray-Freeze Drying. Effect of Atomization Conditions on Particle Size and Stability.** *Pharmaceutical Research* 2000, **17:**1374-1382.
151. Johnson OL, Jaworowicz W, Cleland JL, Bailey L, Charnis M, Duenas E, Wu C, Shepard D, Magil S, Last T, et al: **The stabilization and encapsulation of human growth hormone into biodegradable microspheres.** *Pharm Res* 1997, **14:**730-735.
152. Saluja V, Amorij JP, Kapteyn JC, de Boer AH, Frijlink HW, Hinrichs WL: **A comparison between spray drying and spray freeze drying to produce an influenza subunit vaccine powder for inhalation.** *J Control Release* 2010, **144:**127-133.
153. Steckel H, Thies J, Müller BW: **Micronizing of steroids for pulmonary delivery by supercritical carbon dioxide.** *International Journal of Pharmaceutics* 1997, **152:**99-110.
154. Girotra P, Singh SK, Nagpal K: **Supercritical fluid technology: a promising approach in pharmaceutical research.** *Pharm Dev Technol* 2013, **18:**22-38.
155. Shekunov BY, Feeley JC, Chow AHL, Tong HHY, York P: **Aerosolisation behaviour of micronised and supercritically-processed powders.** *Journal of Aerosol Science* 2003, **34:**553-568.
156. Lobo JM, Schiavone H, Palakodaty S, York P, Clark A, Tzannis ST: **SCF-engineered powders for delivery of budesonide from passive DPI devices.** *Journal of Pharmaceutical Sciences* 2005, **94:**2276-2288.
157. Steckel H, Brandes HG: **A novel spray-drying technique to produce low density particles for pulmonary delivery.** *International Journal of Pharmaceutics* 2004, **278:**187-195.
158. Littringer EM, Mescher A, Schroettner H, Achelis L, Walzel P, Urbanetz NA: **Spray dried mannitol carrier particles with tailored surface properties--the influence of carrier surface roughness and shape.** *Eur J Pharm Biopharm* 2012, **82:**194-204.
159. Littringer EM, Mescher A, Eckhard S, Schröttner H, Langes C, Fries M, Griesser U, Walzel P, Urbanetz NA: **Spray Drying of Mannitol as a Drug Carrier—The Impact of Process Parameters on Product Properties.** *Drying Technology* 2012, **30:**114-124.
160. Vehring R: **Pharmaceutical particle engineering via spray drying.** *Pharmaceutical Research* 2008, **25:**999-1022.
161. Seville PC, Li H-Y, Learoyd TP: **Spray-dried powders for pulmonary drug delivery.** *Critical Reviews in Therapeutic Drug Carrier Systems* 2007, **24:**307-360.
162. Chan HK, Chew NY: **Novel alternative methods for the delivery of drugs for the treatment of asthma.** *Adv Drug Deliv Rev* 2003, **55:**793-805.
163. Duddu SP, Sisk SA, Walter YH, Tarara TE, Trimble KR, Clark AR, Eldon MA, Elton RC, Pickford M, Hirst PH, et al: **Improved lung delivery from a passive dry powder inhaler using an engineered PulmoSphere (R) powder.** *Pharmaceutical Research* 2002, **19:**689-695.
164. Weers JG, Tarara TE, Clark AR: **Design of fine particles for pulmonary drug delivery.** *Expert Opin Drug Deliv* 2007, **4:**297-313.
165. Jin TH, Tsao E, Goudsmit J, Dheenadhayalan V, Sadoff J: **Stabilizing formulations for inhalable powders of an adenovirus 35-vectored tuberculosis (TB) vaccine (AERAS-402).** *Vaccine* 2010, **28:**4369-4375.
166. Lam J, Vaughan S, Parkins MD: **Tobramycin Inhalation Powder (TIP): An Efficient Treatment Strategy for the Management of Chronic Pseudomonas Aeruginosa Infection in Cystic Fibrosis.** *Clin Med Insights Circ Respir Pulm Med* 2013, **7:**61-77.
167. Pilcer G, Amighi K: **Formulation strategy and use of excipients in pulmonary drug delivery.** *Int J Pharm* 2010, **392:**1-19.
168. Steckel H, Bolzen N: **Alternative sugars as potential carriers for dry powder inhalations.** *Int J Pharm* 2004, **270:**297-306.
169. Momin M-N, Hedayati A, Nokhodchi A: **Investigation into Alternative Sugars as Potential Carriers for Dry Powder Formulation of Budesonide.** *BioImpacts : BI* 2011, **1:**105-111.
170. Tee SK, Marriott C, Zeng XM, Martin GP: **The use of different sugars as fine and coarse carriers for aerosolised salbutamol sulphate.** *Int J Pharm* 2000, **208:**111-123.
171. de Boer AH, Chan HK, Price R: **A critical view on lactose-based drug formulation and device studies for dry powder inhalation: which are relevant and what interactions to expect?** *Adv Drug Deliv Rev* 2012, **64:**257-274.

172. Grasmeijer F, Hagedoorn P, Frijlink HW, de Boer AH: **Drug content effects on the dispersion performance of adhesive mixtures for inhalation.** *PLoS One* 2013, **8:**e71339.
173. Young PM, Price R, Tobyn MJ, Buttrum M, Dey F: **Investigation into the effect of humidity on drug-drug interactions using the atomic force microscope.** *J Pharm Sci* 2003, **92:**815-822.
174. Staniforth JN: **Performance-Modifying Influences in Dry Powder Inhalation Systems.** *Aerosol Science and Technology* 1995, **22:**346-353.
175. Ward S, Perkins M, Zhang J, Roberts CJ, Madden CE, Luk SY, Patel N, Ebbens SJ: **Identifying and mapping surface amorphous domains.** *Pharm Res* 2005, **22:**1195-1202.
176. Traini D, Young PM, Jones M, Edge S, Price R: **Comparative study of erythritol and lactose monohydrate as carriers for inhalation: atomic force microscopy and in vitro correlation.** *Eur J Pharm Sci* 2006, **27:**243-251.
177. Frijlink HW, De Boer AH: **Dry powder inhalers for pulmonary drug delivery.** *Expert Opin Drug Deliv* 2004, **1:**67-86.
178. Islam N, Stewart P, Larson I, Hartley P: **Surface roughness contribution to the adhesion force distribution of salmeterol xinafoate on lactose carriers by atomic force microscopy.** *J Pharm Sci* 2005, **94:**1500-1511.
179. Adi H, Larson I, Chiou H, Young P, Traini D, Stewart P: **Role of agglomeration in the dispersion of salmeterol xinafoate from mixtures for inhalation with differing drug to fine lactose ratios.** *Journal of Pharmaceutical Sciences* 2008, **97:**3140-3152.
180. Adi H, Larson I, Stewart PJ: **Adhesion and redistribution of salmeterol xinafoate particles in sugar-based mixtures for inhalation.** *Int J Pharm* 2007, **337:**229-238.
181. Grasmeijer F, Hagedoorn P, Frijlink HW, de Boer HA: **Mixing time effects on the dispersion performance of adhesive mixtures for inhalation.** *PLoS One* 2013, **8:**e69263.
182. Jones MD, Santo JG, Yakub B, Dennison M, Master H, Buckton G: **The relationship between drug concentration, mixing time, blending order and ternary dry powder inhalation performance.** *Int J Pharm* 2010, **391:**137-147.
183. Muller T, Krehl R, Schiewe J, Weiler C, Steckel H: **Influence of small amorphous amounts in hydrophilic and hydrophobic APIs on storage stability of dry powder inhalation products.** *Eur J Pharm Biopharm* 2015, **92:**130-138.
184. Pfeffer R, Dave RN, Wei D, Ramlakhan M: **Synthesis of engineered particulates with tailored properties using dry particle coating.** *Powder Technology* 2001, **117:**40-67.
185. de Boer AH, Hagedoorn P, Gjaltema D, Goede J, Frijlink HW: **Air classifier technology (ACT) in dry powder inhalation - Part I. Introduction of a novel force distribution concept (FDC) explaining the performance of a basic air classifier on adhesive mixtures.** *International Journal of Pharmaceutics* 2003, **260:**187-200.
186. Staniforth JN, Rees JE, Kayes JB: **RELATION BETWEEN MIXING TIME AND SEGREGATION OF ORDERED MIXES.** *Journal of Pharmacy and Pharmacology* 1981, **33:**175-176.
187. Hertel M, Schwarz E, Kobler M, Hauptstein S, Steckel H, Scherliess R: **The influence of high shear mixing on ternary dry powder inhaler formulations.** *Int J Pharm* 2017, **534:**242-250.
188. Staniforth JN, Rees JE, Lai FK, Hersey JA: **Interparticle forces in binary and ternary ordered powder mixes.** *J Pharm Pharmacol* 1982, **34:**141-145.
189. Byron PR, Peart J, Staniforth JN: **Aerosol electrostatics. I: Properties of fine powders before and after aerosolization by dry powder inhalers.** *Pharm Res* 1997, **14:**698-705.
190. Zhou Q, Morton DAV: **Drug–lactose binding aspects in adhesive mixtures: Controlling performance in dry powder inhaler formulations by altering lactose carrier surfaces.** *Advanced Drug Delivery Reviews* 2012, **64:**275-284.
191. Staniforth JN, Rees JE, Lai FK, Hersey TLJA: **Interparticle forces in binary and ternary ordered powder mixes.** *Journal of Pharmacy and Pharmacology* 1982, **34:**141-145.
192. Young PM, Cocconi D, Colombo P, Bettini R, Price R, Steele DF, Tobyn MJ: **Characterization of a surface modified dry powder inhalation carrier prepared by "particle smoothing".** *J Pharm Pharmacol* 2002, **54:**1339-1344.
193. Begat P, Morton DA, Staniforth JN, Price R: **The cohesive-adhesive balances in dry powder inhaler formulations II: influence on fine particle delivery characteristics.** *Pharm Res* 2004, **21:**1826-1833.
194. Qu L, Morton DA, Zhou QT: **Particle Engineering Via Mechanical Dry Coating in the Design of Pharmaceutical Solid Dosage Forms.** *Curr Pharm Des* 2015, **21:**5802-5814.
195. Guchardi R, Frei M, John E, Kaerger JS: **Influence of fine lactose and magnesium stearate on low dose dry powder inhaler formulations.** *International Journal of Pharmaceutics* 2008, **348:**10-17.

196. Visser J: **Particle adhesion and removal: A review.** *Particulate Science and Technology* 1995, **13:**169-196.
197. Podczeck F, Newton JM: **Development of an ultracentrifuge technique to determine the adhesion and friction properties between particles and surfaces.** *Journal of Pharmaceutical Sciences* 1995, **84:**1067-1071.
198. Zeng XM, Martin GP, Marriott C: *Particulate interactions in dry powder formulations for inhalation.* Taylor & Francis; 2001.
199. Telko MJ, Hickey AJ: **Aerodynamic and Electrostatic Properties of Model Dry Powder Aerosols: a Comprehensive Study of Formulation Factors.** *AAPS PharmSciTech* 2014, **15:**1378-1397.
200. M. M: **Particle-particle interactions between tailored mannitol carrier particles and drug particles for inhalation.** Universität Kiel, Mathematisch-Naturwissenschaftliche Fakultät; 2016.
201. Hickey AJ, Mansour HM, Telko MJ, Xu Z, Smyth HDC, Mulder T, McLean R, Langridge J, Papadopoulos D: **Physical Characterization of Component Particles Included in Dry Powder Inhalers. I. Strategy Review and Static Characteristics.** *Journal of Pharmaceutical Sciences*, **96:**1282-1301.
202. Weiler C, Egen M, Trunk M, Langguth P: **Force control and powder dispersibility of spray dried particles for inhalation.** *J Pharm Sci* 2010, **99:**303-316.
203. Concessio NM, Hickey AJ: **Descriptors of irregular particle morphology and powder properties.** *Adv Drug Deliv Rev* 1997, **26:**29-40.
204. Podczeck F: *Particle–Particle Adhesion in Pharmaceutical Powder Handling.* Imperial College Press London UK; 1998.
205. Elajnaf A, Carter P, Rowley G: **The effect of relative humidity on electrostatic charge decay of drugs and excipient used in dry powder inhaler formulation.** *Drug Dev Ind Pharm* 2007, **33:**967-974.
206. Bailey AG: **Electrostatic Phenomena during Powder Handling.** *Powder Technology* 1984, **37:**71-85.
207. Biegaj KW, Rowland MG, Lukas TM, Heng JYY: **Surface Chemistry and Humidity in Powder Electrostatics: A Comparative Study between Tribocharging and Corona Discharge.** *Acs Omega* 2017, **2:**1576-1582.
208. Karner S, Anne Urbanetz N: **The impact of electrostatic charge in pharmaceutical powders with specific focus on inhalation-powders.** *Journal of Aerosol Science* 2011, **42:**428-445.
209. Wong J, Kwok PC, Noakes T, Fathi A, Dehghani F, Chan HK: **Effect of crystallinity on electrostatic charging in dry powder inhaler formulations.** *Pharm Res* 2014, **31:**1656-1664.
210. Ahlneck C, Zografi G: **The Molecular-Basis of Moisture Effects on the Physical and Chemical-Stability of Drugs in the Solid-State.** *International Journal of Pharmaceutics* 1990, **62:**87-95.
211. Tong P, Zografi G: **Effects of water vapor absorption on the physical and chemical stability of amorphous sodium indomethacin.** *AAPS PharmSciTech* 2004, **5:**e26.
212. Price R, Young PM, Edge S, Staniforth JN: **The influence of relative humidity on particulate interactions in carrier-based dry powder inhaler formulations.** *Int J Pharm* 2002, **246:**47-59.
213. Hooton JC, German CS, Allen S, Davies MC, Roberts CJ, Tendler SJ, Williams PM: **An atomic force microscopy study of the effect of nanoscale contact geometry and surface chemistry on the adhesion of pharmaceutical particles.** *Pharm Res* 2004, **21:**953-961.
214. Berard V, Lesniewska E, Andres C, Pertuy D, Laroche C, Pourcelot Y: **Dry powder inhaler: influence of humidity on topology and adhesion studied by AFM.** *Int J Pharm* 2002, **232:**213-224.
215. Young PM, Price R, Tobyn MJ, Buttrum M, Dey F: **The influence of relative humidity on the cohesion properties of micronized drugs used in inhalation therapy.** *J Pharm Sci* 2004, **93:**753-761.
216. Salama R, Hoe S, Chan HK, Traini D, Young PM: **Preparation and characterisation of controlled release co-spray dried drug-polymer microparticles for inhalation 1: influence of polymer concentration on physical and in vitro characteristics.** *Eur J Pharm Biopharm* 2008, **69:**486-495.
217. Buckton G: **Characterisation of small changes in the physical properties of powders of significance for dry powder inhaler formulations.** *Advanced drug delivery reviews* 1997, **26:**17-27.
218. Wagner KG, Dowe U, Zadnik J: **Highly loaded interactive mixtures for dry powder inhalers: prediction of the adhesion capacity using surface energy and solubility parameters.** *Pharmazie* 2005, **60:**339-344.
219. Ho R, Naderi M, Heng JY, Williams DR, Thielmann F, Bouza P, Keith AR, Thiele G, Burnett DJ: **Effect of milling on particle shape and surface energy heterogeneity of needle-shaped crystals.** *Pharm Res* 2012, **29:**2806-2816.
220. Raula J, Thielmann F, Naderi M, Lehto VP, Kauppinen EI: **Investigations on particle surface characteristics vs. dispersion behaviour of L-leucine coated carrier-free inhalable powders.** *Int J Pharm* 2010, **385:**79-85.

221. Thielmann F, Burnett DJ, Heng JY: **Determination of the surface energy distributions of different processed lactose.** *Drug Dev Ind Pharm* 2007, **33:**1240-1253.
222. Traini D, Young PM, Thielmann F, Acharya M: **The influence of lactose pseudopolymorphic form on salbutamol sulfate-lactose interactions in DPI formulations.** *Drug Dev Ind Pharm* 2008, **34:**992-1001.
223. Yla-Maihaniemi PP, Heng JY, Thielmann F, Williams DR: **Inverse gas chromatographic method for measuring the dispersive surface energy distribution for particulates.** *Langmuir* 2008, **24:**9551-9557.
224. Hooton JC, Jones MD, Price R: **Predicting the behavior of novel sugar carriers for dry powder inhaler formulations via the use of a cohesive-adhesive force balance approach.** *J Pharm Sci* 2006, **95:**1288-1297.
225. Jones MD, Harris H, Hooton JC, Shur J, King GS, Mathoulin CA, Nichol K, Smith TL, Dawson ML, Ferrie AR, Price R: **An investigation into the relationship between carrier-based dry powder inhalation performance and formulation cohesive-adhesive force balances.** *Eur J Pharm Biopharm* 2008, **69:**496-507.
226. Chew NYK, Bagster DF, Chan HK: **Effect of particle size, air flow and inhaler device on the aerosolisation of disodium cromoglycate powders.** *International Journal of Pharmaceutics* 2000, **206:**75-83.
227. Glover W, Chan HK, Eberl S, Daviskas E, Verschuer J: **Effect of particle size of dry powder mannitol on the lung deposition in healthy volunteers.** *Int J Pharm* 2008, **349:**314-322.
228. Hickey AJ, Mansour HM, Telko MJ, Xu Z, Smyth HD, Mulder T, McLean R, Langridge J, Papadopoulos D: **Physical characterization of component particles included in dry powder inhalers. I. Strategy review and static characteristics.** *J Pharm Sci* 2007, **96:**1282-1301.
229. Ooi J, Traini D, Hoe S, Wong W, Young PM: **Does carrier size matter? A fundamental study of drug aerosolisation from carrier based dry powder inhalation systems.** *Int J Pharm* 2011, **413:**1-9.
230. Podczeck F: **The influence of particle size distribution and surface roughness of carrier particles on the in vitro properties of dry powder inhalations.** *Aerosol Science and Technology* 1999, **31:**301-321.
231. 9 EP: **Preparations for inhalation: aerodynamic assessment of fine particles 2.9.18.** *European Pharmacopoeia 9* 2017.
232. Martonen TB, Musante CJ, Segal RA, Schroeter JD, Hwang D, Dolovich MA, Burton R, Spencer RM, Fleming JS: **Lung models: strengths and limitations.** *Respir Care* 2000, **45:**712-736.
233. **European Pharmacopeia. Section 2.9.18—Preparations for Inhalation: Aerodynamic Assessment of Fine Particles. 5. Strasbourg: Council of Europe; 2005. pp. 2799–2811.**
234. **United States Pharmacopeia. USP 30-NF 25. Chapter 601—Physical Tests and Determinations: Aerosols. Rockville: United States Pharmacopeia; 2007. pp. 220–240.**
235. Mitchell JP, Nagel MW: **Cascade impactors for the size characterization of aerosols from medical inhalers: their uses and limitations.** *J Aerosol Med* 2003, **16:**341-377.
236. Mitchell J, Newman S, Chan H-K: **In vitro and in vivo aspects of cascade impactor tests and inhaler performance: A review.** *AAPS PharmSciTech* 2007, **8:**237-248.
237. Marple VA, Roberts DL, Romay FJ, Miller NC, Truman KG, Van Oort M, Olsson B, Holroyd MJ, Mitchell JP, Hochrainer D: **Next generation pharmaceutical impactor (a new impactor for pharmaceutical inhaler testing). Part I: Design.** *Journal of aerosol medicine : the official journal of the International Society for Aerosols in Medicine* 2003, **16:**283-299.
238. Mitchell JP, Nagel MW, Avvakoumova V, MacKay H, Ali R: **The Abbreviated Impactor Measurement (AIM) Concept: Part 1—Influence of Particle Bounce and Re-Entrainment—Evaluation with a "Dry" Pressurized Metered Dose Inhaler (pMDI)-Based Formulation.** *AAPS PharmSciTech* 2009, **10:**243-251.
239. Rudolf G, Köbrich R, Stahlhofen W: **Modelling and algebraic formulation of regional aerosol deposition in man.** *Journal of Aerosol Science* 1990, **21:**S403-S406.
240. McKeown PJ, Johnston MV, Murphy DM: **On-line single-particle analysis by laser desorption mass spectrometry.** *Analytical Chemistry* 1991, **63:**2069-2073.
241. Prather KA, Nordmeyer T, Salt K: **Real-Time Characterization of Individual Aerosol-Particles Using Time-of-Flight Mass-Spectrometry.** *Analytical Chemistry* 1994, **66:**1403-1407.
242. Gard E, Mayer JE, Morrical BD, Dienes T, Fergenson DP, Prather KA: **Real-Time Analysis of Individual Atmospheric Aerosol Particles: Design and Performance of a Portable ATOFMS.** *Analytical Chemistry* 1997, **69:**4083-4091.
243. Noble CA, Prather KA: **Real-Time Measurement of Correlated Size and Composition Profiles of Individual Atmospheric Aerosol Particles.** *Environmental Science & Technology* 1996, **30:**2667-2680.

244. Noble CA, Prather KA: **Single Particle Characterization of Albuterol Metered Dose Inhaler Aerosol in Near Real-Time.** *Aerosol Science and Technology* 1998, **29:**294-306.
245. Frank M, Adams KL, Bogan MJ, Farquar GR, Gard EE, Fergenson DP, Martin AN, Riot JV, Steele PT, Tobias HJ, Woods BW: **Single-particle aerosol mass spectrometry (SPAMS) for high-throughput and rapid analysis of biological aerosols and single cells.** In *Abstracts Of Papers Of The American Chemical Society*. 2009
246. **Livermore Instruments Inc.** [http://www.livermoreinstruments.com/spams-overview.html]
247. Fergenson D, Balaxi M, Kohler D, Susz A, Morrical B: **Real-Time Inhalation Analytics Using Single Particle Aerosol Mass Spectrometry (SPAMS).** *Respiratory Drug Delivery* 2014, **1:**259-266.
248. Jetzer MW, Morrical BD, Fergenson DP, Imanidis G: **Particle interactions of fluticasone propionate and salmeterol xinafoate detected with single particle aerosol mass spectrometry (SPAMS).** *Int J Pharm* 2017, **532:**218-228.
249. Jetzer MW, Morrical BD, Schneider M, Edge S, Imanidis G: **Probing the Particulate Microstructure of the Aerodynamic Particle Size Distribution of Dry Powder Inhaler Combination Products.** *Int J Pharm* 2017, **538:**30-39.
250. Marple VA, Roberts DL, Romay FJ, Miller NC, Truman KG, Van Oort M, Olsson B, Holroyd MJ, Mitchell JP, Hochrainer D: **Next generation pharmaceutical impactor (a new impactor for pharmaceutical inhaler testing). Part I: Design.** *Journal of aerosol medicine the official journal of the International Society for Aerosols in Medicine* 2003, **16:**283-299.
251. Susz A, Morrical BD, Fergenson D: **Real time determination of APSD profiles of mono and combination dry powder inhalation products using single particle aerosol mass spectrometry (SPAMS 3.0).** *Respiratory Drug Delivery Europe 2015* 2015, **2:**387-390.
252. **World Health Organization (WHO)** [http://www.who.int/respiratory/en/]
253. Baraniuk JN, Ali M, Brody D, Maniscalco J, Gaumond E, Fitzgerald T, Wong G, Yuta A, Mak JC, Barnes PJ, et al: **Glucocorticoids induce beta2-adrenergic receptor function in human nasal mucosa.** *Am J Respir Crit Care Med* 1997, **155:**704-710.
254. Mak JC, Nishikawa M, Barnes PJ: **Glucocorticosteroids increase beta 2-adrenergic receptor transcription in human lung.** *Am J Physiol* 1995, **268:**L41-46.
255. Michael Y, Snowden MJ, Chowdhry BZ, Ashurst IC, Davies-Cutting CJ, Riley T: **Characterisation of the aggregation behaviour in a salmeterol and fluticasone propionate inhalation aerosol system.** *International Journal of Pharmaceutics* 2001, **221:**165-174.
256. Usmani OS, Maneechotesuwan K, Adcock IM, Barnes PJ: **Glucocorticoid receptor activation following inhaled fluticasone and salmeterol.** *Am J Respir Crit Care Med* 2002, **165:**A616.
257. Johnson M: **Combination therapy for asthma: Complementary effects of long-acting β2-agonists and corticosteroids.** *Curr Allergy Clin Immunol* 2002, **15:**16-22.
258. Orsida BE, Ward C, Li X, Bish R, Wilson JW, Thien F, Walters EH: **Effect of a long-acting beta2-agonist over three months on airway wall vascular remodeling in asthma.** *Am J Respir Crit Care Med* 2001, **164:**117-121.
259. Dowling R, Johnson M, Cole P, Wilson R: **Effect of fluticasone propionate and salmeterol on Pseudomonas aeruginosa infection of the respiratory mucosa in vitro.** *European Respiratory Journal* 1999, **14:**363-369.
260. Korn SH, Jerre A, Brattsand R: **Effects of formoterol and budesonide on GM-CSF and IL-8 secretion by triggered human bronchial epithelial cells.** *European Respiratory Journal* 2001, **17:**1070-1077.
261. Pang L, Knox AJ: **Synergistic inhibition by beta(2)-agonists and corticosteroids on tumor necrosis factor-alpha-induced interleukin-8 release from cultured human airway smooth-muscle cells.** *Am J Respir Cell Mol Biol* 2000, **23:**79-85.
262. Kirby S, Falcoz C, Daniel MJ, Milleri S, Squassante L, Ziviani L, Ventresca GP: **Salmeterol and fluticasone propionate given as a combination. Lack of systemic pharmacodynamic and pharmacokinetic interactions.** *Eur J Clin Pharmacol* 2001, **56:**781-791.
263. Taki M, Ahmed S, Marriott C, Zeng XM, Martin GP: **The 'stage-by-stage' deposition of drugs from commercial single-active and combination dry powder inhaler formulations.** *Eur J Pharm Sci* 2011, **43:**225-235.
264. Traini D, Young PM, Rogueda P, Price R: **In vitro investigation of drug particulates interactions and aerosol performance of pressurised metered dose inhalers.** *Pharm Res* 2007, **24:**125-135.

265. Gordon J, Panos RJ: **Inhaled albuterol/salbutamol and ipratropium bromide and their combination in the treatment of chronic obstructive pulmonary disease.** *Expert Opin Drug Metab Toxicol* 2010, **6:**381-392.
266. Frampton JE: **QVA149 (indacaterol/glycopyrronium fixed-dose combination): a review of its use in patients with chronic obstructive pulmonary disease.** *Drugs* 2014, **74:**465-488.
267. Ashurst IC, Prime D, Haywood PA: **Development of a dry powder inhaler device containing a combination of salmeterol and fluticasone propionate.** *Eur Respir J* 1998, **12 (suppl 28):**93s.
268. Malley TR, Ashurst IC, Daniels GE, Prime D, Stock NJ, Haywood PA: **Fine particle mass of a dry powder inhaler device containing a combination of salmeterol and fluticasone propionate.** *Eur Respir J* 1998, **12 (suppl 29):**8s.
269. Michael Y, Chowdhry BZ, Ashurst IC, Snowden MJ, Davies-Cutting C, Gray S: **The physico-chemical properties of salmeterol and fluticasone propionate in different solvent environments.** *International Journal of Pharmaceutics* 2000, **200:**279-288.
270. Theophilus A, Moore A, Prime D, Rossomanno S, Whitcher B, Chrystyn H: **Co-deposition of salmeterol and fluticasone propionate by a combination inhaler.** *Int J Pharm* 2006, **313:**14-22.
271. Zhou Q, Gengenbach T, Denman JA, Yu HH, Li J, Chan HK: **Synergistic Antibiotic Combination Powders of Colistin and Rifampicin Provide High Aerosolization Efficiency and Moisture Protection.** *The AAPS Journal* 2014, **16:**37-47.
272. Zhou Q, Loh ZH, Yu J, Sun S-p, Gengenbach T, Denman JA, Li J, Chan H-K: **How Much Surface Coating of Hydrophobic Azithromycin Is Sufficient to Prevent Moisture-Induced Decrease in Aerosolisation of Hygroscopic Amorphous Colistin Powder?** *The AAPS Journal* 2016, **18:**1213-1224.
273. Steele PT, Farquar GR, Martin AN, Coffee KR, Riot VJ, Martin SI, Fergenson DP, Gard EE, Frank M: **Autonomous, broad-spectrum detection of hazardous aerosols in seconds.** *Anal Chem* 2008, **80:**4583-4589.
274. Wang L-P, Maxey MR: **Settling velocity and concentration distribution of heavy particles in homogeneous isotropic turbulence.** *Journal of Fluid Mechanics* 2006, **256:**27-68.
275. Pilcer G, Amighi K: **Formulation strategy and use of excipients in pulmonary drug delivery.** *International Journal of Pharmaceutics* 2010, **392:**1-19.
276. Laitinen T, Hartonen K, Kulmala M, Riekkola ML: **Aerosol time-of-flight mass spectrometer for measuring ultrafine aerosol particles.** *Boreal Environment Research* 2009, **14:**539-549.
277. Fergenson DP, Morrical BD, Balaxi M, Brand N: **Real-Time Determination of Aerodynamic Particle Size Profiles and the Presence/Co-Presence of Active Ingredients in Inhalational Pharmaceutical Products Using a SPAMS 3.0.** *RDD Europe 2013* 2013, **2:**317-320.
278. Samir A, Salem H, Abdelkawy M: **New developed spectrophotometric method for simultaneous determination of salmeterol xinafoate and fluticasone propionate in bulk powder and Seritide® diskus inhalation.** *Bulletin of Faculty of Pharmacy, Cairo University* 2012, **50:**121-126.
279. Le VN, Robins E, Flament MP: **Agglomerate behaviour of fluticasone propionate within dry powder inhaler formulations.** *Eur J Pharm Biopharm* 2012, **80:**596-603.
280. Stein SW, Sheth P, Myrdal PB: **A model for predicting size distributions delivered from pMDIs with suspended drug.** *Int J Pharm* 2012, **422:**101-115.
281. Gonda I: **Development of a systematic theory of suspension inhalation aerosols. I. A framework to study the effects of aggregation on the aerodynamic behaviour of drug particles.** *International Journal of Pharmaceutics* 1985, **27:**99-116.
282. Islam N, Gladki E: **Dry powder inhalers (DPIs)--a review of device reliability and innovation.** *Int J Pharm* 2008, **360:**1-11.
283. Morrical BD, Fergenson DP, Prather KA: **Coupling two-step laser desorption/ ionization with aerosol time-of-flight mass spectrometry for the analysis of individual organic particles.** *Journal of the American Society for Mass Spectrometry* 1998, **9:**1068-1073.
284. van der Peyl GJQ, Haverkamp J, Kistemaker PG: **Thermal aspects of laser desorption mass spectrometry.** *International Journal of Mass Spectrometry and Ion Physics* 1982, **42:**125-141.
285. Dale MJ, Jones AC, Pollard SJT, Langridge-Smith PRR: **Direct determination of polycyclic aromatic hydrocarbons in environmental matrices using laser desorption laser photoionization time-of-flight mass spectrometry.** *Analyst* 1994, **119:**571-578.
286. **Draft Guidance for metered dose inhaler (MDI) and dry powder inhaler (DPI) drug products. Chemistry, manufacturing, and controls documentation.**

[http://www.fda.gov/downloads/drugs/guidancecomplianceregulatoryinformation/guidances/ucm070573.pdf]
287. de Boer AH, Gjaltema D, Hagedoorn P, Frijlink HW: **Can 'extrafine' dry powder aerosols improve lung deposition?** *European Journal of Pharmaceutics and Biopharmaceutics* 2015, **96:**143-151.
288. Hamid Q, Song Y, Kotsimbos TC, Minshall E, Bai TR, Hegele RG, Hogg JC: **Inflammation of small airways in asthma.** *J Allergy Clin Immunol* 1997, **100:**44-51.
289. Hogg JC, Chu F, Utokaparch S, Woods R, Elliott WM, Buzatu L, Cherniack RM, Rogers RM, Sciurba FC, Coxson HO, Pare PD: **The nature of small-airway obstruction in chronic obstructive pulmonary disease.** *N Engl J Med* 2004, **350:**2645-2653.
290. Leach CL, Kuehl PJ, Chand R, Ketai L, Norenberg JP, McDonald JD: **Characterization of respiratory deposition of fluticasone-salmeterol hydrofluoroalkane-134a and hydrofluoroalkane-134a beclomethasone in asthmatic patients.** *Ann Allergy Asthma Immunol* 2012, **108:**195-200.
291. 9 EP: **Preparations for inhalation 0671.** *European Pharmacopoeia 9* 2017.
292. Srichana T, Martin GP, Marriott C: **Dry powder inhalers : The influence of device resistance and powder formulation on drug and lactose deposition in vitro.** 1998, **7:**73-80.
293. Price R., J. S: **Physicochemical Evaluation of Powder Aggregates in Guiding Formulation Design.** *RDD Europe* 2013, **1:**185-196.
294. H. K, J. S, S. E, R. P: **Spectroscopic studies into the microstructure of carrier-based dry powder inhaler formulations.** *Drug Delivery to the Lungs* 2009.
295. Virgolini I, Kurtaran A, Leimer M, Smith-Jones P, Agis H, Angelberger P, Kletter K, Valent P, Linkesch W, Eichler HG: **Inhalation scintigraphy with iodine-123-labeled interferon gamma-1b: pulmonary deposition and dose escalation study in healthy volunteers.** *J Nucl Med* 1997, **38:**1475-1481.
296. Pasquali I, Merusi C, Brambilla G, Long EJ, Hargrave GK, Versteeg HK: **Optical diagnostics study of air flow and powder fluidisation in Nexthaler®—Part I: Studies with lactose placebo formulation.** *International Journal of Pharmaceutics* 2015, **496:**780-791.
297. Ruzycki CA, Javaheri E, Finlay WH: **The use of computational fluid dynamics in inhaler design.** *Expert Opin Drug Deliv* 2013, **10:**307-323.
298. NEWMAN SGSK, DAMHUIS RJFFD: **Processes for making lactose utilizing pre-classification techniques and pharmaceutical formulations formed therefrom.** Google Patents; 2007.
299. Farkas Á, Lewis D, Church T, Tweedie A, Mason F, Haddrell AE, Reid JP, Horváth A, Balásházy I: **Experimental and computational study of the effect of breath-actuated mechanism built in the NEXThaler® dry powder inhaler.** *International Journal of Pharmaceutics*.
300. Buttini F, Pasquali I, Brambilla G, Copelli D, Alberi MD, Balducci AG, Bettini R, Sisti V: **Multivariate Analysis of Effects of Asthmatic Patient Respiratory Profiles on the In Vitro Performance of a Reservoir Multidose and a Capsule-Based Dry Powder Inhaler.** *Pharmaceutical Research* 2016, **33:**701-715.
301. Theraputic Goods Administration ADoHaA: **Australian Public Assessment Report for glycopyrronium (as bromide).** *https://wwwtgagovau/sites/default/files/auspar-glycopyrronium-130710pdf* 2013.
302. JN. S, DA. VM, R. G, G. B, R. M, L. F: **Pharmaceutical formulations for dry powder inhalers in the form of hard-pellets.** *EP1274406 B1* 2006.
303. Lau M, Young PM, Traini D: **Co-milled API-lactose systems for inhalation therapy: impact of magnesium stearate on physico-chemical stability and aerosolization performance.** *Drug Development and Industrial Pharmacy* 2017, **43:**980-988.
304. Kanniess F, Scuri M, Vezzoli S, Francisco C, Petruzzelli S: **Extrafine beclomethasone/formoterol combination via a dry powder inhaler (NEXThaler((R))) or pMDI and beclomethasone monotherapy for maintenance of asthma control in adult patients: A randomised, double-blind trial.** *Pulm Pharmacol Ther* 2015, **30:**121-127.
305. Grant AC, Walker R, Hamilton M, Garrill K: **The ELLIPTA(®) Dry Powder Inhaler: Design, Functionality, In Vitro Dosing Performance and Critical Task Compliance by Patients and Caregivers.** *Journal of Aerosol Medicine and Pulmonary Drug Delivery* 2015, **28:**474-485.
306. Shekunov BY, Chattopadhyay P, Tong HHY, Chow AHL: **Particle Size Analysis in Pharmaceutics: Principles, Methods and Applications.** *Pharmaceutical Research* 2006, **24:**203-227.
307. Apte SP: **Excipient-API interactions in dry powder inhalers.** *Journal of Excipients and Food Chemicals* 2012, **3:**129-142.

308. Kawashima Y, Serigano T, Hino T, Yamamoto H, Takeuchi H: **Effect of surface morphology of carrier lactose on dry powder inhalation property of pranlukast hydrate.** *International Journal of Pharmaceutics* 1998, **172:**179-188.
309. Das S, Larson I, Young P, Stewart P: **Influence of Storage Relative Humidity on the Dispersion of Salmeterol Xinafoate Powders for Inhalation.** *Journal of Pharmaceutical Sciences* 2009, **98:**1015-1027.
310. Thalberg K, Berg E, Fransson M: **Modeling dispersion of dry powders for inhalation. The concepts of total fines, cohesive energy and interaction parameters.** *Int J Pharm* 2012, **427:**224-233.
311. Chan LW, Lim LT, Heng PW: **Immobilization of fine particles on lactose carrier by precision coating and its effect on the performance of dry powder formulations.** *J Pharm Sci* 2003, **92:**975-984.
312. Van Vaeck L, Adriaens A, Gijbels R: **Static secondary ion mass spectrometry: (S-SIMS) Part 1. Methodology and structural interpretation.** *Mass Spectrometry Reviews* 1999, **18:**1-47.
313. Wang XL, McMurry PH: **A design tool for aerodynamic lens systems.** *Aerosol Science and Technology* 2006, **40:**320-334.
314. Zeng XM, Martin GP, Tee SK, Marriott C: **The role of fine particle lactose on the dispersion and deaggregation of salbutamol sulphate in an air stream in vitro.** *International Journal of Pharmaceutics* 1998, **176:**99-110.
315. Kumon M, Suzuki M, Kusai A, Yonemochi E, Terada K: **Novel approach to DPI carrier lactose with mechanofusion process with additives and evaluation by IGC.** *Chemical & Pharmaceutical Bulletin* 2006, **54:**1508-1514.
316. Young PM, Edge S, Traini D, Jones MD, Price R, El-Sabawi D, Urry C, Smith C: **The influence of dose on the performance of dry powder inhalation systems.** *Int J Pharm* 2005, **296:**26-33.
317. Le VN, Hoang Thi TH, Robins E, Flament MP: **Dry powder inhalers: study of the parameters influencing adhesion and dispersion of fluticasone propionate.** *AAPS PharmSciTech* 2012, **13:**477-484.
318. Kwok PC, Chan HK: **Effect of relative humidity on the electrostatic charge properties of dry powder inhaler aerosols.** *Pharm Res* 2008, **25:**277-288.
319. Li Q, Rudolph V, Peukert W: **London-van der Waals adhesiveness of rough particles.** *Powder Technology* 2006, **161:**248-255.
320. Cline D, Dalby R: **Predicting the quality of powders for inhalation from surface energy and area.** *Pharmaceutical Research* 2002, **19:**1274-1277.
321. Saleem I, Smyth H, Telko M: **Prediction of dry powder inhaler formulation performance from surface energetics and blending dynamics.** *Drug Development and Industrial Pharmacy* 2008, **34:**1002-1010.
322. Zeng XM, Martin GP, Marriott C, Pritchard J: **The use of lactose recrystallised from carbopol gels as a carrier for aerosolised salbutamol sulphate.** *European Journal of Pharmaceutics and Biopharmaceutics* 2001, **51:**55-62.
323. Louey MD, Van Oort M, Hickey AJ: **Aerosol dispersion of respirable particles in narrow size distributions produced by jet-milling and spray-drying techniques.** *Pharmaceutical Research* 2004, **21:**1200-1206.
324. Tay T, Das S, Stewart P: **Magnesium stearate increases salbutamol sulphate dispersion: What is the mechanism?** *International Journal of Pharmaceutics* 2010, **383:**62-69.
325. Fults KA, Miller IF, Hickey AJ: **Effect of particle morphology on emitted dose of fatty acid-treated disodium cromoglycate powder aerosols.** *Pharmaceutical development and technology* 1997, **2:**67-79.
326. Chew NYK, Shekunov BY, Tong HHY, Chow AHL, Savage C, Wu J, Chan HK: **Effect of amino acids on the dispersion of disodium cromoglycate powders.** *Journal of Pharmaceutical Sciences* 2005, **94:**2289-2300.
327. Lucas P, Anderson K, Potter UJ, Staniforth JN: **Enhancement of small particle size dry powder aerosol formulations using an ultra low density additive.** *Pharmaceutical Research* 1999, **16:**1643-1647.
328. Pu Y, Mazumder M, Cooney C: **Effects of electrostatic charging on pharmaceutical powder blending homogeneity.** *J Pharm Sci* 2009, **98:**2412-2421.
329. Steckel H, Müller BW: **In vitro evaluation of dry powder inhalers II: influence of carrier particle size and concentration on in vitro deposition.** *International Journal of Pharmaceutics* 1997, **154:**31-37.
330. Chew NYK, Chan HK: **Effect of powder polydispersity on aerosol generation.** *Journal of Pharmacy and Pharmaceutical Sciences* 2002, **5:**162-168.
331. Larhrib H, Martin GP, Marriott C, Prime D: **The influence of carrier and drug morphology on drug delivery from dry powder formulations.** *International Journal of Pharmaceutics* 2003, **257:**283-296.

332. Zeng XM, Martin GP, Marriott C, Pritchard J: **The effects of carrier size and morphology on the dispersion of salbutamol sulphate after aerosolization at different flow rates.** *Journal of Pharmacy and Pharmacology* 2000, **52:**1211-1221.
333. Adi H, Traini D, Chan H-K, Young PM: **The influence of drug morphology on the aerosolisation efficiency of dry powder inhaler formulations.** *Journal of Pharmaceutical Sciences* 2008, **97:**2780-2788.
334. Flament MP, Leterme P, Gayot A: **The influence of carrier roughness on adhesion, content uniformity and the in vitro deposition of terbutaline sulphate from dry powder inhalers.** *International Journal of Pharmaceutics* 2004, **275:**201-209.
335. Perkins M, Ebbens SJ, Hayes S, Roberts CJ, Madden CE, Luk SY, Patel N: **Elastic modulus measurements from individual lactose particles using atomic force microscopy.** *International Journal of Pharmaceutics* 2007, **332:**168-175.
336. Chan LW, Lim LT, Heng PWS: **Immobilization of fine particles on lactose carrier by precision coating and its effect on the performance of dry powder formulations.** *Journal of Pharmaceutical Sciences* 2003, **92:**975-984.
337. Chow KT, Zhu K, Tan RB, Heng PW: **Investigation of electrostatic behavior of a lactose carrier for dry powder inhalers.** *Pharm Res* 2008, **25:**2822-2834.
338. Kubavat HA, Shur J, Ruecroft G, Hipkiss D, Price R: **Investigation into the influence of primary crystallization conditions on the mechanical properties and secondary processing behaviour of fluticasone propionate for carrier based dry powder inhaler formulations.** *Pharm Res* 2012, **29:**994-1006.
339. Shur J, Lee S, Adams W, Lionberger R, Tibbatts J, Price R: **Effect of device design on the in vitro performance and comparability for capsule-based dry powder inhalers.** *AAPS J* 2012, **14:**667-676.
340. O'Callaghan C, Lynch J, Cant M, Robertson C: **Improvement in sodium cromoglycate delivery from a spacer device by use of an antistatic lining, immediate inhalation, and avoiding multiple actuations of drug.** *Thorax* 1993, **48:**603-606.
341. Barry PW, O'Callaghan C: **The effect of delay, multiple actuations and spacer static charge on the in vitro delivery of budesonide from the Nebuhaler.** *Br J Clin Pharmacol* 1995, **40:**76-78.
342. Bailey AG: **The inhalation and deposition of charged particles within the human lung.** *Journal of Electrostatics* 1997, **42:**25-32.
343. Braun MA, Oschmann R, Schmidt PC: **Influence of excipients and storage humidity on the deposition of disodium cromoglycate (DSCG) in the Twin Impinger.** *International Journal of Pharmaceutics* 1996, **135:**53-62.
344. Young PM, Price R, Tobyn MJ, Buttrum M, Dey F: **Effect of Humidity on Aerosolization of Micronized Drugs.** *Drug Development and Industrial Pharmacy* 2003, **29:**959-966.
345. Young PM, Price R: **The influence of humidity on the aerosolisation of micronised and SEDS produced salbutamol sulphate.** *Eur J Pharm Sci* 2004, **22:**235-240.
346. Murtomaa M, Mellin V, Harjunen P, Lankinen T, Laine E, Lehto VP: **Effect of particle morphology on the triboelectrification in dry powder inhalers.** *Int J Pharm* 2004, **282:**107-114.
347. Giles CH, MacEwan TH, Nakhwa SN, Smith D: **786. Studies in adsorption. Part XI. A system of classification of solution adsorption isotherms, and its use in diagnosis of adsorption mechanisms and in measurement of specific surface areas of solids.** *Journal of the Chemical Society (Resumed)* 1960**:**3973.
348. Rouagdia K, Nemamcha M, Herous L, Dascalescu L, Mellouki H: **Surface potential decay of DC-corona-charged PET films on humid electrodes.** *Journal of Electrostatics* 2015, **78:**17-21.
349. Chubb JN: **Corona charging of practical materials for charge decay measurements.** *Journal of Electrostatics* 1996, **37:**53-65.
350. Kumara S, Serdyuk YV, Gubanski SM: **Surface charge decay on polymeric materials under different neutralization modes in air.** *IEEE Transactions on Dielectrics and Electrical Insulation* 2011, **18:**1779-1788.
351. Carter PA, Rowley G, Fletcher EJ, Stylianopoulos V: **Measurement of Electrostatic Charge Decay in Pharmaceutical Powders and Polymer Materials Used in Dry Powder Inhaler Devices.** *Drug Development and Industrial Pharmacy* 1998, **24:**1083-1088.
352. Chubb JN: **Comments on methods for charge decay measurement.** *Journal of Electrostatics* 2004, **62:**73-80.
353. **Volume Resistivity of Polymers** [https://omnexus.specialchem.com/polymer-properties/properties/volume-resistivity]

354. Peart J: **Powder Electrostatics: Theory, Techniques and Applications.** *KONA Powder and Particle Journal* 2001, **19**.
355. Elajnaf A, Carter P, Rowley G: **Electrostatic characterisation of inhaled powders: Effect of contact surface and relative humidity.** *European Journal of Pharmaceutical Sciences* 2006, **29:**375-384.
356. Elajnaf A, Carter P, Rowley G: **The effect of relative humidity on electrostatic charge decay of drugs and excipient used in dry powder inhaler formulation.** *Drug Development and Industrial Pharmacy* 2007, **33:**967-974.
357. Trigwell S, Grable N, Yurteri CU, Sharma R, Mazumder MK: **Effects of surface properties on the tribocharging characteristics of polymer powder as applied to industrial processes.** *Ieee Transactions on Industry Applications* 2003, **39:**79-86.
358. Rezende CA, Gouveia RF, da Silva MA, Galembeck F: **Detection of charge distributions in insulator surfaces.** *J Phys Condens Matter* 2009, **21:**263002.
359. Burgo TAD, Rezende CA, Bertazzo S, Galembeck A, Galembeck F: **Electric potential decay on polyethylene: Role of atmospheric water on electric charge build-up and dissipation.** *Journal of Electrostatics* 2011, **69:**401-409.
360. Gouveia RF, Costa CAR, Galembeck F: **Water Vapor Adsorption Effect on Silica Surface Electrostatic Patterning.** *Journal of Physical Chemistry C* 2008, **112:**17193-17199.
361. Gouveia RF, Galembeck F: **Electrostatic charging of hydrophilic particles due to water adsorption.** *J Am Chem Soc* 2009, **131:**11381-11386.
362. Saini D, Biris AS, Srirama PK, Mazumder MK: **Particle Size and Charge Distribution Analysis of Pharmaceutical Aerosols Generated by Inhalers.** *Pharmaceutical Development and Technology* 2007, **12:**35-41.
363. Castle GSP, Schein LB: **General model of sphere-sphere insulator contact electrification.** *Journal of Electrostatics* 1995, **36:**165-173.
364. Telko MJ, Kujanpaa J, Hickey AJ: **Investigation of triboelectric charging in dry powder inhalers using electrical low pressure impactor (ELPI).** *Int J Pharm* 2007, **336:**352-360.
365. Lowell J, Truscott WS: **Triboelectrification of identical insulators. I. An experimental investigation.** *Journal of Physics D: Applied Physics* 1986, **19:**1273.
366. Lowell J, Truscott WS: **Triboelectrification of identical insulators. II. Theory and further experiments.** *Journal of Physics D: Applied Physics* 1986, **19:**1281.
367. Davidson N, Tong HJ, Kalberer M, Seville PC, Ward AD, Kuimova MK, Pope FD: **Measurement of the Raman spectra and hygroscopicity of four pharmaceutical aerosols as they travel from pressurised metered dose inhalers (pMDI) to a model lung.** *International Journal of Pharmaceutics* 2017, **520:**59-69.
368. Hickey AJ, Gonda I, Irwin WJ, Fildes FJ: **Effect of hydrophobic coating on the behavior of a hygroscopic aerosol powder in an environment of controlled temperature and relative humidity.** *J Pharm Sci* 1990, **79:**1009-1014.
369. Borgström L, Asking L, Lipniunas P: **An In Vivo and In Vitro Comparison of Two Powder Inhalers following Storage at Hot/Humid Conditions.** *Journal of Aerosol Medicine* 2005, **18:**304-310.
370. Young PM, Price R, Tobyn MJ, Buttrum M, Dey F: **Effect of humidity on aerosolization of micronized drugs.** *Drug Dev Ind Pharm* 2003, **29:**959-966.
371. Steele DF, Young PM, Price R, Smith T, Edge S, Lewis D: **The potential use of Raman mapping to investigate in vitro deposition of combination pressurized metered-dose inhalers.** *AAPS J* 2004, **6:**e32.
372. Mapel DW, Hurley JS, Dalal AA, Blanchette CM: **The role of combination inhaled corticosteroid/long-acting beta-agonist therapy in COPD management.** *Prim Care Respir J* 2010, **19:**93-103.
373. Liu S, Watts AB, Du J, Bui A, Hengsawas S, Peters JI, Williams RO, 3rd: **Formulation of a novel fixed dose combination of salmeterol xinafoate and mometasone furoate for inhaled drug delivery.** *Eur J Pharm Biopharm* 2015, **96:**132-142.
374. EMEA: **Guideline on the requirements for clinical documentation for Orally Inhaled Products (OIP) including the requirements for demonstration of therapeutic equivalence between two inhaled products for use in the treatment of Asthma and Chronic Obstructive Pulmonary Disease (COPD) in adults and for use in the treatment of Asthma in children and adolescents. European Medicines Agency (EMEA). Committee for Medicinal Products for Human Use (CHMP).** 2009.
375. Lu D, Lee SL, Lionberger RA, Choi S, Adams W, Caramenico HN, Chowdhury BA, Conner DP, Katial R, Limb S, et al: **International Guidelines for Bioequivalence of Locally Acting Orally Inhaled Drug Products: Similarities and Differences.** *AAPS J* 2015, **17:**546-557.

376. Young PM, Kwok P, Adi H, Chan HK, Traini D: **Lactose composite carriers for respiratory delivery.** *Pharm Res* 2009, **26:**802-810.
377. Smutney CC, Grant M, Kinsey PS: **Device factors affecting pulmonary delivery of dry powders.** *Therapeutic Delivery* 2013, **4:**939-949.
378. Ngoc NT, Chang L, Jia X, Lau R: **Experimental investigation of design parameters on dry powder inhaler performance.** *Int J Pharm* 2013, **457:**92-100.
379. Coates MS, Fletcher DF, Chan HK, Raper JA: **Effect of design on the performance of a dry powder inhaler using computational fluid dynamics. Part 1: Grid structure and mouthpiece length.** *J Pharm Sci* 2004, **93:**2863-2876.
380. Coates MS, Chan HK, Fletcher DF, Raper JA: **Effect of design on the performance of a dry powder inhaler using computational fluid dynamics. Part 2: Air inlet size.** *J Pharm Sci* 2006, **95:**1382-1392.
381. Zhou QT, Tong Z, Tang P, Citterio M, Yang R, Chan HK: **Effect of device design on the aerosolization of a carrier-based dry powder inhaler--a case study on Aerolizer((R)) Foradile ((R)).** *AAPS J* 2013, **15:**511-522.
382. Longest PW, Son YJ, Holbrook L, Hindle M: **Aerodynamic factors responsible for the deaggregation of carrier-free drug powders to form micrometer and submicrometer aerosols.** *Pharm Res* 2013, **30:**1608-1627.
383. Chen L, Heng RL, Delele MA, Cai J, Du DZ, Opara UL: **Investigation of dry powder aerosolization mechanisms in different channel designs.** *Int J Pharm* 2013, **457:**143-149.
384. Wong W, Fletcher DF, Traini D, Chan HK, Crapper J, Young PM: **Particle aerosolisation and break-up in dry powder inhalers: evaluation and modelling of the influence of grid structures for agglomerated systems.** *J Pharm Sci* 2011, **100:**4710-4721.
385. Tonnis WF, Lexmond AJ, Frijlink HW, de Boer AH, Hinrichs WLJ: **Devices and formulations for pulmonary vaccination.** *Expert Opinion on Drug Delivery* 2013, **10:**1383-1397.
386. Rottier B, Grasmeijer F, Hagedoorn P, de Boer AH: **Aerosol drug delivery: developments in device design and clinical use.** *Lancet* 2011, **378:**981-982; author reply 982.
387. **Advair/Seretide** [https://www.fiercepharma.com/special-report/advair-seretide]

LIST OF ABBREVIATIONS

ABS	Acrylonitrile butadiene styrene
AFM	Atomic force microscopy
API	Active pharmaceutical ingredient
APS	Aerodynamic particle sizer
APSD	Aerodynamic particle size distribution
BDP	Beclomethasone dipropionate
BUD	Budesonide
CAB	Cohesive-adhesive balance
CFC	Chlorofluorocarbon
COPD	Chronic obstructive pulmonary disease
DPI	Dry powder inhaler
FCA	Force control agent
FF	Formoterol fumarate
FP	Fluticasone propionate
FPF	Fine particle fraction
GINA	Global initiative for asthma
GOLD	Global initiative for chronic obstructive pulmonary disease
HFA	Hydrofluoroalkanes
HPLC	High performance liquid chromatography
HPMC	Hydroxypropyl methylcellulose
IGC	Inverse gas chromatography
ICS	Inhaled corticosteroids
LABA	Long-acting β2-agonist
LOD	Limit of detection
LOQ	Limit of quantification
MgSt	Magnesium stearate
NGI	Next generation impactor

pMDI	(pressurized) metered dose inhaler
RH	Relative humidity
SABA	Short-acting β2-agonists
SCF	Supercritical fluid
SD	Standard deviation
SEM	Scanning electron microscopy
SPAMS	Single particle aerosol mass spectrometry
SS	Salbutamol sulphate
SX	Salmeterol xinafoate
ToF-SIMS	Time-of-flight secondary ion mass spectrometry
XPS	X-ray photoelectron spectroscopy